Discrete Confocal Quadrics and Checkerboard Incircular Nets

vorgelegt von
M.Sc.
Jan Techter

an der Fakultät II – Mathematik und Naturwissenschaften
der Technischen Universität Berlin
zur Erlangung des akademischen Grades

Doktor der Naturwissenschaften
Dr. rer. nat.

genehmigte Dissertation

Promotionsausschuss:

Vorsitzender: Prof. Dr. Mario Kummer
Gutachter: Prof. Dr. Alexander Bobenko
Gutachter: Prof. Dr. Helmut Pottmann (KAUST)
Gutachter: Prof. Dr. Ivan Izmestiev (TU Wien)

Tag der wissenschaftlichen Aussprache: 28.02.2020

Berlin 2021

Abstract

Confocal quadrics constitute a special example of orthogonal coordinate systems. In this cumulative thesis we propose two approaches to the discretization of confocal coordinates, and study the closely related checkerboard incircular nets.

First, we propose a discretization based on factorizable solutions to an integrable discretization of the Euler-Poisson-Darboux equation. The constructed solutions are discrete Koenigs nets and feature a novel discrete orthogonality constraint defined on pairs of dual discrete nets, as well as a corresponding discrete isothermicity condition. The coordinate functions of these discrete confocal coordinates are explicitly given in terms of gamma functions.

Secondly, we show that classical confocal coordinates and their reparametrizations along coordinate lines are characterized by orthogonality and the factorization property. We use these two properties to propose another discretization of confocal coordinates, while again employing the aforementioned discrete orthogonality constraint. In comparison to the first approach, this definition results in a broader class of nets capturing arbitrary reparametrizations also in the discrete case. We show that these discrete confocal coordinate systems may equivalently be constructed geometrically via polarity with respect to a sequence of classical confocal quadrics. Different sequences correspond to different discrete parametrizations. We give several explicit examples, including parametrizations in terms of Jacobi elliptic functions.

A particular example of discrete confocal coordinates in the two-dimensional case is closely related to incircular nets, that is, congruences of straight lines in the plane with the combinatorics of the square grid such that each elementary quadrilateral admits an incircle. Thus, thirdly, we classify and integrate the class of checkerboard incircular nets, which constitute the Laguerre geometric generalization of incircular nets.

Further aspects of the novel discrete orthogonality constraint are studied in the introduction of this thesis. These include discrete Lamé coefficients, discrete focal nets, discrete parallel nets, and discrete isothermicity, as well as the relation to pairs of circular and conical nets.

Zusammenfassung

Konfokale Quadriken bilden ein Beispiel für orthogonale Koordinatensysteme. In dieser kumulativen Dissertation werden zwei Ansätze zur Diskretisierung konfokaler Koordinaten sowie der Zusammenhang zu Schachbrettinkreisnetzen behandelt.

Der erste Ansatz begründet sich auf einer integrablen Diskretisierung der Euler-Poisson-Darboux-Gleichung. Die konstruierten Lösungen sind diskrete Koenigs-Netze und durch eine neue diskrete Orthogonalitätsbedingung gekennzeichnet. Die Koordinatenfunktionen sind explizit durch gamma-Funktionen gegeben.

Für den zweiten Ansatz zeigen wir zunächst, dass klassische konfokale Koordiatensysteme bis auf Umparametrisierung entlang der Koordinatenlinien durch Orthogonalität und die Faktorsierbarkeit bereits charakterisiert sind. Wir übertragen diese beiden Eigenschaften auf eine weitere Definition diskreter konfokaler Koordinaten, wieder unter Verwendung der genannten neuen diskreten Orthogonalitätsbedingung. Diese Definition führt zu einer größeren Klasse von Netzen als im ersten Ansatz und beinhaltet beliebege Umparametriesierungen. Es wird gezeigt, dass diese diskreten konfokalen Koordinaten durch eine äquivalente geometrische Konstruktion durch Polarität in einer Folge von klassischen konfokalen Quadriken charakterisiert ist. Verschiedene Folgen entsprechen verschiedenen diskreten Parametrisierungen. Wir geben eine Vielzahl von konkreten Beispielen an, insebesondere eine Parametrisierung durch Jacobi elliptische Funktionen.

Ein besonderes Beispiel von diskreten konfokalen Koordinaten im zwei-dimensionalen Fall ist durch Inkreisnetze gegeben. Inkreisnetzte sind durch zwei Folgen von Geraden in der Ebene mit der Kombinatorik des Quadratgitters gegeben, so dass alle elementaren Vierecke einen Inkreis besitzen. Wir klassifizieren und integrieren die zugehörige Laguerre-geometrische Verallgemeinerung der Schachbrettinkreisnetze.

Weitere Aspekte der neuen diskreten Orthogonalitätzbedingung werden in der Einleitung behandelt. Unter anderem diskrete Lamé-Koeffizienten, diskrete Fokalnetze, diskrete Parallelnetze, sowie der Zusammenhang zu Paaren von zirkulären und konischen Netzen.

In Loving Memory of
Heinrich-Wilhelm Techter †
and
Heinrich Cox †

Acknowledgements

Beside my advisor

Alexander Bobenko,

and my coauthors

Wolfgang Schief,
Yuri Suris,

I would like to thank the following people for various kind of support:

Niklas Affolter,
Lily Black,
Philip Brozio,
Ulrike Bücking,
Albert Chern,
Shana Choukri,
Renate Cox-Techter,
Hanka Kouřimská,
Wayne Lam,
Christian Müller,
Isabella Retter,
Thilo Rörig,
Andy Sageman-Furnas,
Lara Skuppin,
Ananth Sridhar,
Jonas Tervooren,
Max Techter,

and most importantly

Alexandra Haack.

All 3D renderings (and many of the 2D pictures) were created using `blender`, and, in the introduction, with the help of Oliver Gross.

Contents

Introduction

The main subject of this cumulative doctoral thesis is orthogonal coordinate systems constituted by families of confocal quadrics and their discretization, as well as the closely related checkerboard incircular nets in the plane. The results have been published in the following articles and appear in this thesis as the three enumerated chapters.

[BSST1] A.I. Bobenko, W.K. Schief, Y.B. Suris, J. Techter.
On a discretization of confocal quadrics. I. An integrable systems approach,
Journal of Integrable Systems, Volume 1, Issue 1, January 2016, xyw005,
`https://doi.org/10.1093/integr/xyw005`

[BSST2] A.I. Bobenko, W.K. Schief, Y.B. Suris, J. Techter.
On a discretization of confocal quadrics. II. A geometric approach to general parametrizations,
International Mathematics Research Notices, Volume 2020, Issue 24, December 2020,
Pages 10180–10230, `https://doi.org/10.1093/imrn/rny279`

[BST] A.I. Bobenko, W.K. Schief, J. Techter.
Checkerboard incircular nets. Laguerre geometry and parametrisation,
Geometriae Dedicata, Volume 204, Issue 1, February 2020, Pages 97-129,
`https://doi.org/10.1007/s10711-019-00449-x`

Besides featuring many further beautiful geometric properties and applications (Chapter 1: Section 1, Chapter 2: Section 1), confocal quadrics constitute a special example of orthogonal coordinate systems, i.e., a smooth map $\boldsymbol{x} : \mathbb{R}^N \supset U \to \mathbb{R}^N$ satisfying $\langle \partial_i \boldsymbol{x}, \partial_j \boldsymbol{x} \rangle = 0$ for $i \neq j$.

The fundamental monograph [Da2] by Darboux is solely devoted to the study of orthogonal coordinate systems with the main emphasis on triply orthogonal systems. Therein he classified all triply orthogonal systems whose two-dimensional coordinate surfaces are isothermic. Such coordinate systems are closely related to the separability in Laplace-type equations [SS]. Darboux found several families, all satisfying the Euler-Poisson-Darboux system

$$\partial_i \partial_j \boldsymbol{x} = \frac{\gamma}{u_i - u_j} (\partial_j \boldsymbol{x} - \partial_i \boldsymbol{x}), \qquad i \neq j.$$

with coefficient $\gamma = \pm\frac{1}{2}, -1$, or -2. The case corresponding to $\gamma = \frac{1}{2}$ includes confocal quadrics as factorizable solutions, i.e.,

$$x_k(u_1, \ldots, u_N) = f_1^k(u_1) f_2^k(u_2) \cdots f_N^k(u_N), \qquad i = 1, \ldots, N$$

with some functions $f_i^k(u_i)$.

Discretizing coordinate systems means finding suitable approximating discrete nets $\boldsymbol{x} : \mathbb{Z}^N \supset U \to \mathbb{R}^N$. According to the philosophy of structure preserving discretization [BS], it is crucial not to follow the path of a straightforward discretization of differential equations, but rather to discretize a well chosen collection of essential geometric properties. A discretization of the Euler-Poisson-Darboux system (Chapter 1: Section 5) following this principle has been introduced by Konopelchenko and Schief [KS2],

$$\Delta_i \Delta_j \boldsymbol{x} = \frac{\gamma}{n_i + \varepsilon_i - n_j - \varepsilon_j} (\Delta_j \boldsymbol{x} - \Delta_i \boldsymbol{x}), \qquad i \neq j.$$

In particular, solutions of this discrete system satisfy a well-established notion of discrete Koenigs nets (Chapter 1: Sections 4 and 5). In [BSST1] (Chapter 1), we take this discrete equation as our point of departure to obtain discrete confocal coordinates as certain factorizable solutions of this system, which can be described in terms of gamma functions. The orthogonality in this discretization is implemented by considering pairs of solutions defined on dual square lattices,

$$\boldsymbol{x} : \mathbb{Z}^N \cup \left(\mathbb{Z} + \tfrac{1}{2}\right)^N \supset U \to \mathbb{R}^N,$$

such that each pair of dual edges from the two lattices are orthogonal (Chapter 1: Section 6.2). It turns out that this novel discrete orthogonality constraint generalizes a combined notion of circular and conical nets [PW] (see Section 2.2 of the Introduction). Due to the factorizability of discrete confocal coordinates, the solutions can be extended to the stepsize $\frac{1}{2}$ lattice $\left(\frac{1}{2}\mathbb{Z}\right)^N$.

In [BSST2] (Chapter 2), we show that classical confocal coordinates are already characterized by the factorization property and orthogonality (up to reparametrization along the coordinate lines). Different parametrizations of confocal coordinates exhibit different geometric properties, revealing connections to 3-webs/4-webs in the plane [Ak, Ag] and on quadrics [ABST]. We take the two characterizing properties of factorizability and orthogonality, while again employing the novel discrete orthogonality constraint introduced in [BSST1], to define discrete confocal coordinates. This definition results in a broader class of nets than the one from [BSST1], capturing arbitrary reparametrizations also in the discrete case, and leading to a variety of examples of discrete confocal coordinates, which exhibit many geometric features analogous to the smooth case (Chapter 2: Sections 8, 9, and B). Furthermore, discrete confocal coordinates admit a geometric characterization in terms of polarity with respect to quadrics of a classical confocal family (Chapter 2: Section 6), and satisfy a generalized discrete Euler-Poisson-Darboux system (Chapter 2: Section A.2).

Incircular nets are congruences of straight lines in the plane with the combinatorics of the square grid such that each elementary quadrilateral admits an incircle [Bö, AB]. All lines of an incircular net touch a common conic, while the points of intersection of these lines lie on confocal conics. The incircle centers of such a net provide a further example of discrete confocal conics as introduced in [BSST2] (Chapter 1: Section A and Chapter 2: Sections 8.4 and 8.5). In [BST] (Chapter 3), we study checkerboard incircular nets, which are the Laguerre geometric generalization of incircular nets. We classify generic checkerboard incircular nets based on the classification of hypercycles [Bl], and give explicit parametrizations for the subclass of confocal checkerboard incircular nets in terms of Jacobi elliptic functions.

This introduction serves the following purposes:

- Summarizing the main results of the three publications in a coherent setup.
- Introducing some of the relevant foundations.
- Providing some supplementary results and explanations that support the concepts and definitions from the publications.

Outline of the Introduction In Section 1, we introduce smooth and discrete nets as well as the respective orthogonality conditions. Discrete nets are introduced on pairs of dual square lattices. These pairs of dual discrete nets admit a novel orthogonality constraint and the definition of corresponding Lamé coefficients. As a consequence of a discrete version of Dupin's theorem, pairs of dual discrete orthogonal nets have planar faces, i.e. are discrete conjugate nets. Replacing orthogonal pairs of dual discrete nets by orthogonal sphere congruences leads to a Möbius invariant description.

Orthogonal pairs of two-dimensional dual discrete conjugate nets are discrete analogs of curvature line parametrizations. In Section 2, we show that they generalize pairs of circular and conical nets and admit a definition of discrete focal nets and discrete parallel nets.

In Section 3, discrete isothermic nets are defined by factorizing discrete Lamé coefficients.

In Section 4, confocal coordinates and their characterizing properties of factorizability and orthogonality is introduced, as well as the corresponding definition of discrete confocal coordinates. The corresponding discrete Lamé coefficients are computed and it is shown that all two-dimensional subnets of a discrete confocal coordinate system are discrete isothermic in the sense of Section 3.

The general discrete Euler-Poisson-Darboux system is introduced in Section 5. Its 3D-consistency is shown and different forms of the equation are studied, revealing a discrete Koenigs-type condition.

In Section 6, confocal quadrics are described from the point of view of projective geometry. A geometric proof for the closedness of a dynamical system defined by sequences of quadrics from a dual pencil is given. This system, in particular, describes the geometric construction of discrete confocal coordinates.

In Section 7, incircular nets and their relation to smooth and discrete confocal conics are introduced, as well as their Laguerre geometric generalization of checkerboard incircular nets.

Conclusions and open problems are given in Section 8.

1 Orthogonal nets

1.1 Classical orthogonal nets

We start with the definition of *(regular) nets*, which represent parametrizations of submanifolds of $\mathbb{R}^N$, in particular,

- *parametrized curves* in the case $M = 1$,
- *parametrized surfaces* in the case $M = 2$, and
- *coordinate systems* of (some region of) $\mathbb{R}^N$ in the case $M = N$.

Definition 1.1.

(i) Let $U \subset \mathbb{R}^M$ be open and connected. Then a smooth map

$$\boldsymbol{x} : \mathbb{R}^M \supset U \to \mathbb{R}^N, \qquad (s_1, \ldots, s_M) \mapsto \boldsymbol{x}(s_1, \ldots, s_M)$$

*is called an M-*dimensional (smooth) net*.*

(ii) A net $\boldsymbol{x} : \mathbb{R}^M \supset U \to \mathbb{R}^N$ is called regular *if the M tangent vectors*

$$\partial_1 \boldsymbol{x}, \ldots, \partial_M \boldsymbol{x} \in \mathbb{R}^N$$

are linearly independent at every point in U, where $\partial_i = \frac{\partial}{\partial s_i}$ denotes the i-th partial derivative.

(iii) Let $\boldsymbol{x} : \mathbb{R}^M \supset U \to \mathbb{R}^N$ be a net and $\{i_1, \ldots, i_n\} \subset \{1, \ldots, M\}$ some indices. Then the map

$$(s_{i_1}, \ldots, s_{i_n}) \mapsto \boldsymbol{x}(s_1, \ldots, s_M)$$

*for fixed s_j with complementary indices is called an n-*dimensional subnet *of $\boldsymbol{x}$. In particular, 1-dimensional subnets are called* coordinate lines *and 2-dimensional subnets are called* coordinate surfaces*.*

Remark 1.1. Concerning the "smoothness" of a net, we follow the tradition of classical differential geometry assuming that all required partial derivatives exist without explicitly stating. Furthermore, we assume all appearing nets to be regular unless stated otherwise.

Our main object of interest are *orthogonal nets*.

Definition 1.2.

(i) A net $\boldsymbol{x} : \mathbb{R}^M \supset U \to \mathbb{R}^N$ is called orthogonal *if*

$$\langle \partial_i \boldsymbol{x}, \partial_j \boldsymbol{x} \rangle = 0, \qquad i, j = 1, \ldots, M, \ i \neq j. \tag{1.1}$$

(ii) For an orthogonal net $\boldsymbol{x} : \mathbb{R}^M \supset U \to \mathbb{R}^N$, the functions $H_i : U \to \mathbb{R}_+$,

$$H_i^2 = \langle \partial_i \boldsymbol{x}, \partial_i \boldsymbol{x} \rangle, \qquad i = 1, \ldots, M$$

are called its Lamé coefficients*.*

Remark 1.2.

(i) The notion of orthogonal nets is invariant under Möbius transformations of the codomain.

(ii) The metric of an orthogonal net, or its *first fundamental form*, is diagonal and entirely determined by its Lamé coefficients,

$$\mathrm{I} = H_1^2 \mathrm{d}s_1^2 + \ldots + H_M^2 \mathrm{d}s_M^2.$$

Definition 1.3. *A net* $\boldsymbol{x} : \mathbb{R}^M \supset U \to \mathbb{R}^N$ *is called* conjugate *if*

$$\partial_i \partial_j \boldsymbol{x} \wedge \partial_i \boldsymbol{x} \wedge \partial_j \boldsymbol{x} = 0, \qquad i, j = 1, \ldots, \ i \neq j.$$

Remark 1.3.

(i) The condition of being a conjugate net is a condition on every two-dimensional subnet, and invariant under projective transformations.

(ii) Conjugate nets are governed by partial differential equations of the form

$$\partial_i \partial_j \boldsymbol{x} = a_{ji} \partial_i \boldsymbol{x} + a_{ij} \partial_j \boldsymbol{x} \tag{1.2}$$

with functions $a_{ij}, a_{ji} : U \to \mathbb{R}$ satisfying some consistency conditions if $M \geqslant 3$ (see, e.g., [BS]).

The fundamental monograph [Da2] by Darboux is solely devoted to the study of orthogonal coordinate systems ($M = N$) with the main emphasis on *triply orthogonal systems* ($M = N = 3$). A famous theorem by Dupin states that any two coordinate surfaces of a triply orthogonal system $\boldsymbol{x} : \mathbb{R}^3 \supset U \to \mathbb{R}^3$ intersect in a common *curvature line* (cf. Section 2), i.e., $\boldsymbol{x}$ is orthogonal and conjugate. Its generalization to arbitrary dimension takes the following form.

Theorem 1.4 (Dupin)**.** *For* $N \geqslant 3$ *every orthogonal coordinate system* $\boldsymbol{x} : \mathbb{R}^N \supset U \to \mathbb{R}^N$ *is conjugate.*

Proof. For three distinct $i, j, k = 1, \ldots, N$ differentiating (1.1) with respect to s_k leads to

$$\langle \partial_i \boldsymbol{x}, \partial_j \partial_k \boldsymbol{x} \rangle + \langle \partial_j \boldsymbol{x}, \partial_k \partial_i \boldsymbol{x} \rangle = 0.$$

By permutation of the indices, these are three equations which sum up to

$$2 \left(\langle \partial_i \boldsymbol{x}, \partial_j \partial_k \boldsymbol{x} \rangle + \langle \partial_j \boldsymbol{x}, \partial_k \partial_i \boldsymbol{x} \rangle + \langle \partial_k \boldsymbol{x}, \partial_i \partial_j \boldsymbol{x} \rangle \right) = 0.$$

Dividing by 2 and subtracting one of the first three equations again leads to

$$\langle \partial_i \boldsymbol{x}, \partial_j \partial_k \boldsymbol{x} \rangle = 0.$$

Thus, for $j, k = 1, \ldots, N$, $j \neq k$,

$$\partial_j \partial_k \boldsymbol{x} \in \operatorname{span} \{ \partial_i \boldsymbol{x} \mid i = 1, \ldots, N, \ i \neq j, k \}^{\perp} = \operatorname{span} \{ \partial_j \boldsymbol{x}, \partial_k \boldsymbol{x} \},$$

due to the regularity and orthogonality of $\boldsymbol{x}$. $\square$

1.2 Discrete orthogonal nets

In discrete differential geometry, the classical notion of a net is replaced by that of a *discrete net*, which is defined on the *square lattice* $\mathbb{Z}^M$.

Definition 1.5.

(i) A map

$$\boldsymbol{x} : \mathbb{Z}^M \to \mathbb{R}^N, \qquad \boldsymbol{n} = (n_1, \ldots, n_M) \mapsto \boldsymbol{x}(\boldsymbol{n})$$

is called an M-dimensional discrete net.

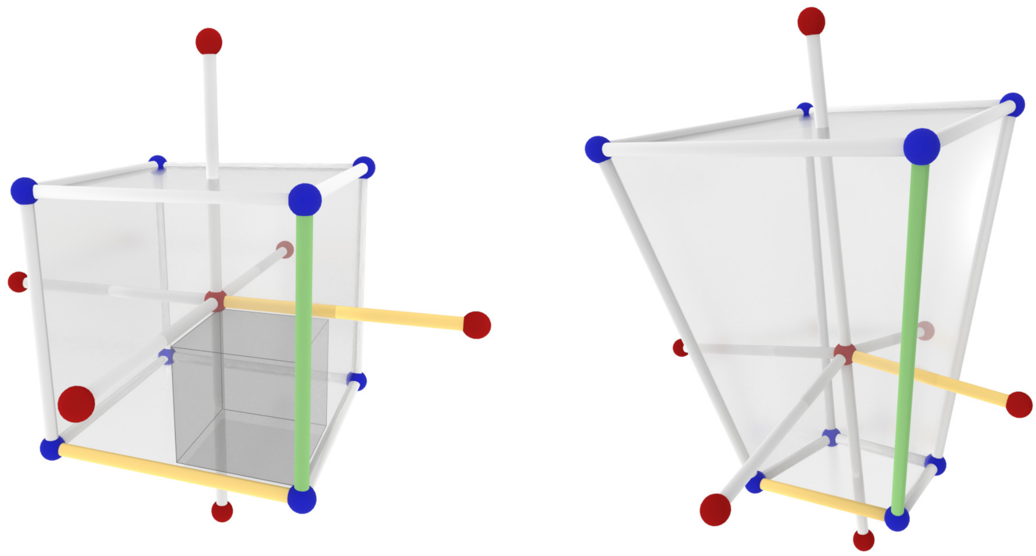

Figure 1.1. *Left:* Elementary cube of the square lattice $\mathbb{Z}^3$ and its dual edges from $\left(\mathbb{Z}+\frac{1}{2}\right)^3$. *Right:* Its image in $\mathbb{R}^3$ such that each pair of dual edges is orthogonal, e.g., the green and its dual yellow edge are orthogonal. The two marked yellow edges contribute to a discrete Lamé coefficient, combinatorially located at the center of the small gray cube.

(ii) *Denote the forward and backward* difference operators*, or* discrete tangent vectors*, by*

$$\Delta_i \boldsymbol{x}(\boldsymbol{n}) = \boldsymbol{x}(\boldsymbol{n}+\boldsymbol{e}_i) - \boldsymbol{x}(\boldsymbol{n}), \qquad \bar{\Delta}_i \boldsymbol{x}(\boldsymbol{n}) = \boldsymbol{x}(\boldsymbol{n}) - \boldsymbol{x}(\boldsymbol{n}-\boldsymbol{e}_i)$$

for any $\boldsymbol{n} \in \mathbb{Z}^M$ and $i = 1,\dots,M$, where $\boldsymbol{e}_i \in \mathbb{Z}^M$ is the unit vector in the i-th coordinate direction. A discrete net $\boldsymbol{x} : \mathbb{Z}^M \to \mathbb{R}^N$ is called regular *if for any $\boldsymbol{n} \in \mathbb{Z}^M$ all choices of M discrete tangent vectors, arbitrarily chosen among $\Delta_i \boldsymbol{x}(\boldsymbol{n})$ and $\bar{\Delta}_i \boldsymbol{x}(\boldsymbol{n})$ for all $i = 1,\dots,M$, are linearly independent.*

(iii) n-dimensional discrete subnets *are defined as for smooth nets (see Definition 1.1).*

Remark 1.4. Note that for now, we assume discrete nets to be defined on the whole lattice $\mathbb{Z}^M$. In some sense, this replaces the openness condition on the domain assuring that, e.g., for every point in the domain all necessary neighbors are contained in the domain as well. Furthermore, as in the smooth case, we assume all appearing discrete nets to be regular unless stated otherwise.

For the purpose of introducing a novel discrete orthogonality condition, instead of using single lattices as our discrete domains, we consider pairs of dual lattices. For the square lattice $\mathbb{Z}^M$ we call $\left(\mathbb{Z}+\frac{1}{2}\right)^M$ its *dual square lattice* (see Figure 1.1, *left*), and say that any two edges

$$[\boldsymbol{n}, \boldsymbol{n}+\boldsymbol{e}_i] \subset \mathbb{Z}^M, \qquad [\boldsymbol{n}+\tfrac{1}{2}\boldsymbol{\sigma}, \boldsymbol{n}+\tfrac{1}{2}\boldsymbol{\sigma}+\boldsymbol{e}_j] \subset \left(\mathbb{Z}+\tfrac{1}{2}\right)^M$$

are *dual edges*, where $\boldsymbol{n} \in \mathbb{Z}^M$ and $\boldsymbol{\sigma} = (\sigma_1,\dots,\sigma_M) \in \{\pm 1\}^M$ with $\sigma_i = 1$ and $\sigma_j = -1$. Furthermore, for a point $\boldsymbol{n} \in \mathbb{Z}^M$, we call the 2^M points $\boldsymbol{n}+\frac{1}{2}\boldsymbol{\sigma} \in \left(\mathbb{Z}+\frac{1}{2}\right)^M$, $\boldsymbol{\sigma} \in \{\pm 1\}^M$, its *adjacent points from the dual lattice.*

Definition 1.6.

(i) *A map*

$$\boldsymbol{x} : \mathbb{Z}^M \cup \left(\mathbb{Z}+\tfrac{1}{2}\right)^M \to \mathbb{R}^N$$

is called a pair of dual discrete nets.

(ii) *A pair of dual discrete nets is called* regular *if the two discrete subnets $\boldsymbol{x}|_{\mathbb{Z}^M}$ and $\boldsymbol{x}|_{\left(\mathbb{Z}+\frac{1}{2}\right)^M}$ are regular.*

For the following, we consider pairs of dual discrete nets (not just each of their two discrete subnets) as discrete analogs of smooth nets, and introduce the following discrete orthogonality condition (see Figure 1.1).

Definition 1.7 (Chapter 1: Definition 6.4, Chapter 2: Definition 4.1)**.**

(i) A pair of dual discrete nets $\boldsymbol{x} : \mathbb{Z}^M \cup \left(\mathbb{Z} + \frac{1}{2}\right)^M \to \mathbb{R}^N$ *is called* orthogonal *if every pair of dual edges is orthogonal in* $\mathbb{R}^N$*, i.e.,*

$$\langle \Delta_i \boldsymbol{x}(\boldsymbol{n}), \Delta_j \boldsymbol{x}(\boldsymbol{n}^*) \rangle = 0, \tag{1.3}$$

for all distinct $i, j = 1, \ldots, M$ *and* $\boldsymbol{n} \in \mathbb{Z}^M$, $\boldsymbol{n}^* = \boldsymbol{n} + \frac{1}{2}\boldsymbol{\sigma} \in \left(\mathbb{Z} + \frac{1}{2}\right)^M$, *where* $\boldsymbol{\sigma} = (\sigma_1, \ldots, \sigma_M) \in \{\pm 1\}^M$ *with* $\sigma_i = 1$ *and* $\sigma_j = -1$.

(ii) For a pair of dual discrete nets $\boldsymbol{x} : \mathbb{Z}^M \cup \left(\mathbb{Z} + \frac{1}{2}\right)^M \to \mathbb{R}^N$ *the* discrete (squared) Lamé coefficients

$$H_i^2 : \left(\mathbb{Z} + \tfrac{1}{4}\right)^M \to \mathbb{R}, \qquad i = 1, \ldots, M$$

are defined by

$$H_i^2(\boldsymbol{n} + \tfrac{1}{4}\boldsymbol{\sigma}) = \begin{cases} \langle \Delta_i \boldsymbol{x}(\boldsymbol{n}), \bar{\Delta}_i \boldsymbol{x}(\boldsymbol{n} + \frac{1}{2}\boldsymbol{\sigma}) \rangle, & \sigma_i = 1 \\ \langle \bar{\Delta}_i \boldsymbol{x}(\boldsymbol{n}), \Delta_i \boldsymbol{x}(\boldsymbol{n} + \frac{1}{2}\boldsymbol{\sigma}) \rangle, & \sigma_i = -1 \end{cases}$$

for all $\boldsymbol{n} \in \mathbb{Z}^M$ *and* $\boldsymbol{\sigma} = (\sigma_1, \ldots, \sigma_M) \in \{\pm 1\}^M$.

Remark 1.5. The discrete orthogonality condition is invariant under similarity transformations. Furthermore, it is invariant under individual translation of each of its two discrete subnets in space.

The standard discretization of conjugate nets is given by discrete nets with planar quadrilaterals.

Definition 1.8. *A discrete net* $\boldsymbol{x} : \mathbb{Z}^M \to \mathbb{R}^N$ *is called* conjugate*, or a* Q-net*, if*

$$\Delta_i \Delta_j \boldsymbol{x} \wedge \Delta_i \boldsymbol{x} \wedge \Delta_j \boldsymbol{x} = 0, \qquad i, j = 1, \ldots, M, \ i \neq j,$$

or equivalently, if all its elementary quadrilaterals $(\boldsymbol{x}(\boldsymbol{n}), \boldsymbol{x}(\boldsymbol{n}+\boldsymbol{e}_i), \boldsymbol{x}(\boldsymbol{n}+\boldsymbol{e}_i+\boldsymbol{e}_j), \boldsymbol{x}(\boldsymbol{n}+\boldsymbol{e}_j))$ *are coplanar.*

With this, we obtain the following discrete version of Theorem 1.4 ("discrete Dupin's theorem").

Theorem 1.9 (Chapter 2: Proposition 4.2)**.** *Let* $N \geqslant 3$ *and* $\boldsymbol{x} : \mathbb{Z}^N \cup \left(\mathbb{Z} + \frac{1}{2}\right)^N \to \mathbb{R}^N$ *be an orthogonal pair of dual discrete nets. Then its two discrete subnets* $\boldsymbol{x}\big|_{\mathbb{Z}^N}$ *and* $\boldsymbol{x}\big|_{\left(\mathbb{Z}+\frac{1}{2}\right)^N}$ *are discrete conjugate nets.*

Remark 1.6. For a discrete conjugate net $\boldsymbol{x} : \mathbb{Z}^M \to \mathbb{R}^N$, $M \leqslant N$, there exists a second conjugate net $\boldsymbol{x}^* : \left(\mathbb{Z} + \frac{1}{2}\right)^M \to \mathbb{R}^N$ such that $\boldsymbol{x}$ and $\boldsymbol{x}^*$ together form an orthogonal pair of dual discrete nets. Thus, from the point of view of a single discrete conjugate net, the discrete orthogonality is not a constraint. Only if we consider pairs of dual discrete nets as discretizations of *one* smooth net does the discrete orthogonality become an actual further constraint.

1.3 Discrete Möbius invariance

The discrete orthogonality constraint is not invariant under mapping each point of an orthogonal pair of dual discrete nets by a Möbius transformation (cf. Remark 2.7). Nevertheless, one can replace the points of the pair of nets by orthogonal spheres to obtain a Möbius invariant description.

Definition 1.10. *Let* $\mathcal{S}$ *be the space of (hyper)spheres in* $\mathbb{R}^N$*. We call a map* $S : \mathbb{Z}^M \cup \left(\mathbb{Z} + \frac{1}{2}\right)^M \to \mathcal{S}$ *an* orthogonal pair of sphere congruences *if each two adjacent spheres from the dual lattices* $S(\boldsymbol{n})$ *and* $S(\boldsymbol{n} + \frac{1}{2}\boldsymbol{\sigma})$, $\boldsymbol{n} \in \mathbb{Z}^M, \boldsymbol{\sigma} \in \{\pm 1\}^M$*, are orthogonal (see Figure 1.2, (left)).*

Orthogonal pairs of sphere congruences are Möbius invariant. Furthermore, given a pair of dual discrete nets $\boldsymbol{x} : \mathbb{Z}^M \cup \left(\mathbb{Z} + \frac{1}{2}\right)^M \to \mathbb{R}^N$ we can construct orthogonal spheres with centers at the points of $\boldsymbol{x}$: Choosing the radius for one sphere at $\boldsymbol{n} \in \mathbb{Z}^M$, the radii of all spheres at adjacent vertices $\boldsymbol{n}^* \in \left(\mathbb{Z} + \frac{1}{2}\right)^M$ of the dual lattice are uniquely determined by the orthogonality condition. Can this be propagated throughout the whole pair of dual lattices $\mathbb{Z}^M \cup \left(\mathbb{Z} + \frac{1}{2}\right)^M$ without contradiction?

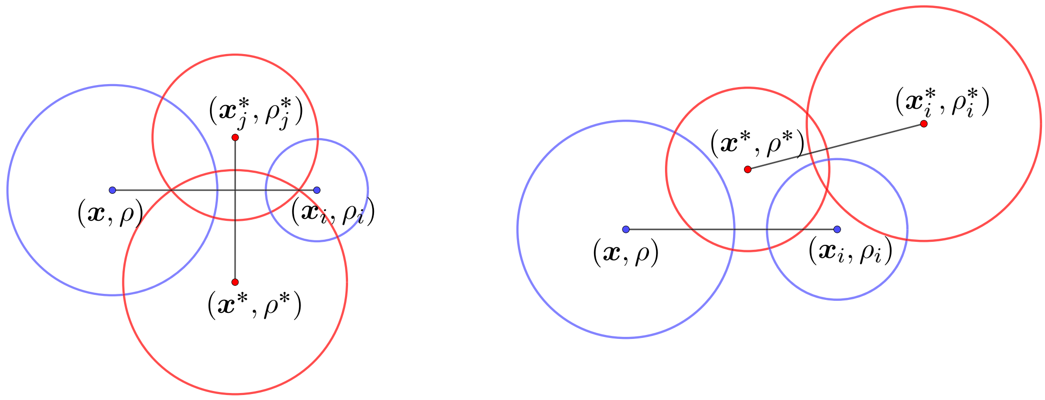

Figure 1.2. *Left:* Two dual edges from an orthogonal pair of sphere congruences. *Right:* Two "parallel" edges from an orthogonal pair of sphere congruences.

Lemma 1.11. *Two spheres in $\mathbb{R}^N$ with centers $\boldsymbol{x}$, $\boldsymbol{x}^*$ and radii r, r^*, respectively, are orthogonal if and only if*

$$\langle \boldsymbol{x}, \boldsymbol{x}^* \rangle = \rho + \rho^*,$$

where

$$\rho = \frac{1}{2}\left(|\boldsymbol{x}|^2 - r^2\right), \qquad \rho^* = \frac{1}{2}\left(|\boldsymbol{x}^*|^2 - (r^*)^2\right).$$

Proof. The orthogonality condition of the two spheres is equivalent to

$$|\boldsymbol{x} - \boldsymbol{x}^*|^2 = r^2 + (r^*)^2 \;\Leftrightarrow\; 2\langle \boldsymbol{x}, \boldsymbol{x}^* \rangle = |\boldsymbol{x}|^2 - r^2 + |\boldsymbol{x}^*|^2 - (r^*)^2.$$

$\square$

Proposition 1.12. *Let $\boldsymbol{x} : \mathbb{Z}^M \cup \left(\mathbb{Z} + \frac{1}{2}\right)^M \to \mathbb{R}^N$ be a pair of dual discrete nets. Then there exists a one-parameter family of orthogonal pairs of sphere congruences with centers in the points of $\boldsymbol{x}$ if and only if the pair of discrete nets $\boldsymbol{x}$ is orthogonal.*

Moreover, let $S : \mathbb{Z}^M \cup \left(\mathbb{Z} + \frac{1}{2}\right)^M \to \mathcal{S}$ be an orthogonal pair of sphere congruences. Then the pair of dual discrete nets $\boldsymbol{x} : \mathbb{Z}^M \cup \left(\mathbb{Z} + \frac{1}{2}\right)^M \to \mathbb{R}^N$ given by the centers of S is orthogonal.

Proof. Consider a pair of dual edges of the net $\boldsymbol{x}$, and denote the involved vertices such that $\Delta_i \boldsymbol{x}(\boldsymbol{n}) = \boldsymbol{x}_i - \boldsymbol{x}$ and $\Delta_j \boldsymbol{x}(\boldsymbol{n}^*) = \boldsymbol{x}_j^* - \boldsymbol{x}^*$ (see Figure 1.2 (*left*)). Assume that the radius r at $\boldsymbol{x}$ is given by $\rho = \frac{1}{2}\left(|\boldsymbol{x}|^2 - r^2\right)$. Then the two radii at $\boldsymbol{x}^*$ and $\boldsymbol{x}_j^*$ are given by

$$\rho^* = \langle \boldsymbol{x}, \boldsymbol{x}^* \rangle - \rho, \qquad \rho_j^* = \langle \boldsymbol{x}, \boldsymbol{x}_j^* \rangle - \rho.$$

Now the radius at $\boldsymbol{x}_i$ may be obtained in two ways

$$\begin{aligned} \rho_i &= \langle \boldsymbol{x}_i, \boldsymbol{x}^* \rangle - \rho^* = \langle \boldsymbol{x}_i, \boldsymbol{x}^* \rangle - \langle \boldsymbol{x}, \boldsymbol{x}^* \rangle + \rho, \\ \tilde{\rho}_i &= \langle \boldsymbol{x}_i, \boldsymbol{x}_j^* \rangle - \rho_j^* = \langle \boldsymbol{x}_i, \boldsymbol{x}_j^* \rangle - \langle \boldsymbol{x}, \boldsymbol{x}_j^* \rangle + \rho. \end{aligned}$$

Thus,

$$\rho_i = \tilde{\rho}_i \;\Leftrightarrow\; \langle \boldsymbol{x}_i - \boldsymbol{x}, \boldsymbol{x}_j^* - \boldsymbol{x}^* \rangle,$$

which is the orthogonality of the two dual edges. $\square$

Now an orthogonal pair of dual discrete nets $\boldsymbol{x} : \mathbb{Z}^M \cup \left(\mathbb{Z}^M\right)^* \to \mathbb{R}^N$ may be transformed in the following way:

- Choose an orthogonal pair of sphere congruences $S : \mathbb{Z}^M \cup (\mathbb{Z}^M)^* \to \mathcal{S}$ with centers in $\boldsymbol{x}$.
- Transform S under a Möbius transformation to obtain $\tilde{S}$.
- Take the centers $\tilde{\boldsymbol{x}}$ of the transformed pair of sphere congruences $\tilde{S}$.

Lemma 1.13. *Let $S : \mathbb{Z}^M \cup \left(\mathbb{Z} + \frac{1}{2}\right)^M \to \mathcal{S}$ be an orthogonal pair of sphere congruences with centers $\boldsymbol{x}$, radii r, and $\rho = \frac{1}{2}\left(|\boldsymbol{x}|^2 - r^2\right)$. Then the corresponding quantities of the image of S under inversion in the unit sphere centered at the origin are given by*

$$\tilde{\boldsymbol{x}} = \frac{\boldsymbol{x}}{2\rho}, \qquad \tilde{r} = \frac{r}{|\boldsymbol{x}|^2 - r^2}, \qquad \tilde{\rho} = \frac{1}{4\rho}.$$

Proof. This reduces to a one-dimensional problem on the line through the origin and the center of each sphere.

$$\begin{aligned}
\tilde{\boldsymbol{x}} &= \frac{1}{2}\left(\frac{1}{\boldsymbol{x} - r} + \frac{1}{\boldsymbol{x} + r}\right) = \frac{\boldsymbol{x}}{|\boldsymbol{x}|^2 - r^2} = \frac{\boldsymbol{x}}{2\rho}, \\
\tilde{r} &= \frac{1}{2}\left(\frac{1}{\boldsymbol{x} - r} - \frac{1}{\boldsymbol{x} + r}\right) = \frac{r}{|\boldsymbol{x}|^2 - r^2} = \frac{r}{2\rho}, \\
\tilde{\rho} &= \frac{1}{2}(|\tilde{\boldsymbol{x}}|^2 - \tilde{r}^2) = \frac{1}{2}\left(\frac{|\boldsymbol{x}|^2}{4\rho^2} - \frac{r^2}{4\rho^2}\right) = \frac{1}{4\rho}.
\end{aligned}$$

□

Lemma 1.14. *Let $S : \mathbb{Z}^M \cup \left(\mathbb{Z} + \frac{1}{2}\right)^M \to \mathcal{S}$ be an orthogonal pair of sphere congruences.*

(i) The discrete Lamé coefficients of the orthogonal pair of dual discrete nets of centers $\boldsymbol{x}$ are given by

$$H_i^2(\boldsymbol{n} + \tfrac{1}{4}\boldsymbol{\sigma}) = \begin{cases} \rho(\boldsymbol{n} + e_i) + \rho(\boldsymbol{n} + \frac{1}{2}\boldsymbol{\sigma} - e_i) - \langle \boldsymbol{x}(\boldsymbol{n} + \boldsymbol{e}_i), \boldsymbol{x}(\boldsymbol{n} + \frac{1}{2}\boldsymbol{\sigma} - \boldsymbol{e}_i)\rangle, & \sigma_i = 1 \\ \rho(\boldsymbol{n} - e_i) + \rho(\boldsymbol{n} + \frac{1}{2}\boldsymbol{\sigma} + \boldsymbol{e}_i) - \langle \boldsymbol{x}(\boldsymbol{n} - \boldsymbol{e}_i), \boldsymbol{x}(\boldsymbol{n} + \frac{1}{2}\boldsymbol{\sigma} + \boldsymbol{e}_i)\rangle, & \sigma_i = -1 \end{cases}$$

for $i = 1, \ldots, M$, $\boldsymbol{n} \in \mathbb{Z}^M$, $\boldsymbol{\sigma} \in \{\pm 1\}^M$.

(ii) The discrete Lamé coefficients transform under inversion in the unit sphere centered at the origin by

$$\tilde{H}_i^2(\boldsymbol{n} + \tfrac{1}{4}\boldsymbol{\sigma}) = \begin{cases} \frac{1}{4\rho(\boldsymbol{n}+e_i)\rho(\boldsymbol{n}+1/2\boldsymbol{\sigma}-\boldsymbol{e}_i)} H_i^2(\boldsymbol{n} + \frac{1}{4}\boldsymbol{\sigma}) & \sigma_i = 1 \\ \frac{1}{4\rho(\boldsymbol{n}-e_i)\rho(\boldsymbol{n}+1/2\boldsymbol{\sigma}+\boldsymbol{e}_i)} H_i^2(\boldsymbol{n} + \frac{1}{4}\boldsymbol{\sigma}) & \sigma_i = -1 \end{cases}$$

for $i = 1, \ldots, M$, $\boldsymbol{n} \in \mathbb{Z}^M$, $\boldsymbol{\sigma} \in \{\pm 1\}^M$.

Proof. Let $\boldsymbol{\sigma} \in \{\pm 1\}^M$ with $\sigma_i = 1$. Denote the involved centers such that $\bar{\Delta}_i \boldsymbol{x}(\boldsymbol{n}) = \boldsymbol{x}_i - \boldsymbol{x}$ and $\Delta_i \boldsymbol{x}(\boldsymbol{n} + \frac{1}{2}\boldsymbol{\sigma}) = \boldsymbol{x}_i^* - \boldsymbol{x}^*$ (see Figure 1.13 (*right*)).

(i) Then the discrete Lamé coefficients at $\boldsymbol{n} + \frac{1}{4}\boldsymbol{\sigma}$ are given by

$$\begin{aligned}
H_i^2(\boldsymbol{n} + \tfrac{1}{4}\boldsymbol{\sigma}) &= \langle \Delta_i \boldsymbol{x}(\boldsymbol{n}), \bar{\Delta}_i \boldsymbol{x}(\boldsymbol{n} + \tfrac{1}{2}\boldsymbol{\sigma})\rangle \\
&= \langle \boldsymbol{x}, \boldsymbol{x}^*\rangle - \langle \boldsymbol{x}^*, \boldsymbol{x}_i\rangle + \langle \boldsymbol{x}_i, \boldsymbol{x}_i^*\rangle - \langle \boldsymbol{x}_i^*, \boldsymbol{x}\rangle \\
&= \rho + \rho^* - \rho^* - \rho_i + \rho_i + \rho_+^* - \langle \boldsymbol{x}_i^*, \boldsymbol{x}\rangle \\
&= \rho + \rho_i^* - \langle \boldsymbol{x}_i^*, \boldsymbol{x}\rangle.
\end{aligned}$$

(ii) By Lemma 1.13 the discrete Lamé coefficients transform by

$$\tilde{H}_i^2 = \frac{1}{4\rho} + \frac{1}{4\rho_i^*} - \langle \frac{\boldsymbol{x}}{4\rho}, \frac{\boldsymbol{x}_i^*}{4\rho_i^*}\rangle = \frac{1}{4\rho\rho_i^*}\left(\rho + \rho_i^* - \langle \boldsymbol{x}_i^*, \boldsymbol{x}\rangle\right) = \frac{1}{4\rho\rho_i^*} H_i^2.$$

□

2 Curvature lines, focal nets, and parallel nets

2.1 Classical curvature line parametrizations

Let $\boldsymbol{x} : \mathbb{R}^2 \supset U \to \mathbb{R}^3$ be a net, i.e., a (regular) parametrization of a surface in $\mathbb{R}^3$. We denote its *unit normal field* by

$$\boldsymbol{\nu}(s_1, s_2) = \frac{\partial_1 \boldsymbol{x} \times \partial_2 \boldsymbol{x}}{|\partial_1 \boldsymbol{x} \times \partial_2 \boldsymbol{x}|}, \qquad (s_1, s_2) \in U,$$

its *first fundamental form* by

$$\mathrm{I} = E\,\mathrm{d}s_1^2 + 2F\,\mathrm{d}s_1\mathrm{d}s_2 + G\,\mathrm{d}s_2^2$$

where $E = \langle \partial_1 \boldsymbol{x}, \partial_1 \boldsymbol{x} \rangle$, $F = \langle \partial_1 \boldsymbol{x}, \partial_2 \boldsymbol{x} \rangle$, $G = \langle \partial_2 \boldsymbol{x}, \partial_2 \boldsymbol{x} \rangle$, and its *second fundamental form* by

$$\mathrm{II} = e\,\mathrm{d}s_1^2 + 2f\,\mathrm{d}s_1\mathrm{d}s_2 + g\,\mathrm{d}s_2^2$$

where $e = \langle \partial_1 \boldsymbol{\nu}, \partial_1 \boldsymbol{x} \rangle$, $f = \langle \partial_1 \boldsymbol{\nu}, \partial_2 \boldsymbol{x} \rangle = \langle \partial_2 \boldsymbol{\nu}, \partial_1 \boldsymbol{x} \rangle$, $g = \langle \partial_2 \boldsymbol{\nu}, \partial_2 \boldsymbol{x} \rangle$.

Remark 2.1. For an orthogonally parametrized surface, i.e., $G = 0$, its Lamé coefficients are given by $H_1^2 = E$ and $H_2^2 = G$.

Locally, and away from umbilic points, every surface in $\mathbb{R}^3$ has a unique *curvature line parametrization*, i.e., a parametrization along *principal directions*. We denote by $\kappa_1, \kappa_2 : U \to \mathbb{R}$ the corresponding *principal curvatures* and for the following of this section we assume that the net $\boldsymbol{x}$ has no umbilic and no parabolic points, i.e., $\kappa_1 \neq \kappa_2$ and $\kappa_1\kappa_2 \neq 0$ at every point of U.

Proposition 2.1. *A net $\boldsymbol{x} : \mathbb{R}^2 \supset U \to \mathbb{R}^3$ is a* curvature line parametrization *if and only if one of the following two equivalent conditions is satisfied:*

(i) The first and second fundamental form are diagonal, i.e., $F = f = 0$.

(ii) The net $\boldsymbol{x}$ is orthogonal and conjugate.

Remark 2.2.

(i) The property of being a curvature line parametrization is Möbius invariant.

(ii) A parametrized surface is a two-parameter family of points in $\mathbb{R}^3$. Alternatively, it can be described as the envelope of a two-parameter family of (oriented) planes, namely its tangent planes. For a regular non-developable surface these two descriptions are equivalent. Yet the characterization of a curvature line parametrization in terms of its tangent planes is invariant under Laguerre transformations.

Focal nets

The normal direction $\boldsymbol{\nu}$ defines a line

$$\lambda \mapsto \boldsymbol{x}(s_1, s_2) + \lambda \boldsymbol{\nu}(s_1, s_2), \qquad \lambda \in \mathbb{R}$$

at every point $(s_1, s_2) \in U$, together constituting the *normal congruence* of the net $\boldsymbol{x}$.

Proposition 2.2. *Let $\boldsymbol{x} : \mathbb{R}^2 \supset U \to \mathbb{R}^3$ be a conjugate net. Then $\boldsymbol{x}$ is orthogonal, i.e., a curvature line parametrization, if and only if one of the following two equivalent conditions is satisfied:*

(i) $\boldsymbol{\nu} \wedge \partial_1 \boldsymbol{\nu} \wedge \partial_1 \boldsymbol{x} = 0$ and $\boldsymbol{\nu} \wedge \partial_2 \boldsymbol{\nu} \wedge \partial_2 \boldsymbol{x} = 0$.

(ii) The two families of ruled surfaces contained in the normal congruence along the coordinate lines of $\boldsymbol{x}$

$$(s_i, \lambda) \mapsto \boldsymbol{x}(s_1, s_2) + \lambda \boldsymbol{\nu}(s_1, s_2), \qquad i = 1, 2, \tag{2.1}$$

are developable.

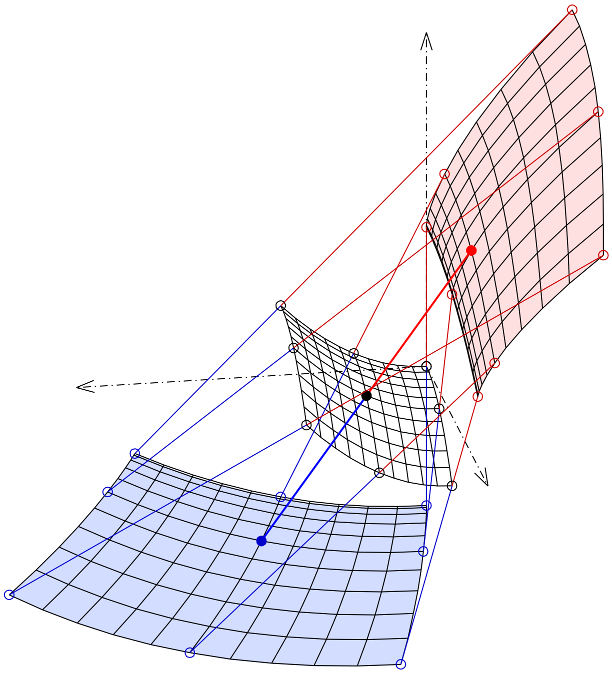

Figure 2.1. A curvature line parametrized surface (white) and its two focal nets (red and blue). [Image by Ag2gaeh, CC BY-SA 4.0]

Intuitively the condition in Proposition 2.2 means that infinitesimally close normal lines along the principal directions intersect. Along a curvature line the points of intersection are given by the centers of the osculating circles, which have radii $\frac{1}{\kappa_i}$, $i = 1, 2$, and together form the line of striction of the developable surface (2.1). For each principal direction these lines of striction constitute one of the two *focal nets* of $\boldsymbol{x}$ (see Figure 2.1),

$$\boldsymbol{f}_i : U \to \mathbb{R}^3, \qquad (s_1, s_2) \mapsto \boldsymbol{x}(s_1, s_2) + \frac{1}{\kappa_i(s_1, s_2)} \boldsymbol{\nu}(s_1, s_2), \qquad i = 1, 2. \tag{2.2}$$

Remark 2.3. The focal net $\boldsymbol{f}_i$ is regular at each point $(s_1, s_2) \in U$ with $\partial_i \kappa_i(s_1, s_2) \neq 0$. Furthermore,

$$\partial_i \kappa_i(s_1, s_2) = 0 \;\Leftrightarrow\; \partial_i \boldsymbol{f}_i(s_1, s_2) = 0.$$

Proposition 2.3. *The two focal nets* (2.2) *are conjugate nets.*

Remark 2.4. The envelope of a one-parameter family of spheres in $\mathbb{R}^3$ is called a *channel surface*. The curvature lines in one direction of a channel surface are circles, and thus one of its focal nets degenerates to a curve, i.e., $\partial_i \boldsymbol{f}_i = 0$ for one $i = 1, 2$ (cf. Remark 2.3). In fact, this property characterizes channel surfaces. A *Dupin cyclide* is a channel surface in both directions, i.e., the envelope of two distinct one-parameter families of spheres, and therefore characterized by the condition that both of its focal nets degenerate to curves.

Parallel nets

A *parallel surface* is a surface of constant offset in normal direction to a given surface. It is a special case of a *Combescure transform*, i.e., corresponding tangent planes are parallel. A net $\boldsymbol{x} : \mathbb{R}^2 \supset U \to \mathbb{R}^3$ can be extended to a three-dimensional net by a family of parallel nets, given by

$$\tilde{\boldsymbol{x}} : U \times I \to \mathbb{R}^3, \qquad (s_1, s_2, s_3) \mapsto \boldsymbol{x}(s_1, s_2) + \rho(s_3)\boldsymbol{\nu}(s_1, s_2), \tag{2.3}$$

with some smooth function $\rho : I \to \mathbb{R}$ on an open interval $I \subset \mathbb{R}$. Away from the focal points, which in the case of a curvature line parametrization are given by (2.2), the three-dimensional net of parallel surfaces

$\tilde{\boldsymbol{x}}$ is regular. By Dupin's Theorem (cf. Theorem 1.4) a two-dimensional net can be a subnet of a three-dimensional orthogonal net, i.e., a triply orthogonal system, only if it is a curvature line parametrization. Yet every curvature line parametrization can be extended to a triply orthogonal system by its parallel nets.

Proposition 2.4. *Let $\boldsymbol{x} : \mathbb{R}^2 \supset U \to \mathbb{R}^3$ be an orthogonal conjugate net, i.e., a curvature line parametrization. Then the three-dimensional net of parallel surfaces $\tilde{\boldsymbol{x}}$ given by* (2.3) *is orthogonal with the third Lamé coefficient given by $H_3^2 = (\rho')^2$, which only depends on s_3.*

Remark 2.5. In particular, this implies that curvature line parametrizations are Möbius invariant (cf. Remark 2.2). Indeed, by Proposition 2.4, a curvature line parametrization $\boldsymbol{x} : \mathbb{R}^2 \supset U \to \mathbb{R}^3$ can be extended to a triply orthogonal systems $\tilde{\boldsymbol{x}}$. Application of a Möbius transformation maps $\tilde{\boldsymbol{x}}$ to a triply orthogonal system and thus, by Theorem 1.4 and Proposition 2.1, it maps $\boldsymbol{x}$ to a curvature line parametrization.

2.2 Discrete curvature line parametrizations

Two well-established discretizations of curvature line parametrizations are given by *circular nets* and *conical nets.*

Definition 2.5. *Let $\boldsymbol{x} : \mathbb{Z}^2 \to \mathbb{R}^3$ be a discrete conjugate net.*

(i) The net $\boldsymbol{x}$ is called a circular net *if all its elementary quadrilaterals are circular, i.e., each four points $(\boldsymbol{x}(\boldsymbol{n}), \boldsymbol{x}(\boldsymbol{n}+\boldsymbol{e}_i), \boldsymbol{x}(\boldsymbol{n}+\boldsymbol{e}_i+\boldsymbol{e}_j), \boldsymbol{x}(\boldsymbol{n}+\boldsymbol{e}_j))$ lie on a circle.*

(ii) The net $\boldsymbol{x}$ is called a conical net *if all four planes corresponding to any elementary quadrilateral containing a common vertex touch a common cone.*

Remark 2.6.

(i) The notion of circular nets is invariant under Möbius transformations.

(ii) Conical nets are more naturally described as maps from the dual lattice into the set of (oriented) planes of $\mathbb{R}^3$. Thus, they correspond to the description of a net in terms of its tangent planes (cf. Remark 2.2 (ii)). The notion of conical nets is invariant under Laguerre transformations.

As described in [PW] circular nets and conical nets are intimately related. Given a circular net there exists a canonical three-parameter family of corresponding conical nets:

- Let $\boldsymbol{x} : \mathbb{Z}^2 \to \mathbb{R}^3$ be a circular net.
- Associate to each edge $[\boldsymbol{n}, \boldsymbol{n}+\boldsymbol{e}_i]$ of $\mathbb{Z}^2$ the length bisecting plane of the segment $[\boldsymbol{x}(\boldsymbol{n}), \boldsymbol{x}(\boldsymbol{n}+\boldsymbol{e}_i)]$.
- Choose a plane at some $\boldsymbol{n} \in \mathbb{Z}^2$ and reflect it in all bisecting planes.

This process is well-defined on $\mathbb{Z}^2$ in the sense that it closes along every cycle. Every four planes associated to an elementary quadrilateral of $\mathbb{Z}^2$ intersect in a point, constituting an *associated conical net* $\boldsymbol{x}^* : (\mathbb{Z} + \frac{1}{2})^2 \to \mathbb{R}^3$ on the dual lattice.

Vice versa, given a conical net there exists a canonical three-parameter family of corresponding circular nets:

- Let $\boldsymbol{x} : \left(\mathbb{Z}^2 + \frac{1}{2}\right)^2 \to \mathbb{R}^3$ be a conical net.
- Associate to each edge $[\boldsymbol{n}^*, \boldsymbol{n}^* + \boldsymbol{e}_i]$ of $\left(\mathbb{Z} + \frac{1}{2}\right)^2$ the angle bisecting plane of the two adjacent face planes.
- Choose a point at some $\boldsymbol{n} \in \mathbb{Z}^2$ and reflect it in all bisecting planes.

This process is well-defined on $\mathbb{Z}^2$ and constitutes an *associated circular net* $\boldsymbol{x} : \mathbb{Z}^2 \to \mathbb{R}^3$ on the dual lattice.

We call two nets $\boldsymbol{x} : \mathbb{Z}^2 \to \mathbb{R}^3$ and $\boldsymbol{x}^* : (\mathbb{Z} + \frac{1}{2})^2 \to \mathbb{R}^3$ obtained by either of the previously described procedures a *pair of associated circular and conical nets.*

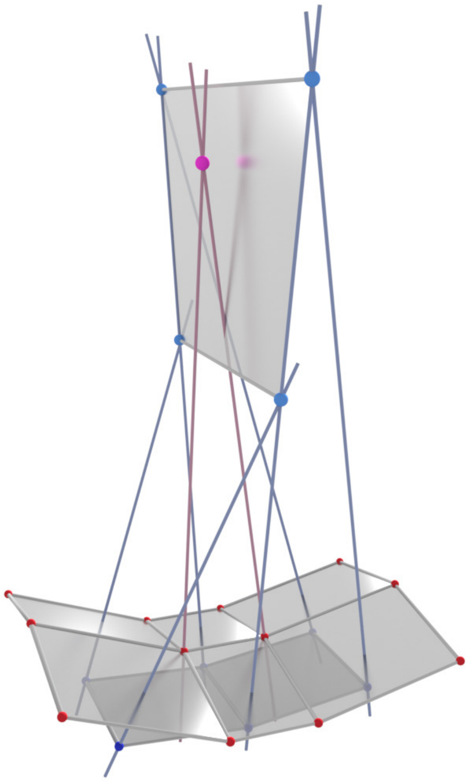

Figure 2.2. Patch of an orthogonal pair of dual discrete conjugate nets, its normal congruence, and one quadrilateral of one of its two focal nets.

Proposition 2.6. *A pair of associated circular and conical nets constitutes an orthogonal pair of dual discrete nets (in the sense of Definition 1.7).*

Proof. Consider one of the bisecting planes Π. A plane and its reflection in Π intersect in Π. On the other hand, the line through a point and its reflection in Π is orthogonal to Π. □

Thus, orthogonal pairs of dual discrete conjugate nets are generalizations of pairs of associated circular and conical nets, and we view them as *discrete curvature line parametrizations.*

Remark 2.7. While circular nets are invariant under Möbius transformations and conical nets are invariant under Laguerre transformations, the associated pairs of such nets are invariant under the intersection of these transformation groups, i.e., similarity transformations. Similarly, general orthogonal pairs of dual discrete nets are invariant under similarity transformations, but not under general Möbius or Laguerre transformations (though cf. Section 1.3).

Discrete focal nets

For a pair of dual discrete conjugate nets $\boldsymbol{x} : \mathbb{Z}^2 \cup \left(\mathbb{Z} + \frac{1}{2}\right)^2 \to \mathbb{R}^3$ we associate to every vertex $\boldsymbol{n} \in \mathbb{Z}^2 \cup \left(\mathbb{Z} + \frac{1}{2}\right)^2$ the unit normal vector of the corresponding dual face plane, i.e.,

$$\boldsymbol{\nu}(\boldsymbol{n}) = \frac{\Delta_1 \boldsymbol{x}(\boldsymbol{n}^*) \times \Delta_2 \boldsymbol{x}(\boldsymbol{n}^*)}{|\Delta_1 \boldsymbol{x}(\boldsymbol{n}^*) \times \Delta_2 \boldsymbol{x}(\boldsymbol{n}^*)|},$$

where $\boldsymbol{n}^* = \boldsymbol{n} - \left(\frac{1}{2}, \frac{1}{2}\right)$. The corresponding normal lines

$$\ell(\boldsymbol{n}) : \lambda \mapsto \boldsymbol{x}(\boldsymbol{n}) + \lambda \boldsymbol{\nu}(\boldsymbol{n}), \qquad \lambda \in \mathbb{R}.$$

together constitute the *discrete normal congruence* of the pair of discrete nets $\boldsymbol{x}$, for which we immediately obtain a discrete version of Proposition 2.2.

Proposition 2.7. *Let $\boldsymbol{x} : \mathbb{Z}^2 \cup \left(\mathbb{Z} + \frac{1}{2}\right)^2 \to \mathbb{R}^3$ be a pair of dual discrete conjugate nets. Then $\boldsymbol{x}$ is orthogonal, i.e., a discrete curvature line parametrization, if and only if one of the following two equivalent conditions is satisfied:*

(i) $\boldsymbol{\nu} \wedge \Delta_1 \boldsymbol{\nu} \wedge \Delta_1 \boldsymbol{x} = 0$ *and* $\boldsymbol{\nu} \wedge \Delta_2 \boldsymbol{\nu} \wedge \Delta_2 \boldsymbol{x} = 0$

(ii) Any two adjacent normals $\ell(\boldsymbol{n})$ and $\ell(\boldsymbol{n} + \boldsymbol{e}_i)$, $i = 1, 2$, intersect (see Figure 2.2).

Proof. Let $\boldsymbol{n} \in \mathbb{Z}^2 \cup \left(\mathbb{Z} + \frac{1}{2}\right)^2$ and $\boldsymbol{n}^* = \boldsymbol{n} + \left(\frac{1}{2}, -\frac{1}{2}\right)$ so that $\Delta_1 \boldsymbol{x}(\boldsymbol{n})$ and $\Delta_2 \boldsymbol{x}(\boldsymbol{n}^*)$ are dual edges and therefore

$$\boldsymbol{\nu}(\boldsymbol{n}), \boldsymbol{\nu}(\boldsymbol{n} + \boldsymbol{e}_1) \perp \Delta_2 \boldsymbol{x}(\boldsymbol{n}^*).$$

Thus, under the assumption $\boldsymbol{\nu}(\boldsymbol{n}) \neq \boldsymbol{\nu}(\boldsymbol{n} + \boldsymbol{e}_1)$, we obtain

$$(\boldsymbol{\nu} \wedge \Delta_1 \boldsymbol{\nu} \wedge \Delta_1 \boldsymbol{x})(\boldsymbol{n}) = \boldsymbol{\nu}(\boldsymbol{n}) \wedge \boldsymbol{\nu}(\boldsymbol{n} + \boldsymbol{e}_1) \wedge \Delta_1 \boldsymbol{x}(\boldsymbol{n}) = 0 \;\Leftrightarrow\; \Delta_1 \boldsymbol{x}(\boldsymbol{n}) \perp \Delta_2 \boldsymbol{x}(\boldsymbol{n}^*).$$

□

Remark 2.8. Condition (ii) of Proposition 2.7 may be interpreted in the sense that the two families of "discrete ruled surfaces" contained in the discrete normal congruence along the coordinate lines of $\boldsymbol{x}$ are "discrete developable surfaces".

For an orthogonal pair of dual discrete conjugate nets $\boldsymbol{x} : \mathbb{Z}^2 \cup \left(\mathbb{Z} + \frac{1}{2}\right)^2 \to \mathbb{R}^3$ we define their *discrete focal nets* $\boldsymbol{f}_i$, $i = 1, 2$, by the points of intersection of neighboring normal lines (see Figure 2.2)

$$\boldsymbol{f}_i : \boldsymbol{n} \mapsto \ell(\boldsymbol{n}) \cap \ell(\boldsymbol{n} + \boldsymbol{e}_i). \tag{2.4}$$

Proposition 2.8. *The two discrete focal nets* (2.4) *are discrete conjugate nets.*

Proof. The two points $\boldsymbol{f}_i(\boldsymbol{n})$ and $\boldsymbol{f}_i(\boldsymbol{n} + \boldsymbol{e}_i)$ lie on the line $\ell(\boldsymbol{n} + \boldsymbol{e}_i)$, while the two points $\boldsymbol{f}_i(\boldsymbol{n} + \boldsymbol{e}_j)$ and $\boldsymbol{f}_i(\boldsymbol{n} + \boldsymbol{e}_i + \boldsymbol{e}_j)$ lie on the line $\ell(\boldsymbol{n} + \boldsymbol{e}_i + \boldsymbol{e}_j)$. By Proposition 2.7 these two lines intersect. □

Furthermore, comparing with Remark 2.4, we obtain natural definitions for *discrete channel surfaces* and *discrete Dupin cyclides*, whose properties are studied in a forthcoming publication.

Definition 2.9. *Let $\boldsymbol{x} : \mathbb{Z}^2 \cup \left(\mathbb{Z} + \frac{1}{2}\right)^2 \to \mathbb{R}^3$ be a discrete curvature line parametrization.*

(i) Then $\boldsymbol{x}$ is called a discrete channel surface *if one of its discrete focal nets degenerates to a curve, i.e., $\Delta_i \boldsymbol{f}_i = 0$ for one $i = 1, 2$.*

(ii) It is called a discrete Dupin cyclide *if both of its discrete focal nets degenerate to curves, i.e., $\Delta_i \boldsymbol{f}_i = 0$ for both $i = 1, 2$.*

Discrete parallel nets

For an orthogonal pair of dual discrete conjugate nets $\boldsymbol{x} : \mathbb{Z}^2 \cup \left(\mathbb{Z} + \frac{1}{2}\right)^2 \to \mathbb{R}^3$, a one-parameter family of *discrete parallel surfaces* is defined by (see Figure 2.3)

$$\tilde{\boldsymbol{x}} : \mathbb{Z}^3 \cup \left(\mathbb{Z} + \tfrac{1}{2}\right)^3 \to \mathbb{R}^3, \qquad (n_1, n_2, n_3) \mapsto \boldsymbol{x}(n_1, n_2) + \rho(n_1, n_2, n_3)\boldsymbol{\nu}(n_1, n_2), \tag{2.5}$$

where $\rho : \mathbb{Z}^2 \cup \left(\mathbb{Z} + \frac{1}{2}\right)^3 \to \mathbb{R}$ is chosen such that for $i = 1, 2$ the edges $\Delta_i \boldsymbol{x}(n_1, n_2, n_3)$ are parallel for all values of n_3. This is always possible due to the fact that neighboring normal lines of $\boldsymbol{x}$ intersect (see, e.g., [BS]). Thus, the function ρ may only be chosen at one point for each layer $n_3 = const.$, and each two coordinate surfaces $\tilde{\boldsymbol{x}}(n_1, n_2, n_3 = const.)$ are *discrete Combescure transforms* of each other, i.e., they are discrete conjugate nets with parallel faces.

Similar to the smooth case, $\boldsymbol{x}$ can be extended to a discrete triply orthogonal system by its parallel surfaces.

Proposition 2.10. *Let $\boldsymbol{x} : \mathbb{Z}^2 \cup \left(\mathbb{Z} + \frac{1}{2}\right)^2 \to \mathbb{R}^3$ be an orthogonal pair of dual discrete conjugate nets. Then the pair of discrete three-dimensional nets of parallel surfaces $\tilde{\boldsymbol{x}}$ given by* (2.5) *is orthogonal with the third discrete Lamé coefficient H_3^2 only depending on n_3.*

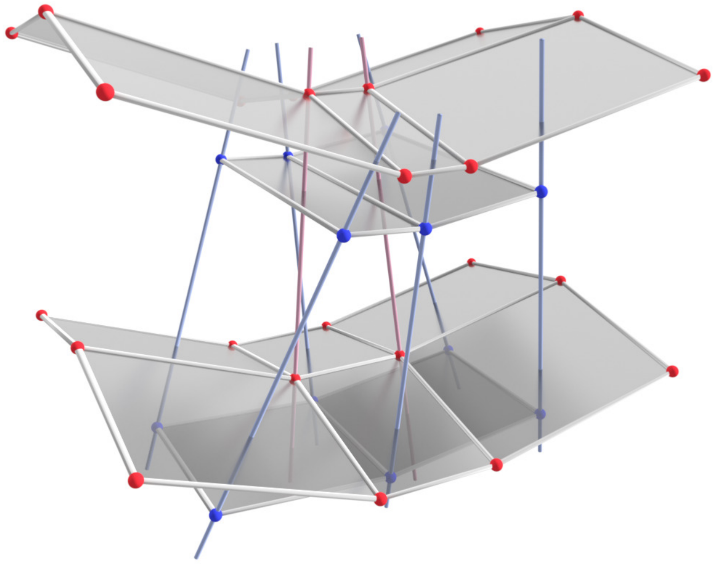

Figure 2.3. Patch of an orthogonal pair of dual discrete conjugate nets, and one layer of a discrete parallel pair of nets.

Proof. The orthogonality of two dual edges $\Delta_1\tilde{\boldsymbol{x}}(\boldsymbol{n})$ and $\Delta_2\tilde{\boldsymbol{x}}(\boldsymbol{n}^*)$ follows from parallelity to the corresponding edges of $\boldsymbol{x}$. An edge $\Delta_3\tilde{\boldsymbol{x}}(\boldsymbol{n})$ is always parallel to the discrete normal vector $\boldsymbol{\nu}(n_1,n_2)$, which in turn is orthogonal to any dual edge $\Delta_1\tilde{\boldsymbol{x}}(\boldsymbol{n}^*)$ and $\Delta_2\tilde{\boldsymbol{x}}(\boldsymbol{n}^*)$.

Let $\boldsymbol{n} \in \mathbb{Z}^3 \cup \left(\mathbb{Z}+\frac{1}{2}\right)^3$, $\boldsymbol{\sigma}_1 = (-1,1,1)$, $\boldsymbol{\sigma}_2 = (1,1,1)$, $\boldsymbol{n}_1^* = \boldsymbol{n} + \frac{1}{2}\boldsymbol{\sigma}_1$, $\boldsymbol{n}_2^* = \boldsymbol{n} + \frac{1}{2}\boldsymbol{\sigma}_2$, and consider the two corresponding adjacent values of H_3^2. Then

$$
\begin{aligned}
H_3^2(\boldsymbol{n}+\tfrac{1}{4}\boldsymbol{\sigma}_2) - H_3^2(\boldsymbol{n}+\tfrac{1}{4}\boldsymbol{\sigma}_1) &= \langle \Delta_3\boldsymbol{x}(\boldsymbol{n}), \bar{\Delta}_3\boldsymbol{x}(\boldsymbol{n}_2^*)\rangle - \langle \Delta_3\boldsymbol{x}(\boldsymbol{n}), \bar{\Delta}_3\boldsymbol{x}(\boldsymbol{n}_1^*)\rangle \\
&= \langle \Delta_3(\boldsymbol{n}), \Delta_1\bar{\Delta}_3\boldsymbol{x}(\boldsymbol{n}_1^*)\rangle \\
&= \langle \Delta_3(\boldsymbol{n}), \bar{\Delta}_3\boldsymbol{x}\Delta_1(\boldsymbol{n}_1^*)\rangle \\
&= \langle \Delta_3(\boldsymbol{n}), \Delta_1(\boldsymbol{n}_1^*)\rangle - \langle \Delta_3(\boldsymbol{n}), \Delta_1(\boldsymbol{n}_1^* - \boldsymbol{e}_3)\rangle = 0.
\end{aligned}
$$

□

3 Isothermic nets

3.1 Classical isothermic nets

A surface is called *isothermic* if it (locally) possesses a *conformal* curvature line parametrization, i.e., a parametrization $\boldsymbol{x} : \mathbb{R}^2 \supset U \to \mathbb{R}^3$ with

$$F = f = 0, \qquad E = G.$$

Definition 3.1. *A net $\boldsymbol{x} : \mathbb{R}^2 \supset U \to \mathbb{R}^3$ is called* isothermic *if it is a curvature line parametrization and conformal up to reparametrization along the coordinate lines, i.e., $F = f = 0$ and the coefficients of the first fundamental form satisfy*

$$\partial_1\partial_2 \log \frac{E}{G} = 0,$$

or equivalently,

$$\frac{E}{G} = \frac{\alpha(s_1)}{\beta(s_2)},$$

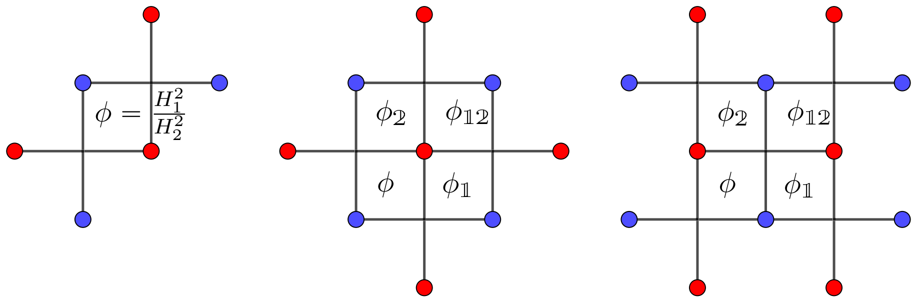

Figure 3.1. *Left:* The edges of a pair of dual nets involved in the discrete isothermicity condition. *Middle:* The four quotients of discrete Lamé coefficients around a vertex. *Right:* The four quotients of discrete Lamé coefficients around a pair of dual edges. The double stroked indices denote half-integer shifts in the corresponding lattice direction.

with some functions α and β only depending on s_1 and s_2, respectively.

The Möbius invariant notion of isothermic nets may be decomposed into the Möbius invariant notion of orthogonal nets and the projectively invariant notion of Koenigs nets.

Definition 3.2. *A net $\boldsymbol{x} : \mathbb{R}^2 \supset U \to \mathbb{R}^3$ is called* a Koenigs net *if there exists a function $\nu : U \to \mathbb{R}_+$ such that*

$$\partial_1\partial_2\boldsymbol{x} = \frac{\partial_2\nu}{\nu}\,\partial_1\boldsymbol{x} + \frac{\partial_1\nu}{\nu}\,\partial_2\boldsymbol{x}.$$

Remark 3.1. Comparing with (1.2) we see that Koenigs nets are special conjugate nets. For a conjugate net $\boldsymbol{x} : \mathbb{R}^2 \supset U \to \mathbb{R}^3$ satisfying the equation

$$\partial_1\partial_2\boldsymbol{x} = a\,\partial_1\boldsymbol{x} + b\,\partial_2\boldsymbol{x}.$$

its *Laplace invariants* are given by

$$\hat{a} = \partial_1 a - ab, \qquad \hat{b} = \partial_2 b - ab.$$

Thus, Koenigs nets are conjugate nets with equal Laplace invariants.

Proposition 3.3. *A net $\boldsymbol{x} : \mathbb{R}^2 \supset U \to \mathbb{R}^3$ is isothermic if it is an orthogonal Koenigs net.*

3.2 Discrete isothermic nets

Having a definition for discrete Lamé coefficients, we can immediately discretize Definition 3.1 in the following sense:

Definition 3.4. *An orthogonal pair of dual discrete conjugate nets $\boldsymbol{x} : \mathbb{Z}^2 \cup \left(\mathbb{Z} + \frac{1}{2}\right)^2 \to \mathbb{R}^3$ is called* a discrete isothermic net *if its discrete Lamé coefficients $H_1^2, H_2^2 : \left(\frac{1}{2}\mathbb{Z} + \frac{1}{4}\right)^2 \to \mathbb{R}$ satisfy the following factorization condition:*

$$\frac{H_1^2}{H_2^2} = \frac{\alpha(n_1)}{\beta(n_2)}, \qquad n_1, n_2 \in \tfrac{1}{2}\mathbb{Z} + \tfrac{1}{4}, \tag{3.1}$$

where $\alpha, \beta : \left(\frac{1}{2}\mathbb{Z} + \frac{1}{4}\right) \to \mathbb{R}$ are two functions depending on n_1 and n_2 only, respectively.

If we denote the quotient of the discrete Lamé coefficients by

$$\phi = \frac{H_1^2}{H_2^2} : \left(\tfrac{1}{2}\mathbb{Z} + \tfrac{1}{4}\right)^2 \to \mathbb{R},$$

the factorization condition (3.1) is equivalent to

$$\phi(n_1, n_2)\,\phi(n_1 + \tfrac{1}{2}, n_2 + \tfrac{1}{2}) = \phi(n_1 + \tfrac{1}{2}, n_2)\,\phi(n_1, n_2 + \tfrac{1}{2}) \tag{3.2}$$

for every $(n_1, n_2) \in \left(\frac{1}{2}\mathbb{Z} + \frac{1}{4}\right)^2$. Equation (3.2) describes two combinatorially different configurations, depending on whether the four values of ϕ are located around a vertex of the net $\boldsymbol{x}$ or around two dual edges of it (see Figure 3.1).

Proposition 3.5. *Let $\boldsymbol{x} : \mathbb{Z}^2 \cup \left(\mathbb{Z} + \frac{1}{2}\right)^2 \to \mathbb{R}^3$ be an orthogonal pair of dual discrete conjugate nets. Then the four values of ϕ around any vertex $\boldsymbol{n} \in \mathbb{Z}^2 \cup \left(\mathbb{Z} + \frac{1}{2}\right)^2$ satisfy* (3.2) *(see Figure 3.1 (middle)).*

Proof. Denote the plane of the quadrilateral through the four points $\boldsymbol{x}(\boldsymbol{n} + \frac{1}{2}(\pm 1, \pm 1))$ by Π. Orthogonal projection of the four edges $\Delta_1\boldsymbol{x}(\boldsymbol{n}), \bar{\Delta}_1\boldsymbol{x}(\boldsymbol{n}), \Delta_2\boldsymbol{x}(\boldsymbol{n}), \bar{\Delta}_2\boldsymbol{x}(\boldsymbol{n})$ onto Π preserves the orthogonality constraint as well as the involved Lamé coefficients. Thus, we may restrict ourselves to the planar case.

For simplicity, assume that all Lamé coefficients are positive, $H_i^2 > 0$. Then we find

$$\phi(n_1 + \tfrac{1}{4}, n_2 + \tfrac{1}{4}) = \frac{\langle \Delta_1\boldsymbol{x}(n_1, n_2), \Delta_1\boldsymbol{x}(n_1 - \frac{1}{2}, n_2 + \frac{1}{2})\rangle}{\langle \Delta_2\boldsymbol{x}(n_1, n_2), \Delta_2\boldsymbol{x}(n_1 + \frac{1}{2}, n_2 - \frac{1}{2})\rangle} = \frac{|\Delta_1\boldsymbol{x}(n_1, n_2)|\,|\Delta_1\boldsymbol{x}(n_1 - \frac{1}{2}, n_2 + \frac{1}{2})|}{|\Delta_2\boldsymbol{x}(n_1, n_2)|\,|\Delta_2\boldsymbol{x}(n_1 + \frac{1}{2}, n_2 - \frac{1}{2})|},$$

and similarly for the other values of ϕ. Thus, in (3.2) all lengths appear twice and cancel. □

Thus, for an orthogonal pair of discrete conjugate nets the discrete isothermicity condition (3.2) only needs to be checked around every pair of dual edges (Figure 3.1 (*right*)).

Remark 3.2. From Lemma 1.14 we immediately see that the factorization condition (3.1) is not invariant under Möbius transformations for orthogonal pairs of sphere congruences as they are defined in Section 1.3. Yet, as mentioned in Remark 2.7, Möbius invariance is not necessarily to be expected in the setup of orthogonal pairs of dual discrete nets.

4 Confocal quadrics

An important example of an orthogonal coordinate system in which all coordinate surfaces are isothermic is given by *confocal coordinates* (also known as *elliptic coordinates*).

4.1 Classical confocal coordinates

For given $a_1 > a_2 > \cdots > a_N$, we consider the one-parameter family of confocal quadrics in $\mathbb{R}^N$ given by

$$\mathcal{Q}_\lambda = \left\{ \boldsymbol{x} = (x_1, \ldots, x_N) \in \mathbb{R}^N : \sum_{k=1}^{N} \frac{x_k^2}{a_k + \lambda} = 1 \right\}, \quad \lambda \in \mathbb{R}. \tag{4.1}$$

Note that the quadrics of this family are centered at the origin and have their principal axes aligned along the coordinate directions. For a given point $\boldsymbol{x} = (x_1, \ldots, x_N) \in \mathbb{R}^N$ with $x_1 x_2 \ldots x_N \neq 0$, the equation $\sum_{k=1}^N x_k^2/(a_k + \lambda) = 1$ is, after clearing the denominators, a polynomial equation of degree N in λ, with N real roots $u_1, \ldots, u_N$ lying in the intervals

$$-a_1 < u_1 < -a_2 < u_2 < \cdots < -a_N < u_N,$$

so that

$$\sum_{k=1}^{N} \frac{x_k^2}{\lambda + a_k} - 1 = -\frac{\prod_{m=1}^N (\lambda - u_m)}{\prod_{m=1}^N (\lambda + a_m)}. \tag{4.2}$$

These N roots correspond to the N confocal quadrics of the family (4.1) that intersect at the point $\boldsymbol{x} = (x_1, \ldots, x_N)$:

$$\sum_{k=1}^{N} \frac{x_k^2}{a_k + u_i} = 1, \quad i = 1, \ldots, N \quad \Leftrightarrow \quad \boldsymbol{x} \in \bigcap_{i=1}^{N} \mathcal{Q}_{u_i}. \tag{4.3}$$

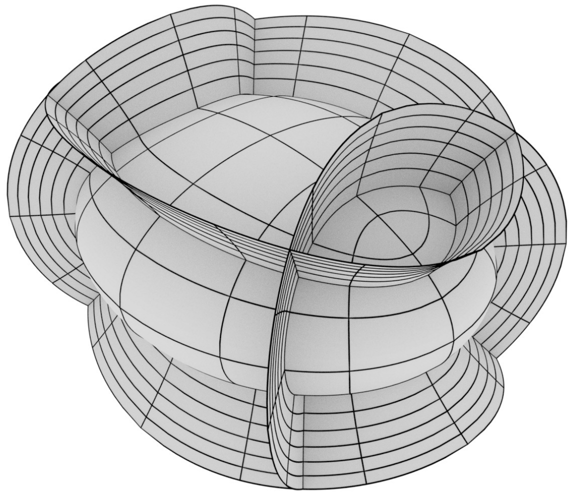

Figure 4.1. Three confocal quadrics in $\mathbb{R}^3$.

The N quadrics $\mathcal{Q}_{u_i}$ are all of different (affine) signatures. Evaluating the residue of the right-hand side of (4.2) at $\lambda = -a_k$, one can easily express x_k^2 through $u_1, \dots, u_N$:

$$x_k^2 = \frac{\prod_{i=1}^N (u_i + a_k)}{\prod_{i \neq k} (a_k - a_i)}, \quad k = 1, \dots, N. \tag{4.4}$$

Thus, for each point $(x_1, \dots, x_N) \in \mathbb{R}^N$ with $x_1 x_2 \dots x_N \neq 0$, there is exactly one solution $(u_1, \dots, u_N) \in \mathcal{U}$ of (4.4), where

$$\mathcal{U} = \left\{ (u_1, \dots, u_N) \in \mathbb{R}^N \mid -a_1 < u_1 < -a_2 < u_2 < \dots < -a_N < u_N \right\}.$$

On the other hand, for each $(u_1, \dots, u_N) \in \mathcal{U}$ there are exactly 2^N solutions $(x_1, \dots, x_N) \in \mathbb{R}^N$, which are mirror symmetric with respect to the coordinate hyperplanes. Thus, we are dealing with a parametrization of, say, the first hyperoctant of $\mathbb{R}^N$,

$$\boldsymbol{x} : \mathcal{U} \to \mathbb{R}_+^N, \qquad \boldsymbol{u} = (u_1, \dots, u_N) \mapsto \boldsymbol{x} = (x_1, \dots, x_N)$$

given by

$$x_k = \frac{\prod_{i=1}^{k-1} \sqrt{-(u_i + a_k)} \prod_{i=k}^N \sqrt{u_i + a_k}}{\prod_{i=1}^{k-1} \sqrt{a_i - a_k} \prod_{i=k+1}^N \sqrt{a_k - a_i}}, \quad k = 1, \dots, N,$$

such that the coordinate hyperplanes $u_i = \text{const}$ are mapped to (parts of) the respective quadrics given by (4.3). The coordinates $(u_1, \dots, u_N)$ are called *confocal coordinates.*

Proposition 4.1. *The system of confocal coordinates $\boldsymbol{x} : \mathcal{U} \to \mathbb{R}_+^N$ is orthogonal. Its Lamé coefficients are given by*

$$H_i^2(\boldsymbol{u}) = \frac{1}{4} \frac{\prod_{j \neq i} (u_i - u_j)}{\prod_{k=1}^N (u_i - a_k)}, \qquad i = 1, \dots, N. \tag{4.5}$$

Remark 4.1.

(i) By Theorem 1.4 the system of confocal coordinates is conjugate. In particular, it satisfies the *Euler-Poisson-Darboux system* (cf. Section 5)

$$\partial_i \partial_j \boldsymbol{x}(\boldsymbol{u}) = \frac{1}{2(u_i - u_j)} (\partial_j \boldsymbol{x}(\boldsymbol{u}) - \partial_i \boldsymbol{x}(\boldsymbol{u})), \qquad i, j = 1, \dots, N, \ i \neq j.$$

Comparing with Definition 3.2 we find that all two-dimensional coordinate subnets of $\boldsymbol{x}$ are Koenigs nets, and thus, by Proposition 3.3, isothermic nets, which is also imminent from the form of the Lamé coefficients (4.5).

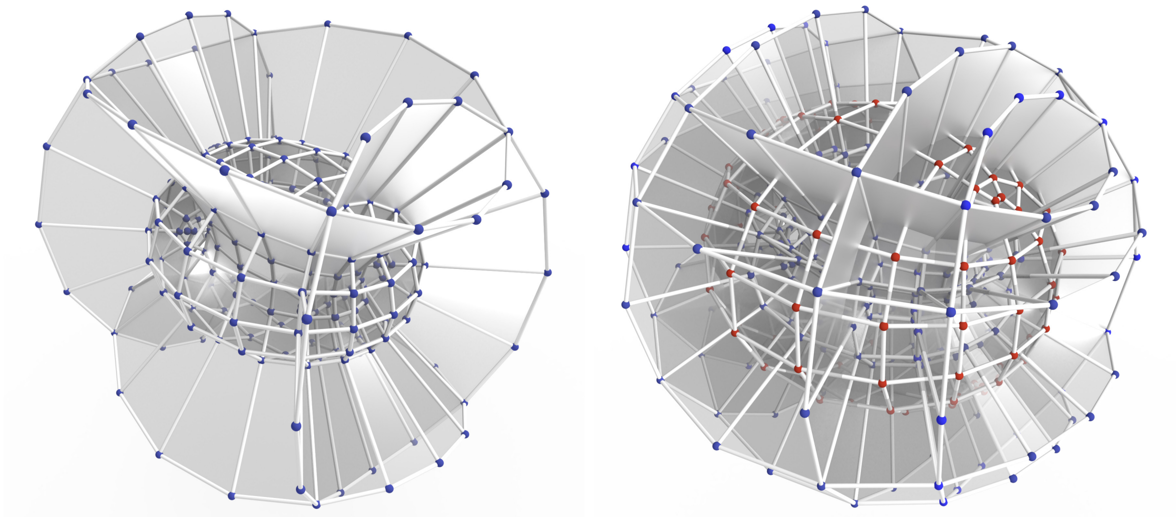

Figure 4.2. *Left:* Three discrete confocal quadrics as part of a (stepsize 1) subnet of a discrete confocal coordinate system in $\mathbb{R}^3$. *Right:* Part of an orthogonal pair of dual discrete conjugate nets which are (stepsize 1) subnets of a discrete confocal coordinate system in $\mathbb{R}^3$.

(ii) The orthogonal coordinate systems with coordinate hypersurfaces belonging to a common family of confocal quadrics are uniquely defined only up to reparametrization along the coordinate lines $u_i = u_i(s_i)$, $i = 1, \dots, N$. This reparametrization leads to different nets with different geometric properties (see Chapter 2: Section 8, Section 9, and Appendix B, as well as [Ak, Ag, ABST]). Note that under reparametrization the Lamé coefficients (4.5) take the form

$$H_i^2(\boldsymbol{s}) = \frac{1}{4}\left(u_i'(s_i)\right)^2 \frac{\prod_{j\neq i}(u_i(s_i) - u_j(s_j))}{\prod_{k=1}^N (u_i(s_i) - a_k)}, \qquad i = 1, \dots, N.$$

The system of confocal coordinates is orthogonal and its coordinate functions factorize in the sense that each coordinate function is a product of functions each depending on only one of the N variables. It turns out that these two properties characterize confocal coordinates (up to reparametrization along the coordinate lines).

Theorem 4.2 (Chapter 2: Theorem 3.1)**.** *If a coordinate system* $\boldsymbol{x} : \mathbb{R}^N \supset U \to \mathbb{R}^N$ *satisfies two conditions:*

(i) $\boldsymbol{x}(\boldsymbol{s})$ factorizes, *in the sense that*

$$\begin{cases} x_1(\boldsymbol{s}) = f_1^1(s_1) f_2^1(s_2) \cdots f_N^1(s_N), \\ x_2(\boldsymbol{s}) = f_1^2(s_1) f_2^2(s_2) \cdots f_N^2(s_N), \\ \dots \\ x_N(\boldsymbol{s}) = f_1^N(s_1) f_2^N(s_2) \cdots f_N^N(s_N), \end{cases}$$

with all $f_i^k(s_i) \neq 0$ *and* $\left(f_i^k\right)'(s_i) \neq 0$*, and*

(ii) $\boldsymbol{x}$ *is* orthogonal, *that is,*

$$\langle \partial_i \boldsymbol{x}, \partial_j \boldsymbol{x} \rangle = 0, \qquad i, j = 1, \dots, N,\ i \neq j,$$

then all coordinate hypersurfaces are confocal quadrics.

4.2 Discrete confocal coordinates

Consider applying a factorizability condition, similar to (3.1),

$$x_i(\boldsymbol{n}) = f_1^i(n_1) f_2^i(n_2) \cdots f_N^i(n_N), \qquad i = 1, \dots, N,$$

to an orthogonal pair of dual discrete nets $\boldsymbol{x} : \mathbb{Z}^N \cup \left(\mathbb{Z} + \frac{1}{2}\right)^N \to \mathbb{R}^N$ defined on the dual pair of square lattices $\mathbb{Z}^N$ and $\left(\mathbb{Z} + \frac{1}{2}\right)^N$. Then the functions f_i^k must each be defined on $\frac{1}{2}\mathbb{Z}$, and thus, the net $\boldsymbol{x}$ can be extended to all of $\left(\frac{1}{2}\mathbb{Z}\right)^N$. The two dual lattices $\mathbb{Z}^M$ and $\left(\mathbb{Z} + \frac{1}{2}\right)^M$ are just one pair of dual sublattices of $\left(\frac{1}{2}\mathbb{Z}\right)^M$. More generally we call two lattices

$$\mathbb{Z}^M + \tfrac{1}{2}\boldsymbol{\delta}, \qquad \mathbb{Z}^M + \tfrac{1}{2}\bar{\boldsymbol{\delta}},$$

a *pair of dual sublattices* of $\left(\frac{1}{2}\mathbb{Z}\right)^M$, where

$$\boldsymbol{\delta} = (\delta_1, \ldots, \delta_M) \in \{0,1\}^M, \qquad \bar{\boldsymbol{\delta}} = (1 - \delta_1, \ldots, 1 - \delta_M) \in \{0,1\}^M.$$

The stepsize $\frac{1}{2}$ square lattice $\left(\frac{1}{2}\mathbb{Z}\right)^M$ has 2^{M-1} such pairs of dual sublattices.

Definition 4.3.

(i) A map

$$\boldsymbol{x} : \left(\tfrac{1}{2}\mathbb{Z}\right)^M \to \mathbb{R}^N$$

is called a stepsize $\frac{1}{2}$ discrete net.

(ii) A stepsize $\frac{1}{2}$ discrete net is called regular *if all of its 2^M (stepsize 1) discrete subnets are regular.*

(iii) A stepsize $\frac{1}{2}$ discrete net is called orthogonal *if all of its 2^{M-1} pairs of dual discrete subnets are orthogonal.*

Remark 4.2.

(i) For a general stepsize $\frac{1}{2}$ discrete net, the discrete orthogonality constraint (1.3) only correlates the two nets from each pair of dual discrete subnets. The 2^{M-1} different pairs of dual discrete subnets are not mutually correlated by this condition unless an additional constraint, like the factorizability, is introduced.

(ii) Each of the 2^{M-1} different pairs of dual discrete subnets leads to a different definition of discrete Lamé coefficients on the lattice $\left(\frac{1}{2}\mathbb{Z} + \frac{1}{4}\right)^M$. In general these do not coincide.

We turn the characterizing properties of classical confocal coordinates (Theorem 4.2) into a definition for discrete confocal coordinates using stepsize $\frac{1}{2}$ discrete nets.

Definition 4.4 (Chapter 2: Definition 5.1)**.** *A discrete coordinate system $\boldsymbol{x} : \left(\frac{1}{2}\mathbb{Z}\right)^N \supset \mathcal{U} \to \mathbb{R}^N$ is called* a discrete confocal coordinate system *if it satisfies two conditions:*

(i) $\boldsymbol{x}(\boldsymbol{n})$ factorizes*, in the sense that for any $\boldsymbol{n} \in \mathcal{U}$*

$$\begin{cases} x_1(\boldsymbol{n}) = f_1^1(n_1) f_2^1(n_2) \cdots f_N^1(n_N), \\ x_2(\boldsymbol{n}) = f_1^2(n_1) f_2^2(n_2) \cdots f_N^2(n_N), \\ \ldots \\ x_N(\boldsymbol{n}) = f_1^N(n_1) f_2^N(n_2) \cdots f_N^N(n_N), \end{cases}$$

with $f_i^k(n_i) \neq 0$ and $\bar{\Delta} f_i^k(n_i) = f_i^k(n_i) - f_i^k(n_i - 1) \neq 0$, and

(ii) $\boldsymbol{x}$ is orthogonal*, in the sense of Definition 4.3.*

The quadratic equations (4.1) identifying the coordinate surfaces in the smooth case as confocal quadrics are replaced by bilinear identities relating adjacent points in the dual sublattices.

Theorem 4.5 (Chapter 2: Theorem 5.2)**.** *For a discrete confocal coordinate system, there exist $a_1, \ldots, a_N \in \mathbb{R}$, and sequences $u_i : \left(\frac{1}{2}\mathbb{Z} + \frac{1}{4}\right) \to \mathbb{R}$, $i = 1, \ldots, N$, such that*

$$\sum_{k=1}^{N} \frac{x_k(\boldsymbol{n}) x_k(\boldsymbol{n} + \frac{1}{2}\boldsymbol{\sigma})}{a_k + u_i} = 1, \quad u_i = u_i(n_i + \tfrac{1}{4}\sigma_i), \qquad i = 1, \ldots, N. \tag{4.6}$$

for any $\boldsymbol{n} \in \mathcal{U}$ and $\boldsymbol{\sigma} \in \{\pm 1\}^N$, or equivalently,

$$x_k(\boldsymbol{n})x_k(\boldsymbol{n} + \tfrac{1}{2}\boldsymbol{\sigma}) = \frac{\prod_{j=1}^N (u_j + a_k)}{\prod_{j \neq k}(a_k - a_j)}, \quad u_j = u_j(n_j + \tfrac{1}{4}\sigma_j), \qquad k = 1, \ldots, N.$$

Remark 4.3.

(i) Different choices for the discrete functions u_i lead to different "discrete reparametrizations" of the system of confocal coordinates, which resemble many of the geometric properties from the smooth case (see Chapter 2: Section 8, Section 9, and Appendix B).

(ii) Equation (4.6) leads to a remarkable geometric interpretation via polarity with respect to sequences of classical confocal quadrics (see Section 6.4).

Proposition 4.6. *Let $\boldsymbol{x} : \left(\tfrac{1}{2}\mathbb{Z}\right)^N \to \mathbb{R}^N$ be a discrete confocal coordinate system. Then at each $\boldsymbol{n} \in \left(\tfrac{1}{2}\mathbb{Z}\right)^N$ and for $i = 1, \ldots, N$ the 2^{N-1} scalar products*

$$\langle \Delta_i \boldsymbol{x}(\boldsymbol{n} + \tfrac{1}{2}\boldsymbol{\delta}), \bar{\Delta}_i \boldsymbol{x}(\boldsymbol{n} + \tfrac{1}{2}\boldsymbol{\sigma} + \tfrac{1}{2}\bar{\boldsymbol{\delta}}) \rangle$$

are equal for all $\boldsymbol{\delta} = (\delta_1, \ldots, \delta_M) \in \{0,1\}^M$ and $\bar{\boldsymbol{\delta}} = (1 - \delta_1, \ldots, 1 - \delta_M)$ and $\boldsymbol{\sigma} = (1, \ldots, 1)$. Thus, the discrete Lamé coefficients defined by the different pairs of dual discrete subnets coincide on $\left(\tfrac{1}{2}\mathbb{Z} + \tfrac{1}{4}\right)^N$. They are given by

$$H_i^2(\boldsymbol{n}) = \left(u_i(n_i + \tfrac{1}{2}) - u_i(n_i)\right)\left(u_i(n_i) - u_i(n_i - \tfrac{1}{2})\right) \frac{\prod_{j \neq i} \left(u_i(n_i) - u_j(n_j)\right)}{\prod_{k=1}^N \left(u_i(n_i) - a_k\right)}. \tag{4.7}$$

Proof. Let $i = 1, \ldots, N$, $\boldsymbol{n} \in \left(\tfrac{1}{2}\mathbb{Z}\right)^N$, and $\boldsymbol{\sigma} = (1, \ldots, 1)$. For $k = 1, \ldots, N$ the discrete differences satisfy

$$\begin{aligned} \Delta_i x_k(\boldsymbol{n}) &= x_k(\boldsymbol{n}) \frac{u_i(n_i + \frac{3}{4}) - u_i(n_i + \frac{1}{4})}{u_i(n_i + \frac{1}{4}) + a_k}, \\ \bar{\Delta}_i x_k(\boldsymbol{n} + \tfrac{1}{2}\boldsymbol{\sigma}) &= x_k(\boldsymbol{n} + \tfrac{1}{2}\boldsymbol{\sigma}) \frac{u_i(n_i + \frac{1}{4}) - u_i(n_i - \frac{1}{4})}{u_i(n_i + \frac{1}{4}) + a_k}, \end{aligned}$$

and thus,

$$\begin{aligned} &\langle \Delta_i \boldsymbol{x}(\boldsymbol{n}), \bar{\Delta}_i \boldsymbol{x}(\boldsymbol{n} + \tfrac{1}{2}\boldsymbol{\sigma}) \rangle = \\ &\left(u_i(n_i + \tfrac{3}{4}) - u_i(n_i + \tfrac{1}{4})\right)\left(u_i(n_i + \tfrac{1}{4}) - u_i(n_i - \tfrac{1}{4})\right) \sum_{k=1}^N \frac{x_k(\boldsymbol{n})x_k(\boldsymbol{n} + \frac{1}{2}\boldsymbol{\sigma})}{(u_i(n_i + \frac{1}{4}) + a_k),}, \end{aligned}$$

which by Lemma 4.7 yields (4.7). By symmetry, adding different choices of $\boldsymbol{\delta}$ and $\bar{\boldsymbol{\delta}}$ gives the same result. ☐

Lemma 4.7. *The system of discrete confocal coordinates $\boldsymbol{x} : \left(\tfrac{1}{2}\mathbb{Z}\right)^N \to \mathbb{R}^N$ satisfies*

$$\sum_{k=1}^N \frac{x_k(\boldsymbol{n})x_k(\boldsymbol{n} + \frac{1}{2}\boldsymbol{\sigma})}{(u_i(n_i + \frac{1}{4}) + a_k)^2} = \frac{\prod_{j \neq i}(u_i(n_i + \frac{1}{4}) - u_j(n_j + \frac{1}{4}))}{\prod_{k=1}^N (u_i(n_i + \frac{1}{4}) + a_k)}.$$

Proof. This is the remarkable identity (3.10) from Chapter 1 that immediately carries over to the discrete setting. ☐

That the Lamé coefficients coincide for all pairs of dual discrete subnets implies together with Proposition 3.5, that all pairs of dual discrete subnets are discrete isothermic in the sense of Definition 3.4. On the other hand, this also follows immediately from the explicit expressions of the Lamé coefficients (4.7).

Proposition 4.8. *Let $\boldsymbol{x} : \left(\tfrac{1}{2}\mathbb{Z}\right)^N \to \mathbb{R}^N$ be a discrete confocal coordinate system. All two-dimensional pairs of dual discrete subnets $\boldsymbol{x}|_{(\mathbb{Z}^N + \frac{1}{2}\boldsymbol{\delta})}$ and $\boldsymbol{x}|_{(\mathbb{Z}^N + \frac{1}{2}\bar{\boldsymbol{\delta}})}$ are discrete isothermic. In particular, for $i, j = 1, \ldots, N$, $i < j$,*

$$\begin{aligned} H_i^2(\boldsymbol{n}) &= \alpha_{ij}(n_1, \ldots, n_{j-1}, n_{j+1}, \ldots, n_N) s_{ij}^2(n_i, n_j), \\ H_j^2(\boldsymbol{n}) &= \beta_{ij}(n_1, \ldots, n_{i-1}, n_{i+1}, \ldots, n_N) s_{ij}^2(n_i, n_j), \end{aligned}$$

with

$$
\begin{aligned}
s_{ij}^2 &= u_j(n_j) - u_i(n_i),\\
\alpha_{ij} &= -\left(u_i(n_i+\tfrac{1}{2}) - u_i(n_i)\right)\left(u_i(n_i) - u_i(n_i-\tfrac{1}{2})\right)\frac{\prod_{l\neq i,j}\left(u_i(n_i)-u_l(n_l)\right)}{\prod_{k=1}^{N}\left(u_i(n_i)-a_k\right)},\\
\beta_{ij} &= \left(u_j(n_j+\tfrac{1}{2}) - u_j(n_j)\right)\left(u_j(n_j) - u_j(n_j-\tfrac{1}{2})\right)\frac{\prod_{l\neq i,j}\left(u_j(n_j)-u_l(n_l)\right)}{\prod_{k=1}^{N}\left(u_j(n_j)-a_k\right)}.
\end{aligned}
$$

Remark 4.4. For a discrete Koenigs condition satisfied by the discrete confocal coordinates see Section 5.2.

5 Euler-Poisson-Darboux equation

5.1 Classical Euler-Poisson-Darboux equation

The classical *Euler-Poisson-Darboux system* is given by

$$\partial_i\partial_j \boldsymbol{x}(\boldsymbol{u}) = \frac{\gamma}{u_i-u_j}\left(\partial_j\boldsymbol{x}(\boldsymbol{u}) - \partial_i\boldsymbol{x}(\boldsymbol{u})\right), \quad i,j=1,\dots,N,\ i\neq j$$

with some constant $\gamma\in\mathbb{R}$. Confocal coordinates constitute certain factorizable solutions of this system (see Chapter 1: Proposition 3.6).

Eisenhart classified conjugate nets in $\mathbb{R}^3$ with all two-dimensional coordinate surfaces being Koenigs nets [Ei1]. The generic case is described by solutions of the Euler-Poisson-Darboux system with an arbitrary coefficient γ. Darboux classified orthogonal nets in $\mathbb{R}^3$ whose two-dimensional coordinate surfaces are isothermic [Da2, Livre II, Chap. III–V]. He found several families, all satisfying the Euler-Poisson-Darboux system with coefficient $\gamma = \pm\frac{1}{2}, -1$, or -2. The family corresponding to $\gamma=\frac{1}{2}$ consists of confocal cyclides and includes the case of confocal quadrics (or their Möbius images).

To factor in arbitrary reparametrizations along the coordinate lines $u_i = u_i(s_i)$ the Euler-Poisson-Darboux system should be replaced by

$$\partial_i\partial_j\boldsymbol{x}(\boldsymbol{s}) = \frac{\gamma}{u_i(s_i)-u_j(s_j)}\left(u_i'(s_i)\partial_j\boldsymbol{x}(\boldsymbol{s}) - u_j'(s_j)\partial_i\boldsymbol{x}(\boldsymbol{s})\right).$$

Considering only one component and two independent directions we obtain the *Euler-Poisson-Darboux equation*, which may equivalently be written as

$$
\begin{aligned}
\partial_1\partial_2 x &= \gamma\left(\frac{\partial_2\tau}{\tau}\partial_1 x + \frac{\partial_1\tau}{\tau}\partial_2 x\right)\\
\partial_1\partial_2\tau &= 0,
\end{aligned}
$$

where $\tau = u_1 - u_2$.

Remark 5.1. Note that the Euler-Poisson-Darboux equation can further be rewritten as

$$\partial_1\partial_2 x = \left(\frac{\partial_2\nu}{\nu}\partial_1 x + \frac{\partial_1\nu}{\nu}\partial_2 x\right)$$

with $\nu = |\tau|^\gamma$. Comparing with Definition 3.2 this reflects the fact that all solutions are *Koenigs nets.*

5.2 Discrete Euler-Poisson-Darboux equation

It turns out that discrete confocal coordinate systems also satisfy a corresponding discrete Euler-Poisson-Darboux system.

Theorem 5.1 (Chapter 2: Theorem A.2)**.** *Discrete confocal coordinate systems satisfy the discrete Euler-Poisson-Darboux system with $\gamma=\frac{1}{2}$:*

$$\Delta_i\Delta_j\boldsymbol{x} = \frac{1}{u_i-u_j}\left(\Delta^{1/2}u_i\Delta_j\boldsymbol{x} - \Delta^{1/2}u_j\Delta_i\boldsymbol{x}\right), \tag{5.1}$$

where $\boldsymbol{x}=\boldsymbol{x}(\boldsymbol{n})$, $u_i = u_i(n_i+\frac{1}{4})$, and

$$\Delta^{1/2}u_i = u_i(n_i+\tfrac{3}{4}) - u_i(n_i+\tfrac{1}{4}).$$

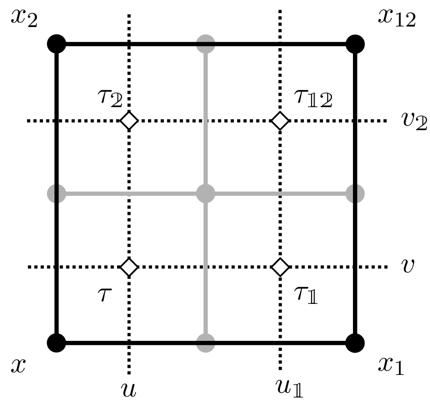

Figure 5.1. Combinatorial picture for the locations of the values of u, v, and τ in the discrete Euler-Poisson-Darboux equation.

Remark 5.2.

(i) The choice of $\gamma = \frac{1}{2}$ in (5.2) is encoded in the half-differences of the functions u_i and thus also in the stepsize $\frac{1}{2}$ of the lattice which serves as the domain for $\boldsymbol{x}$.

(ii) In the case $u_i(n_i + \frac{1}{4}) = n_i + \varepsilon_i$ we recover the version of the discrete Euler-Poisson-Darboux equation that was introduced in [KS2], and used in [BSST1] (see Chapter 1) to obtain discrete confocal coordinates.

The discrete Euler-Poisson-Darboux system satisfies the following discrete integrability condition.

Proposition 5.2. *Equation* (5.1) *is 3D-consistent.*

Proof. For 3D-consistency as a discrete integrability condition see [BS]. One computes that

$$\Delta_i\Delta_j\Delta_k\boldsymbol{x} = \frac{\Delta^{1/2}u_j\Delta^{1/2}u_k}{(u_i-u_j)(u_i-u_k)}\Delta_i\boldsymbol{x} + \frac{\Delta^{1/2}u_k\Delta^{1/2}u_i}{(u_j-u_i)(u_j-u_k)}\Delta_j\boldsymbol{x} + \frac{\Delta^{1/2}u_i\Delta^{1/2}u_j}{(u_k-u_i)(u_k-u_j)}\Delta_k\boldsymbol{x},$$

which is symmetric with respect to permutations of i, j, k. ☐

Consider the corresponding discrete Euler-Poisson-Darboux equation

$$\Delta_1\Delta_2 x = \frac{\Delta^{1/2}u}{u-v}\Delta_2 x - \frac{\Delta^{1/2}v}{u-v}\Delta_1 x \tag{5.2}$$

where $u = u(n_1 + \frac{1}{4})$ and $v = v(n_2 + \frac{1}{4})$ are functions on $\frac{1}{2}\mathbb{Z} + \frac{1}{4}$.

Proposition 5.3. *Let* $\tau = \tau\left(n_1 + \frac{1}{4}, n_2 + \frac{1}{4}\right)$ *be a function on* $\left(\frac{1}{2}\mathbb{Z} + \frac{1}{4}\right)^2$ *satisfying*

$$\Delta_1^{1/2}\Delta_2^{1/2}\tau = \tau_{\mathbb{12}} - \tau_{\mathbb{1}} - \tau_{\mathbb{2}} + \tau = 0. \tag{5.3}$$

Then the following three equations are equivalent:

$$\Delta_1\Delta_2 x = \frac{\tau_{\mathbb{2}}\tau_{\mathbb{12}} - \tau\tau_{\mathbb{1}}}{\tau(\tau_{\mathbb{1}} + \tau_{\mathbb{2}})}\Delta_1 x + \frac{\tau_{\mathbb{1}}\tau_{\mathbb{12}} - \tau\tau_{\mathbb{2}}}{\tau(\tau_{\mathbb{1}} + \tau_{\mathbb{2}})}\Delta_2 x, \tag{5.4}$$

$$\Delta_1\Delta_2 x = \frac{\Delta_2^{1/2}\tau}{\tau}\Delta_1 x + \frac{\Delta_1^{1/2}\tau}{\tau}\Delta_2 x, \tag{5.5}$$

$$\tau_{\mathbb{12}}x + \tau x_{12} = \tau_{\mathbb{1}}x_2 + \tau_{\mathbb{2}}x_1, \tag{5.6}$$

where the double stroked indices denote half-integer shifts $\tau_{\mathbb{1}} = \tau\left(n_1 + \frac{3}{4}, n_2 + \frac{1}{4}\right)$, $\tau_{\mathbb{2}} = \tau\left(n_1 + \frac{1}{4}, n_2 + \frac{3}{4}\right)$, *etc. (see Figure 5.1).*

Proof. Resolving the differences in (5.4) one obtains

$$(\tau_{\mathbb{1}} + \tau_{\mathbb{2}})(\tau_{\mathbb{12}} x + \tau x_{12}) = (\tau + \tau_{\mathbb{12}})(\tau_{\mathbb{1}} x_2 + \tau_{\mathbb{2}} x_1).$$

Analogously, for (5.5) one obtains

$$(\tau_{\mathbb{1}} + \tau_{\mathbb{2}} - \tau)x + \tau x_{12} = \tau_{\mathbb{1}} x_2 + \tau_{\mathbb{2}} x_1,$$

Under the assumption (5.3) both equations become equivalent to (5.6). □

Condition (5.3) is equivalent to

$$\tau\left(n_1 + \tfrac{1}{4}, n_2 + \tfrac{1}{4}\right) = u\left(n_1 + \tfrac{1}{4}\right) - v\left(n_2 + \tfrac{1}{4}\right)$$

for some functions u and v. Substituting this into (5.5) one immediately obtains (5.2). Thus, the discrete Euler-Poisson-Darboux equation (5.2) is equivalent to any of the three equations from Proposition 5.3.

Remark 5.3.

(i) While equation (5.4) resembles the equation for the standard notion of discrete Koenigs nets (see equation (4.1) from Chapter 1), it is yet different, due to the half-integer shifts in the τ's. The values of τ are assigned to the faces of the stepsize $\frac{1}{2}$ lattice $\left(\frac{1}{2}\mathbb{Z}\right)^2$. Thus, there are four values of τ that belong to one face of any integer sublattice (see Figure 5.1). But adjacent faces of an integer sublattice do not share any values of τ. Thus, on one integer sublattice, equation (5.4) poses no restriction on a net $\boldsymbol{x}$ beyond having planar faces. The restriction here comes from $\boldsymbol{x}$ being defined on the whole stepsize $\frac{1}{2}$ lattice $\left(\frac{1}{2}\mathbb{Z}\right)^2$, and, in the case of the Euler-Poisson-Darboux equation, from the additional harmonicity condition (5.3).

(ii) An analogous discretization of the Euler-Poisson-Darboux equation in the case of $\gamma = 1$ is given by

$$\tau_{12} x + \tau x_{12} = \tau_1 x_2 + \tau_2 x_1$$
$$\tau_{12} + \tau = \tau_1 + \tau_2$$

where x and τ are functions on the integer lattice $\mathbb{Z}^2$. Here we are back to the case of a standard discrete Koenigs net, and the surfaces satisfying this equation are projective translational surfaces (see [BPR]).

6 Confocal quadrics as dual pencils of quadrics

From the point of view of projective geometry, confocal quadrics are special dual pencils of quadrics, where one of the quadrics in the pencil is distinguished to induce the metric.

6.1 Quadrics in projective space

Consider the N-dimensional *real projective space*

$$\mathbb{RP}^N = \mathrm{P}(\mathbb{R}^{N+1}) = \left(\mathbb{R}^{N+1} \setminus \{0\}\right) \big/ \sim$$

as it is generated via projectivization from its *homogeneous coordinate space* $\mathbb{R}^{N+1}$ by the equivalence relation $x \sim y \Leftrightarrow x = \lambda y$ for some $\lambda \in \mathbb{R}$. We denote points in $\mathbb{RP}^N$ and their *homogeneous coordinates* by $\boldsymbol{x} = [x_1, \ldots, x_{N+1}]$. *Projective subspaces* of $\mathbb{RP}^N$ are induced by linear subspaces of $\mathbb{R}^{N+1}$, and the group of *projective transformations* is induced by the group of general linear transformations of $\mathbb{R}^{N+1}$ and denoted by $\mathrm{PGL}(N+1)$.

The N-dimensional *dual real projective space* is given by

$$(\mathbb{RP}^N)^* = \mathrm{P}\left((\mathbb{R}^{N+1})^*\right),$$

where $(\mathbb{R}^{N+1})^*$ is the space of linear functionals on $\mathbb{R}^{N+1}$. We identify $(\mathbb{RP}^N)^{**} = \mathbb{RP}^N$ in the canonical way, and obtain a bijection between projective subspaces $U \subset \mathbb{RP}^N$ and their *dual projective subspaces*

$$U^\star = \left\{ \boldsymbol{y} \in (\mathbb{RP}^N)^* \mid y(x) = 0 \text{ for all } x \in \mathbb{R}^{N+1} \text{ with } \boldsymbol{x} \in U \right\},$$

which satisfies $\dim U + \dim U^\star = N - 1$. Every projective transformation $f \in \mathrm{PGL}(N+1)$ induces a *dual projective transformation* $f^\star : (\mathbb{RP}^N)^* \to (\mathbb{RP}^N)^*$ satisfying

$$f(U)^\star = f^\star(U^\star)$$

for every projective subspace $U \subset \mathbb{RP}^N$. Introduce a basis on $\mathbb{R}^{N+1}$, say the canonical basis, and its dual basis on $(\mathbb{R}^{N+1})^*$. Then, if $F \in \mathbb{R}^{(N+1)\times(N+1)}$ is a matrix representing the transformation $f = [F]$, a matrix $F^\star \in \mathbb{R}^{(N+1)\times(N+1)}$ representing the dual transformation $f^\star = [F^\star]$ is given by the inverse transposed matrix

$$F^\star = F^{-\mathsf{T}}.$$

A *quadric* in $\mathbb{RP}^N$ is given by

$$\mathcal{Q} = \left\{ \boldsymbol{x} \in \mathbb{RP}^N \mid \langle x, x \rangle = 0 \right\},$$

where $\langle \cdot, \cdot \rangle$ is a non-zero symmetric bilinear form on $\mathbb{R}^{N+1}$. Its *signature* (r, s, t) (up to interchanging r and s) characterizes the quadric up to projective transformations. The quadric $\mathcal{Q}$ is called *non-degenerate* if $t = 0$. To ensure that the bilinear form corresponding to a quadric is well-defined up to a non-zero scalar multiple for all signatures, we consider the complexification of real quadrics. For non-neutral signature, i.e., $r \neq s$, the subgroup of projective transformations that preserve the quadric $\mathcal{Q}$ is given by the *projective orthogonal group* $\mathrm{PO}(r, s, t)$.

If we denote the *Gram matrix* of the bilinear form $\langle \cdot, \cdot \rangle$ by

$$Q \in \mathbb{R}^{(N+1)\times(N+1)}, \qquad Q_{ij} = \langle e_i, e_j \rangle,$$

one can write

$$\langle x, y \rangle = x^\mathsf{T} Q y.$$

A quadric induces the notion of *polarity* by the map $\pi_{\mathcal{Q}} = [Q] : \mathbb{RP}^N \to (\mathbb{RP}^N)^*$. The *polar subspace* of a projective subspace $U \subset \mathbb{RP}^N$ is given by

$$\pi_{\mathcal{Q}}(U)^\star = U^\perp = \left\{ \boldsymbol{y} \in \mathbb{RP}^N \mid \langle x, y \rangle = 0 \text{ for all } x \in \mathbb{R}^{N+1} \text{ with } \boldsymbol{x} \in U \right\}.$$

Any two points $\boldsymbol{x}, \boldsymbol{y} \in \mathbb{RP}^N$ lying in polar subspaces, i.e., satisfying $\langle x, y \rangle = 0$, are called *conjugate*. The involutory nature of the polarity relation is expressed by $\pi_{\mathcal{Q}}^\star \circ \pi_{\mathcal{Q}} = \mathrm{id}$.

Dual quadrics

For a quadric $\mathcal{Q} \subset \mathbb{RP}^N$ its *dual quadric* $\mathcal{Q}^\star \subset (\mathbb{RP}^N)^*$ may be defined as the set of points dual to the tangent hyperplanes of $\mathcal{Q}$. For a non-degenerate quadric $\mathcal{Q} \subset \mathbb{RP}^N$ of signature (r, s) its dual quadric $\mathcal{Q}^\star \subset (\mathbb{RP}^N)^*$ is a non-degenerate quadric with the same signature, and its Gram-matrix is given by

$$Q^\star = Q^{-1}.$$

For a once-degenerate quadric $\mathcal{Q} \subset \mathbb{RP}^N$ of signature $(r, s, 1)$, i.e., a cone its dual quadric $\mathcal{Q}^\star \subset (\mathbb{RP}^N)^*$ consists of the set of points on a lower dimensional quadric of signature (r, s) contained in the hyperplane $\boldsymbol{v}^\star \subset (\mathbb{RP}^N)^*$ where $\boldsymbol{v} \in \mathcal{Q}$ is the vertex of the cone. Thus, it is in itself not a quadric in $(\mathbb{RP}^N)^*$.

Remark 6.1. A more involved concept of quadrics considers them as pairs of primal and dual objects. This can be advantageous when considering more than once-degenerate quadrics (see [Kl]).

6.2 Cayley-Klein metric and orthogonality

A non-degenerate quadric $\mathcal{Q} \subset \mathbb{RP}^N$ with corresponding symmetric bilinear form $\langle \cdot, \cdot \rangle$ induces a *Cayley-Klein metric* on the projective space by

$$K_{\mathcal{Q}}(\boldsymbol{x}, \boldsymbol{y}) = \frac{\langle x, y \rangle^2}{\langle x, x \rangle \langle y, y \rangle}, \qquad \boldsymbol{x}, \boldsymbol{y} \in \mathbb{RP}^N \tag{6.1}$$

The quadric $\mathcal{Q}$ is called the corresponding *absolute quadric.*

- An absolute quadric $\mathcal{Q}$ with signature $(N, 1, 0)$ induces *hyperbolic geometry.* The hyperbolic distance d of two points $\boldsymbol{x}, \boldsymbol{y} \in \mathbb{RP}^N$ "inside" $\mathcal{Q}$ is given by

  $$\cosh^2 d(\boldsymbol{x}, \boldsymbol{y}) = K_{\mathcal{Q}}(\boldsymbol{x}, \boldsymbol{y}),$$

  while the angle α between two hyperbolic hyperplanes $\boldsymbol{n}^\star, \boldsymbol{m}^\star$ with $\boldsymbol{n}, \boldsymbol{m} \in \left(\mathbb{RP}^N\right)^*$ "outside" $\mathcal{Q}^\star$ is given by

  $$\cos^2 \alpha(\boldsymbol{m}^\star, \boldsymbol{n}^\star) = K_{\mathcal{Q}^\star}(\boldsymbol{m}, \boldsymbol{n}).$$

- An absolute quadric $\mathcal{Q}$ with signature $(N+1, 0, 0)$ induces *elliptic geometry.* The elliptic distance d of two points $\boldsymbol{x}, \boldsymbol{y} \in \mathbb{RP}^N$ is given by

  $$\cos^2 d(\boldsymbol{x}, \boldsymbol{y}) = K_{\mathcal{Q}}(\boldsymbol{x}, \boldsymbol{y}),$$

  while the angle α between two elliptic hyperplanes $\boldsymbol{n}^\star, \boldsymbol{m}^\star$ with $\boldsymbol{n}, \boldsymbol{m} \in \left(\mathbb{RP}^N\right)^*$ is given by

  $$\cos^2 \alpha(\boldsymbol{m}^\star, \boldsymbol{n}^\star) = K_{\mathcal{Q}^\star}(\boldsymbol{m}, \boldsymbol{n}).$$

- While *Euclidean geometry* can not be introduced by taking an absolute quadric in $\mathbb{RP}^N$, it can be introduced by a (once) degenerate quadric $\mathcal{Q} \subset \left(\mathbb{RP}^N\right)^*$ of signature $(N, 0, 1)$ on the dual space. The corresponding dual quadric $\mathcal{Q}^\star \subset \mathbb{RP}^N$ is not a quadric in $\mathbb{RP}^N$, but a quadric contained in the "hyperplane at infinity". Thus, while the Cayley-Klein metric can not be defined on the primal space in the usual way as in (6.1), it can still be defined on the dual space leading to the notion of angle between two Euclidean hyperplanes $\boldsymbol{n}^\star, \boldsymbol{m}^\star$ with $\boldsymbol{n}, \boldsymbol{m} \in \left(\mathbb{RP}^N\right)^*$, which is given by

  $$\cos^2 \alpha(\boldsymbol{m}^\star, \boldsymbol{n}^\star) = K_{\mathcal{Q}}(\boldsymbol{m}, \boldsymbol{n}).$$

Remark 6.2. The group of transformations preserving the absolute quadric $\mathcal{Q} \subset \left(\mathbb{RP}^N\right)^*$ in the Euclidean case is the group of similarity transformations. The Euclidean metric and the group of Euclidean transformations can still be obtained by a limiting procedure in an appropriately chosen pencil of absolute quadrics (see, e.g., [Kl]).

We find that in all above examples, two hyperplanes are orthogonal if the corresponding dual points are conjugate with respect to the absolute quadric on the dual space. We take this as the general definition of *orthogonality* with respect to an absolute quadric.

Definition 6.1. *Let $\mathcal{Q} \subset \left(\mathbb{RP}^N\right)^*$ be a quadric with corresponding symmetric bilinear form $\langle \cdot, \cdot \rangle$. Then two hyperplanes $\boldsymbol{m}^\star, \boldsymbol{n}^\star \subset \mathbb{RP}^N$ are* orthogonal *(with respect to $\mathcal{Q}$) if the two points $\boldsymbol{m}, \boldsymbol{n} \in \left(\mathbb{RP}^N\right)^*$ are conjugate, i.e.,*

$$\langle m, n \rangle = 0.$$

6.3 Pencils and dual pencils of quadrics

Let $\mathcal{Q}_1, \mathcal{Q}_2 \subset \mathbb{RP}^N$ be two distinct quadrics with corresponding bilinear forms $\langle \cdot, \cdot \rangle_1$ and $\langle \cdot, \cdot \rangle_2$, respectively. Every linear combination of these two bilinear forms yields a new quadric. The family of quadrics obtained by all linear combinations of the two bilinear forms is called a *pencil of quadrics* (see Figure 6.1, *left*):

$$\mathcal{Q}_1 \wedge \mathcal{Q}_2 = \left(\mathcal{Q}_{[\lambda_1,\lambda_2]}\right)_{[\lambda_1,\lambda_2] \in \mathbb{RP}^1}, \qquad \mathcal{Q}_{[\lambda_1,\lambda_2]} := \left\{\boldsymbol{x} \in \mathbb{RP}^N \mid \lambda_1 \langle x, x \rangle_1 + \lambda_2 \langle x, x \rangle_2 = 0\right\}.$$

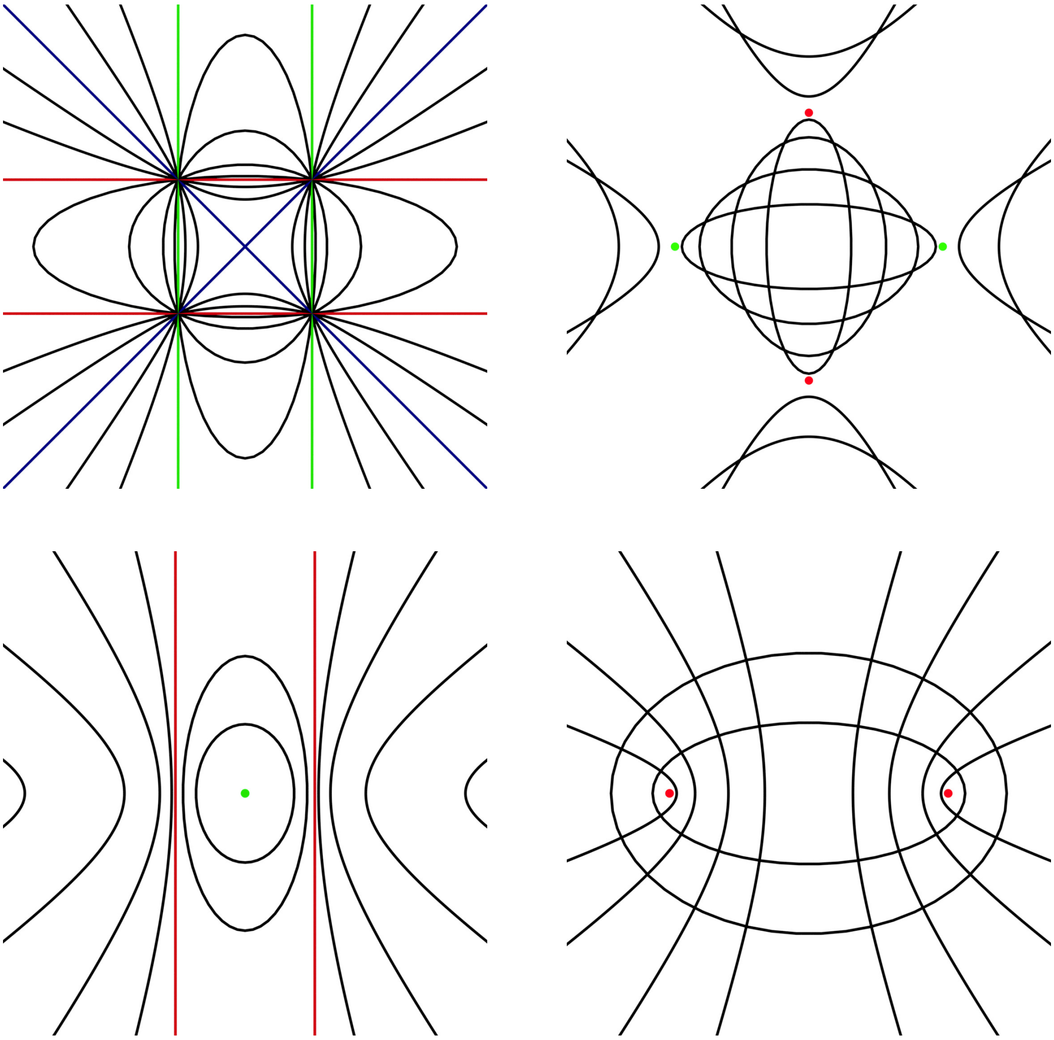

Figure 6.1. *Top:* A pencil of conics *(left)* containing three pairs of lines as degenerate conics (colored) and the corresponding dual pencil *(right)*.
Bottom: A pencil of conics *(left)* containing a real pair of lines, an imaginary pair of lines, and a pair of complex conjugate lines intersecting in a real point as degenerate conics, and the corresponding dual pencil *(right)*.

It is a line in the *projective space of quadrics of* $\mathbb{RP}^N$. In the following, we additionally assume a pencil of quadrics to be *non-degenerate*, i.e., not exclusively consisting of degenerate quadrics, in which case it contains at most $N+1$ degenerate quadrics (exactly $N+1$ counting imaginary solutions and multiplicity).

A point contained in two quadrics from a pencil of quadrics is called a *base point*. It is then contained in every quadric of the pencil. The variety of base points has codimension (at least) 2.

- For a generic point there exists a unique quadric from the pencil containing that point.
- For a generic hyperplane on the other hand there exist N quadrics from the pencil tangent to that hyperplane (counting imaginary solutions and multiplicity).

The different points of tangency of a single hyperplane are conjugate.

Lemma 6.2. *Let $(\mathcal{Q}_\lambda)_{\lambda\in\mathbb{RP}1}$ be a pencil of quadrics. Let Π be a common tangent plane of two distinct quadrics from the pencil touching them in the points $\boldsymbol{x}_1$ and $\boldsymbol{x}_2$, respectively. Then $\boldsymbol{x}_1$ and $\boldsymbol{x}_2$ are conjugate.*

While a single quadric induces the notion of polarity, a pencil of quadrics induces the following relation.

Lemma 6.3. *Let $(\mathcal{Q}_\lambda)_{\lambda\in\mathbb{RP}1}$ be a pencil of quadrics. Let $\boldsymbol{x}$ be a point. Then the polar hyperplanes with respect to all quadrics from the pencil intersect in a common subspace U of codimension (at most) 2. Vice versa, all polar hyperplanes of points in U contain the point $\boldsymbol{x}$.*

Remark 6.3. Generically a pencil of quadrics defines a map $x \mapsto U$ of points to codimension 2 subspaces. Note that every point in U is conjugate to x with respect to every quadric from the pencil.

Remark 6.4. The classification of pencils of quadrics in $\mathbb{RP}^N$ can be done by the theory of *elementary divisors* [Ki, Ca], or, for $N = 2$, by more elementary methods [Le].

Dual pencils of quadrics

The pencil of quadrics $\mathcal{Q}_1 \wedge \mathcal{Q}_2$ induces a *dual pencil of quadrics* (see Figure 6.1, *right*)

$$(\mathcal{Q}_1 \wedge \mathcal{Q}_2)^\star = \left(\mathcal{Q}^\star_{[\lambda_1,\lambda_2]}\right)_{[\lambda_1,\lambda_2]\in\mathbb{RP}^1}.$$

Note that a dual pencil of quadrics is itself not a pencil of quadrics.

- For a generic hyperplane there exists a unique quadric from the dual pencil tangent to that hyperplane.
- For a generic point there exist N quadrics from the dual pencil through that point (counting imaginary solutions and multiplicity).

By dualization of Lemma 6.2 we obtain the following statement:

Lemma 6.4. *Let $(\mathcal{Q}_\lambda)_{\lambda\in\mathbb{RP}1}$ be a dual pencil of quadrics. Let $\boldsymbol{x}$ be a point of intersection of two quadrics from the dual pencil and Π_1 and Π_1 the two tangent planes at $\boldsymbol{x}$, respectively. Then Π_1 and Π_2 are orthogonal with respect to every quadric in the pencil.*

And by dualization of Lemma 6.3:

Lemma 6.5. *Let Π be a hyperplane. Then all poles of Π (with respect to all quadrics from the dual pencil) lie on a common line ℓ. Vice versa, all poles of hyperplanes containing the line ℓ lie in Π.*

Remark 6.5. Generically, a dual pencil of quadrics defines a map $\Pi \mapsto \ell$ of hyperplanes into the space of lines. Note that the line ℓ is orthogonal to the hyperplane Π with respect to every quadric from the dual pencil in the sense that every hyperplane containing ℓ is orthogonal to Π.

Confocal quadrics

From the projective point of view, *confocal quadrics* can be introduced on every Cayley-Klein space.

Definition 6.6. *Let $\mathcal{Q} \subset \left(\mathbb{RP}^N\right)^*$ be an (at most once degenerate) absolute quadric on the dual projective space. Then a dual pencil of quadrics in $\mathbb{RP}^N$ is called a* confocal pencil of quadrics *if it contains the absolute quadric $\mathcal{Q}^\star$.*

Remark 6.6. The well-known metric/optical properties of confocal quadrics follow from this definition. For the two-dimensional case of confocal conics in hyperbolic and elliptic space see, e.g., [Iz].

From Lemma 6.4 we immediately find:

Proposition 6.7. *Any two confocal quadrics intersect orthogonally.*

Together with the fact that, generically, in a point of space there intersect N confocal quadrics, we find, that this definition of confocal quadrics again constitutes special orthogonal coordinate systems.

Finally, we convince ourselves that our main example from Section 4.1 of Euclidean confocal quadrics is indeed a dual pencil containing the absolute quadric. The absolute quadric on the dual space is given by the quadratic form

$$r(x) = x_1^2 + \ldots + x_N^2 = 0,$$

while a generic quadric on the dual space may be written as

$$q(x) = a_1 x_1 + \ldots + a_N x_N^2 - x_{N+1}^2 = 0.$$

with some $a_1 < \ldots < a_N$. Therefore, a generic pencil containing the absolute quadric is given by

$$q(x) + \lambda r(x) = 0 \qquad \lambda \in \mathbb{R} \cup \{\infty\}$$

After dualization, and introducing affine coordinates ($x_{N+1} = 1$) we obtain the generic form of a dual pencil in Euclidean space containing the absolute quadric

$$\frac{x_1^2}{a_1 + \lambda} + \ldots + \frac{x_N^2}{a_N + \lambda} = 1,$$

which coincides with (4.1).

6.4 A discrete dynamical system from dual pencils

Let $(\mathcal{Q}_\lambda)_{\lambda \in \mathbb{RP}1}$ be a dual pencil of quadrics. Take N arbitrary discrete subfamilies of quadrics by choosing maps

$$u_k : \left(\tfrac{1}{2}\mathbb{Z} + \tfrac{1}{4}\right) \to \mathbb{RP}^1.$$

On $\left(\mathbb{Z}^N \cup \left(Z + \frac{1}{2}\right)^N\right) \times \mathbb{RP}^N$ define the maps

$$C_{\boldsymbol{\sigma}} : (\boldsymbol{n}, \boldsymbol{x}) \mapsto \left(\boldsymbol{n} + \tfrac{1}{2}\boldsymbol{\sigma}, \bigcap_{k=1}^{N} \pi_{\mathcal{Q}_{u_k(n_k + \frac{1}{4}\sigma_k)}}(\boldsymbol{x})\right).$$

for $\boldsymbol{\sigma} \in \{\pm 1\}^N$. It maps a point on the square lattice $\mathbb{Z}^N$ to an adjacent point on the dual square lattice $\left(\mathbb{Z} + \frac{1}{2}\right)^N$ via polarity with respect to N quadrics from the dual pencil, and vice versa. We may propagate one initial value for $(\boldsymbol{x}, \boldsymbol{n})$ throughout the whole pair of dual lattices using this map. To see that this results in a well-defined pair of dual discrete nets

$$\boldsymbol{x} : \mathbb{Z}^N \cup \left(\mathbb{Z} + \tfrac{1}{2}\right)^N \to \mathbb{RP}^N, \quad \left(\boldsymbol{n} + \tfrac{1}{2}\boldsymbol{\sigma}, \boldsymbol{x}\left(\boldsymbol{n} + \tfrac{1}{2}\boldsymbol{\sigma}\right)\right) = C_{\boldsymbol{\sigma}}(\boldsymbol{n}, \boldsymbol{x}(\boldsymbol{n})),$$

that does not depend on the path along which this construction is applied, we show the following closedness condition:

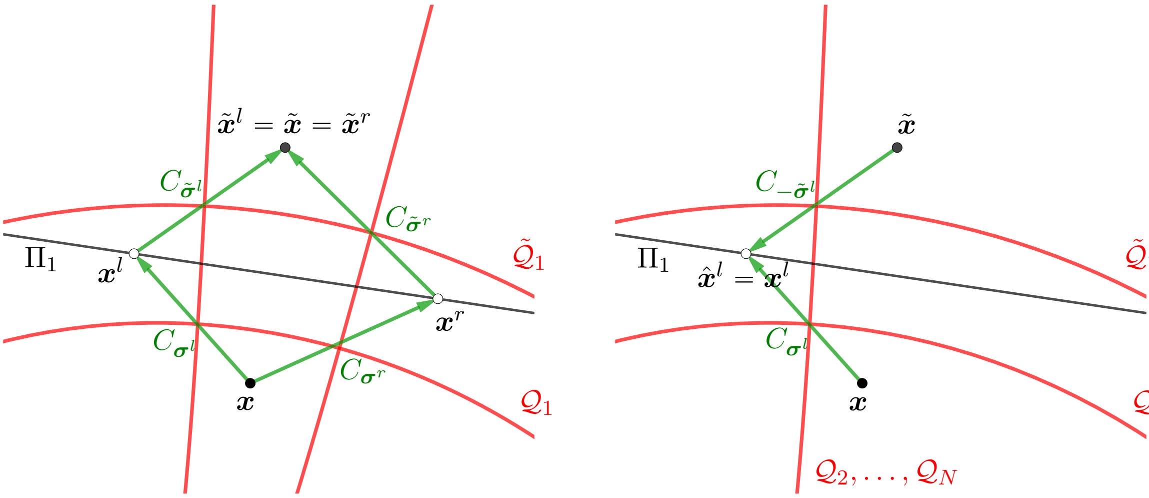

Figure 6.2. Closedness of the discrete dynamical system defined by sequences from a dual pencil of quadrics.

Theorem 6.8. *The maps C satisfy:*

(i) $\quad C_{\boldsymbol{\sigma}} \circ C_{-\boldsymbol{\sigma}} = \mathrm{id}, \qquad$ *for any* $\boldsymbol{\sigma} \in \{\pm 1\}^N$.

(ii) $\quad C_{\tilde{\boldsymbol{\sigma}}^l} \circ C_{\boldsymbol{\sigma}^l} = C_{\tilde{\boldsymbol{\sigma}}^r} \circ C_{\boldsymbol{\sigma}^r}, \qquad$ *for any* $\boldsymbol{\sigma}^l, \tilde{\boldsymbol{\sigma}}^l, \boldsymbol{\sigma}^r, \tilde{\boldsymbol{\sigma}}^r \in \{\pm 1\}^N$
with $\frac{1}{2}(\boldsymbol{\sigma}^l + \tilde{\boldsymbol{\sigma}}^l) = \frac{1}{2}(\boldsymbol{\sigma}^r + \tilde{\boldsymbol{\sigma}}^r) = \pm \boldsymbol{e}_i$
for some $i = 1, \ldots, N$.

Proof.

(i) This identity is the involutivity of the polarity relation $\pi^\star_{\mathcal{Q}} \circ \pi_{\mathcal{Q}} = \mathrm{id}$ for any (non-degenerate) quadric $\mathcal{Q} \subset \mathbb{R}\mathrm{P}^N$.

(ii) W.l.o.g. $\frac{1}{2}(\boldsymbol{\sigma}^l, \tilde{\boldsymbol{\sigma}}^l) = \frac{1}{2}(\boldsymbol{\sigma}^r, \tilde{\boldsymbol{\sigma}}^r) = \boldsymbol{e}_1$. Let $\boldsymbol{x} \in \mathbb{R}\mathrm{P}^N$ and define $\boldsymbol{x}^l, \tilde{\boldsymbol{x}}^l, \boldsymbol{x}^r, \tilde{\boldsymbol{x}}^r$ by (see Figure 6.2 (*left*))

$$\boldsymbol{x} \xmapsto{C_{\boldsymbol{\sigma}^l}} \boldsymbol{x}^l \xmapsto{C_{\tilde{\boldsymbol{\sigma}}^l}} \tilde{\boldsymbol{x}}^l,$$
$$\boldsymbol{x} \xmapsto{C_{\boldsymbol{\sigma}^r}} \boldsymbol{x}^r \xmapsto{C_{\tilde{\boldsymbol{\sigma}}^r}} \tilde{\boldsymbol{x}}^r.$$

Further define

$$\mathcal{Q}_1 = \mathcal{Q}_{u_1\left(n_1 + \frac{1}{4}\right)} = \mathcal{Q}_{u_1\left(n_1 + \frac{1}{4}\sigma^l_1\right)} = \mathcal{Q}_{u_1\left(n_1 + \frac{1}{4}\sigma^r_1\right)},$$
$$\tilde{\mathcal{Q}}_1 = \mathcal{Q}_{u_1\left(n_1 + \frac{3}{4}\right)} = \mathcal{Q}_{u_1\left(n_1 + \frac{3}{4}\sigma^l_1\right)} = \mathcal{Q}_{u_1\left(n_1 + \frac{3}{4}\sigma^r_1\right)},$$

and $\tilde{\boldsymbol{x}}$ by

$$\boldsymbol{x} \xmapsto{\pi_{\mathcal{Q}_1}} \Pi_1 \xmapsto{\pi_{\tilde{\mathcal{Q}}_1}} \tilde{\boldsymbol{x}}.$$

We show that $\tilde{\boldsymbol{x}}^l = \tilde{\boldsymbol{x}}$ (and by symmetry $\tilde{\boldsymbol{x}}^r = \tilde{\boldsymbol{x}}$), i.e.,

$$C_{\tilde{\boldsymbol{\sigma}}^l} \circ C_{\boldsymbol{\sigma}^l} = \pi_{\tilde{\mathcal{Q}}_1} \circ \pi_{\mathcal{Q}_1} = C_{\tilde{\boldsymbol{\sigma}}^r} \circ C_{\boldsymbol{\sigma}^r}.$$

Due to (i) we may equivalently show that with $\hat{\boldsymbol{x}}^l := C_{-\tilde{\boldsymbol{\sigma}}^l}(\tilde{\boldsymbol{x}})$ we have $\boldsymbol{x}^l = \hat{\boldsymbol{x}}^l$ (see Figure 6.2 (*right*)). Denote

$$\mathcal{Q}_k := \mathcal{Q}_{u_k\left(n_k + \frac{1}{4}\sigma^l_k\right)}, \qquad k = 2, \ldots, N$$

and

$$\Pi_k := \pi_{\mathcal{Q}_k}(\boldsymbol{x}), \quad \tilde{\Pi}_k := \pi_{\mathcal{Q}_k}(\tilde{\boldsymbol{x}}), \qquad k = 2, \ldots, N.$$

We now show that

$$\Pi_k \cap \tilde{\Pi}_k \subset \Pi_1.$$

Indeed, let ℓ be the line through $\boldsymbol{x}$ and $\tilde{\boldsymbol{x}}$, and let $\boldsymbol{y} \in \Pi_k \cap \tilde{\Pi}_k$ for some $k = 2, \ldots, N$. Then, from the involutivity of the polarity relation, we get $\ell \subset \pi_{\mathcal{Q}_k}(\boldsymbol{y})$. Since $\mathcal{Q}_1, \tilde{\mathcal{Q}}_1, \mathcal{Q}_k$ come from a dual pencil of quadrics, this implies, by Lemma 6.9, that the pole of $\pi_{\mathcal{Q}_k}(\boldsymbol{y})$ with respect to $\mathcal{Q}_k$ must lie on Π_1, i.e.,

$$y = \pi_{\mathcal{Q}_k} \circ \pi_{\mathcal{Q}_k}(\boldsymbol{y}) \in \Pi_1.$$

Thus, we have

$$\Pi_2 \cap \tilde{\Pi}_2, \ldots, \Pi_N \cap \tilde{\Pi}_N \subset \Pi_1.$$

But the intersection of $N-1$ subspaces of dimension $N-2$ in an $(N-1)$-dimensional subspace generically is a point. Therefore,

$$\bigcap_{k=2}^{N} \Pi_k \cap \tilde{\Pi}_k = \bigcap_{k=1}^{N} \Pi_k = \boldsymbol{x}^l$$

and, on the other hand,

$$\bigcap_{k=2}^{N} \Pi_k \cap \tilde{\Pi}_k = \Pi_1 \cap \bigcap_{k=2}^{N} \tilde{\Pi}_k = \hat{\boldsymbol{x}}^l.$$

□

Lemma 6.9. *Let $\mathcal{Q}, \tilde{\mathcal{Q}}, \mathcal{Q}'$ be three non-degenerate quadrics from a dual pencil of quadrics. Let Π be a hyperplane and set*

$$\boldsymbol{x} := \pi_{\mathcal{Q}}(\Pi), \qquad \tilde{\boldsymbol{x}} := \pi_{\tilde{\mathcal{Q}}}(\Pi).$$

Let ℓ be the line through $\boldsymbol{x}$ and $\tilde{\boldsymbol{x}}$. Then

$$\pi_{\mathcal{Q}'}(\Pi) \in \ell.$$

Furthermore, let Π' be a hyperplane with $\ell \subset \Pi'$. Then

$$\pi_{\mathcal{Q}'}(\boldsymbol{x}) \in \Pi.$$

Proof. Follows from Lemma 6.5. □

Discrete confocal coordinate systems, as described in Section 4.2 constitute a special case of this construction. Indeed, as we have seen in Section 6.3, the system of (Euclidean) confocal quadrics is a dual pencil, while equation (4.6) describes the polarity of adjacent points from dual lattices with respect to quadrics from this pencil.

7 Checkerboard incircular nets

7.1 Incircular nets and discrete confocal conics

Incircular nets are defined as congruences of straight lines in the plane with the combinatorics of the square grid such that each elementary quadrilateral admits an incircle.

Definition 7.1. *A discrete net $f : \mathbb{Z}^2 \supset U \to \mathbb{R}^2$ is called an* incircular net *if*

(i) The points $f_{i,j}$ with $i = \text{const}$, respectively $j = \text{const}$, lie on straight lines, preserving the order.

(ii) Every elementary quadrilateral $(f_{i,j}, f_{i+1,j}, f_{i+1,j+1}, f_{i,j+1})$ has an incircle.

All lines of an incircular net touch a common conic α (see Figure 7.1). The relation to confocal conics is revealed by the classical Graves-Chasles theorem:

Theorem 7.2. *Suppose that all sides of a complete quadrilateral touch a conic α. Denote pairs of its opposite vertices by $\{\boldsymbol{a}, \boldsymbol{c}\}$, $\{\boldsymbol{b}, \boldsymbol{d}\}$, and $\{\boldsymbol{e}, \boldsymbol{f}\}$ (see Figure 7.2). Then, the following four properties are equivalent:*

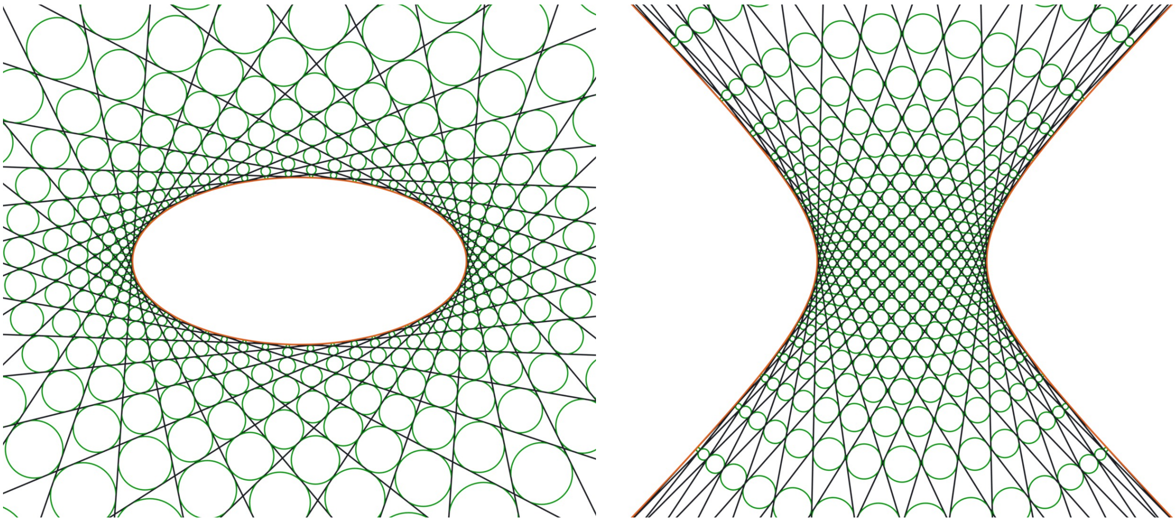

Figure 7.1. Periodic incircular nets. All lines are tangent to a common conic.

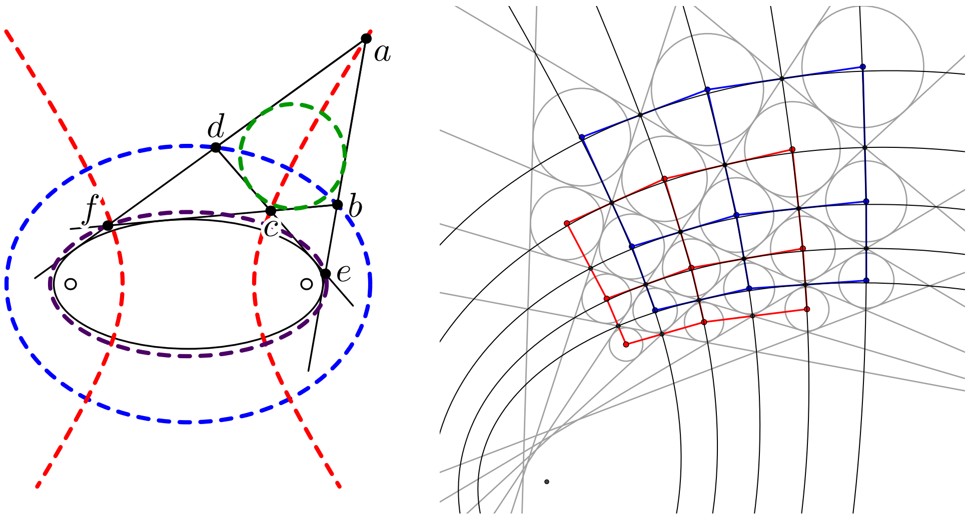

Figure 7.2. *Left:* Graves–Chasles theorem. *Right:* A pair of dual discrete nets from incircle centers of an incircular net.

(i) ($\boldsymbol{abcd}$) *circumscribes a circle,*

(ii) Points $\boldsymbol{a}$ *and* $\boldsymbol{c}$ *lie on a conic confocal with* α*,*

(iii) Points $\boldsymbol{b}$ *and* $\boldsymbol{d}$ *lie on a conic confocal with* α*,*

(iv) Points $\boldsymbol{e}$ *and* $\boldsymbol{f}$ *lie on a conic confocal with* α*.*

Remark 7.1. The Graves-Chasles theorem also holds in the hyperbolic and elliptic plane and is best proven in a projective setting [Iz].

Thus, the vertices of incircular nets lie on conics confocal with α (see Figure 7.2 (*left*)). Furthermore, the incircle centers constitute pairs of dual discrete nets (see Figure 7.2 (*right*)) that possess the following properties:

Proposition 7.3 (Chapter 1: Theorem A.2, Chapter 2: Proposition 8.2 and Proposition 8.4)**.** *Let* $\boldsymbol{x} : \mathbb{Z}^2 \cup \left(\mathbb{Z} + \frac{1}{2}\right)^2 \to \mathbb{R}^2$ *be the pair of dual discrete nets of incircle centers of an incircular net. Then*

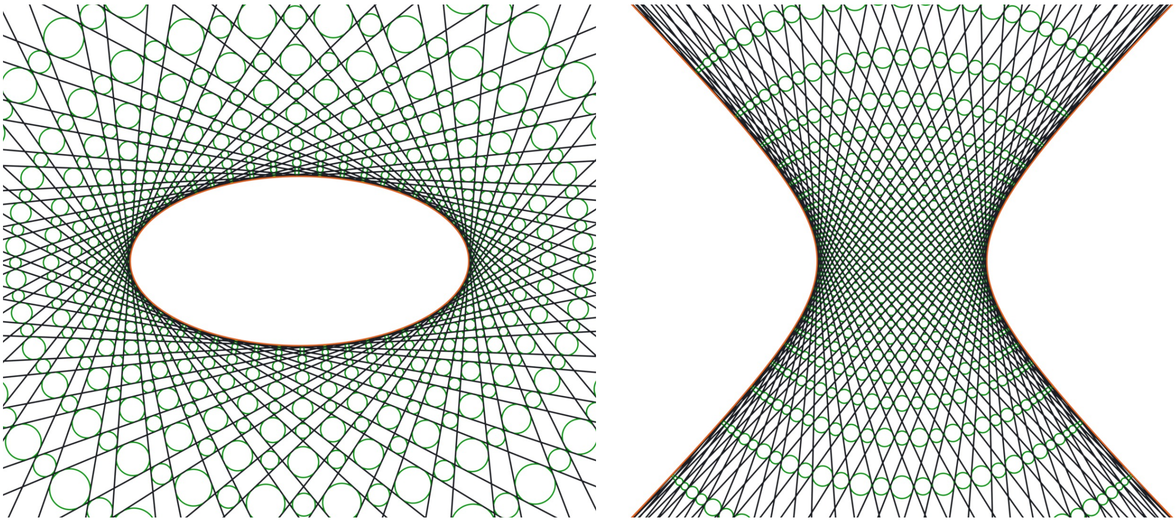

Figure 7.3. Periodic confocal checkerboard incircular nets.

(i) $\boldsymbol{x}$ *is an orthogonal pair of dual discrete nets from a system of discrete confocal coordinates,*

(ii) *each of the two subnets of* $\boldsymbol{x}$ *is circular and conical, i.e., opposite angles in each quadrilateral and at each vertex sum up to* $\frac{\pi}{2}$*,*

(iii) *each of the two subnets of* $\boldsymbol{x}$ *is a discrete Koenigs net.*

7.2 Checkerboard incircular nets

Planar *Laguerre geometry* is the geometry of oriented lines, oriented circles, and their oriented contact in the Euclidean plane. A projective model of Laguerre geometry is given by the *Blaschke cylinder*, a degenerate quadric $\mathcal{Z} \subset \mathbb{R}\mathrm{P}^3$ of signature $(2, 1, 1)$. Every point on $\mathcal{Z}$ corresponds to an oriented line, while every plane constitutes an oriented circle.

Due to the combinatorial structure of incircular nets, their lines and circles may not be consistently oriented in such a manner that they are in oriented contact. However, *checkerboard incircular nets*, which constitute the Laguerre geometric generalization of incircular nets exhibit this feature. Once again, the (oriented) lines of a checkerboard incircular net have the combinatorics of the square grid, but it is only required that every second quadrilateral (in a checkerboard manner) admits an incircle (see Figure 7.3).

All lines of a checkerboard incircular net are tangent to a hypercycle (see Figure 7.4 and Chapter 3: Theorem 3.5), which are curves corresponding to the intersection of the Blaschke cylinder with another quadric. Thus, hypercycles are in correspondence to base curves of pencils of quadrics in $\mathbb{R}\mathrm{P}^3$ that contain the Blaschke cylinder.

Confocal checkerboard incircular nets constitute an important subclass of checkerboard incircular nets and are characterized by their lines being tangent to a conic as in the case of incircular nets (see Figure 7.3). The corresponding base curve of the hypercycle can be parametrized by elliptic functions, which in turn leads to explicit parametrizations for confocal checkerboard incircular nets, and all checkerboard incircular nets that are obtained under Laguerre transformation of those (see Chapter 3: Section 5).

Different generalizations of checkerboard incircular nets to three dimensions are described in [ABST].

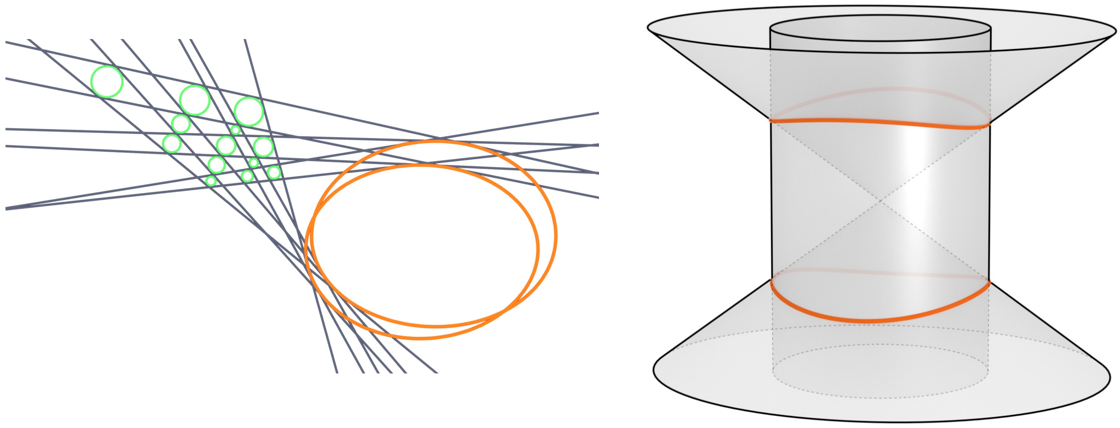

Figure 7.4. *Left:* All lines of a checkerboard incircular net are tangent to a common hypercycle. *Right:* The corresponding base curve as the intersection of the Blaschke cylinder with another quadric.

8 Conclusion

In this thesis we introduce discrete confocal coordinate systems, which are characterized, as in the smooth case, by factorizability and orthogonality.

The main open questions are whether the theory of pairs of discrete nets and in particular the theory of discrete orthogonal coordinate systems using the novel discrete orthogonality constraint can be further extended.

- Discrete surfaces with planar curvature lines employing the novel orthogonality constraint, in particular discrete Dupin cyclides, as well as discrete focal conics are the subject of a forthcoming publication. Are there more interesting examples making use of the novel orthogonality constraint?
- Is there a sensible definition for a discrete first and second fundamental form and corresponding principal curvatures for pairs of discrete nets? The discrete orthogonality corresponds to a diagonal first fundamental form, while the discrete Lamé coefficients provide the remaining coefficients. Conjugacy (planar faces) corresponds to a diagonal second fundamental form, while certain additional factorization properties of discrete confocal coordinates suggest the form of the remaining coefficients.
- Is there a geometric characterization of the discrete isothermicity condition for pairs of discrete nets, e.g., a discrete Christoffel dual, and is there a corresponding notion of discrete Koenigs nets?
- Is the novel discrete orthogonality constraint applicable to a discrete theory of separability in Laplace-type equations?

Chapter 1

On a discretization of confocal quadrics. I. An integrable systems approach

Alexander I. Bobenko[1], Wolfgang K. Schief[2], Yuri B. Suris[1], Jan Techter[1]

[1]Institut für Mathematik, TU Berlin,
Str. des 17. Juni 136, 10623 Berlin, Germany

[2]School of Mathematics and Statistics and
Australian Research Council Centre of Excellence for
Mathematics and Statistics of Complex Systems,
The University of New South Wales, Sydney, NSW 2052, Australia

Abstract. Confocal quadrics lie at the heart of the system of confocal coordinates (also called elliptic coordinates, after Jacobi). We suggest a discretization which respects two crucial properties of confocal coordinates: separability and all two-dimensional coordinate subnets being isothermic surfaces (that is, allowing a conformal parametrization along curvature lines, or, equivalently, supporting orthogonal Koenigs nets). Our construction is based on an integrable discretization of the Euler-Poisson-Darboux equation and leads to discrete nets with the separability property, with all two-dimensional subnets being Koenigs nets, and with an additional novel discrete analog of the orthogonality property. The coordinate functions of our discrete nets are given explicitly in terms of gamma functions.

Acknowledgements. This research is supported by the DFG Collaborative Research Center TRR 109 "Discretization in Geometry and Dynamics". We would like to acknowledge the stimulating role of the research visit to TU Berlin by I. Taimanov in summer 2014. In our construction, we combine the fact that the confocal coordinate system satisfies continuous Euler-Poisson-Darboux equations, which we learned from I. Taimanov, with the discretization of Euler-Poisson-Darboux equations recently proposed (in a different context) by one of the authors [KS2].

The pictures in this paper were generated using `blender`, `matplotlib`, `geogebra`, and `inkscape`.

Journal of Integrable Systems, Volume 1, Issue 1, January 2016, xyw005,
`https://doi.org/10.1093/integr/xyw005`

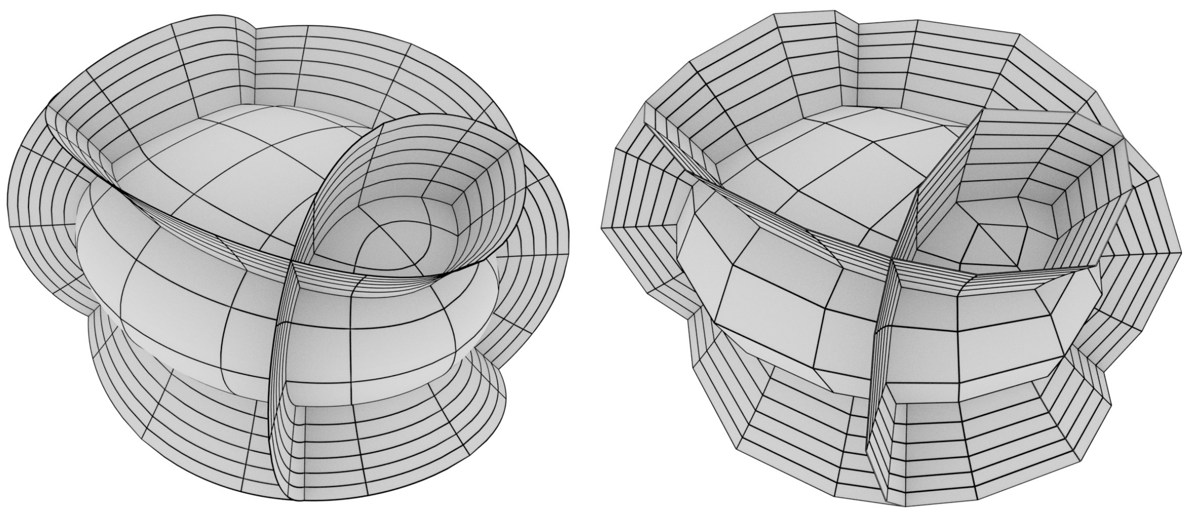

Figure 0.1. Left: three quadrics of different signature from a family of confocal quadrics in $\mathbb{R}^3$. Right: the corresponding three discrete quadrics from a family introduced in the present paper.

1 Introduction

Confocal quadrics in $\mathbb{R}^N$ belong to the favorite objects of classical mathematics, due to their beautiful geometric properties and numerous relations and applications to various branches of mathematics. To mention just a few well-known examples:

- Optical properties of quadrics and their confocal families were discovered by the ancient Greeks and continued to fascinate mathematicians for many centuries, culminating in the famous Ivory and Chasles theorems from 19th century given a modern interpretation by Arnold [Ar].
- Dynamical systems: integrability of geodesic flows on quadrics (discovered by Jacobi) and of billiards in quadrics was given a far reaching generalization, with applications to the spectral theory, by Moser [Mo].
- Gravitational properties of ellipsoids were studied in detail starting with Newton and Ivory, see [Ar, Appendix 15], [FT, Part 8], and are based to a large extent on the geometric properties of confocal quadrics.
- Quadrics in general and confocal systems of quadrics in particular serve as favorite objects in differential geometry. They deliver a non-trivial example of isothermic surfaces which form one of the most interesting classes of “integrable” surfaces, that is, surfaces described by integrable differential equations and possessing a rich theory of transformations with remarkable permutability properties.
- Confocal quadrics lie at the heart of the system of confocal coordinates which allows for separation of variables in the Laplace operator. As such, they support a rich theory of special functions including Lamé functions and their generalizations [EMOT].

In the present paper, we are interested in a discretization of a system of confocal quadrics, or, what is the same, of a system of confocal coordinates in $\mathbb{R}^N$. In general, coordinate systems are instances of *smooth nets*, that is, maps $\mathbb{R}^M \supset U \to \mathbb{R}^N$. Discretizing them consists of finding suitable approximating *discrete nets*, that is, maps $\mathbb{Z}^M \supset U \to \mathbb{R}^N$. According to the philosophy of structure preserving discretization [BS], it is crucial not to follow the path of a straightforward discretization of differential equations, but rather to discretize a well chosen collection of essential geometric properties. In the case of confocal quadrics, the choice of properties to be preserved in the course of discretization becomes especially difficult, due to the above-mentioned abundance of complementary geometric and analytic features.

A number of attempts to discretize quadrics in general and confocal systems of quadrics in particular are available in the literature. In [Ts] a discretization of the defining property of a conic as an image of a circle under a projective transformation is considered. Since a natural discretization of a circle is a regular polygon, one ends up with a class of discrete curves which are projective images of regular polygons. More sophisticated geometric constructions are developed in [AB] and lead to a very interesting class of quadrilateral nets in a plane and in space, with all quadrilaterals possessing an incircle, resp. all hexahedra possessing an inscribed sphere. The rich geometric content of these constructions still waits for an adequate analytic description.

Our approach here is based on a discretization of the classical Euler-Poisson-Darboux equation which has been introduced in [KS2] in the context of discretization of semi-Hamiltonian systems of hydrodynamic type. The discrete Euler-Poisson-Darboux equation is integrable in the sense of multi-dimensional consistency [BS], which, in turn, gives rise to Darboux-type transformations with remarkable permutability properties. As we will demonstrate, the integrable nature of the discrete Euler-Poisson-Darboux equation is reflected in the preservation of a suite of algebraic and geometric properties of the confocal coordinate systems.

Our proposal takes as a departure point two properties of the confocal coordinates: they are separable, and all two-dimensional coordinate subnets are isothermic surfaces (which is equivalent to being conjugate nets with equal Laplace invariants and with orthogonal coordinate curves). We propose here a novel concept of discrete isothermic nets. Remarkably, the incircular nets of [AB] turn out to be another instance of this geometry, see Appendix A. Discretization of confocal coordinate systems based on more general curvature line parametrizations will be addressed in [BSST2].

2 Euler-Poisson-Darboux equation

Definition 2.1. *Let $U \subset \mathbb{R}^M$ be open and connected. We say that a net*

$$\boldsymbol{x} : U \to \mathbb{R}^N, \quad (u_1, \ldots, u_M) \mapsto (x_1, \ldots, x_N)$$

satisfies the Euler-Poisson-Darboux system *if all its two-dimensional subnets satisfy the (vector) Euler-Poisson-Darboux equation with the same parameter γ:*

$$\frac{\partial^2 \boldsymbol{x}}{\partial u_i \partial u_j} = \frac{\gamma}{u_i - u_j} \left(\frac{\partial \boldsymbol{x}}{\partial u_j} - \frac{\partial \boldsymbol{x}}{\partial u_i} \right) \tag{EPD$_\gamma$}$$

for all $i, j \in \{1, \ldots, M\}$, $i \neq j$.

For any s distinct indices $i_1, \ldots, i_s \in \{1, \ldots, M\}$, we write

$$U_{i_1 \ldots i_s} := \{(u_{i_1}, \ldots, u_{i_s}) \in \mathbb{R}^s \mid (u_1, \ldots, u_M) \in U\}.$$

Definition 2.2. *A two-dimensional subnet of a net $\boldsymbol{x} : \mathbb{R}^M \supset U \to \mathbb{R}^N$ corresponding to the coordinate directions $i, j \in \{1, \ldots, M\}$, $i \neq j$, is called* a Koenigs net*, or, classically,* a conjugate net with equal Laplace invariants*, if there exists a function $\nu : U_{ij} \to \mathbb{R}_+$ such that*

$$\frac{\partial^2 \boldsymbol{x}}{\partial u_i \partial u_j} = \frac{1}{\nu} \frac{\partial \nu}{\partial u_j} \frac{\partial \boldsymbol{x}}{\partial u_i} + \frac{1}{\nu} \frac{\partial \nu}{\partial u_i} \frac{\partial \boldsymbol{x}}{\partial u_j}. \tag{2.1}$$

Proposition 2.3. *Let $\boldsymbol{x} : \mathbb{R}^M \supset U \to \mathbb{R}^N$ be a net satisfying the Euler-Poisson-Darboux system* (EPD$_\gamma$)*. Then all two-dimensional subnets of $\boldsymbol{x}$ are Koenigs nets.*

Proof. The function $\nu(u_i, u_j) = |u_i - u_j|^\gamma$ solves

$$\frac{1}{\nu} \frac{\partial \nu}{\partial u_i} = \frac{\gamma}{u_i - u_j}, \qquad \frac{1}{\nu} \frac{\partial \nu}{\partial u_j} = \frac{\gamma}{u_j - u_i},$$

thus the Euler-Poisson-Darboux system (EPD$_\gamma$) is of the Koenigs form (2.1). □

Remark 2.1. Eisenhart classified conjugate nets in $\mathbb{R}^3$ with all two-dimensional coordinate surfaces being Koenigs nets [Ei1]. The generic case is described by solutions of the Euler-Poisson-Darboux system (EPD$_\gamma$) with an arbitrary coefficient γ.

3 Confocal coordinates

For given $a_1 > a_2 > \cdots > a_N > 0$, we consider the one-parameter family of confocal quadrics in $\mathbb{R}^N$ given by

$$Q_\lambda = \left\{ \boldsymbol{x} = (x_1, \ldots, x_N) \in \mathbb{R}^N : \sum_{k=1}^{N} \frac{x_k^2}{a_k + \lambda} = 1 \right\}, \quad \lambda \in \mathbb{R}. \tag{3.1}$$

Note that the quadrics of this family are centered at the origin and have the principal axes aligned along the coordinate directions. For a given point $\boldsymbol{x} = (x_1, \ldots, x_N) \in \mathbb{R}^N$ with $x_1 x_2 \ldots x_N \neq 0$, equation $\sum_{k=1}^N x_k^2/(a_k + \lambda) = 1$ is, after clearing the denominators, a polynomial equation of degree N in λ, with N real roots $u_1, \ldots, u_N$ lying in the intervals

$$-a_1 < u_1 < -a_2 < u_2 < \cdots < -a_N < u_N,$$

so that

$$\sum_{k=1}^{N} \frac{x_k^2}{\lambda + a_k} - 1 = -\frac{\prod_{m=1}^N (\lambda - u_m)}{\prod_{m=1}^N (\lambda + a_m)}. \tag{3.2}$$

These N roots correspond to the N confocal quadrics of the family (3.1) that intersect at the point $\boldsymbol{x} = (x_1, \ldots, x_N)$:

$$\sum_{k=1}^{N} \frac{x_k^2}{a_k + u_i} = 1, \quad i = 1, \ldots, N \quad \Leftrightarrow \quad \boldsymbol{x} \in \bigcap_{i=1}^{N} Q_{u_i}. \tag{3.3}$$

Each of the quadrics Q_{u_i} is of a different signature. Evaluating the residue of the right-hand side of (3.2) at $\lambda = -a_k$, one can easily express x_k^2 through $u_1, \ldots, u_N$:

$$x_k^2 = \frac{\prod_{i=1}^N (u_i + a_k)}{\prod_{i \neq k} (a_k - a_i)}, \quad k = 1, \ldots, N. \tag{3.4}$$

Thus, for each point $(x_1, \ldots, x_N) \in \mathbb{R}^N$ with $x_1 x_2 \ldots x_N \neq 0$, there is exactly one solution $(u_1, \ldots, u_N) \in \mathcal{U}$ of (3.4), where

$$\mathcal{U} = \left\{ (u_1, \ldots, u_N) \in \mathbb{R}^N \mid -a_1 < u_1 < -a_2 < u_2 < \ldots < -a_N < u_N \right\}.$$

On the other hand, for each $(u_1, \ldots, u_N) \in \mathcal{U}$ there are exactly 2^N solutions $(x_1, \ldots, x_N) \in \mathbb{R}^N$, which are mirror symmetric with respect to the coordinate hyperplanes. In what follows, when we refer to a solution of (3.4), we always mean the solution with values in

$$\mathbb{R}_+^N = \left\{ (x_1, \ldots, x_N) \in \mathbb{R}^N \mid x_1 > 0, \ldots, x_N > 0 \right\}.$$

Thus, we are dealing with a parametrization of the first hyperoctant of $\mathbb{R}^N$, $\boldsymbol{x} : \mathcal{U} \ni (u_1, \ldots, u_N) \mapsto (x_1, \ldots, x_N) \in \mathbb{R}_+^N$, given by

$$x_k = \frac{\prod_{i=1}^{k-1} \sqrt{-(u_i + a_k)} \prod_{i=k}^{N} \sqrt{u_i + a_k}}{\prod_{i=1}^{k-1} \sqrt{a_i - a_k} \prod_{i=k+1}^{N} \sqrt{a_k - a_i}}, \quad k = 1, \ldots, N, \tag{3.5}$$

such that the coordinate hyperplanes $u_i = \text{const}$ are mapped to the respective quadrics given by (3.3). The coordinates $(u_1, \ldots, u_N)$ are called *confocal coordinates* (or *elliptic coordinates*, following Jacobi [Ja, Vorlesung 26]).

3.1 Confocal coordinates and isothermic surfaces

Proposition 3.1. *The net $\boldsymbol{x} : \mathcal{U} \to \mathbb{R}_+^N$ given by* (3.5) *satisfies the Euler-Poisson-Darboux system* (EPD_γ) *with $\gamma = \frac{1}{2}$. As a consequence, all two-dimensional subnets of $\boldsymbol{x}$ are Koenigs nets.*

Proof. The partial derivatives of (3.5) satisfy

$$\frac{\partial x_k}{\partial u_i} = \frac{1}{2}\frac{x_k}{(a_k+u_i)}. \tag{3.6}$$

From this we compute the second order partial derivatives for $i \neq j$:

$$\begin{aligned}\frac{\partial^2 x_k}{\partial u_i \partial u_j} &= \frac{1}{2(a_k+u_i)}\frac{\partial x_k}{\partial u_j} = \frac{x_k}{4(a_k+u_i)(a_k+u_j)} \\ &= \frac{x_k}{4(u_i-u_j)}\left(\frac{1}{a_k+u_j} - \frac{1}{a_k+u_i}\right) \\ &= \frac{1}{2(u_i-u_j)}\left(\frac{\partial x_k}{\partial u_j} - \frac{\partial x_k}{\partial u_i}\right).\end{aligned}$$

□

Proposition 3.2. *The net $\boldsymbol{x} : \mathcal{U} \to \mathbb{R}^N_+$ given by (3.5) is orthogonal, and thus gives a curvature line parametrization of any of its two-dimensional coordinate surfaces.*

Proof. With the help of (3.6), we compute, for $i \neq j$, the scalar product

$$\begin{aligned}\left\langle \frac{\partial \boldsymbol{x}}{\partial u_i}, \frac{\partial \boldsymbol{x}}{\partial u_j} \right\rangle &= \frac{1}{4}\sum_{k=1}^N \frac{x_k^2}{(a_k+u_i)(a_k+u_j)} \\ &= \frac{1}{4(u_i-u_j)}\sum_{k=1}^N \left(\frac{x_k^2}{a_k+u_j} - \frac{x_k^2}{a_k+u_i}\right) = 0,\end{aligned}$$

since $\boldsymbol{x}(u_1,\ldots,u_N)$ satisfies (3.3) for u_i and for u_j. □

We recall the following classical definition.

Definition 3.3. *A curvature line parametrized surface $\boldsymbol{x} : U_{ij} \to \mathbb{R}^N$ is called an* isothermic surface *if its first fundamental form is conformal, possibly upon a reparametrization of independent variables $u_i \mapsto \varphi_i(u_i)$, $u_j \mapsto \varphi_j(u_j)$, that is, if*

$$\frac{|\partial \boldsymbol{x}/\partial u_i|^2}{|\partial \boldsymbol{x}/\partial u_j|^2} = \frac{\alpha_i(u_i)}{\alpha_j(u_j)}$$

at every point $(u_i, u_j) \in U_{ij}$.

In other words, isothermic surfaces are characterized by the relations $\partial^2 \boldsymbol{x}/\partial u_i \partial u_j \in \operatorname{span}(\partial \boldsymbol{x}/\partial u_i, \partial \boldsymbol{x}/\partial u_j)$ and

$$\left\langle \frac{\partial \boldsymbol{x}}{\partial u_i}, \frac{\partial \boldsymbol{x}}{\partial u_j} \right\rangle = 0, \quad \left|\frac{\partial \boldsymbol{x}}{\partial u_i}\right|^2 = \alpha_i(u_i)s^2, \quad \left|\frac{\partial \boldsymbol{x}}{\partial u_j}\right|^2 = \alpha_j(u_j)s^2, \tag{3.7}$$

with a conformal metric coefficient $s : U_{ij} \to \mathbb{R}_+$ and with the functions α_i, α_j, each depending on the respective variable u_i, u_j only. These conditions may be equivalently represented as

$$\frac{\partial^2 \boldsymbol{x}}{\partial u_i \partial u_j} = \frac{1}{s}\frac{\partial s}{\partial u_j}\frac{\partial \boldsymbol{x}}{\partial u_i} + \frac{1}{s}\frac{\partial s}{\partial u_i}\frac{\partial \boldsymbol{x}}{\partial u_j}, \quad \left\langle \frac{\partial \boldsymbol{x}}{\partial u_i}, \frac{\partial \boldsymbol{x}}{\partial u_j} \right\rangle = 0.$$

Comparison with (2.1) shows that isothermic surfaces are nothing but orthogonal Koenigs nets.

Thus, Propositions 3.1, 3.2 immediately imply the first statement of the following proposition.

Proposition 3.4. *All two-dimensional coordinate surfaces $\boldsymbol{x} : \mathcal{U}_{ij} \to \mathbb{R}^N$ (for fixed values of u_m, $m \neq i, j$) of a confocal coordinate system are isothermic. Specifically, one has (3.7) with*

$$s = s(u_i, u_j) = |u_i - u_j|^{1/2}, \tag{3.8}$$

$$\frac{\alpha_i(u_i)}{\alpha_j(u_j)} = -\frac{\prod_{m\neq i,j}(u_i-u_m)}{\prod_{m=1}^N(u_i+a_m)} \cdot \frac{\prod_{m=1}^N(u_j+a_m)}{\prod_{m\neq i,j}(u_j-u_m)}. \tag{3.9}$$

Proof. Differentiate both sides of (3.2) with respect to u_i. Taking into account (3.6), we find:

$$\sum_{k=1}^{N} \frac{x_k^2}{(u_i + a_k)(\lambda + a_k)} = \frac{\prod_{m \neq i}(\lambda - u_m)}{\prod_{m=1}^{N}(\lambda + a_m)}.$$

Setting $\lambda = u_i$, we finally arrive at

$$\left|\frac{\partial \boldsymbol{x}}{\partial u_i}\right|^2 = \sum_{k=1}^{N} \left(\frac{\partial x_k}{\partial u_i}\right)^2 = \frac{1}{4} \sum_{k=1}^{N} \frac{x_k^2}{(u_i + a_k)^2} = \frac{1}{4} \frac{\prod_{m \neq i}(u_i - u_m)}{\prod_{m=1}^{N}(u_i + a_m)}. \tag{3.10}$$

This proves (3.7) with (3.8), (3.9). ☐

Remark 3.1. Darboux classified orthogonal nets in $\mathbb{R}^3$ whose two-dimensional coordinate surfaces are isothermic [Da2, Livre II, Chap. III–V] . He found several families, all satisfying the Euler-Poisson-Darboux system with coefficient $\gamma = \pm\frac{1}{2}, -1$, or -2. The family corresponding to $\gamma = \frac{1}{2}$ consists of confocal cyclides and includes the case of confocal quadrics (or their Möbius images).

3.2 Confocal coordinates and separability

From (3.5) we observe that confocal coordinates are described by very special (separable) solutions of Euler-Poisson-Darboux equations (EPD_γ). We will now show that the separability property is almost characteristic for confocal coordinates.

Proposition 3.5. *A separable function $x : \mathbb{R}^N \supset U \to \mathbb{R}$,*

$$x(u_1, \ldots, u_N) = \prod_{i=1}^{N} \rho_i(u_i) \tag{3.11}$$

is a solution of the Euler-Poisson-Darboux system (EPD_γ) *iff the functions $\rho_i : U_i \to \mathbb{R}$, $i = 1, \ldots, N$, satisfy*

$$\frac{\rho_i'(u_i)}{\rho_i(u_i)} = \frac{\gamma}{c + u_i} \tag{3.12}$$

for some $c \in \mathbb{R}$ and for all $u_i \in U_i$.

Proof. Computing the derivatives of (3.11) for $i = 1, \ldots, N$, we obtain:

$$\frac{\partial x}{\partial u_i} = x \cdot \frac{\rho_i'(u_i)}{\rho_i(u_i)},$$

and for the second derivatives ($i \neq j$):

$$\frac{\partial^2 x}{\partial u_i \partial u_j} = x \cdot \frac{\rho_i'(u_i)}{\rho_i(u_i)} \frac{\rho_j'(u_j)}{\rho_j(u_j)}. \tag{3.13}$$

On the other hand, x satisfies the Euler-Poisson-Darboux system (EPD_γ), which implies

$$\frac{\partial^2 x}{\partial u_i \partial u_j} = \frac{\gamma}{u_i - u_j} \left(\frac{\rho_j'(u_j)}{\rho_j(u_j)} - \frac{\rho_i'(u_i)}{\rho_i(u_i)}\right) x. \tag{3.14}$$

From (3.13) and (3.14) we obtain

$$u_i - u_j = \gamma \left(\frac{\rho_i(u_i)}{\rho_i'(u_i)} - \frac{\rho_j(u_j)}{\rho_j'(u_j)}\right),$$

or

$$\gamma \frac{\rho_i(u_i)}{\rho_i'(u_i)} - u_i = \gamma \frac{\rho_j(u_j)}{\rho_j'(u_j)} - u_j$$

for all $i, j = 1, ..., N$, $i \neq j$, and $(u_i, u_j) \in U_{ij}$. Thus, both the left-hand side and the right-hand side of the last equation do not depend on u_i, u_j. So, there exists a $c \in \mathbb{R}$ such that (3.12) is satisfied. ☐

For $\gamma = \frac{1}{2}$ general solutions of (3.12) are given, up to constant factors, by

$$\rho_i(u_i, c) = \sqrt{u_i + c} \qquad \text{for} \quad u_i > -c,$$

respectively by

$$\rho_i(u_i, c) = \sqrt{-(u_i + c)} \quad \text{for} \quad u_i < -c.$$

A separable solution of the Euler-Poisson-Darboux system (EPD_γ) with $\gamma = \frac{1}{2}$ finally takes the form

$$x(u_1, \ldots, u_N) = D \prod_{i=1}^{N} \rho_i(u_i, c)$$

with some $c \in \mathbb{R}$, and with a constant $D \in \mathbb{R}$, which is the product of all the constant factors of $\rho_i(u_i, c)$ mentioned above.

Proposition 3.6. *Let $a_1 > \cdots > a_N$ and set*

$$\mathcal{U} = \left\{(u_1, \ldots, u_N) \in \mathbb{R}^N \mid -a_1 < u_1 < -a_2 < u_2 < \cdots < -a_N < u_N\right\}.$$

a) *Let $x_k : \mathcal{U} \to \mathbb{R}_+$, $k = 1, \ldots, N$, be N independent separable solutions of the Euler-Poisson-Darboux system* (EPD_γ) *with $\gamma = \frac{1}{2}$ defined on $\mathcal{U}$ and satisfying there the following boundary conditions:*

$$\lim_{u_k \searrow (-a_k)} x_k(u_1, \ldots, u_N) = 0 \quad \textit{for} \quad k = 1, \ldots, N, \tag{3.15}$$

$$\lim_{u_{k-1} \nearrow (-a_k)} x_k(u_1, \ldots, u_N) = 0 \quad \textit{for} \quad k = 2, \ldots, N. \tag{3.16}$$

Then

$$x_k(u_1, \ldots, u_N) = D_k \prod_{i=1}^{N} \rho_i(u_i, a_k), \quad k = 1, \ldots, N, \tag{3.17}$$

with some $D_1, \ldots, D_N > 0$ and with

$$\rho_i(u_i, a_k) = \begin{cases} \sqrt{u_i + a_k} & \textit{for} \quad i \geqslant k, \\ \sqrt{-(u_i + a_k)} & \textit{for} \quad i < k. \end{cases}$$

Thus, the net $\boldsymbol{x} = (x_1, \ldots, x_N) : \mathcal{U} \to \mathbb{R}_+^N$ coincides with the confocal coordinates (3.5) *on the positive hyperoctant, up to independent scaling along the coordinate axes $(x_1, \ldots, x_N) \mapsto (C_1 x_1, \ldots, C_N x_N)$ with some $C_1, \ldots, C_N > 0$.*

b) *The choice of the constants $D_1, \ldots, D_N > 0$ that specifies the system of confocal coordinates* (3.5) *among the separable solutions* (3.17)*, namely*

$$D_k^{-2} = \prod_{i<k} (a_i - a_k) \prod_{i>k} (a_k - a_i),$$

is the unique scaling (up to a common factor) such that the parameter curves are pairwise orthogonal.

Proof. a) We have

$$x_k(u_1, \ldots, u_N) = D_k \cdot \rho_1(u_1, c_k) \cdot \ldots \cdot \rho_N(u_N, c_k), \quad k = 1, \ldots, N.$$

Boundary conditions (3.15), (3.16) yield that the constants are given by $c_k = a_k$, and that the solutions are actually given by (3.17). Formulas (3.5) are now equivalent to a specific choice of the constants D_k.

b) From (3.6) we compute:

$$\left\langle \frac{\partial \boldsymbol{x}}{\partial u_i}, \frac{\partial \boldsymbol{x}}{\partial u_j} \right\rangle = \frac{1}{4} \sum_{k=1}^{N} \frac{x_k^2}{(u_i + a_k)(u_j + a_k)} = \frac{1}{4} \sum_{k=1}^{N} (-1)^{k-1} D_k^2 \prod_{l \neq i,j} (u_l + a_k). \tag{3.18}$$

We have:

$$\prod_{l\neq i,j}(u_l+a_k)=\sum_{m=0}^{N-2}p_{ij}^{(N-2-m)}(\boldsymbol{u})a_k^m,$$

where $p_{ij}^{(N-2-m)}(\boldsymbol{u})$ is an elementary symmetric polynomial of degree $N-2-m$ in u_l, $l\neq i,j$. Thus,

$$\left\langle\frac{\partial\boldsymbol{x}}{\partial u_i},\frac{\partial\boldsymbol{x}}{\partial u_j}\right\rangle=\frac{1}{4}\sum_{m=0}^{N-2}\left(\sum_{k=1}^{N}(-1)^{k-1}a_k^mD_k^2\right)p_{ij}^{(N-2-m)}(\boldsymbol{u}).$$

Since the polynomials $p_{ij}^{(N-2-m)}(\boldsymbol{u})$ are independent on $\mathcal{U}$, the latter expression is equal to zero if and only if

$$\sum_{k=1}^{N}(-1)^{k-1}a_k^mD_k^2=0,\qquad m=0,\dots,N-2.$$

This system of $N-1$ linear homogeneous equations for the N unknowns D_k^2 does not depend on i,j. Supplying it by the non-homogeneous equation $\sum_{k=1}^{N}(-1)^{k-1}a_k^{N-1}D_k^2=1$, we find the unique solution of the resulting system as quotients of Vandermonde determinants, or finally $(-1)^{k-1}D_k^2=1/\prod_{i\neq k}(a_k-a_i)$. □

Remark 3.2. The boundary conditions ensure that the $2N-1$ faces of the boundary of $\mathcal{U}$ are mapped into coordinate hyperplanes. Their images are degenerate quadrics of the confocal family (3.1).

4 Discrete Koenigs nets

For a function f on $\mathbb{Z}^M$ we define the *difference operator* in the standard way:

$$\Delta_if(\boldsymbol{n})=f(\boldsymbol{n}+\boldsymbol{e}_i)-f(\boldsymbol{n})$$

for all $\boldsymbol{n}\in\mathbb{Z}^M$, where $\boldsymbol{e}_i$ is the i-th coordinate vector of $\mathbb{Z}^M$.

Definition 4.1. *A two-dimensional discrete net $\boldsymbol{x}:\mathbb{Z}^M\supset U_{ij}\to\mathbb{R}^N$ corresponding to the coordinate directions $i,j\in\{1,\dots,M\}$, $i\neq j$, is called* a discrete Koenigs net *if there exists a function $\nu:U_{ij}\to\mathbb{R}_+$ such that*

$$\Delta_i\Delta_j\boldsymbol{x}=\frac{\nu_{(j)}\nu_{(ij)}-\nu\nu_{(i)}}{\nu(\nu_{(i)}+\nu_{(j)})}\Delta_i\boldsymbol{x}+\frac{\nu_{(i)}\nu_{(ij)}-\nu\nu_{(j)}}{\nu(\nu_{(i)}+\nu_{(j)})}\Delta_j\boldsymbol{x}.\tag{4.1}$$

Here we use index notation to denote shifts of ν:

$$\nu_{(i)}(\boldsymbol{n}):=\nu(\boldsymbol{n}+\boldsymbol{e}_i),\qquad\nu_{(ij)}(\boldsymbol{n}):=\nu(\boldsymbol{n}+\boldsymbol{e}_i+\boldsymbol{e}_j),\qquad\boldsymbol{n}\in\mathbb{Z}^M.$$

The geometric meaning of this algebraic definition is as follows. Like in the continuous case, discrete Königs nets constitute a subclass of discrete conjugate nets (Q-nets), in the sense that all two-dimensional subnets have planar faces. See [BS] for more information on Q-nets, as well as on geometric properties of discrete Koenigs nets. Consider an elementary planar quadrilateral $(\boldsymbol{x},\boldsymbol{x}_{(i)},\boldsymbol{x}_{(ij)},\boldsymbol{x}_{(j)})$ of a Q-net governed by the discrete Darboux equation

$$\Delta_i\Delta_j\boldsymbol{x}=A\Delta_i\boldsymbol{x}+B\Delta_j\boldsymbol{x}.\tag{4.2}$$

Let M be the intersection point of its diagonals $[\boldsymbol{x},\boldsymbol{x}_{(ij)}]$ and $[\boldsymbol{x}_{(i)},\boldsymbol{x}_{(j)}]$. Then one can easily compute that M divides the corresponding diagonals in the following relations:

$$\overrightarrow{\boldsymbol{x}_{(i)}M}:\overrightarrow{M\boldsymbol{x}_{(j)}}=(B+1):(A+1),\quad\overrightarrow{\boldsymbol{x}M}:\overrightarrow{M\boldsymbol{x}_{(ij)}}=1:(A+B+1).$$

A Q-net is called a Koenigs net, if there is a positive function ν defined at the vertices of the net such that

$$\overrightarrow{\boldsymbol{x}_{(i)}M}:\overrightarrow{M\boldsymbol{x}_{(j)}}=\nu_{(i)}:\nu_{(j)},\quad\overrightarrow{\boldsymbol{x}M}:\overrightarrow{M\boldsymbol{x}_{(ij)}}=\nu:\nu_{(ij)}.$$

One can show [BS] that this happens if and only if the intersection points of the diagonals of four adjacent quadrilaterals are coplanar. The function ν should satisfy

$$(A+1)\nu_{(i)} = (B+1)\nu_{(j)}, \quad \nu_{(ij)} = (A+B+1)\nu. \tag{4.3}$$

This is clearly equivalent to

$$A = \frac{\nu_{(j)}\nu_{(ij)} - \nu\nu_{(i)}}{\nu(\nu_{(i)} + \nu_{(j)})}, \quad B = \frac{\nu_{(i)}\nu_{(ij)} - \nu\nu_{(j)}}{\nu(\nu_{(i)} + \nu_{(j)})}.$$

The pair of linear equations (4.3) is compatible if and only if the following nonlinear equation is satisfied for the coefficients A, B associated with four adjacent quadrilaterals:

$$\frac{A_{(ij)}+1}{B_{(ij)}+1} = \frac{(A_{(j)}+B_{(j)}+1)}{(A_{(i)}+B_{(i)}+1)}\frac{(A+1)}{(B+1)}. \tag{4.4}$$

If this relation for the coefficients A, B of the discrete Darboux equation (4.2) holds true everywhere, then the linear equations (4.3) determine a function ν uniquely, as soon as initial data are prescribed, consisting, for instance, of the values of ν at two neighboring vertices. The associated discrete Darboux equation is then of Koenigs type (4.1).

5 Discrete Euler-Poisson-Darboux equation

Definition 5.1. *Let $U \subset \mathbb{Z}^M$. We say that a discrete net*

$$\boldsymbol{x} : U \to \mathbb{R}^N, \quad (n_1, \ldots, n_M) \mapsto (x_1, \ldots, x_N)$$

satisfies the discrete Euler-Darboux system *if all of its two-dimensional subnets satisfy the (vector) discrete Euler-Poisson-Darboux equation with the same parameter γ:*

$$\Delta_i\Delta_j\boldsymbol{x} = \frac{\gamma}{n_i+\varepsilon_i-n_j-\varepsilon_j}(\Delta_j\boldsymbol{x} - \Delta_i\boldsymbol{x}) \tag{dEPD$_\gamma$}$$

for all $i, j \in \{1, \ldots, M\}$, $i \neq j$, and some $\gamma \in \mathbb{R}$, $\varepsilon_1, \ldots, \varepsilon_M \in \mathbb{R}$.

Remark 5.1. This discretization of the Euler-Poisson-Darboux system was introduced by Konopelchenko and Schief [KS2].

Proposition 5.2. *Let $\boldsymbol{x} : \mathbb{Z}^M \supset U \to \mathbb{R}^N$ be a discrete net satisfying the discrete Euler-Poisson-Darboux system* (dEPD$_\gamma$). *Then all two-dimensional subnets of $\boldsymbol{x}$ are discrete Koenigs nets.*

Proof. It is straightforward to verify that the coefficients

$$A = -B = \frac{\gamma}{n_i+\varepsilon_i-n_j-\varepsilon_j}$$

indeed obey the Koenigs condition (4.4). □

We now show that for a discrete net satisfying the discrete Euler-Poisson-Darboux equation (dEPD$_\gamma$), the function ν can be found explicitly. For this aim, use the ansatz

$$\nu(n_i, n_j) = \mu(n_i - n_j),$$

so that $\nu_{(ij)} = \nu(n_i+1, n_j+1) = \nu(n_i, n_j) = \nu$. Under this ansatz, equation (4.1) simplifies to

$$\Delta_i\Delta_j\boldsymbol{x} = \frac{\nu_{(j)} - \nu_{(i)}}{\nu_{(i)} + \nu_{(j)}}\Delta_i\boldsymbol{x} + \frac{\nu_{(i)} - \nu_{(j)}}{\nu_{(i)} + \nu_{(j)}}\Delta_j\boldsymbol{x}.$$

Comparing with (dEPD$_\gamma$) we obtain

$$
\begin{aligned}
&\frac{\nu_{(i)}-\nu_{(j)}}{\nu_{(i)}+\nu_{(j)}}=\frac{\gamma}{n_i+\varepsilon_i-n_j-\varepsilon_j}\\
\Leftrightarrow\ &\nu_{(i)}\left(1-\frac{\gamma}{n_i+\varepsilon_i-n_j-\varepsilon_j}\right)=\nu_{(j)}\left(1+\frac{\gamma}{n_i+\varepsilon_i-n_j-\varepsilon_j}\right)\\
\Leftrightarrow\ &\nu(n_i+1,n_j)=\nu(n_i,n_j+1)\ \frac{n_i+\varepsilon_i-n_j-\varepsilon_j+\gamma}{n_i+\varepsilon_i-n_j-\varepsilon_j-\gamma}.
\end{aligned}
$$

Thus, the function μ should satisfy

$$\mu(m+1)=\mu(m-1)\ \frac{m+\varepsilon_i-\varepsilon_j+\gamma}{m+\varepsilon_i-\varepsilon_j-\gamma}.$$

This equation is easily solved:

$$\mu(m)=\frac{\Gamma\left(\frac{1}{2}(m+\varepsilon_i-\varepsilon_j+\gamma+1)\right)}{\Gamma\left(\frac{1}{2}(m+\varepsilon_i-\varepsilon_j-\gamma+1)\right)}b(m),$$

where Γ denotes the gamma function and b is any function of period 2. It is recalled that $\Gamma(x+1)=x\Gamma(x)$.

6 Discrete confocal quadrics

We have seen in the continuous case (Proposition 3.6) that confocal quadrics are described, up to a componentwise scaling, by separable solutions of the Euler-Poisson-Darboux system (EPD$_\gamma$) with $\gamma=\frac{1}{2}$. It is therefore natural to consider separable solutions of the discrete Euler-Poisson-Darboux system.

6.1 Separability

Proposition 6.1. [KS2] *A separable function $x:\mathbb{Z}^N\supset U\to\mathbb{R}$,*

$$x(n_1,\dots,n_N)=\rho_1(n_1)\cdots\rho_N(n_N),\tag{6.1}$$

is a solution of the discrete Euler-Poisson-Darboux system (dEPD$_\gamma$) *iff the functions $\rho_i:U_i\to\mathbb{R}$, $i=1,\dots,N$, satisfy*

$$\Delta\rho_i(n_i)=\frac{\gamma\rho_i(n_i)}{n_i+\varepsilon_i+c},\tag{6.2}$$

or, equivalently,

$$\rho_i(n_i+1)=\rho_i(n_i)\frac{n_i+\varepsilon_i+c+\gamma}{n_i+\varepsilon_i+c}\tag{6.3}$$

for some $c\in\mathbb{R}$ and for all $n_i\in U_i$.

Proof. Substituting (6.1) into (dEPD$_\gamma$) we obtain

$$
\begin{aligned}
&\big(\rho_i(n_i+1)-\rho_i(n_i)\big)\big(\rho_j(n_j+1)-\rho_j(n_j)\big)\\
&\quad=\frac{\gamma}{n_i+\varepsilon_i-n_j-\varepsilon_j}\Big(\rho_i(n_i)\big(\rho_j(n_j+1)-\rho_j(n_j)\big)\\
&\qquad\qquad-\rho_j(n_j)\big(\rho_i(n_i+1)-\rho_i(n_i)\big)\Big),
\end{aligned}
$$

which is equivalent to

$$n_i+\varepsilon_i-n_j-\varepsilon_j=\frac{\gamma\rho_i(n_i)}{\rho_i(n_i+1)-\rho_i(n_i)}-\frac{\gamma\rho_j(n_j)}{\rho_j(n_j+1)-\rho_j(n_j)}.$$

So, the expression

$$\frac{\gamma\rho_i(n_i)}{\rho_i(n_i+1)-\rho_i(n_i)}-(n_i+\varepsilon_i)=c$$

depends neither on n_i nor on n_j, i.e., is a constant. This is equivalent to (6.2) and thus to (6.3). ☐

If the constants γ, c and ε_i are such that neither $\varepsilon_i + c$ nor $\varepsilon_i + c + \gamma$ is an integer, then the general solution of (6.3) is given by

$$\rho_i(n_i, \varepsilon_i + c) = d_i \frac{\Gamma(n_i + \varepsilon_i + c + \gamma)}{\Gamma(n_i + \varepsilon_i + c)} = \tilde{d}_i \frac{\Gamma(-n_i - \varepsilon_i - c + 1)}{\Gamma(-n_i - \varepsilon_i - c - \gamma + 1)}$$

for all $n_i \in \mathbb{Z}$ with some constants $d_i, \tilde{d}_i \in \mathbb{R}$.

In what follows, we will use the Pochhammer symbol $(u)_\gamma$ with a not necessarily integer index γ:

$$(u)_\gamma = \frac{\Gamma(u + \gamma)}{\Gamma(u)}, \quad u, \gamma > 0.$$

Because of the asymptotics $(u)_\gamma \sim u^\gamma$ as $u \to +\infty$, which can also be put as

$$\lim_{\varepsilon \to 0} \varepsilon^\gamma \left(\frac{u}{\varepsilon}\right)_\gamma = u^\gamma,$$

the function $(u)_\gamma$ has been considered as a discretization of u^γ in [GGR, p. 47]. With this notation, the above formulas take the form

$$\rho_i(n_i, \varepsilon_i + c) = d_i(n_i + \varepsilon_i + c)_\gamma = \tilde{d}_i(-n_i - \varepsilon_i - c - \gamma + 1)_\gamma.$$

Definition 6.2. *The* discrete square root function *is defined by*

$$(u)_{1/2} = \frac{\Gamma(u + \frac{1}{2})}{\Gamma(u)}.$$

To achieve boundary conditions similar to (3.15) and (3.16), we will be more interested in the cases where solutions are only defined on an integer half-axis, and vanish at its boundary point. For $\gamma = \frac{1}{2}$ this is the case if:

- either $\varepsilon_i + c \in \mathbb{Z}$, and then the general solution to the right of $-c - \varepsilon_i$ is given by multiples of
$$\rho_i(n_i, \varepsilon_i + c) = (n_i + \varepsilon_i + c)_{1/2} \quad \text{for} \quad n_i \geqslant -c - \varepsilon_i, \tag{6.4}$$
- or $\varepsilon_i + c + \frac{1}{2} \in \mathbb{Z}$, and then the general solution to the left of $-c - \varepsilon + \frac{1}{2}$ is given by multiples of
$$\rho_i(n_i, \varepsilon_i + c) = (-n_i - \varepsilon_i - c + \tfrac{1}{2})_{1/2} \quad \text{for} \quad n_i \leqslant -c - \varepsilon_i + \frac{1}{2}. \tag{6.5}$$

In terms of discrete square roots, the expressions for the separable solutions of the discrete Euler-Poisson-Darboux system for $\gamma = \frac{1}{2}$ now resemble their classical counterparts.

Proposition 6.3. *Let $\alpha_1, \ldots, \alpha_N \in \mathbb{Z}$ with $\alpha_1 > \alpha_2 > \cdots > \alpha_N$, and set*

$$\mathcal{U} = \left\{(n_1, \ldots, n_N) \in \mathbb{Z}^N \mid -\alpha_1 \leqslant n_1 \leqslant -\alpha_2 \leqslant n_2 \leqslant \cdots \leqslant -\alpha_N \leqslant n_N\right\}.$$

Let $x_k : \mathcal{U} \to \mathbb{R}_+$, $k = 1, \ldots, N$, be N independent separable solutions of the discrete Euler-Poisson-Darboux system (dEPD$_\gamma$) *with $\gamma = \frac{1}{2}$ defined on $\mathcal{U}$ and satisfying the following boundary conditions:*

$$x_k|_{n_k = -\alpha_k} = 0 \qquad \text{for} \quad k = 1, \ldots, N, \tag{6.6}$$

$$x_k|_{n_{k-1} = -\alpha_k} = 0 \quad \text{for} \quad k = 2, \ldots, N. \tag{6.7}$$

Then the shifts ε_i of the variables n_i are given by

$$\varepsilon_i - \varepsilon_j = \frac{j - i}{2} \quad \text{for} \quad i, j = 1, \ldots, N, \tag{6.8}$$

and the solutions are expressed by

$$x_k(n_1, \ldots, n_N) = D_k \prod_{i=1}^{N} \rho_i^{(k)}(n_i), \tag{6.9}$$

for some constants $D_1, \ldots, D_N > 0$ and

$$\rho_i^{(k)}(n_i) = \begin{cases} (n_i + \alpha_k + \frac{k-i}{2})_{1/2} & \text{for} \quad i \geqslant k, \\ (-n_i - \alpha_k - \frac{k-i}{2} + \frac{1}{2})_{1/2} & \text{for} \quad i < k. \end{cases} \tag{6.10}$$

Proof. Separable solutions of (dEPD$_\gamma$) with $\gamma = \frac{1}{2}$ are of the general form (6.9), where each $\rho_i^{(k)}(n_i) = \rho_i(n_i, \varepsilon_i + c_k)$ is defined by one of the formulas (6.4), (6.5), and all multiplicative constants are collected in $D_1, \ldots, D_N > 0$. We have to determine suitable constants ε_i and c_k.

The boundary conditions (6.6) and (6.7) imply that x_k is defined for $n_k \geqslant -\alpha_k$, while vanishing for $n_k = -\alpha_k$, and also that x_k is defined for $n_{k-1} \leqslant -\alpha_k$, while vanishing for $n_{k-1} = -\alpha_k$. This shows that

$$\alpha_k = c_k + \varepsilon_k = c_k + \varepsilon_{k-1} - \frac{1}{2}.$$

We obtain $\varepsilon_k - \varepsilon_{k-1} = -\frac{1}{2}$, and equation (6.8) follows. Together with $c_k + \varepsilon_k = a_k$ this implies that

$$c_k + \varepsilon_i = \alpha_k + \frac{k-i}{2}. \tag{6.11}$$

It remains to substitute (6.11) into (6.4) and (6.5). ☐

6.2 Orthogonality

The remaining scaling freedom (multiplicative constants D_k) of the components x_k as given by (6.9) is the same as in the continuous case. As we have seen in Proposition 3.6, in the continuous case, one can fix the scaling by imposing the orthogonality condition $(\partial \boldsymbol{x}/\partial u_i) \perp (\partial \boldsymbol{x}/\partial u_j)$. In the discrete case, it turns out to be possible to introduce a notion of orthogonality, which will allow us to fix the scaling in a similar way.

Definition 6.4. *Let $\mathcal{U} \subset \mathbb{Z}^N$, $\mathcal{U}^* \subset (\mathbb{Z}^N)^*$, where $(\mathbb{Z}^N)^* = (\mathbb{Z} + \frac{1}{2})^N$. Consider a function*

$$\boldsymbol{x} : \mathcal{U} \cup \mathcal{U}^* \to \mathbb{R}^N,$$

such that both restrictions $\boldsymbol{x}(\mathcal{U})$ and $\boldsymbol{x}(\mathcal{U}^*)$ are Q-nets. We say that the discrete net $\boldsymbol{x}$ is orthogonal *if each edge of $\boldsymbol{x}(\mathcal{U})$ is orthogonal to the dual facet of $\boldsymbol{x}(\mathcal{U}^*)$.*

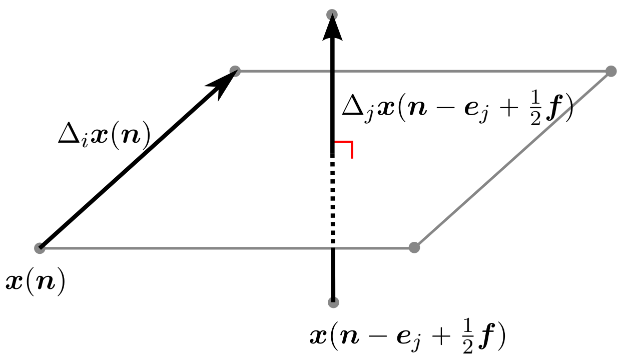

Figure 6.1. Discrete orthogonality for a system of Q-nets defined on a square lattice and on its dual.

The (space of the) facet of $\boldsymbol{x}(\mathcal{U}^*)$ dual to the edge $[\boldsymbol{x}(\boldsymbol{n}), \boldsymbol{x}(\boldsymbol{n}+\boldsymbol{e}_i)]$ of $\boldsymbol{x}(\mathcal{U})$ is spanned by the $N-1$ edges $[\boldsymbol{x}(\boldsymbol{n}-\boldsymbol{e}_j+\frac{1}{2}\boldsymbol{f}), \boldsymbol{x}(\boldsymbol{n}+\frac{1}{2}\boldsymbol{f})]$ with $j \neq i$, where $\boldsymbol{f} = (1, \ldots, 1)$. Therefore, the orthogonality condition in the sense of Definition 6.4 reads:

$$\left\langle \Delta_i \boldsymbol{x}(\boldsymbol{n}), \Delta_j \boldsymbol{x}(\boldsymbol{n} - \boldsymbol{e}_j + \tfrac{1}{2}\boldsymbol{f}) \right\rangle = 0 \tag{6.12}$$

for all $i \neq j$ and $\boldsymbol{n} \in \mathbb{Z}^N$. From this it is easy to see that $\boldsymbol{x}(\mathcal{U})$ and $\boldsymbol{x}(\mathcal{U}^*)$ actually play symmetric roles in Definition 6.4 (that is, each edge of $\boldsymbol{x}(\mathcal{U}^*)$ is orthogonal to the dual facet of $\boldsymbol{x}(\mathcal{U})$, compare Fig. 6.1).

Turning to separable solutions of the discrete Euler-Poisson-Darboux system (dEPD$_\gamma$) with $\gamma = \frac{1}{2}$, we extend the function $\boldsymbol{x} = (x_1, \ldots, x_N)$ defined in Proposition 6.3 to a bigger domain:

$$\boldsymbol{x} : \mathcal{U} \cup \mathcal{U}^* \to \mathbb{R}_+^N,$$

where

$$\mathcal{U}^* = \left\{(n_1, \dots, n_N) \in (\mathbb{Z}^N)^* \mid -\alpha_1 \leqslant n_1 \leqslant -\alpha_2 \leqslant n_2 \leqslant \dots \leqslant -\alpha_N \leqslant n_N\right\}.$$

It is emphasized that the lattices $\boldsymbol{x}(\mathcal{U})$ and $\boldsymbol{x}(\mathcal{U}^*)$ are on equal footing except that the boundary conditions do not apply to $\boldsymbol{x}(\mathcal{U}^*)$.

Proposition 6.5. *Let $\alpha_1, \dots, \alpha_N \in \mathbb{Z}$ with $\alpha_1 > \alpha_2 > \dots > \alpha_N$. Then the net $\boldsymbol{x} : \mathcal{U} \cup \mathcal{U}^* \to \mathbb{R}^N_+$ defined by* (6.9) *and* (6.10) *is orthogonal if and only if*

$$D_k^{-2} = C \prod_{i<k} (\alpha_i - \alpha_k + \tfrac{i-k}{2}) \prod_{i>k} (\alpha_k - \alpha_i + \tfrac{k-i}{2}) \tag{6.13}$$

with some $C \in \mathbb{R}_+$.

Proof. We will use the following formulas for the "discrete derivative" of the "discrete square root function" $(u)_{1/2} = \Gamma(u + \frac{1}{2})/\Gamma(u)$, which are immediate consequences of the identity $\Gamma(u+1) = u\Gamma(u)$:

$$\Delta\big((u)_{1/2}\big) = \frac{1}{2(u + \frac{1}{2})_{1/2}}, \qquad \Delta\big((-u)_{1/2}\big) = -\frac{1}{2(-u - \frac{1}{2})_{1/2}}, \tag{6.14}$$

where $\Delta f(u) = f(u+1) - f(u)$. We also note that the "discrete squares" of discrete square roots obey the relations

$$(u)_{1/2}(u + \tfrac{1}{2})_{1/2} = u, \qquad (-u)_{1/2}(-u - \tfrac{1}{2})_{1/2} = -u - \tfrac{1}{2}. \tag{6.15}$$

Substituting (6.11) and $\gamma = \frac{1}{2}$ into (6.2), we obtain:

$$\Delta\rho_i^{(k)}(n_i) = \frac{\rho_i^{(k)}(n_i)}{2(n_i + \alpha_k + \frac{k-i}{2})}. \tag{6.16}$$

Upon using property (6.15) and expressions (6.10), we arrive at

$$\rho_i^{(k)}(n_i)\rho_i^{(k)}(n_i + \tfrac{1}{2}) = \begin{cases} n_i + \alpha_k + \frac{k-i}{2}, & i \geqslant k, \\ -(n_i + \alpha_k + \frac{k-i}{2}), & i < k. \end{cases} \tag{6.17}$$

We use (6.9), (6.16), (6.17) to compute the left-hand side of equation (6.12):

$$\big\langle \Delta_i \boldsymbol{x}(\boldsymbol{n}), \Delta_j \boldsymbol{x}(\boldsymbol{n} - \boldsymbol{e}_j + \tfrac{1}{2}\boldsymbol{f})\big\rangle = \frac{1}{4}\sum_{k=1}^{N} (-1)^{k-1} D_k^2 \prod_{l \neq i,j} \left(n_l + \alpha_k + \frac{k-l}{2}\right).$$

Observe that this literally coincides with the analogous expression in the continuous case (3.18), if we set

$$a_k = \alpha_k + \frac{k}{2}, \quad u_l = n_l - \frac{l}{2}.$$

Therefore, the proof of part b) of Proposition 3.6 can be literally repeated, leading to the condition $D_k^{-2} = C\prod_{i<k}(a_i - a_k)\prod_{i>k}(a_k - a_i)$, which coincides with (6.13). □

6.3 Definition of discrete confocal coordinates

Definition 6.6. *Let $\alpha_1, \dots, \alpha_N \in \mathbb{Z}$ with $\alpha_1 > \alpha_2 > \dots > \alpha_N$.* Discrete confocal coordinates *are given by the discrete net $\boldsymbol{x} : \mathcal{U} \cup \mathcal{U}^* \to \mathbb{R}^N_+$ defined by*

$$x_k(\boldsymbol{n}) = D_k \prod_{i=1}^{k-1} (-n_i - \alpha_k - \tfrac{k-i}{2} + \tfrac{1}{2})_{1/2} \prod_{i=k}^{N} (n_i + \alpha_k + \tfrac{k-i}{2})_{1/2}$$

with

$$D_k^{-1} = \prod_{i=1}^{k-1} \sqrt{\alpha_i - \alpha_k + \tfrac{i-k}{2}} \prod_{i=k+1}^{N} \sqrt{\alpha_k - \alpha_i + \tfrac{k-i}{2}}.$$

The characteristic properties of this net can be summarized as follows.

(i) Each two-dimensional subnet of $\boldsymbol{x}(\mathcal{U})$ and of $\boldsymbol{x}(\mathcal{U}^*)$ satisfies (dEPD$_\gamma$) with $\gamma = \frac{1}{2}$;

(ii) Therefore each two-dimensional subnet of $\boldsymbol{x}(\mathcal{U})$ and of $\boldsymbol{x}(\mathcal{U}^*)$ is a Koenigs net;

(iii) The net $\boldsymbol{x}(\mathcal{U} \cup \mathcal{U}^*)$ is orthogonal in the sense of Definition 6.4;

(iv) Both nets $\boldsymbol{x}(\mathcal{U})$ and $\boldsymbol{x}(\mathcal{U}^*)$ are separable;

(v) Boundary conditions (6.6), (6.7) are satisfied.

Properties (ii) and (iii) lead to a novel discretization of the notion of isothermic surfaces.

Property (v) allows us to define *discrete confocal quadrics* by reflecting the net $\boldsymbol{x}$ in the coordinate hyperplanes. Like in the continuous case, the boundary conditions correspond to the $2N-1$ degenerate quadrics of the confocal family lying in the coordinate hyperplanes.

Remark 6.1. In [BSST2] we will describe more general discrete confocal quadrics, corresponding to general reparametrizations of the curvature lines. They will be defined in a more geometric way, less based on integrable difference equations.

6.4 Further properties of discrete confocal coordinates

We now obtain a variety of properties of discrete confocal quadrics and discrete confocal coordinates, which serve as discretizations of their respective continuous analogs.

Proposition 6.7. *For any N-tuple of signs $\boldsymbol{\sigma} = (\sigma_1, \ldots, \sigma_N)$, $\sigma_i = \pm 1$, we have:*

$$x_k(\boldsymbol{n}) \cdot x_k(\boldsymbol{n} + \tfrac{1}{2}\boldsymbol{\sigma}) = \frac{\prod_{i=1}^N \left(n_i + \alpha_k + \frac{k-i}{2} - \frac{1}{4}(1-\sigma_i)\right)}{\prod_{i\neq k}\left(\alpha_k - \alpha_i + \frac{k-i}{2}\right)}, \tag{6.18}$$

and therefore

$$\sum_{k=1}^N \frac{x_k(\boldsymbol{n}) x_k(\boldsymbol{n} + \frac{1}{2}\boldsymbol{\sigma})}{n_i + \alpha_k + \frac{k-i}{2} - \frac{1}{4}(1-\sigma_i)} = 1, \qquad i = 1, \ldots, N. \tag{6.19}$$

Proof. Equation (6.18) is obtained by straightforward computation. Using this result, equation (6.19) follows from the continuous equations (3.3), (3.4) upon replacing $a_k = \alpha_k + \frac{k}{2}$ and $u_i = n_i - \frac{i}{2} - \frac{1}{4}(1 - \sigma_i)$. □

We notice that (6.18) can be seen as a discrete version of the parametrization formulas (3.4), while (6.19) can be seen as a discrete version of the quadric equation (3.3). The above formulas take the simplest form for $\boldsymbol{\sigma} = \boldsymbol{f} = (1, \ldots, 1)$:

$$x_k(\boldsymbol{n}) \cdot x_k(\boldsymbol{n} + \tfrac{1}{2}\boldsymbol{f}) = \frac{\prod_{i=1}^N \left(n_i + \alpha_k + \frac{k-i}{2}\right)}{\prod_{i\neq k}\left(\alpha_k - \alpha_i + \frac{k-i}{2}\right)} \tag{6.20}$$

and

$$\sum_{k=1}^N \frac{x_k(\boldsymbol{n}) x_k(\boldsymbol{n} + \frac{1}{2}\boldsymbol{f})}{n_i + \alpha_k + \frac{k-i}{2}} = 1, \qquad i = 1, ..., N. \tag{6.21}$$

In the continuous setting one can obtain from (3.4)

$$\langle \boldsymbol{x}(\boldsymbol{u}), \boldsymbol{x}(\boldsymbol{u}) \rangle = \sum_{k=1}^N x_k^2(\boldsymbol{u}) = \sum_{k=1}^N (u_k + a_k), \tag{6.22}$$

so that the hypersurfaces $\sum_{k=1}^N u_k = \text{const}$ are (parts) of spheres. In particular, this implies that

$$\left\langle \boldsymbol{x}, \frac{\partial \boldsymbol{x}}{\partial u_i} \right\rangle = \frac{1}{2},$$

for all $i = 1, \ldots, N$, which can be regarded as a characterization of the particular parametrization of the confocal quadrics considered in this paper. In the discrete case one obtains the following:

Proposition 6.8. *For any N-tuple of signs $\boldsymbol{\sigma} = (\sigma_1, \dots, \sigma_N)$, $\sigma_k = \pm 1$, we have:*

$$\langle \boldsymbol{x}(\boldsymbol{n}), \boldsymbol{x}(\boldsymbol{n} + \tfrac{1}{2}\boldsymbol{\sigma})\rangle = \sum_{k=1}^{N} \left(n_k + \alpha_k - \tfrac{1}{4}(1-\sigma_k)\right), \tag{6.23}$$

and therefore, for any $i = 1, \dots, N$ and for any $\boldsymbol{\sigma}$ with $\sigma_i = -1$:

$$\langle \boldsymbol{x}(\boldsymbol{n}), \Delta_i \boldsymbol{x}(\boldsymbol{n} + \tfrac{1}{2}\boldsymbol{\sigma})\rangle = \frac{1}{2}.$$

Proof. The right-hand sides of (3.4) and (6.18) may be identified by setting $a_k = \alpha_k + \frac{k}{2}$ and $u_i = n_i - \frac{i}{2} - \frac{1}{4}(1-\sigma_i)$ and hence the right-hand side of (6.22) also applies in the discrete case, leading upon the above identification to (6.23). □

Finally, we obtain a factorization similar to (3.7), (3.8), (3.9), which characterizes isothermic surfaces in the continuous case.

Proposition 6.9. *For $i \neq j$ we have*

$$\langle \Delta_i \boldsymbol{x}(\boldsymbol{n}), \Delta_i \boldsymbol{x}(\boldsymbol{n} + \tfrac{1}{2}\boldsymbol{f})\rangle = s^2 \phi_i(n_i),$$

$$\langle \Delta_j \boldsymbol{x}(\boldsymbol{n} - \boldsymbol{e}_j + \tfrac{1}{2}\boldsymbol{f}), \Delta_j \boldsymbol{x}(\boldsymbol{n} - \boldsymbol{e}_j + \boldsymbol{f})\rangle = s^2 \phi_j(n_j),$$

where

$$s(n_i, n_j) = \left| n_i - n_j + \frac{j-i}{2} + \frac{1}{2} \right|^{1/2},$$

and

$$\frac{\phi_i(n_i)}{\phi_j(n_j)} = -\frac{\prod_{m \neq i,j}(n_i - n_m + \frac{m-i}{2} + \frac{1}{2})}{\prod_{m=1}^{N}(n_i + \alpha_m - \frac{m-i}{2} + \frac{1}{2})} \cdot \frac{\prod_{m=1}^{N}(n_j + \alpha_m - \frac{m-j}{2})}{\prod_{m \neq i,j}(n_j - n_m + \frac{m-j}{2} - \frac{1}{2})}.$$

Proof. For any i, k we compute

$$\Delta_i x_k(\boldsymbol{n}) \cdot \Delta_i x_k(\boldsymbol{n} + \tfrac{1}{2}\boldsymbol{f}) = \frac{1}{4} \frac{1}{\prod_{m \neq k}(\alpha_k - \alpha_m + \frac{k-m}{2})} \frac{\prod_{m \neq i}(n_m + \alpha_k + \frac{k-m}{2})}{n_i + \alpha_k + \frac{k-i}{2} + \frac{1}{2}}.$$

Here, the right-hand side can be identified with the right-hand side of the corresponding continuous expression, put as

$$\left(\frac{\partial x_k}{\partial u_i}\right)^2 = \frac{1}{4} \frac{1}{\prod_{m \neq k}(a_k - a_m)} \frac{\prod_{m \neq i}(u_m + a_k)}{(u_i + a_k)},$$

upon replacing

$$a_k = \alpha_k + \frac{k}{2}, \quad u_m = \begin{cases} n_m - \frac{m}{2}, & \text{for } m \neq i, \\ n_i - \frac{i}{2} + \frac{1}{2}, & \text{for } m = i. \end{cases}$$

Therefore, the continuous identity (3.10) upon the above identification implies

$$\langle \Delta_i \boldsymbol{x}(\boldsymbol{n}), \Delta_i \boldsymbol{x}(\boldsymbol{n} + \tfrac{1}{2}\boldsymbol{f})\rangle = \frac{\prod_{m \neq i}(n_i - n_m + \frac{m-i}{2} + \frac{1}{2})}{4\prod_{m=1}^{N}(n_i + \alpha_m - \frac{m-i}{2} + \frac{1}{2})}.$$

Similarly, we find:

$$\langle \Delta_j \boldsymbol{x}(\boldsymbol{n} - \boldsymbol{e}_j + \tfrac{1}{2}\boldsymbol{f}), \Delta_j \boldsymbol{x}(\boldsymbol{n} - \boldsymbol{e}_j + \boldsymbol{f})\rangle = \frac{\prod_{m \neq j}(n_j - n_m + \frac{m-j}{2} - \frac{1}{2})}{4\prod_{m=1}^{N}(n_j + \alpha_m - \frac{m-j}{2})}.$$

The observation that the only factors in each of the latter two expressions which depends on both n_i and n_j are equal (up to sign) finishes the proof. □

Remark 6.2. Similar to equations (6.20), (6.21) it is possible to generalize Proposition 6.9 by replacing the vector $\boldsymbol{f}$ by a vector of signs $\boldsymbol{\sigma}$ with $\sigma_i = \sigma_j = 1$ and all other components components being arbitrary.

7 The case $N = 2$

Here, and in the following section, we examine in greater detail the general theory set down in the preceding in the cases $N = 2$ and $N = 3$. For the benefit of the reader, these two sections are made as self-contained as possible.

7.1 Continuous confocal coordinates

Let $a > b > 0$. Then formulas

$$\begin{aligned} x(u_1, u_2) &= \frac{\sqrt{u_1 + a}\sqrt{u_2 + a}}{\sqrt{a-b}}, \\ y(u_1, u_2) &= \frac{\sqrt{-(u_1 + b)}\sqrt{u_2 + b}}{\sqrt{a-b}}, \end{aligned} \tag{7.1}$$

define a parametrization of the first quadrant of $\mathbb{R}^2$ by confocal coordinates

$$\mathcal{U} = \left\{(u_1, u_2) \in \mathbb{R}^2 \mid -a < u_1 < -b < u_2\right\} \to \mathbb{R}^2_+.$$

A family of confocal conics is obtained by reflections in the coordinate axes.

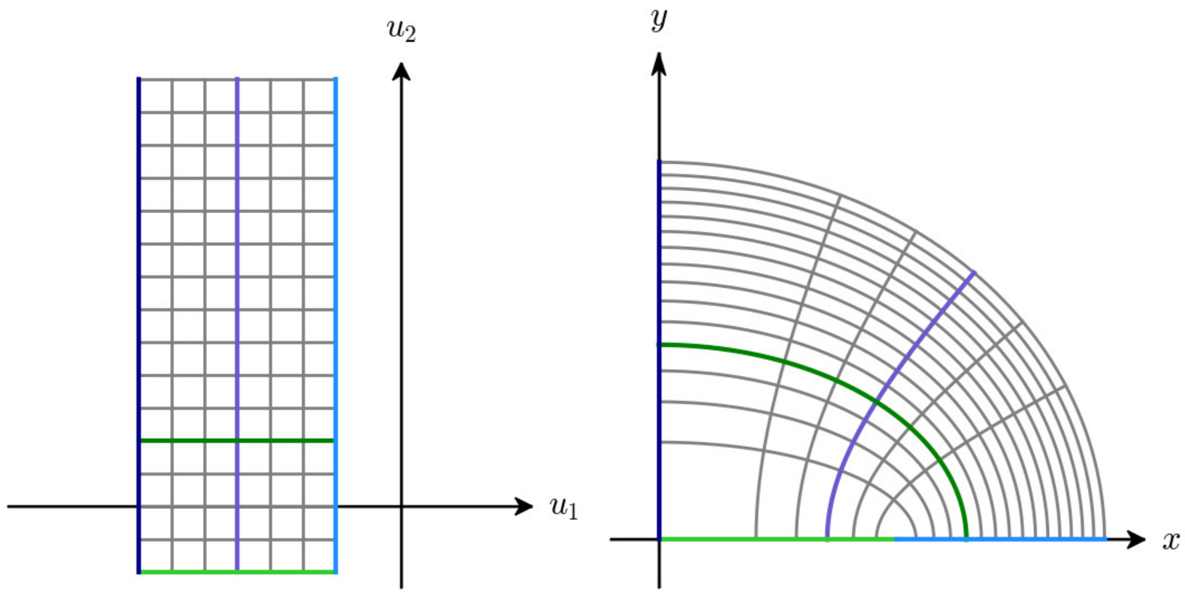

Figure 7.1. Square grid on the domain $\mathcal{U}$ and its image under the map (7.1). The horizontal lines $u_2 = const$ are mapped to ellipses with the degenerate case $u_2 \searrow -b$, which is mapped to a line segment on the x-axis. The vertical lines $u_1 = const$ are mapped to hyperbolas with the degenerate cases $u_1 \nearrow -b$, which is mapped to a ray on the x-axis, and $u_2 \searrow -a$, which is mapped to the positive y-axis.

7.2 Discrete confocal coordinates

We start with the general formula

$$x(n_1, n_2) = D_1(n_1 + \varepsilon_1 + c_1)_{1/2}(n_2 + \varepsilon_2 + c_1)_{1/2},$$

$$y(n_1, n_2) = D_2(-n_1 - \varepsilon_1 - c_2 + \tfrac{1}{2})_{1/2}(n_2 + \varepsilon_2 + c_2)_{1/2}$$

for a separable solution of the discrete Euler-Poisson-Darboux system (dEPD$_\gamma$) with $\gamma = \frac{1}{2}$, where a suitable choice of solutions (6.4), (6.5) has already been made according to the continuous case. We use the above ansatz to illustrate the choice of the coordinate shifts ε_i and c_k according to boundary conditions (6.6) and (6.7). For $\alpha, \beta \in \mathbb{Z}$ with $\alpha > \beta$, we define c_1, c_2 and $\varepsilon_1, \varepsilon_2$ such that we obtain a map

$$\mathcal{U} = \left\{(n_1, n_2) \in \mathbb{Z}^2 \mid -\alpha \leqslant n_1 \leqslant -\beta \leqslant n_2\right\} \to \mathbb{R}^2_+ \ ,$$

where the boundary components $n_1 = -\alpha$, $n_1 = -\beta$, and $n_2 = -\beta$ correspond to degenerate conics that lie on the coordinate axes:

$$\begin{aligned} x|_{n_1=-\alpha} &= 0 \quad \text{(degenerate hyperbola)},\\ y|_{n_1=-\beta} &= 0 \quad \text{(degenerate hyperbola)},\\ y|_{n_2=-\beta} &= 0 \quad \text{(degenerate ellipse)}. \end{aligned}$$

For this, the following linear system of equations has to be satisfied:

$$\begin{aligned} \varepsilon_1 + c_1 &= \alpha,\\ \varepsilon_1 + c_2 &= \beta + \frac{1}{2},\\ \varepsilon_2 + c_2 &= \beta. \end{aligned}$$

As a consequence, we find:

$$\varepsilon_2 + c_1 = \alpha - \frac{1}{2}.$$

Thus, we end up with the formula

$$\boldsymbol{x}(\boldsymbol{n}) = \begin{pmatrix} D_1(n_1+\alpha)_{1/2}(n_2+\alpha-\frac{1}{2})_{1/2} \\ D_2(-n_1-\beta)_{1/2}(n_2+\beta)_{1/2} \end{pmatrix}. \tag{7.2}$$

Up to scaling along the coordinate axes, the latter defines discrete confocal coordinates on the first quadrant of $\mathbb{R}^2$, if the domain $\mathcal{U}$ is extended to $\mathcal{U} \cup \mathcal{U}^*$ as demonstrated below. From this we generate a family of discrete confocal conics by reflections in the coordinate axes.

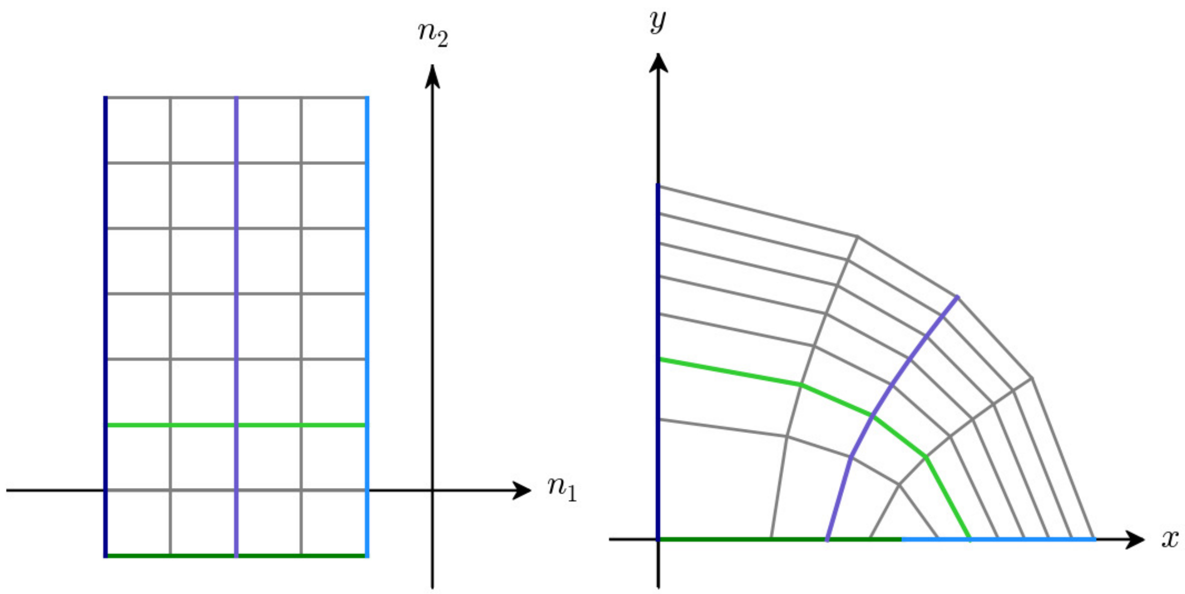

Figure 7.2. Points of the square grid on the domain $\mathcal{U}$ and their images under the map (7.2), joined by straight line segments respectively. The horizontal lines $n_2 =$ const are mapped to discrete ellipses with the degenerate case $n_2 = -\beta$, which is mapped to a line segment on the x-axis. The vertical lines $n_1 =$ const are mapped to discrete hyperbolas with the degenerate cases $n_1 = -\beta$, which is mapped to a ray on the x-axis, and $n_1 = -\alpha$, which is mapped to the positive y-axis.

In order to implement the orthogonality condition, we extend $\boldsymbol{x}$ to $\mathcal{U}^*$, and compute the discrete derivatives of the extension of $\boldsymbol{x}$ along the dual edges of the two dual square lattices $\mathcal{U}$ and $\mathcal{U}^*$. Formulas

(6.14) for the "discrete derivatives" of the discrete square root immediately lead to

$$\Delta_1 \boldsymbol{x}(\boldsymbol{n}) = \frac{1}{2}\begin{pmatrix} D_1 \dfrac{(n_2+\alpha-\frac{1}{2})_{1/2}}{(n_1+\alpha+\frac{1}{2})_{1/2}} \\[2ex] -D_2 \dfrac{(n_2+\beta)_{1/2}}{(-n_1-\beta-\frac{1}{2})_{1/2}} \end{pmatrix}$$

and

$$\Delta_2 \boldsymbol{x}(\boldsymbol{n}) = \frac{1}{2}\begin{pmatrix} D_1 \dfrac{(n_1+\alpha)_{1/2}}{(n_2+\alpha)_{1/2}} \\[2ex] D_2 \dfrac{(-n_1-\beta)_{1/2}}{(n_2+\beta+\frac{1}{2})_{1/2}} \end{pmatrix}.$$

If we introduce the notation

$$\boldsymbol{n}^{\sigma_1,\sigma_2} = \boldsymbol{n} + \tfrac{1}{2}(\sigma_1,\sigma_2), \quad \sigma_i = \pm 1,$$

then it turns out that

$$\langle \Delta_1 \boldsymbol{x}(\boldsymbol{n}), \Delta_2 \boldsymbol{x}(\boldsymbol{n}^{+-})\rangle = \tfrac{1}{4}(D_1^2 - D_2^2),$$

so that dual edges are orthogonal if and only if

$$D_1^2 = D_2^2.$$

We make the choice

$$D_1^2 = D_2^2 = \frac{1}{\alpha-\beta-\frac{1}{2}}. \tag{7.3}$$

Formulas (7.2) with the constants (7.3) constitute a discretization of the parametrization (7.1).

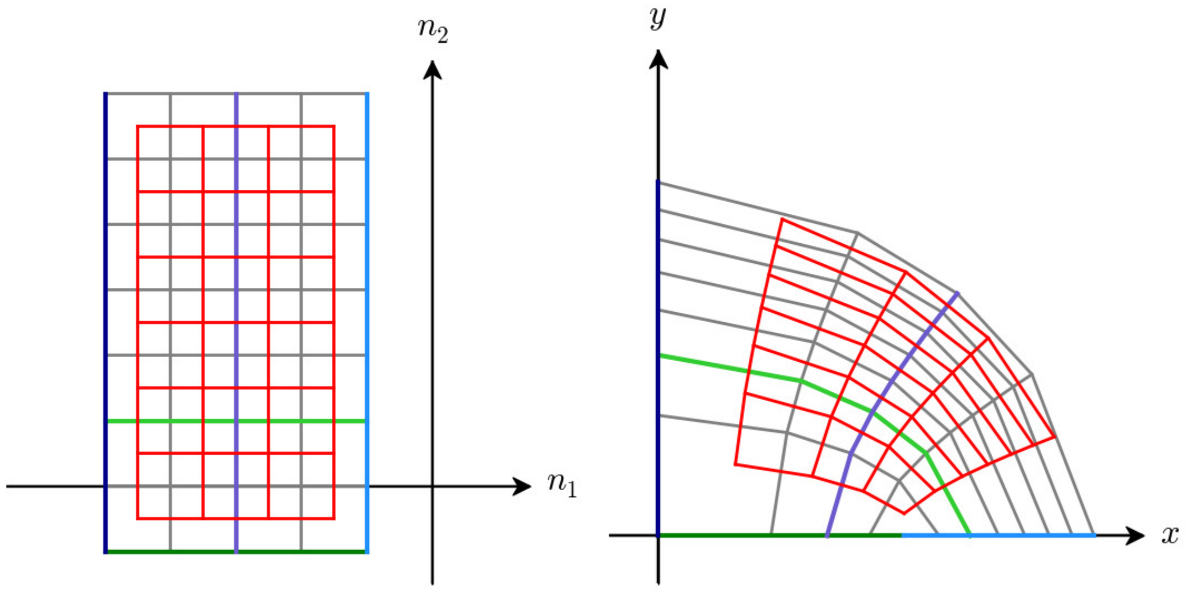

Figure 7.3. Points of the square grid on the domain $\mathcal{U} \cup \mathcal{U}^*$ and their images under the map (7.2). All pairs of corresponding dual edges are mutually orthogonal.

It is readily verified that with the choice (7.3), a lattice point $\boldsymbol{x}(\boldsymbol{n})$ and its nearest neighbours $\boldsymbol{x}(\boldsymbol{n}^{++})$ and $\boldsymbol{x}(\boldsymbol{n}^{+-})$ are related by

$$\begin{aligned} x(\boldsymbol{n})x(\boldsymbol{n}^{++}) &= \frac{(n_1+\alpha)(n_2+\alpha-\frac{1}{2})}{\alpha-\beta-\frac{1}{2}}, \\ y(\boldsymbol{n})y(\boldsymbol{n}^{++}) &= \frac{(n_1+\beta+\frac{1}{2})(n_2+\beta)}{\beta-\alpha+\frac{1}{2}}, \end{aligned} \tag{7.4}$$

respectively by

$$\begin{aligned} x(\boldsymbol{n})x(\boldsymbol{n}^{+-}) &= \frac{(n_1+\alpha)(n_2+\alpha-1)}{\alpha-\beta-\frac{1}{2}}, \\ y(\boldsymbol{n})y(\boldsymbol{n}^{+-}) &= \frac{(n_1+\beta+\frac{1}{2})(n_2+\beta-\frac{1}{2})}{\beta-\alpha+\frac{1}{2}}, \end{aligned} \tag{7.5}$$

which are natural discretizations of the formulas

$$x^2 = \frac{(u_1+a)(u_2+a)}{a-b}, \quad y^2 = \frac{(u_1+b)(u_2+b)}{b-a}$$

for the squares of coordinates. From (7.4), (7.5) one easily derives

$$\begin{aligned} \frac{x(\boldsymbol{n})x(\boldsymbol{n}^{++})}{n_1+\alpha} + \frac{y(\boldsymbol{n})y(\boldsymbol{n}^{++})}{n_1+\beta+\frac{1}{2}} &= 1, \\ \frac{x(\boldsymbol{n})x(\boldsymbol{n}^{++})}{n_2+\alpha-\frac{1}{2}} + \frac{y(\boldsymbol{n})y(\boldsymbol{n}^{++})}{n_2+\beta} &= 1, \end{aligned}$$

and

$$\begin{aligned} \frac{x(\boldsymbol{n})x(\boldsymbol{n}^{+-})}{n_1+\alpha} + \frac{y(\boldsymbol{n})y(\boldsymbol{n}^{+-})}{n_1+\beta+\frac{1}{2}} &= 1, \\ \frac{x(\boldsymbol{n})x(\boldsymbol{n}^{+-})}{n_2+\alpha-1} + \frac{y(\boldsymbol{n})y(\boldsymbol{n}^{+-})}{n_2+\beta-\frac{1}{2}} &= 1, \end{aligned}$$

which can be considered as discretizations of the defining equations of the two confocal conics through the point $(x, y) \in \mathbb{R}^2$:

$$\begin{aligned} \frac{x^2}{u_1+a} + \frac{y^2}{u_1+b} &= 1, \\ \frac{x^2}{u_2+a} + \frac{y^2}{u_2+b} &= 1. \end{aligned}$$

Observe that relations (7.4) and (7.5) may be regarded as two maps

$$\tau^{++} : \boldsymbol{x}(\boldsymbol{n}) \mapsto \boldsymbol{x}(\boldsymbol{n}^{++}), \quad \tau^{+-} : \boldsymbol{x}(n) \mapsto \boldsymbol{x}(\boldsymbol{n}^{+-}),$$

whose commutativity $\tau^{++} \circ \tau^{+-} = \tau^{+-} \circ \tau^{++}$ is directly verified. Thus, the net $\boldsymbol{x}$ can be uniquely determined from its value at a single vertex.

Proposition 6.9 in the case $N = 2$ can be shown by simple calculations starting either with the explicit parametrization (7.2) or the maps (7.4), (7.5). For instance, a factorization property associated with τ^{++} (shift by $\frac{1}{2}\boldsymbol{f}$) reads:

$$\frac{\left\langle \Delta_1 \boldsymbol{x}(\boldsymbol{n}), \Delta_1 \boldsymbol{x}(\boldsymbol{n}+\frac{1}{2}\boldsymbol{f}) \right\rangle}{\left\langle \Delta_2 \boldsymbol{x}(\boldsymbol{n}-\boldsymbol{e}_2+\frac{1}{2}\boldsymbol{f}), \Delta_2 \boldsymbol{x}(\boldsymbol{n}-\boldsymbol{e}_2+\boldsymbol{f}) \right\rangle} = \frac{\phi_1(n_1)}{\phi_2(n_2)}, \tag{7.6}$$

where

$$\frac{\phi_1(n_1)}{\phi_2(n_2)} = -\frac{(n_2+\alpha-\frac{1}{2})(n_2+\beta)}{(n_1+\alpha+\frac{1}{2})(n_1+\beta+1)},$$

and a similar property is associated with the map τ^{+-}. This can be seen as a discretization of the isothermicity property of the system of confocal conics which reads

$$\frac{|\partial \boldsymbol{x}/\partial u_1|^2}{|\partial \boldsymbol{x}/\partial u_2|^2} = \frac{\alpha_1(u_1)}{\alpha_2(u_2)},$$

where

$$\frac{\alpha_1(u_1)}{\alpha_2(u_2)} = -\frac{(u_2+a)(u_2+b)}{(u_1+a)(u_1+b)}.$$

The combinatorics of the factorization property (7.6) is illustrated in Figure 7.4.

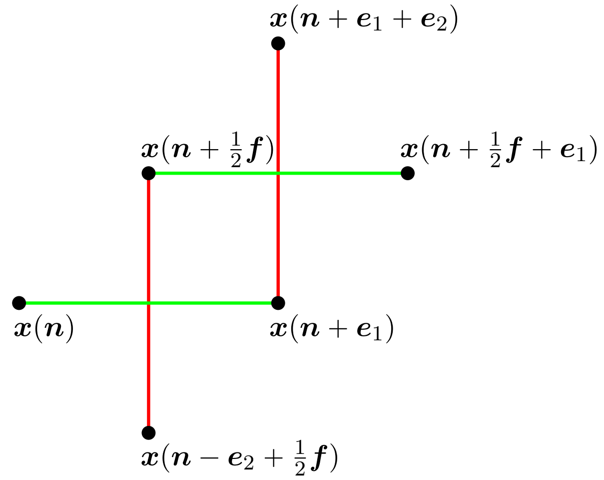

Figure 7.4. Combinatorics of the factorization property (7.6).

8 The case $N = 3$

8.1 Continuous confocal coordinates

Let $a > b > c > 0$. Then formulas

$$
\begin{aligned}
x(u_1,u_2,u_3) &= \frac{\sqrt{u_1+a}\sqrt{u_2+a}\sqrt{u_3+a}}{\sqrt{a-b}\sqrt{a-c}},\\
y(u_1,u_2,u_3) &= \frac{\sqrt{-(u_1+b)}\sqrt{u_2+b}\sqrt{u_3+b}}{\sqrt{a-b}\sqrt{b-c}},\\
z(u_1,u_2,u_3) &= \frac{\sqrt{-(u_1+c)}\sqrt{-(u_2+c)}\sqrt{u_3+c}}{\sqrt{a-c}\sqrt{b-c}}
\end{aligned}
$$

define a parametrization of the first octant of $\mathbb{R}^3$ by confocal coordinates,

$$
\mathcal{U} = \{(u_1,u_2,u_3) \mid -a < u_1 < -b < u_2 < -c < u_3\} \to \mathbb{R}^3_+ .
$$

Confocal quadrics are obtained by reflections of the coordinate surfaces (corresponding to $u_i = \text{const}$ for $i = 1, 2$ or 3) in the coordinate planes of $\mathbb{R}^3$, see Figure 0.1, left.

- The planes $u_3 = \text{const}$ are mapped to ellipsoids. In the degenerate case $u_3 \searrow -c$ one has $z = 0$, while $x(u_1,u_2)$ and $y(u_1,u_2)$ exactly recover the two-dimensional case (7.1) on the interior of an ellipse given by $u_2 \nearrow -c$.
- The planes $u_2 = \text{const}$ are mapped to one-sheeted hyperboloids with the two degenerate cases corresponding to $u_2 \nearrow -c$ and $u_2 \searrow -b$.
- The planes $u_1 = \text{const}$ are mapped to two-sheeted hyperboloids with the two degenerate cases corresponding to $u_1 \nearrow -b$ and $u_1 \searrow -a$.

8.2 Discrete confocal coordinates

Let $\alpha, \beta, \gamma \in \mathbb{Z}$ with $\alpha > \beta > \gamma$. Then the formula

$$
\boldsymbol{x}(\boldsymbol{n}) = \begin{pmatrix} D_1(n_1+\alpha)_{1/2}(n_2+\alpha-\frac{1}{2})_{1/2}(n_3+\alpha-1)_{1/2} \\ D_2(-n_1-\beta)_{1/2}(n_2+\beta)_{1/2}(n_3+\beta-\frac{1}{2})_{1/2} \\ D_3(-n_1-\gamma-\frac{1}{2})_{1/2}(-n_2-\gamma)_{1/2}(n_3+\gamma)_{1/2} \end{pmatrix} \tag{8.1}
$$

with $\boldsymbol{x}(\boldsymbol{n}) = (x(\boldsymbol{n}), y(\boldsymbol{n}), z(\boldsymbol{n}))$ defines a discrete net in the first octant of $\mathbb{R}^3$ (discrete confocal coordinate system), that is, a map

$$
\mathcal{U} = \left\{(n_1,n_2,n_3) \in \mathbb{Z}^3 \mid -\alpha \leqslant n_1 \leqslant -\beta \leqslant n_2 \leqslant -\gamma \leqslant n_3\right\} \to \mathbb{R}^3_+
$$

which is a separable solution of ($\mathrm{dEPD}_{1/2}$). If this net is extended to $\mathcal{U} \cup \mathcal{U}^*$ then discrete confocal quadrics are obtained by reflections of the coordinate surfaces (n_i = const for $i = 1, 2$ or 3) in the coordinate planes of $\mathbb{R}^3$, see Figure 0.1, right, provided that the constants D_k are chosen in the manner described below. The five boundary components $n_1 = -\alpha$, $n_1 = -\beta$, $n_2 = -\beta$, $n_2 = -\gamma$, and $n_3 = -\gamma$ are mapped to degenerate quadrics that lie in the coordinate planes of $\mathbb{R}^3$.

One computes the discrete derivatives with the help of formulas (6.14):

$$\Delta_1 \boldsymbol{x}(\boldsymbol{n}) = \frac{1}{2}\begin{pmatrix} D_1 \dfrac{(n_2+\alpha-\frac{1}{2})_{1/2}(n_3+\alpha-1)_{1/2}}{(n_1+\alpha+\frac{1}{2})_{1/2}} \\[2ex] -D_2 \dfrac{(n_2+\beta)_{1/2}(n_3+\beta-\frac{1}{2})_{1/2}}{(-n_1-\beta-\frac{1}{2})_{1/2}} \\[2ex] -D_3 \dfrac{(-n_2-\gamma)_{1/2}(n_3+\gamma)_{1/2}}{(-n_1-\gamma-1)_{1/2}} \end{pmatrix},$$

$$\Delta_2 \boldsymbol{x}(\boldsymbol{n}) = \frac{1}{2}\begin{pmatrix} D_1 \dfrac{(n_1+\alpha)_{1/2}(n_3+\alpha-1)_{1/2}}{(n_2+\alpha)_{1/2}} \\[2ex] D_2 \dfrac{(-n_1-\beta)_{1/2}(n_3+\beta-\frac{1}{2})_{1/2}}{(n_2+\beta+\frac{1}{2})_{1/2}} \\[2ex] -D_3 \dfrac{(-n_1-\gamma-\frac{1}{2})_{1/2}(n_3+\gamma)_{1/2}}{(-n_2-\gamma-\frac{1}{2})_{1/2}} \end{pmatrix}$$

and

$$\Delta_3 \boldsymbol{x}(\boldsymbol{n}) = \frac{1}{2}\begin{pmatrix} D_1 \dfrac{(n_1+\alpha)_{1/2}(n_2+\alpha-\frac{1}{2})_{1/2}}{(n_3+\alpha-\frac{1}{2})_{1/2}} \\[2ex] D_2 \dfrac{(-n_1-\beta)_{1/2}(n_2+\beta)_{1/2}}{(n_3+\beta)_{1/2}} \\[2ex] D_3 \dfrac{(-n_1-\gamma-\frac{1}{2})_{1/2}(-n_2-\gamma)_{1/2}}{(n_3+\gamma+\frac{1}{2})_{1/2}} \end{pmatrix}.$$

In accordance with the general orthogonality condition, we now demand that dual pairs of edges and faces of the nets $\boldsymbol{x}(\mathcal{U})$ and $\boldsymbol{x}(\mathcal{U}^*)$ be orthogonal, so that

$$\begin{aligned}
\langle \Delta_1 \boldsymbol{x}(\boldsymbol{n}), \Delta_2 \boldsymbol{x}(\boldsymbol{n} - \boldsymbol{e}_2 + \tfrac{1}{2}\boldsymbol{f})\rangle &= 0,\\
\langle \Delta_1 \boldsymbol{x}(\boldsymbol{n}), \Delta_3 \boldsymbol{x}(\boldsymbol{n} - \boldsymbol{e}_3 + \tfrac{1}{2}\boldsymbol{f})\rangle &= 0,\\
\langle \Delta_2 \boldsymbol{x}(\boldsymbol{n}), \Delta_3 \boldsymbol{x}(\boldsymbol{n} - \boldsymbol{e}_3 + \tfrac{1}{2}\boldsymbol{f})\rangle &= 0.
\end{aligned}$$

Evaluation of the above conditions leads to

$$\begin{aligned}
D_1^2(n_3+a-\tfrac{3}{2}) - D_2^2(n_3+b-\tfrac{3}{2}) + D_3^2(n_3+c-\tfrac{3}{2}) &= 0,\\
D_1^2(n_2+a-1) - D_2^2(n_2+b-1) + D_3^2(n_2+c-1) &= 0,\\
D_1^2(n_1+a-\tfrac{1}{2}) - D_2^2(n_1+b-\tfrac{1}{2}) + D_3^2(n_1+c-\tfrac{1}{2}) &= 0,
\end{aligned} \tag{8.2}$$

where

$$a = \alpha + \tfrac{1}{2}, \quad b = \beta + 1, \quad c = \gamma + \tfrac{3}{2}.$$

These are, *mutatis mutandis*, identical with their classical continuous counterparts as demonstrated in connection with the general case analyzed in Section 6. Since the coefficients D_i are independent of, for instance, n_3, the first condition in (8.2) splits into the pair

$$\begin{aligned}
D_1^2 - D_2^2 + D_3^2 &= 0,\\
D_1^2 a - D_2^2 b + D_3^2 c &= 0,
\end{aligned}$$

and it is evident that the remaining two conditions constitute linear combinations thereof. Accordingly, the orthogonality requirement leads to the unique relative scaling

$$\frac{D_1^2}{b-c} = \frac{D_2^2}{a-c} = \frac{D_3^2}{a-b} =: D^2.$$

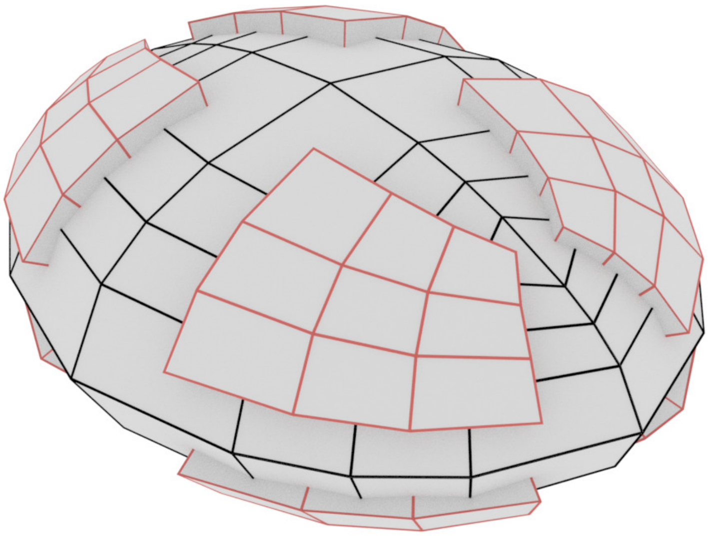

Figure 8.1. A discrete ellipsoid (n_1, n_2 integer, n_3 = const) from the system (8.1) and its two adjacent layers from the dual n (n_1, n_2 half-integer, n_3 = const $\pm \frac{1}{2}$). All faces are planar and orthogonal to the corresponding edges of the other net.

Remark 8.1. The curvature lines of a smooth surface are characterized by the following properties: they form a conjugate net, and along each curvature line two infinitesimally close normals intersect. In the case of discrete confocal coordinates the edges of the dual net $\boldsymbol{x}(\mathcal{U}^*)$ can be interpreted as normals to the faces of the net $\boldsymbol{x}(\mathcal{U})$. Since both nets have planar faces, any two neighboring normals intersect. Thus, extended edges of $\boldsymbol{x}(\mathcal{U}^*)$ constitute a *discrete line congruence* normal to the faces of the Q-net (discrete conjugate net) $\boldsymbol{x}(\mathcal{U})$ (cf. [BS] for the notion of a discrete line congruence).

The bilinear relations between a lattice point $\boldsymbol{x}(\boldsymbol{n})$ and its nearest neighbours $\boldsymbol{x}(\boldsymbol{n} + \frac{1}{2}\boldsymbol{\sigma})$ may be formulated as follows:

$$\frac{x(\boldsymbol{n})x(\boldsymbol{n}+\frac{1}{2}\boldsymbol{\sigma})}{u+a} + \frac{y(\boldsymbol{n})y(\boldsymbol{n}+\frac{1}{2}\boldsymbol{\sigma})}{u+b} + \frac{z(\boldsymbol{n})z(\boldsymbol{n}+\frac{1}{2}\boldsymbol{\sigma})}{u+c} = 1,$$

$$\frac{x(\boldsymbol{n})x(\boldsymbol{n}+\frac{1}{2}\boldsymbol{\sigma})}{v+a} + \frac{y(\boldsymbol{n})y(\boldsymbol{n}+\frac{1}{2}\boldsymbol{\sigma})}{v+b} + \frac{z(\boldsymbol{n})z(\boldsymbol{n}+\frac{1}{2}\boldsymbol{\sigma})}{v+c} = 1,$$

$$\frac{x(\boldsymbol{n})x(\boldsymbol{n}+\frac{1}{2}\boldsymbol{\sigma})}{w+a} + \frac{y(\boldsymbol{n})y(\boldsymbol{n}+\frac{1}{2}\boldsymbol{\sigma})}{w+b} + \frac{z(\boldsymbol{n})z(\boldsymbol{n}+\frac{1}{2}\boldsymbol{\sigma})}{w+c} = 1,$$

provided that

$$D^2 = \frac{1}{(a-b)(a-c)(b-c)},$$

and

$$u = n_1 + \tfrac{1}{4}\sigma_1 - \tfrac{3}{4}, \quad v = n_2 + \tfrac{1}{4}\sigma_2 - \tfrac{5}{4}, \quad w = n_3 + \tfrac{1}{4}\sigma_3 - \tfrac{7}{4}.$$

8.3 Discrete umbilics and discrete focal conics

An interesting feature of discrete confocal quadrics which is not present in the two-dimensional case is obtained by considering the "discrete umbilics" (that is, vertices of valence different from 4) of the discrete ellipsoids $n_3 = \text{const}$ and the discrete two-sheeted hyperboloids $n_1 = \text{const}$. In the case of the discrete ellipsoids, these have valence 2 and are located at $n_1 = n_2 = -\beta$ so that (8.1) reduces to the planar discrete curve

$$\boldsymbol{x}(n_3) = \begin{pmatrix} D_1(\alpha - \beta - \frac{1}{2})(n_3 + \alpha - 1)_{1/2} \\ 0 \\ D_3(\beta - \gamma - \frac{1}{2})(n_3 + \gamma)_{1/2} \end{pmatrix}.$$

Once again, it turns out convenient to extend the domain of this one-dimensional lattice to the appropriate subset of $\mathbb{Z} \cup \mathbb{Z}^*$ so that

$$\frac{x(n_3)x(n_3 + \frac{1}{2})}{\alpha - \beta - \frac{1}{2}} - \frac{z(n_3)z(n_3 + \frac{1}{2})}{\beta - \gamma - \frac{1}{2}} = 1.$$

The latter constitutes a discretization of the focal hyperbola [So]

$$\frac{x^2}{a - b} - \frac{z^2}{b - c} = 1$$

which is known to be the locus of the umbilical points of confocal ellipsoids. Similarly, evaluation of (8.1) at $n_2 = n_3 = -\gamma$ produces the planar discrete curve

$$\boldsymbol{x}(n_1) = \begin{pmatrix} D_1(\alpha - \gamma - 1)(n_1 + \alpha)_{1/2} \\ D_2(\beta - \gamma - \frac{1}{2})(-n_1 - \beta)_{1/2} \\ 0 \end{pmatrix}$$

which consists of the discrete umbilics of the discrete two-sheeted hyperboloids. Extension to half-integers yields

$$\frac{x(n_1)x(n_1 + \frac{1}{2})}{\alpha - \gamma - 1} + \frac{y(n_1)y(n_1 + \frac{1}{2})}{\beta - \gamma - \frac{1}{2}} = 1,$$

which reproduces, in the formal continuum limit, the classical focal ellipse

$$\frac{x^2}{a - c} + \frac{y^2}{b - c} = 1$$

as the locus of the umbilical points of confocal two-sheeted hyperboloids.

A Incircular nets as orthogonal Koenigs nets

A geometric discretization of confocal conics as incircular nets (IC-nets) was recently suggested in [AB]. This version of discrete confocal conics is given via a simple local geometric condition: one considers a congruence of straight lines with the combinatorics of the square grid such that all the quadrilaterals formed by neighboring lines possess inscribed circles. In this appendix we show that, surprisingly, IC-nets share two crucial properties with discrete confocal coordinates introduced in the present paper, namely the Koenigs property and the orthogonality in the sense of Definition 6.4. One should mention however that IC-nets are not separable, therefore they do not constitute a special case of discrete confocal conics as defined in Defintion 6.6.[1]

Definition A.1. *A discrete net* $f : \mathbb{Z}^2 \supset U \to \mathbb{R}^2$ *is called an* incircular net (IC-net) *if*

(i) The points $f_{i,j}$ *with* $i = \text{const}$*, respectively* $j = \text{const}$*, lie on straight lines, preserving the order.*

(ii) Every elementary quadrilateral $(f_{i,j}, f_{i+1,j}, f_{i+1,j+1}, f_{i,j+1})$ *has an incircle.*

All lines of an IC-net touch some conic α, while all vertices of one diagonal $i + j = \text{const}$, resp. $i - j = \text{const}$, lie on a conic confocal to α.

[1]This observation, made on the basis of numerical experiments, was not correct (cf. Chapter 2: Remark 8.1). In fact IC-nets do constitute a special case of discrete confocal conics (see Chapter 2: Sections 8.4 and 8.5).

Denote the incenter of the quadrilateral $(f_{i,j}, f_{i+1,j}, f_{i+1,j+1}, f_{i,j+1})$ by $\omega_{i,j}$. So, $\omega : U \to \mathbb{R}^2$ is the net of incenters of f. Note that ω also possesses property (i). Denote the two dual subnets of ω, corresponding to (i,j) with $2k := i+j$ and $2l := j-i$ even, respectively odd, by η and $\tilde{\eta}$:

$$\eta_{k,l} := \omega_{k-l,k+l},\ (k,l) \in \mathbb{Z}^2 \quad \text{and} \quad \tilde{\eta}_{k,l} := \omega_{k-l,k+l},\ (k,l) \in (\mathbb{Z}^2)^*.$$

In Figure A.1, the edges of the nets η and $\tilde{\eta}$ are shown. The intersection points of dual pairs of edges happen to be points of the underlying IC-net f. At each such point, the intersecting edges of η and of $\tilde{\eta}$ are tangent to the confocal conics mentioned above (the conics through $f_{i,j}$ with $i+j = 2k = \text{const}$, resp. with $j - i = 2l = \text{const}$). Therefore, the dual pairs of edges are orthogonal. We show that these nets also possess the Koenigs property and collect their important properties in the following theorem.

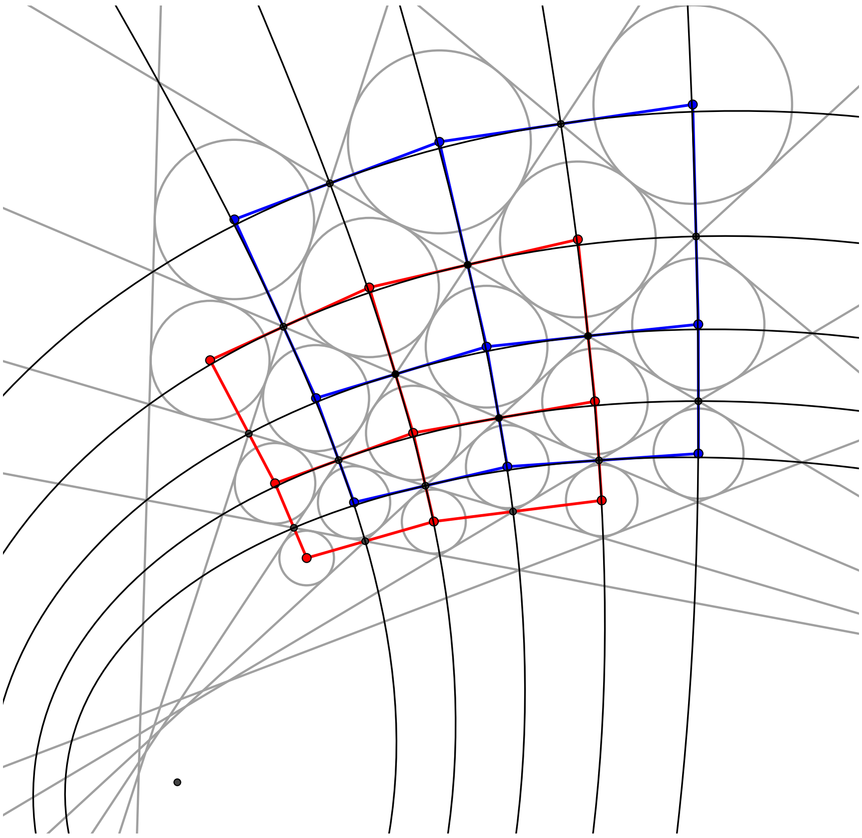

Figure A.1. Two dual subnets η and $\tilde{\eta}$ of the net of incenters of an IC-net. The edges are tangent to confocal conics, and corresponding edges of the two nets are orthogonal.

Theorem A.2. *For the two dual subnets η and $\tilde{\eta}$ of the incenter-net of an IC-net:*

(i) *the edges are tangent to confocal conics, the points of tangency being the points of the IC-net;*

(ii) *each subnet consists of intersection points of diagonals of elementary quadrilaterals of the other subnet;*

(iii) *both subnets are circular-conical (that is, opposite angles sum up to π in each quadrilateral and at each vertex-star);*

(iv) *each pair of dual edges intersects orthogonally;*

(v) *both subnets are Koenigs nets.*

Proof.

(i) See [AB].

(ii) This holds for the two dual subnets of any net consisting of straight lines.

(iii) Each of the dual nets corresponds to the incenters of a checkerboard IC-net, that is, a net having incircles in every other quadrilateral (both checkerboard IC-nets fitting perfectly into each other forming a regular IC-net). Checkerboard IC-nets have been observed to be circular-conical in [AB].

(iv) Dual edges intersect at a point where two lines of the IC-net intersect. The dual edges of η and of $\tilde{\eta}$ are the two angle bisectors of those two lines of the IC-net, and therefore are mutually orthogonal.

(v) From now on, we use the shift notation, like in Section 4, so that $\eta_{(\pm i)}(\boldsymbol{n}) := \eta(\boldsymbol{n} \pm \boldsymbol{e}_i)$ and $\eta_{(ij)}(\boldsymbol{n}) := \eta(\boldsymbol{n} + \boldsymbol{e}_i + \boldsymbol{e}_j)$, with the understanding that the argument of η, $\tilde{\eta}$ is (k,l), while the argument of f is (i,j). Consider four quadrilaterals of the net η adjacent to one vertex (compare Figure A.2). The points of intersection of diagonals of these four quadrilaterals are the points $\tilde{\eta}$, $\tilde{\eta}_{(1)}$, $\tilde{\eta}_{(12)}$, $\tilde{\eta}_{(2)}$ of the net $\tilde{\eta}$. We show that

$$\frac{|\eta_{(1)}\tilde{\eta}_{(12)}|}{|\tilde{\eta}_{(12)}\eta_{(2)}|} \cdot \frac{|\eta_{(2)}\tilde{\eta}_{(2)}|}{|\tilde{\eta}_{(2)}\eta_{(-1)}|} \cdot \frac{|\eta_{(-1)}\tilde{\eta}|}{|\tilde{\eta}\eta_{(-2)}|} \cdot \frac{|\eta_{(-2)}\tilde{\eta}_{(1)}|}{|\tilde{\eta}_{(1)}\eta_{(1)}|} = 1.$$

This is equivalent to the net η being Koenigs (see [BS, p. 52]).

Considering one of the four quotients on the left-hand side, we find:

$$\frac{|\eta_{(1)}\tilde{\eta}_{(12)}|}{|\tilde{\eta}_{(12)}\eta_{(2)}|} = \frac{\operatorname{area}(\eta_{(1)}, \tilde{\eta}_{(12)}, \eta)}{\operatorname{area}(\tilde{\eta}_{(12)}, \eta_{(2)}, \eta)} = \frac{|f_{(1)}\tilde{\eta}_{(12)}| \cdot |\eta\eta_{(1)}|}{|f_{(12)}\tilde{\eta}_{(12)}| \cdot |\eta\eta_{(2)}|},$$

since the dual edges of η and of $\tilde{\eta}$ are orthogonal. In the product the lengths of the edges $|\eta\eta_{(i)}|$ cancel out, and we obtain

$$\begin{aligned} &\frac{|\eta_{(1)}\tilde{\eta}_{(12)}|}{|\tilde{\eta}_{(12)}\eta_{(2)}|} \cdot \frac{|\eta_{(2)}\tilde{\eta}_{(2)}|}{|\tilde{\eta}_{(2)}\eta_{(-1)}|} \cdot \frac{|\eta_{(-1)}\tilde{\eta}|}{|\tilde{\eta}\eta_{(-2)}|} \cdot \frac{|\eta_{(-2)}\tilde{\eta}_{(1)}|}{|\tilde{\eta}_{(1)}\eta_{(1)}|} \\ &\quad = \left(\frac{|\tilde{\eta}f|}{|f\tilde{\eta}_{(1)}|} \cdot \frac{|\tilde{\eta}_{(1)}f_{(1)}|}{|f_{(1)}\tilde{\eta}_{(12)}|} \cdot \frac{|\tilde{\eta}_{(12)}f_{(12)}|}{|f_{(12)}\tilde{\eta}_{(2)}|} \cdot \frac{|\tilde{\eta}_{(2)}f_{(2)}|}{|f_{(2)}\tilde{\eta}|} \right)^{-1}. \end{aligned}$$

The latter product is equal to 1 since the triangles $(\tilde{\eta}, f, f_{(2)})$ and $(\tilde{\eta}_{(12)}, f_{(1)}, f_{(12)})$ are perspective triangles (Menelaus condition for Desargues configuration, cf. [BS, p. 361]). We mention that the right-hand side of the latter formula being equal to 1 is the Koenigs condition for the net ω, while the left-hand side being equal to 1 is the Koenigs condition for the net η. $\square$

Apparently, there also holds:

(vi) *the dual subnets η and $\tilde{\eta}$ satisfy the discrete factorization property* (7.6),

but at present this only has been checked via numerical experiments.

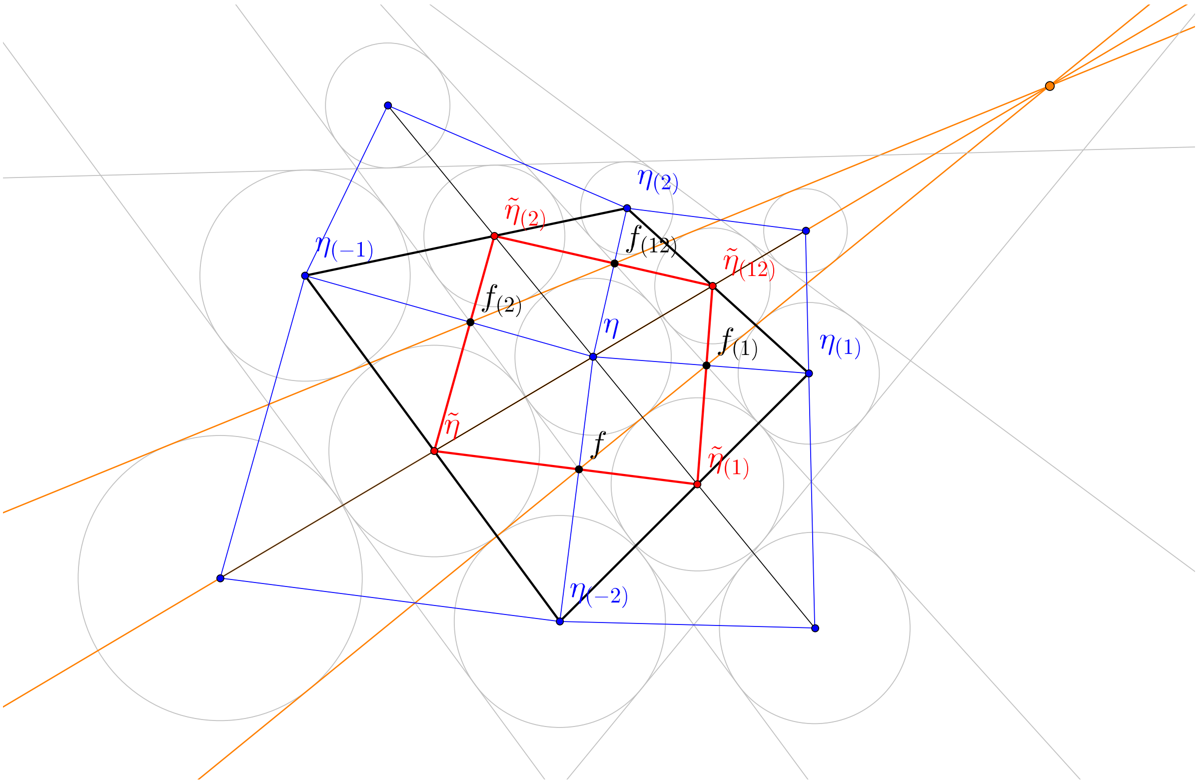

Figure A.2. Koenigs property of the incenter net ω of an IC-net implies the Koenigs property for its two diagonal nets η and $\tilde{\eta}$.

References

[AB] [Ar] [BSST2] [BS] [Da2] [Ei1] [Ei2] [EMOT] [FT] [GGR] [Ja] [KS2] [Mo] [So] [Ts]

Chapter 2

On a discretization of confocal quadrics. II. A geometric approach to general parametrizations

Alexander I. Bobenko[1], Wolfgang K. Schief[2], Yuri B. Suris[1], Jan Techter[1]

[1]Institut für Mathematik, TU Berlin,
Str. des 17. Juni 136, 10623 Berlin, Germany

[2]School of Mathematics and Statistics,
The University of New South Wales, Sydney, NSW 2052, Australia

Abstract. We propose a discretization of classical confocal coordinates. It is based on a novel characterization thereof as factorizable orthogonal coordinate systems. Our geometric discretization leads to factorizable discrete nets with a novel discrete analog of the orthogonality property. A discrete confocal coordinate system may be constructed geometrically via polarity with respect to a sequence of classical confocal quadrics. Various sequences correspond to various discrete parametrizations. The coordinate functions of discrete confocal quadrics are computed explicitly. The theory is illustrated with a variety of examples in two and three dimensions. These include confocal coordinate systems parametrized in terms of Jacobi elliptic functions. Connections with incircular (IC) nets and a generalized Euler-Poisson-Darboux system are established.

Acknowledgements. This research was supported by the DFG Collaborative Research Center TRR 109 "Discretization in Geometry and Dynamics". W.S. was also supported by the Australian Research Council (DP1401000851).

International Mathematics Research Notices, Volume 2020, Issue 24, December 2020, Pages 10180–10230,
`https://doi.org/10.1093/imrn/rny279`

1 Introduction

Confocal quadrics have played a prominent role in classical mathematics due to their beautiful geometric properties and numerous relations and applications to various branches of mathematics. Optical properties of quadrics and their confocal families were already discovered by the ancient Greeks and continued to fascinate mathematicians for many centuries, culminating in the famous Ivory and Chasles theorems from 19th century given a modern interpretation by Arnold [Ar, Appendix 15]. Geodesic flows on quadrics and billiards in quadrics are classical examples of integrable systems [Ja, Mo, Ve, FT]. Gravitational properties of ellipsoids were studied in detail by Newton, Ivory and others, see [FT, Part 8], and are based to a large extent on the geometric properties of confocal quadrics. Quadrics in general and confocal systems of quadrics in particular constitute popular objects in geometry. Poncelet and Ivory theorems play a central role there [DR, IT]. In differential geometry quadrics provide non-trivial examples of isothermic surfaces which form one of the most interesting classes of "integrable" surfaces, that is, surfaces which are governed by integrable differential equations and possess a rich theory of transformations with remarkable permutability properties [BS]. Importantly, confocal quadrics also lie at the heart of confocal coordinate systems which give rise to separation of variables in the Laplace operator. As such, they support a rich theory of special functions, including Lamé functions and their generalizations [EMOT, WW].

In general, coordinate systems are instances of *smooth nets*, that is, maps $\mathbb{R}^M \supset U \to \mathbb{R}^N$. In this paper we present a novel characterization of confocal coordinate systems: a coordinate system $\mathbb{R}^N \supset U \ni \boldsymbol{s} \mapsto \boldsymbol{x}(\boldsymbol{s}) \in \mathbb{R}^N$ is confocal if and only if it is orthogonal and the coordinates x_i factorize as functions of the parameters s_j, that is,

$$x_i(\boldsymbol{s}) = f_1^i(s_1) f_2^i(s_2) \cdots f_N^i(s_N), \quad i = 1, \ldots, N$$

(see Section 3).

Orthogonal coordinate systems constitute a classical topic in differential geometry. They were extensively treated in the fundamental monograph by Darboux [Da2]. From the viewpoint of the theory of integrable systems they were investigated in [Za]. Algebro-geometric orthogonal coordinate systems were constructed in [Kr]. Although it is natural to expect that confocal coordinate systems belong to this class, it remains an open problem to include them in Krichever's construction (see [MT]).

Discretizing coordinate systems consists of finding suitable approximating *discrete nets*, that is, maps $\mathbb{Z}^M \supset U \to \mathbb{R}^N$. Various discretizations of orthogonal coordinate systems have been proposed. The most investigated variant is the class of circular nets [Bo, CDS, KS1], where all elementary quadrilaterals are inscribed in circles. This class inherits the property of orthogonal coordinate systems to be invariant under Möbius transformations. A special case of Darboux-Egorov metrics was discretized in [AVK] as circular nets whose quadrilaterals have two opposite right angles. Another discretization of orthogonal nets is given by conical nets [LPWYW], which are characterized by the property that any four neighboring planar quadrilaterals are tangent to a sphere. This class is preserved by Laguerre transformations. Circular and conical nets may be unified in the context of Lie geometry as principal contact element nets [BS, PW].

Recently, in [BSST1], we have proposed an integrability-preserving discretization of systems of confocal quadrics or, equivalently, systems of confocal coordinates in $\mathbb{R}^N$. The discretization is based on a discrete version [KS2] of the Euler-Poisson-Darboux system, which is known to encode algebraically classical systems of confocal quadrics. This algebraic approach resulted in particular in a new geometric orthogonality condition, which is of central importance in the current paper. In this new sense, a discrete coordinate system $(\frac{1}{2}\mathbb{Z})^N \supset U \ni \boldsymbol{n} \mapsto \boldsymbol{x}(\boldsymbol{n}) \in \mathbb{R}^N$ is discrete orthogonal if any edge of any of the $\mathbb{Z}^N$ sublattices is orthogonal to the dual facet of the dual $\mathbb{Z}^N$ sublattice (see Section 4).

In Section 5 we define *discrete confocal coordinate systems* as orthogonal (in the new sense) nets $(\frac{1}{2}\mathbb{Z})^N \supset U \ni \boldsymbol{n} \mapsto \boldsymbol{x}(\boldsymbol{n}) \in \mathbb{R}^N$ such that the coordinates x_i factorize as functions of the lattice arguments n_j, that is,

$$x_i(\boldsymbol{n}) = f_1^i(n_1) f_2^i(n_2) \cdots f_N^i(n_N), \quad i = 1, \ldots, N.$$

We provide an explicit description of discrete confocal coordinate systems in Theorems 5.2, 5.5, 5.6.

In Section 6 we show that discrete confocal coordinate systems admit a geometric characterization in terms of polarity with respect to quadrics of a classical confocal family. The connection with the particular case discussed in [BSST1] is set down in Section 7.

Sections 8–9 contain an extensive collection of examples of discrete confocal coordinates in the cases $N = 2$ and $N = 3$. We begin by presenting in Section 8.2 the discrete analogue of the classical parametrization of systems of confocal conic sections in terms of trigonometric and hyperbolic functions. Then, in Sections 8.4–8.5 we record a novel parametrization of confocal coordinate systems in $\mathbb{R}^2$, both continuous and discrete, in terms of Jacobi elliptic functions. The discrete confocal coordinate systems of these families are intimately related to incircular (IC) nets studied in [AB]. In Section 9, we show that the classical confocal coordinate systems in $\mathbb{R}^3$ parametrized in terms of Jacobi elliptic functions admit a natural discrete analogue. Finally, in the Appendix, we present a generalized discrete Euler-Poisson-Darboux systems which algebraically encodes discrete confocal coordinate systems.

2 Classical confocal coordinate systems

For given $a_1 > a_2 > \cdots > a_N > 0$, we consider the one-parameter family of confocal quadrics in $\mathbb{R}^N$ given by

$$Q(\lambda) = \left\{ \boldsymbol{x} = (x_1, \ldots, x_N) \in \mathbb{R}^N : \sum_{k=1}^{N} \frac{x_k^2}{a_k + \lambda} = 1 \right\}, \quad \lambda \in \mathbb{R}. \tag{2.1}$$

Note that the quadrics of this family are centered at the origin and have the principal axes aligned along the coordinate directions. For a given point $\boldsymbol{x} = (x_1, \ldots, x_N) \in \mathbb{R}^N$ with $x_1 x_2 \ldots x_N \neq 0$, equation $\sum_{k=1}^N x_k^2/(a_k + \lambda) = 1$ is, after clearing the denominators, a polynomial equation of degree N in λ, with N real roots $u_1, \ldots, u_N$ lying in the intervals

$$-a_1 < u_1 < -a_2 < u_2 < \cdots < -a_N < u_N, \tag{2.2}$$

so that

$$\sum_{k=1}^{N} \frac{x_k^2}{\lambda + a_k} - 1 = -\frac{\prod_{m=1}^N (\lambda - u_m)}{\prod_{m=1}^N (\lambda + a_m)}. \tag{2.3}$$

These N roots correspond to the N confocal quadrics of the family (2.1) that intersect at the point $\boldsymbol{x} = (x_1, \ldots, x_N)$:

$$\sum_{k=1}^{N} \frac{x_k^2}{a_k + u_i} = 1, \quad i = 1, \ldots, N \quad \Leftrightarrow \quad \boldsymbol{x} \in \bigcap_{i=1}^{N} Q(u_i). \tag{2.4}$$

The N quadrics $Q(u_i)$ are all of different signatures. Evaluating the residue of the right-hand side of (2.3) at $\lambda = -a_k$, one can easily express x_k^2 through $u_1, \ldots, u_N$:

$$x_k^2 = \frac{\prod_{i=1}^N (u_i + a_k)}{\prod_{i \neq k} (a_k - a_i)}, \quad k = 1, \ldots, N. \tag{2.5}$$

Thus, for each point $(x_1, \ldots, x_N) \in \mathbb{R}^N$ with $x_1 x_2 \ldots x_N \neq 0$, there is exactly one solution $(u_1, \ldots, u_N) \in \mathcal{U}$ of (2.5), where

$$\mathcal{U} = \left\{ (u_1, \ldots, u_N) \in \mathbb{R}^N \mid -a_1 < u_1 < -a_2 < u_2 < \ldots < -a_N < u_N \right\}.$$

On the other hand, for each $(u_1, \ldots, u_N) \in \mathcal{U}$ there are exactly 2^N solutions $(x_1, \ldots, x_N) \in \mathbb{R}^N$, which are mirror symmetric with respect to the coordinate hyperplanes. In what follows, when we refer to a solution of (2.5), we always mean the solution with values in

$$\mathbb{R}_+^N = \left\{ (x_1, \ldots, x_N) \in \mathbb{R}^N \mid x_1 > 0, \ldots, x_N > 0 \right\}.$$

Thus, we are dealing with a parametrization of the first hyperoctant of $\mathbb{R}^N$, $\boldsymbol{x} : \mathcal{U} \ni (u_1, \ldots, u_N) \mapsto (x_1, \ldots, x_N) \in \mathbb{R}_+^N$, given by

$$x_k = \frac{\prod_{i=1}^{k-1} \sqrt{-(u_i + a_k)} \prod_{i=k}^{N} \sqrt{u_i + a_k}}{\prod_{i=1}^{k-1} \sqrt{a_i - a_k} \prod_{i=k+1}^{N} \sqrt{a_k - a_i}}, \quad k = 1, \ldots, N, \tag{2.6}$$

such that the coordinate hyperplanes $u_i = \text{const}$ are mapped to (parts of) the respective quadrics given by (2.4). The coordinates $(u_1, \dots, u_N)$ are called *confocal coordinates* (or *elliptic coordinates*, following Jacobi [Ja, Vorlesung 26]).

For various applications, it is often useful to re-parametrize the coordinate lines according to $u_i = u_i(s_i)$, $i = 1, \dots, N$. One of the reasons of the usefulness of this procedure is the possibility to uniformize the square roots in the above formulas, that is, to present them as single-valued functions of the new coordinates s_i. A classical example in the dimension $N = 2$, where

$$x_1 = \frac{\sqrt{u_1 + a_1}\sqrt{u_2 + a_1}}{\sqrt{a_1 - a_2}}, \quad x_2 = \frac{\sqrt{-(u_1 + a_2)}\sqrt{u_2 + a_2}}{\sqrt{a_1 - a_2}},$$

is to set

$$u_1 = -a_1 \sin^2 s_1 - a_2 \cos^2 s_1, \quad u_2 = a_1 \sinh^2 s_2 - a_2 \cosh^2 s_2,$$

so that

$$u_1 + a_1 = (a_1 - a_2)\cos^2 s_1, \quad -(u_1 + a_2) = (a_1 - a_2)\sin^2 s_1,$$

and

$$u_2 + a_1 = (a_1 - a_2)\cosh^2 s_2, \quad u_2 + a_2 = (a_1 - a_2)\sinh^2 s_2.$$

Accordingly, one obtains a version of elliptic coordinates in the plane free from branch points and naturally periodic with respect to s_1:

$$x_1 = \sqrt{a_1 - a_2}\cos s_1 \cosh s_2, \quad x_2 = \sqrt{a_1 - a_2}\sin s_1 \sinh s_2.$$

Such a re-parametrization, being a relatively trivial operation for classical coordinate systems, does not have a simple counterpart in the discrete context. Actually, the lack of the notion of a re-parametrization is one of the main and fundamental differences between discrete differential geometry and discrete analysis, on the one hand, and their classical analogs, on the other hand. It is one of the principal goals of this paper to present a natural geometric construction of a general parametrization for discrete confocal coordinate systems.

3 Characterization of confocal coordinate systems

Our main subject in this paper are coordinate systems, i.e., maps $\boldsymbol{x} : \mathbb{R}^N \supset U \to \mathbb{R}^N$ on open sets U such that $\det(\partial x_i/\partial s_j)_{i,j=1}^N \neq 0$. We now demonstrate that the two properties, factorization and orthogonality, are sufficient to characterize confocal coordinates. For the sake of simplicity, we restrict ourselves to coordinate systems satisfying the additional condition $\partial x_i/\partial s_j \neq 0$, which excludes degenerate cases like cylindric, spherical coordinates etc.

Theorem 3.1. *If a coordinate system $\boldsymbol{x} : \mathbb{R}^N \supset U \to \mathbb{R}^N$ satisfies two conditions:*

i) $\boldsymbol{x}(\boldsymbol{s})$ factorizes, *in the sense that*

$$\begin{cases} x_1(\boldsymbol{s}) = f_1^1(s_1) f_2^1(s_2) \cdots f_N^1(s_N), \\ x_2(\boldsymbol{s}) = f_1^2(s_1) f_2^2(s_2) \cdots f_N^2(s_N), \\ \dots \\ x_N(\boldsymbol{s}) = f_1^N(s_1) f_2^N(s_2) \cdots f_N^N(s_N), \end{cases} \tag{3.1}$$

with all $f_i^k(s_i) \neq 0$ and $\left(f_i^k\right)'(s_i) \neq 0$;

ii) $\boldsymbol{x}$ *is* orthogonal, *that is,*

$$\langle \partial_i \boldsymbol{x}, \partial_j \boldsymbol{x} \rangle = 0 \quad for \quad i \neq j, \tag{3.2}$$

then all coordinate hypersurfaces are confocal quadrics.

Proof. One easily computes that the orthogonality condition (3.2) for a factorized net (3.1) is equivalent to

$$\sum_{k=1}^{N} \big(f_i^k\big)'(s_i) f_i^k(s_i) \big(f_j^k\big)'(s_j) f_j^k(s_j) \prod_{\ell \neq i,j} \big(f_\ell^k(s_\ell)\big)^2 = 0,$$

or

$$\sum_{k=1}^{N} \big(F_i^k\big)'(s_i) \big(F_j^k\big)'(s_j) \prod_{\ell \neq i,j} F_\ell^k(s_\ell) = 0, \tag{3.3}$$

where $F_i^k(s_i) = \big(f_i^k(s_i)\big)^2$.

Lemma 3.2. *Equation* (3.3) *is equivalent to*

$$\sum_{k=1}^{N} F_1^k(s_1) F_2^k(s_2) \cdots F_N^k(s_N) = A_1(s_1) + A_2(s_2) + \ldots + A_N(s_N), \tag{3.4}$$

with some functions $A_i(s_i)$.

Proof. Equation (3.3) reads: $\partial^2 F / \partial s_i \partial s_j = 0$, where the function F is the left-hand side of (3.4). Induction with respect to N shows that this is equivalent to F being a sum of functions of single arguments. □

Lemma 3.3. *Assume that all* $f_i^k \neq 0$ *and* $\big(f_i^k\big)' \neq 0$. *Then, for each* $i = 1, \ldots, N$ *there exists a function* $F_i(s_i)$ *such that*

$$F_i^k(s_i) = \alpha_i^k F_i(s_i) + \beta_i^k, \quad k = 1, \ldots, N, \tag{3.5}$$

for some constants $\alpha_i^k \neq 0$ *and* β_i^k.

Proof. Note that the assumption of lemma is equivalent to $\big(F_i^k\big)' \neq 0$. We will prove that for each $i = 1, \ldots, N$ we have

$$\begin{pmatrix} \big(F_i^1\big)'(s_i) \\ \ldots \\ \big(F_i^N\big)'(s_i) \end{pmatrix} \in \mathbb{R} \begin{pmatrix} \alpha_i^1 \\ \ldots \\ \alpha_i^N \end{pmatrix}. \tag{3.6}$$

For any fixed i, equation (3.3) can be formulated as the following $N-1$ orthogonality conditions:

$$\begin{pmatrix} \big(F_i^1\big)' \\ \ldots \\ \big(F_i^N\big)' \end{pmatrix} \perp \begin{pmatrix} \big(F_j^1\big)' \prod_{\ell \neq i,j} F_\ell^1 \\ \ldots \\ \big(F_j^N\big)' \prod_{\ell \neq i,j} F_\ell^N \end{pmatrix}, \quad j \neq i. \tag{3.7}$$

To prove (3.6), we will show that the $N-1$ vectors on the right-hand side of (3.7) span an $(N-1)$-dimensional subspace of $\mathbb{R}^N$ which is obviously independent of s_i. Thus, its orthogonal complement is a one-dimensional space which does not depend on s_i. To prove the claim about the dimension, we multiply the $N-1$ vectors on the right-hand side of (3.7) from the left by the non-degenerate matrix

$$\mathrm{diag}\Big(\prod_{\ell \neq i} F_\ell^1, \ldots, \prod_{\ell \neq i} F_\ell^N\Big)^{-1},$$

to obtain vectors

$$\begin{pmatrix} \big(F_j^1\big)'/F_j^1 \\ \ldots \\ \big(F_j^N\big)'/F_j^N \end{pmatrix} = \frac{1}{2} \begin{pmatrix} \big(f_j^1\big)'/f_j^1 \\ \ldots \\ \big(f_j^N\big)'/f_j^N \end{pmatrix}, \quad j \neq i.$$

Multiplying the latter vectors from the left by the non-degenerate matrix

$$\mathrm{diag}\Big(\prod_{\ell=1}^{N} f_\ell^1, \ldots, \prod_{\ell=1}^{N} f_\ell^N\Big),$$

we obtain vectors

$$\frac{1}{2}\begin{pmatrix} (f_j^1)' \prod_{\ell\neq j} f_\ell^1 \\ \dots \\ (f_j^N)' \prod_{\ell\neq j} f_\ell^N \end{pmatrix} = \frac{1}{2}\partial_j \boldsymbol{x}, \quad j \neq i.$$

By definition of a coordinate system, the latter vectors are linearly independent and span an $(N-1)$-dimensional subspace of $\mathbb{R}^N$. This finishes the proof of Lemma 3.3. □

Substituting (3.5) into the left-hand side of equation (3.4), we arrive at an expression which may be represented as the polynomial

$$\sum_{k=1}^{N} (\alpha_1^k z_1 + \beta_1^k)\cdots(\alpha_N^k z_N + \beta_N^k)$$

of degree N in N formal variables $z_1, \dots, z_N$, evaluated at $z_i = F_i(s_i)$. It is easy to deduce that the result is a sum of functions of single variables, as in (3.4), if and only if in the above polynomial all monomials of degree $\geqslant 2$ vanish, leaving us with

$$\sum_{k=1}^{N} \left(\alpha_1^k z_1 + \beta_1^k\right)\cdots\left(\alpha_N^k z_N + \beta_N^k\right) = \sum_{i=1}^{N} \rho_i z_i + c. \tag{3.8}$$

We can identify the coefficients of the monomials of degree $\leqslant 1$:

$$\rho_i = \sum_{k=1}^{N} \alpha_i^k \prod_{\ell\neq i} \beta_\ell^k, \qquad c = \sum_{k=1}^{N}\prod_{\ell=1}^{N} \beta_\ell^k,$$

while the vanishing of the coefficients of all monomials of degree $\geqslant 2$ can be expressed as a certain set of equations for the coefficients α_i^k, β_i^k. As a result, (3.4) adopts the concrete form

$$\sum_{k=1}^{N} \left(\alpha_1^k F_1(s_1) + \beta_1^k\right)\cdots\left(\alpha_N^k F_N(s_N) + \beta_N^k\right) = \sum_{i=1}^{N} \rho_i F_i(s_i) + c.$$

It turns out that the above mentioned equations for the coefficients α_i^k, β_i^k imply certain identities involving functions of $N-1$ variables.

Lemma 3.4. *The following formulas hold true for all $i = 1, 2, \dots, N$:*

$$\sum_{k=1}^{N} \alpha_i^k \prod_{\ell\neq i} F_\ell^k(s_\ell) = \rho_i. \tag{3.9}$$

Proof. Differentiate equation (3.4), written as

$$\sum_{k=1}^{N}\prod_{\ell=1}^{N} F_\ell^k(s_\ell) = \sum_{i=1}^{N} \rho_i F_i(s_i) + c,$$

with respect to s_i:

$$\sum_{k=1}^{N} \left(F_i^k\right)'(s_i) \prod_{\ell\neq i} F_\ell^k(s_\ell) = \rho_i F_i'(s_i).$$

Taking into account equation (3.5) and dividing by $F_i' \neq 0$, we arrive at (3.9). □

Equations (3.9) describe coordinate hypersurfaces $s_i = \text{const}$. Indeed, observe that, according to (3.1) and to $F_i^k = \left(f_i^k\right)^2$, these equations can be expressed as quadrics:

$$\sum_{k=1}^{N} \frac{\alpha_i^k}{F_i^k(s_i)} x_k^2 = \rho_i,$$

or, equivalently, due to (3.5),

$$\sum_{k=1}^{N} \frac{x_k^2}{\rho_i F_i(s_i) + \rho_i \beta_i^k/\alpha_i^k} = 1. \tag{3.10}$$

In order to show that these quadrics for all $i = 1, \ldots, N$ and for any values of s_i belong to a confocal family

$$\sum_{k=1}^{N} \frac{x_k^2}{\lambda + a_k} = 1,$$

it remains to show that, for any two indices $k \neq m$ from $1, \ldots, N$, the expressions

$$\rho_i \left(\frac{\beta_i^k}{\alpha_i^k} - \frac{\beta_i^m}{\alpha_i^m} \right),$$

which should be equal to $a_k - a_m$, do not depend on i. Upon setting in identity (3.8)

$$z_1 = -\frac{\beta_1^{(k_1)}}{\alpha_1^{(k_1)}}, \quad \ldots, \quad z_N = -\frac{\beta_N^{(k_N)}}{\alpha_N^{(k_N)}}$$

for an arbitrary permutation $(k_1, \ldots, k_N)$ of $(1, \ldots, N)$, which makes one of the factors in each term on the left-hand side of (3.8) vanish, we arrive at

$$\rho_1 \frac{\beta_1^{(k_1)}}{\alpha_1^{(k_1)}} + \ldots + \rho_N \frac{\beta_N^{(k_N)}}{\alpha_N^{(k_N)}} = c.$$

Subtracting two such equations for two permutations, differing at only two positions i, j, where they take values k, m and m, k, respectively, we arrive at

$$\rho_i \frac{\beta_i^k}{\alpha_i^k} + \rho_j \frac{\beta_j^m}{\alpha_j^m} = \rho_i \frac{\beta_i^m}{\alpha_i^m} + \rho_j \frac{\beta_j^k}{\alpha_j^k},$$

or

$$\rho_i \left(\frac{\beta_i^k}{\alpha_i^k} - \frac{\beta_i^m}{\alpha_i^m} \right) = \rho_j \left(\frac{\beta_j^k}{\alpha_j^k} - \frac{\beta_j^m}{\alpha_j^m} \right).$$

This is the desired result, since i and j are arbitrary.

We have demonstrated that the equations of the coordinate hypersurfaces of a factorized orthogonal coordinate system (3.1) can be put as

$$\sum_{k=1}^{N} \frac{x_k^2}{u_i + a_k} = 1, \quad i = 1, \ldots, N, \tag{3.11}$$

where the parameters a_k are given by

$$a_k = \rho_i \frac{\beta_i^k}{\alpha_i^k} + c_i, \quad k = 1, \ldots, N, \tag{3.12}$$

with suitable constants c_i (which ensure that the right-hand side of (3.12) does not depend on i), while the quantities

$$u_i = u_i(s_i) = \rho_i F_i(s_i) - c_i, \quad i = 1, \ldots, N$$

can be considered as the confocal coordinates of the points $\boldsymbol{x}(\boldsymbol{s})$.

Observe that $a_k \neq a_m$ for $k \neq m$. Indeed, $a_k = a_m$ would imply $\beta_i^k/\alpha_i^k = \beta_i^m/\alpha_i^m$ for all i. Due to (3.5) this implies the proportionality $F_i^k(s_i) = (\alpha_i^k/\alpha_i^m) F_i^m(s_i)$ for all i, and finally $x_k(\boldsymbol{s})/x_m(\boldsymbol{s}) = \text{const}$. This contradicts to $\boldsymbol{x}$ being a coordinate system. This finishes the proof of Theorem 3.1. □

We remark that, since confocal quadrics of the same signature do not intersect, the N confocal coordinates should belong to N disjoint intervals (2.2) (possibly, upon a re-numbering).

The statement converse to Theorem 3.1 is almost obvious. We know that for any confocal coordinate system, equation (3.11) is equivalent to

$$x_k^2 = \frac{\prod_{i=1}^N (u_i + a_k)}{\prod_{i\neq k}(a_k - a_i)}, \quad k = 1, \dots, N,$$

and positivity of these expressions is equivalent to (2.2). Thus, formulas for x_k contain square roots $\sqrt{\pm(u_i + a_k)}$ (see (2.6)). Suppose that these square roots are uniformized by the re-parametrization

$$\big(f_i^k(s_i)\big)^2 = \begin{cases} u_i + a_k, & k \leqslant i, \\ -\big(u_i + a_k\big), & k > i. \end{cases}$$

The latter equations are consistent, if for any $1 \leqslant i \leqslant N$ the squares of the functions $f_i^k(s_i)$, $1 \leqslant k \leqslant N$, satisfy a system of $N-1$ linear equations:

$$\begin{cases} \big(f_i^1(s_i)\big)^2 - \big(f_i^k(s_i)\big)^2 = a_1 - a_k, & k \leqslant i, \\ \big(f_i^1(s_i)\big)^2 + \big(f_i^k(s_i)\big)^2 = a_1 - a_k, & k > i. \end{cases}$$

Under such a re-parametrization, formulas for confocal coordinates can be written as

$$x_k(\boldsymbol{s}) = \frac{\prod_{j=1}^N f_j^k(s_j)}{\prod_{i=1}^{k-1}\sqrt{a_i - a_k}\prod_{i=k+1}^N \sqrt{a_k - a_i}}, \quad k = 1, \dots, N \tag{3.13}$$

and, hence, the coordinate system factorizes. Note that (3.13) is equivalent to (3.1) modulo a scaling of the functions f_i^k.

4 Discrete orthogonality

We will use the discrete version of the characteristic properties from Theorem 3.1 to define discrete confocal coordinate systems. These will be special nets defined on the square lattice of stepsize 1/2,

$$\boldsymbol{x} : (\tfrac{1}{2}\mathbb{Z})^N \supset \mathcal{U} \to \mathbb{R}^N. \tag{4.1}$$

The suitable notion of orthogonality is a novel one, introduced in [BSST1]. We denote by $\boldsymbol{e}_i$ the unit vector of the coordinate direction i.

Definition 4.1. *A net* (4.1) *is called* orthogonal *if for each edge* $[\boldsymbol{n}, \boldsymbol{n}+\boldsymbol{e}_i]$*, all* 2^{N-1} *vertices of the dual facet,*

$$\boldsymbol{x}(\boldsymbol{n} + \tfrac{1}{2}\boldsymbol{\sigma}) \ \ \textit{for all} \ \ \boldsymbol{\sigma} = (\sigma_1, \dots, \sigma_N) \in \{\pm 1\}^N \ \ \textit{with} \ \ \sigma_i = 1,$$

lie in a hyperplane orthogonal to the line $(\boldsymbol{x}(\boldsymbol{n}), \boldsymbol{x}(\boldsymbol{n}+\boldsymbol{e}_i))$ *(see Fig. 4.1).*

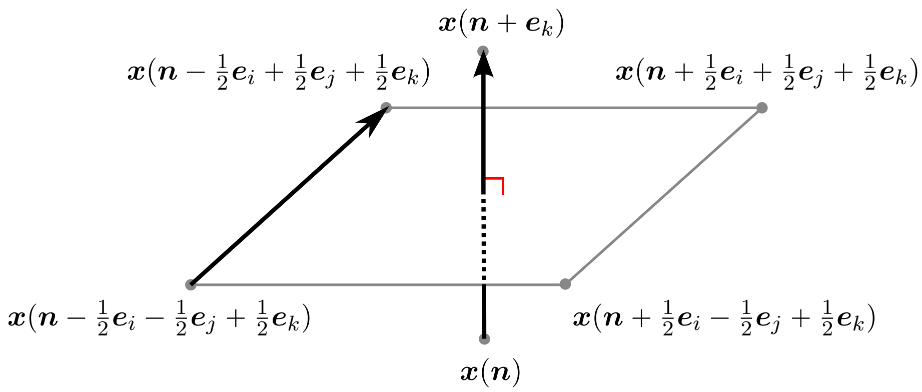

Figure 4.1. Discrete orthogonality in dimension $N = 3$.

Note that the original definition from [BSST1] referred to pairs of nets defined on two dual lattices $\mathbb{Z}^N$ and $(\mathbb{Z}+\frac{1}{2})^N$. The lattice $(\frac{1}{2}\mathbb{Z})^N$ contains 2^{N-1} pairs of dual sublattices of this type, namely

$$\mathbb{Z}^N+\tfrac{1}{2}\boldsymbol{\delta} \quad \text{and} \quad \mathbb{Z}^N+\tfrac{1}{2}\bar{\boldsymbol{\delta}},$$

for any $\boldsymbol{\delta}=(\delta_1,\ldots,\delta_N)\in\{0,1\}^N$ and $\bar{\boldsymbol{\delta}}=(1-\delta_1,\ldots,1-\delta_N)\in\{0,1\}^N$.

Proposition 4.2. *All elementary quadrilaterals*

$$(\boldsymbol{x}(\boldsymbol{n}),\boldsymbol{x}(\boldsymbol{n}+\boldsymbol{e}_j),\boldsymbol{x}(\boldsymbol{n}+\boldsymbol{e}_j+\boldsymbol{e}_k),\boldsymbol{x}(\boldsymbol{n}+\boldsymbol{e}_k)) \tag{4.2}$$

of a generic orthogonal net are planar.

Proof. An elementary quadrilateral (4.2) can be considered as the intersection of $N-2$ facets dual to the edges

$$\Big[\boldsymbol{x}\big(\boldsymbol{n}+\tfrac{1}{2}\sum_{\ell\neq i}\boldsymbol{e}_\ell-\tfrac{1}{2}\boldsymbol{e}_i\big),\boldsymbol{x}\big(\boldsymbol{n}+\tfrac{1}{2}\sum_{\ell\neq i}\boldsymbol{e}_\ell+\tfrac{1}{2}\boldsymbol{e}_i\big)\Big], \quad i\neq j,k$$

of the dual sublattice. Each of these $N-2$ facets lies in a hyperplane. The intersection of $N-2$ hyperplanes in $\mathbb{R}^N$ is generically a two-dimensional plane. ☐

Clearly, the definition of orthogonality can be equivalently formulated as follows: the two lines containing any pair of dual edges are orthogonal:

$$\big(\boldsymbol{x}(\boldsymbol{n}),\boldsymbol{x}(\boldsymbol{n}+\boldsymbol{e}_i)\big)\perp\big(\boldsymbol{x}(\boldsymbol{n}+\tfrac{1}{2}\boldsymbol{\sigma}),\boldsymbol{x}(\boldsymbol{n}+\tfrac{1}{2}\boldsymbol{\sigma}+\boldsymbol{e}_j)\big), \tag{4.3}$$

where $\boldsymbol{\sigma}\in\{\pm1\}^N$ is any N-tuple of signs with $\sigma_i=1$ and $\sigma_j=-1$ (and orthogonality is understood in the sense of orthogonality of the direction vectors). From this it is easy to see that pairs of dual sublattices actually play symmetric roles in the definition of orthogonality.

5 Discrete confocal coordinate systems

For discrete nets $\boldsymbol{x}:\mathbb{Z}^N\supset\mathcal{U}\to\mathbb{R}^N$, at any point $\boldsymbol{n}\in\mathcal{U}$ and for any coordinate direction $j=1,\ldots,N$, there exist two natural discrete tangent vectors, $\Delta_j\boldsymbol{x}(\boldsymbol{n})=\boldsymbol{x}(\boldsymbol{n}+\boldsymbol{e}_j)-\boldsymbol{x}(\boldsymbol{n})$ and $\bar{\Delta}_j\boldsymbol{x}(\boldsymbol{n})=\boldsymbol{x}(\boldsymbol{n})-\boldsymbol{x}(\boldsymbol{n}-\boldsymbol{e}_j)$. We call such a net a *discrete coordinate system* if at any $\boldsymbol{n}\in\mathcal{U}$, the N discrete tangent vectors (arbitrarily chosen among $\Delta_j\boldsymbol{x}(\boldsymbol{n})$ and $\bar{\Delta}_j\boldsymbol{x}(\boldsymbol{n})$ for any j) are linearly independent.

A net $\boldsymbol{x}:\big(\frac{1}{2}\mathbb{Z}\big)^N\to\mathbb{R}^N$ defined on the lattice of a half stepsize can be considered as consisting of 2^N subnets defined on sublattices $\mathbb{Z}^N+\frac{1}{2}\boldsymbol{\delta}$ for $\boldsymbol{\delta}\in\{0,1\}^N$, and we call it a discrete coordinate system if all 2^N subnets satisfy the above condition.

Definition 5.1. *A discrete coordinate system* $\boldsymbol{x}:\big(\frac{1}{2}\mathbb{Z}\big)^N\supset\mathcal{U}\to\mathbb{R}^N$ *is called* a discrete confocal coordinate system *if it satisfies two conditions:*

i) $\boldsymbol{x}(\boldsymbol{n})$ factorizes*, in the sense that for any* $\boldsymbol{n}\in\mathcal{U}$

$$\begin{cases} x_1(\boldsymbol{n})=f_1^1(n_1)f_2^1(n_2)\cdots f_N^1(n_N),\\ x_2(\boldsymbol{n})=f_1^2(n_1)f_2^2(n_2)\cdots f_N^2(n_N),\\ \cdots\\ x_N(\boldsymbol{n})=f_1^N(n_1)f_2^N(n_2)\cdots f_N^N(n_N), \end{cases} \tag{5.1}$$

with $f_i^k(n_i)\neq0$ *and* $\bar{\Delta}f_i^k(n_i)=f_i^k(n_i)-f_i^k(n_i-1)\neq0$*;*

ii) $\boldsymbol{x}$ *is* orthogonal *in the sense of Definition 4.1.*

Theorem 5.2. *For a discrete confocal coordinate system, there exist N real numbers a_k, $1 \leqslant k \leqslant N$, and N sequences $u_i : \frac{1}{2}\mathbb{Z} + \frac{1}{4} \to \mathbb{R}$ such that the following equations are satisfied for any $\boldsymbol{n} \in \mathcal{U}$ and for any $\boldsymbol{\sigma} \in \{\pm 1\}^N$:*

$$\sum_{k=1}^{N} \frac{x_k(\boldsymbol{n}) x_k(\boldsymbol{n} + \frac{1}{2}\boldsymbol{\sigma})}{a_k + u_i} = 1, \quad u_i = u_i(n_i + \tfrac{1}{4}\sigma_i), \quad i = 1, \ldots, N.$$

Equivalently,

$$x_k(\boldsymbol{n}) x_k(\boldsymbol{n} + \tfrac{1}{2}\boldsymbol{\sigma}) = \frac{\prod_{j=1}^{N}(u_j + a_k)}{\prod_{j \neq k}(a_k - a_j)}, \quad u_j = u_j(n_j + \tfrac{1}{4}\sigma_j), \quad k = 1, \ldots, N. \tag{5.2}$$

Proof. Orthogonality condition (4.3) written in full reads:

$$\sum_{k=1}^{N} (f_i^k(n_i + 1) - f_i^k(n_i)) f_i^k(n_i + \tfrac{1}{2}) \cdot \\ (f_j^k(n_j + \tfrac{1}{2}) - f_j^k(n_j - \tfrac{1}{2})) f_j^k(n_j) \cdot \prod_{\ell \neq i,j} f_\ell^k(n_\ell) f_\ell^k(n_\ell + \tfrac{1}{2}\sigma_\ell) = 0.$$

We introduce the quantities

$$F_i^k(n_i + \tfrac{1}{4}) = f_i^k(n_i) f_i^k(n_i + \tfrac{1}{2}),$$

assigned to the points of the lattice $\frac{1}{2}\mathbb{Z} + \frac{1}{4}$, and the difference operator

$$\Delta^{1/2} F(n) = F(n + \tfrac{1}{4}) - F(n - \tfrac{1}{4}).$$

With this notation, relation (5.3) takes the form

$$\sum_{k=1}^{N} \Delta^{1/2} F_i^k(n_i + \tfrac{1}{2}) \cdot \Delta^{1/2} F_j^k(n_j) \cdot \prod_{\ell \neq i,j} F_\ell^k(n_\ell + \tfrac{1}{4}\sigma_\ell) = 0.$$

Since it is supposed that this relation holds true for all $\boldsymbol{n} \in (\frac{1}{2}\mathbb{Z})^N$, we write it, omitting all arguments due to their arbitrariness, as

$$\sum_{k=1}^{N} \Delta^{1/2} F_i^k \cdot \Delta^{1/2} F_j^k \cdot \prod_{\ell \neq i,j} F_\ell^k = 0. \tag{5.4}$$

Now one sees immediately that the following analogues of Lemmas 3.2, 3.3 hold true in the discrete context *mutatis mutandis.*

Lemma 5.3. *Equation* (5.4) *is equivalent to*

$$\sum_{k=1}^{N} F_1^k(n_1 + \tfrac{1}{4}) \cdot \ldots \cdot F_N^k(n_N + \tfrac{1}{4}) = A_1(n_1) + \ldots + A_N(n_N),$$

with some functions $A_i(n_i)$.

Lemma 5.4. *Assume that all $f_i^k \neq 0$ and $\bar{\Delta} f_i^k \neq 0$. Then, for each $i = 1, \ldots, N$ there exists a function $F_i(n_i + \frac{1}{4})$ such that*

$$F_i^k(n_i + \tfrac{1}{4}) = \alpha_i^k F_i(n_i + \tfrac{1}{4}) + \beta_i^k, \quad k = 1, \ldots, N \tag{5.5}$$

for some constants $\alpha_i^k \neq 0$ and β_i^k.

Proof. Note that the assumption of lemma is equivalent to $\Delta^{1/2} F_i^k \neq 0$. The statement of lemma is equivalent to

$$\begin{pmatrix} \Delta^{1/2} F_i^1(n_i) \\ \ldots \\ \Delta^{1/2} F_i^N(n_i) \end{pmatrix} \in \mathbb{R} \begin{pmatrix} \alpha_i^1 \\ \ldots \\ \alpha_i^N \end{pmatrix}. \tag{5.6}$$

To prove this, take equation (5.4) with all $\sigma_\ell = 1$ and observe that, for any fixed i, it can be formulated as the following $N-1$ orthogonality conditions:

$$\begin{pmatrix} \Delta^{1/2} F_i^1 \\ \dots \\ \Delta^{1/2} F_i^N \end{pmatrix} \perp \begin{pmatrix} \Delta^{1/2} F_j^1 \cdot \prod_{\ell \neq i,j} F_\ell^1 \\ \dots \\ \Delta^{1/2} F_j^N \cdot \prod_{\ell \neq i,j} F_\ell^N \end{pmatrix}, \quad j \neq i. \tag{5.7}$$

Multiplying the $N-1$ vectors on the right-hand side from the left by the non-degenerate matrix

$$\mathrm{diag}\Big(\prod_{\ell \neq i} F_\ell^1, \dots, \prod_{\ell \neq i} F_\ell^N \Big)^{-1},$$

we obtain vectors

$$\begin{pmatrix} (\Delta^{1/2} F_j^1)/F_j^1 \\ \dots \\ (\Delta^{1/2} F_j^N)/F_j^N \end{pmatrix}, \quad j \neq i.$$

We have:

$$\frac{\Delta^{1/2} F_j^1}{F_j^1} = \frac{(f_j^k(n_j + \frac{1}{2}) - f_j^k(n_j - \frac{1}{2})) f_j^k(n_j)}{f_j^k(n_j + \frac{1}{2}) f_j^k(n_j)} = \frac{\bar{\Delta}_j f_j^k(n_j + \frac{1}{2})}{f_j^k(n_j + \frac{1}{2})}.$$

Multiplying the latter vectors from the left by the non-degenerate matrix

$$\mathrm{diag}\Big(\prod_{\ell=1}^N f_\ell^1(n_\ell + \tfrac{1}{2}), \dots, \prod_{\ell=1}^N f_\ell^N(n_\ell + \tfrac{1}{2}) \Big),$$

we obtain vectors

$$\bar{\Delta}_j \boldsymbol{x}(\boldsymbol{n} + \tfrac{1}{2}\boldsymbol{\sigma}), \quad j \neq i.$$

The latter vectors are linearly independent and span an $(N-1)$-dimensional subspace of $\mathbb{R}^N$. Thus, the vector on the left-hand side of (5.7) lies in the orthogonal complement of an $(N-1)$-dimensional subspace which is manifestly independent of n_i. This orthogonal complement is a one-dimensional space which does not depend on n_i. This proves (5.6). ☐

As a result, a discrete analogue of Lemma 3.4 holds true:

$$\sum_{k=1}^N \alpha_i^k \prod_{\ell \neq i} F_\ell^k(n_\ell + \tfrac{1}{4}\sigma_\ell) = \rho_i. \tag{5.8}$$

Now observe that, according to $F_i^k(n_i + \frac{1}{4}) = f_i^k(n_i) f_i^k(n_i + \frac{1}{2})$, to (5.1), and to (5.5), equations (5.8) can be expressed as follows:

$$\sum_{k=1}^N \frac{x_k(\boldsymbol{n}) x_k(\boldsymbol{n} + \frac{1}{2}\boldsymbol{\sigma})}{\rho_i F_i(n_i + \frac{1}{4}\sigma_i) + \rho_i \beta_i^k / \alpha_i^k} = 1.$$

The same arguments as after equation (3.10) show that the expressions

$$\rho_i \left(\frac{\beta_i^k}{\alpha_i^k} - \frac{\beta_i^m}{\alpha_i^m} \right),$$

which should be equal to $a_k - a_m$, do not depend on i. Thus, we can set

$$a_k = \rho_i \frac{\beta_i^k}{\alpha_i^k} + c_i,$$

with suitable constants c_i, and

$$u_i(n_i + \tfrac{1}{4}) = \rho_i F_i(n_i + \tfrac{1}{4}) - c_i.$$

Like in the continuous case, we show that $a_k \neq a_m$ for $k \neq m$. Indeed, $a_k = a_m$ would imply $\beta_i^k/\alpha_i^k = \beta_i^m/\alpha_i^m$ for all i. Due to (5.5) this implies the proportionality $F_i^k(n_i + \frac{1}{4}) = (\alpha_i^k/\alpha_i^m) F_i^m(n_i + \frac{1}{4})$ for all i. This, in turn, implies that $x_k(\boldsymbol{n}) x_k(\boldsymbol{n} + \frac{1}{2}\boldsymbol{\sigma}) / x_m(\boldsymbol{n}) x_m(\boldsymbol{n} + \frac{1}{2}\boldsymbol{\sigma}) = \text{const}$ for any $\boldsymbol{\sigma} \in \{\pm 1\}^N$. As a consequence, $x_k(\boldsymbol{n})/x_m(\boldsymbol{n}) = \text{const}$ on any sublattice $\mathbb{Z}^N + \frac{1}{2}\boldsymbol{\delta}$ with $\boldsymbol{\delta} \in \{0,1\}^N$ of the lattice $(\frac{1}{2}\mathbb{Z})^N$. This contradicts to $\boldsymbol{x}$ being a discrete coordinate system. This finishes the proof of Theorem 5.2. ☐

Upon a re-numbering, we can assume that $a_1 > a_2 > \cdots > a_N > 0$. Formula (5.2) shows that, as long as the points $\boldsymbol{x}(\boldsymbol{n})$ and $\boldsymbol{x}(\boldsymbol{n} + \frac{1}{2}\boldsymbol{\sigma})$ stay in one hyperoctant like $\mathbb{R}^N_+$, the quantities $u_i = u_i(n_i + \frac{1}{2}\sigma_i)$ lie in the intervals (2.2). If the points $\boldsymbol{x}(\boldsymbol{n})$ and $\boldsymbol{x}(\boldsymbol{n} + \frac{1}{2}\boldsymbol{\sigma})$ lie on different sides of a coordinate hyperplane $x_i = 0$ of $\boldsymbol{x}$, the corresponding quantity u_i is outside the corresponding interval.

It is convenient to re-scale the functions $f_j^k(n_j)$ in (5.1) by certain constant factors so that it takes the form

$$x_k(\boldsymbol{n}) = \frac{\prod_{j=1}^N f_j^k(n_j)}{\prod_{i=1}^{k-1} \sqrt{a_i - a_k} \prod_{i=k+1}^N \sqrt{a_k - a_i}}, \quad k = 1, \ldots, N. \tag{5.9}$$

Thus, relations (5.2) give rise to the following theorem.

Theorem 5.5. *For given sequences $u_i : \frac{1}{2}\mathbb{Z} + \frac{1}{4} \to \mathbb{R}$, $1 \leqslant i \leqslant N$, consider functions $f_i^k(n_i)$ as solutions of the respective difference equations*

$$f_i^k(n_i) f_i^k(n_i + \tfrac{1}{2}) = \begin{cases} u_i(n_i + \frac{1}{4}) + a_k, & k \leqslant i, \\ -\big(u_i(n_i + \frac{1}{4}) + a_k\big), & k > i. \end{cases} \tag{5.10}$$

Given a sequence u_i, equations (5.10) *define the functions f_i^k, $k = 1, \ldots, N$ uniquely by prescribing their values at one point. Then, $\boldsymbol{x}$ defined by* (5.9) *constitutes a discrete confocal coordinate system. The right-hand sides of equations* (5.10) *are positive as long as $\boldsymbol{x}(\boldsymbol{n})$ and $\boldsymbol{x}(\boldsymbol{n} + \frac{1}{2}(\boldsymbol{e}_1 + \ldots + \boldsymbol{e}_N))$ stay in one hyperoctant of $\mathbb{R}^N$.*

Formulas (5.10) may be regarded as a discrete parametrization of the variables u_i. Another interpretation of equations (5.10) (and the corresponding *modus operandi*) is as follows.

Theorem 5.6. *For $i = 1, \ldots, N$, consider a system of $N - 1$ functional equations for functions $f_i^k(n_i)$, $1 \leqslant k \leqslant N$:*

$$\begin{cases} f_i^1(n_i) f_i^1(n_i + \frac{1}{2}) - f_i^k(n_i) f_i^k(n_i + \frac{1}{2}) = a_1 - a_k, & k \leqslant i, \\ f_i^1(n_i) f_i^1(n_i + \frac{1}{2}) + f_i^k(n_i) f_i^k(n_i + \frac{1}{2}) = a_1 - a_k, & k > i. \end{cases} \tag{5.11}$$

For any solution of these N systems, the function $\boldsymbol{x}$ defined by (5.9) *constitutes a discrete confocal coordinate system. The corresponding values $u_i(n_i + \frac{1}{4})$ are determined by equations* (5.10).

Proof. We arrive at equations (5.11) by eliminating u_i between equations (5.10). Note that equations (5.11) do not depend on $u_i = u_i(n_i + \frac{1}{4})$. The latter can be determined *a posteriori* from any of equations (5.10). ☐

It is well known that functional equations (5.11) admit solutions in terms of trigonometric/hyperbolic functions if $N = 2$, and in terms of elliptic functions if $N = 3$. We discuss these solutions in Sections 8, 9, respectively.

6 Geometric interpretation

The main formula from Theorem 5.2,

$$\sum_{k=1}^N \frac{x_k(\boldsymbol{n}) x_k(\boldsymbol{n} + \frac{1}{2}\boldsymbol{\sigma})}{a_k + u_i} = 1, \quad u_i = u_i(n_i + \tfrac{1}{4}\sigma_i), \quad i = 1, \ldots, N, \tag{6.1}$$

admits a remarkable geometric interpretation. Recall that the *polarity* with respect to a non-degenerate quadric is a projective transformation between the points $\boldsymbol{x} \in \mathbb{P}^N$ and the hyperplanes $\Pi \in (\mathbb{P}^N)^*$. In homogeneous coordinates, if the quadric Q is given by a quadratic form $Q(\boldsymbol{x}) = 0$, then the hyperplane Π polar to a point $\boldsymbol{x} = [x_1 : \ldots : x_{N+1}] \in \mathbb{P}^N$ with respect to Q consists of all points $\boldsymbol{y} = [y_1 : \ldots : y_{N+1}] \in \mathbb{P}^N$ satisfying $\bar{Q}(\boldsymbol{x}, \boldsymbol{y}) = 0$, where $\bar{Q}$ is the symmetric bilinear form corresponding to the quadratic form Q. We write $\boldsymbol{x} = P_Q(\Pi)$ and $\Pi = P_Q(\boldsymbol{x})$. Returning to affine coordinates (with $x_{N+1} = 1$), formula (6.1) is equivalent to saying that *the point $\boldsymbol{x}(\boldsymbol{n}+\frac{1}{2}\boldsymbol{\sigma})$ lies in the intersection of the polar hyperplanes of $\boldsymbol{x}(\boldsymbol{n})$ with respect to the confocal quadrics $Q(u_i)$, $i = 1, \ldots, N$:*

$$\boldsymbol{x}(\boldsymbol{n}+\tfrac{1}{2}\boldsymbol{\sigma}) = \bigcap_{i=1}^{N} P_{Q(u_i)}(\boldsymbol{x}(\boldsymbol{n})), \quad u_i = u_i(n_i + \tfrac{1}{4}\sigma_i). \tag{6.2}$$

Of course, the roles of $\boldsymbol{x}(\boldsymbol{n})$ and $\boldsymbol{x}(\boldsymbol{n}+\frac{1}{2}\boldsymbol{\sigma})$ in this formula are completely symmetric.

This interpretation can be used to give a *geometric construction* of a discrete confocal coordinate system $\boldsymbol{x} : (\frac{1}{2}\mathbb{Z})^N \supset \mathcal{U} \to \mathbb{R}^N$, or, better, of its restriction to two dual sublattices like $\mathbb{Z}^N$ and $(\mathbb{Z}+\frac{1}{2})^N$. Suppose that for each $i = 1, \ldots, N$ a sequence of quadrics of the confocal family (2.1) is chosen, with the parameters

$$u_i : \left(\tfrac{1}{2}\mathbb{Z} + \tfrac{1}{4}\right) \cap \mathcal{I}_i \to \mathbb{R},$$

indexed by a discrete variable $n_i + \frac{1}{4} \in \mathcal{I}_i$, where $n_i \in \frac{1}{2}\mathbb{Z}$. It is convenient to think of $u_i(n_i + \frac{1}{4})$ as being assigned to the interval $[n_i, n_i + \frac{1}{2}]$, for which $n_i + \frac{1}{4}$ is the midpoint. We denote by $\mathcal{V}$, $\mathcal{V}^*$ the parts of the respective lattices $\mathbb{Z}^N$, $(\mathbb{Z}+\frac{1}{2})^N$ lying in the region $\prod_{i=1}^N \mathcal{I}_i$. We construct a discrete net $\boldsymbol{x} : \mathcal{V} \cup \mathcal{V}^* \to \mathbb{R}^N$ recurrently, starting with an arbitrary point $\boldsymbol{x}(\boldsymbol{n}_0)$, as long as the components of $\boldsymbol{x}(\boldsymbol{n})$ are non-vanishing.

Construction (cf. Figure 6.1). *Let $\boldsymbol{n}$ and $\boldsymbol{n}^*$ be two neighboring points in the two dual sublattices, in the sense that*

$$\boldsymbol{n}^* = \boldsymbol{n} + \tfrac{1}{2}\boldsymbol{\sigma}, \quad \boldsymbol{\sigma} = (\sigma_1, \ldots, \sigma_N), \quad \sigma_i = \pm 1.$$

Suppose that $\boldsymbol{x}(\boldsymbol{n}) = \boldsymbol{x}$ is already known. Then $\boldsymbol{x}(\boldsymbol{n}^*) = \boldsymbol{x}^*$ is constructed as the intersection point of the N polar hyperplanes

$$\boldsymbol{x}^* = C_{\boldsymbol{n},\frac{1}{2}\boldsymbol{\sigma}}(\boldsymbol{x}) := \bigcap_{i=1}^{N} P_{Q(u_i)}(\boldsymbol{x}), \quad u_i = u_i(n_i + \tfrac{1}{4}\sigma_i).$$

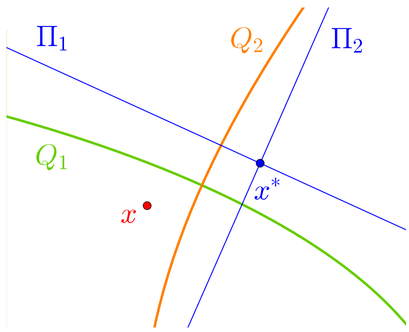

Figure 6.1. Geometric construction of $\boldsymbol{x}^*$ in the case $N = 2$ as the intersection of the polar lines Π_1 and Π_2 of $\boldsymbol{x}$ with respect to the confocal conics Q_1 and Q_2.

In order to show that this construction is well defined, the following statement is required.

Proposition 6.1. *The following diagram is commutative for any $\boldsymbol{\sigma}, \tilde{\boldsymbol{\sigma}} \in \{\pm 1\}^N$:*

$$\begin{tikzcd}
\mathbb{R}^N \arrow[r, "C_{\boldsymbol{n},\frac{1}{2}\tilde{\boldsymbol{\sigma}}}"] \arrow[d, "C_{\boldsymbol{n},\frac{1}{2}\boldsymbol{\sigma}}"'] & \mathbb{R}^N \arrow[d, "C_{\boldsymbol{n}+\frac{1}{2}\tilde{\boldsymbol{\sigma}},\frac{1}{2}\boldsymbol{\sigma}}"] \\
\mathbb{R}^N \arrow[r, "C_{\boldsymbol{n}+\frac{1}{2}\boldsymbol{\sigma},\frac{1}{2}\tilde{\boldsymbol{\sigma}}}"'] & \mathbb{R}^N
\end{tikzcd}$$

Thus, applying the above construction along a path depends only on the initial and the end points of the path and not on the path itself.

Proof. Denote the right-hand side of (5.2) by

$$x_k(\boldsymbol{n})x_k(\boldsymbol{n}+\tfrac{1}{2}\boldsymbol{\sigma}) = B_k(\boldsymbol{n},\boldsymbol{\sigma}) := \frac{\prod_{j=1}^{N}(u_j(n_j+\frac{1}{4}\sigma_j)+a_k)}{\prod_{j\neq k}(a_k-a_j)}.$$

Then the commutativity of the diagram is equivalent to

$$\frac{B_k(\boldsymbol{n}+\frac{1}{2}\boldsymbol{\sigma},\tilde{\boldsymbol{\sigma}})}{B_k(\boldsymbol{n},\boldsymbol{\sigma})} = \frac{B_k(\boldsymbol{n}+\frac{1}{2}\tilde{\boldsymbol{\sigma}},\boldsymbol{\sigma})}{B_k(\boldsymbol{n},\tilde{\boldsymbol{\sigma}})}, \tag{6.3}$$

or

$$\frac{\prod_{j=1}^{N}(u_j(n_j+\frac{1}{2}\sigma_j+\frac{1}{4}\tilde{\sigma}_j)+a_k)}{\prod_{j=1}^{N}(u_j(n_j+\frac{1}{4}\sigma_j)+a_k)} = \frac{\prod_{j=1}^{N}(u_j(n_j+\frac{1}{2}\tilde{\sigma}_j+\frac{1}{4}\sigma_j)+a_k)}{\prod_{j=1}^{N}(u_j(n_j+\frac{1}{4}\tilde{\sigma}_j)+a_k)}. \tag{6.4}$$

For each j, we have either $\tilde{\sigma}_j=\sigma_j$, or $\tilde{\sigma}_j=-\sigma_j$. In the first case, the corresponding factors in the numerators of both sides of (6.4) are equal, as well as the corresponding factors in the denominators. In the second case, the corresponding factors in the numerator and in the denominator on the left-hand side are equal, and the same holds true for the corresponding factors in the numerator and in the denominator on the right-hand side. This proves (6.3). □

The discrete orthogonality property is now a consequence of the following lemma (cf. Figure 6.2).

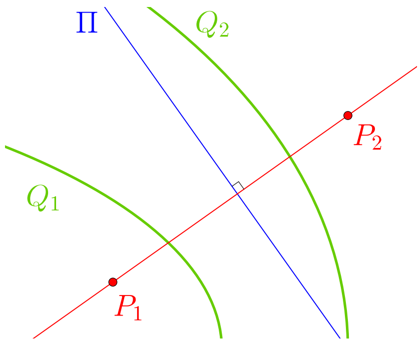

Figure 6.2. Orthogonality in the case $N=2$: If P_2 is related to P_1 via polarity in two confocal conics, that is, $\Pi=P_{Q_1}(P_1)$ and $P_2=P_{Q_2}(\Pi)$, then the line through P_1 and P_2 is orthogonal to Π.

Lemma 6.2. *Let Π be a hyperplane. Then the poles of Π with respect to all quadrics of the confocal family* (2.1) *lie on a line ℓ. This line ℓ is orthogonal to Π.*

Proof. Let the equation of the hyperplane Π be $\sum_{k=1}^{N} c_k x_k = 1$, where $\boldsymbol{c}=(c_1,\dots,c_N)$ is a normal vector for Π. Take two quadrics of the confocal family, $Q_1=Q(u)$ and $Q_2=Q(v)$. Set

$$P_1 = P_{Q_1}(\Pi) = (y_1,\dots,y_N) \quad\text{and}\quad P_2 = P_{Q_2}(\Pi) = (z_1,\dots,z_N).$$

Then we get the following two forms of the equation of the hyperplane Π:

$$\sum_{i=1}^{N}\frac{x_i y_i}{a_i+u} = 1 \quad\text{and}\quad \sum_{i=1}^{N}\frac{x_i z_i}{a_i+v} = 1.$$

Thus,

$$c_i = \frac{y_i}{a_i+u} = \frac{z_i}{a_i+v},$$

and, hence,

$$y_i - z_i = c_i(a_i+u) - c_i(a_i+v) = c_i(u-v),$$

so that the vector P_2-P_1 is proportional to $\boldsymbol{c}$ and therefore is orthogonal to Π. Thus, denoting by ℓ the line which passes through P_1 orthogonally to Π, we see that the pole P_2 of the hyperplane Π with respect to the quadric Q_2 lies on ℓ. It remains to note that Q_2 is an arbitrary quadric of the confocal family of Q_1. □

Theorem 6.3. *The nets $\boldsymbol{x}(\mathcal{V})$ and $\boldsymbol{x}(\mathcal{V}^*)$ are orthogonal in the sense of Definition 4.1.*

Proof. From (6.2) it follows that, for a fixed index k, all points $\boldsymbol{x}(\boldsymbol{n}+\frac{1}{2}\boldsymbol{\sigma})$ with $\sigma_k = 1$ lie in the hyperplane $\Pi = P_{Q_1}(\boldsymbol{x}(\boldsymbol{n}))$, where $Q_1 = Q(u_k(n_k + \frac{1}{4}))$. These points are exactly the vertices of the facet of $\boldsymbol{x}(\mathcal{V}^*)$ dual to the edge $[\boldsymbol{x}(\boldsymbol{n}), \boldsymbol{x}(\boldsymbol{n} + \boldsymbol{e}_k)]$ of $\boldsymbol{x}(\mathcal{V})$. Now, since

$$\boldsymbol{x}(\boldsymbol{n}) = P_{Q_1}(\Pi), \quad \boldsymbol{x}(\boldsymbol{n} + \boldsymbol{e}_k) = P_{Q_2}(\Pi),$$

where $Q_2 = Q(u_k(n_k + \frac{3}{4}))$, it follows from Lemma 6.2 that the line $(\boldsymbol{x}(\boldsymbol{n}), \boldsymbol{x}(\boldsymbol{n} + \boldsymbol{e}_k))$ is orthogonal to the hyperplane Π. $\square$

7 Discrete confocal coordinates in terms of gamma functions

There exists an important particular case when the difference equations (5.10) admit an explicit solution, namely by the choice

$$u_i(n_i + \tfrac{1}{4}) = n_i + \varepsilon_i, \quad i = 1, \dots, N,$$

where $\varepsilon_i \in \mathbb{R}$ are some fixed shifts. This can be considered to correspond to the smooth case (2.6) where we take the quantities u_i as coordinates without further re-parametrization. With this choice, equations (5.10) turn into

$$f_i^k(n_i) f_i^k(n_i + \tfrac{1}{2}) = \begin{cases} n_i + a_k + \varepsilon_i, & k \leqslant i, \\ -\big(n_i + a_k + \varepsilon_i\big), & k > i. \end{cases} \tag{7.1}$$

These equations can be solved in terms of the "discrete square root" function defined as

$$(u)_{1/2} = \frac{\Gamma(u + \frac{1}{2})}{\Gamma(u)},$$

which satisfies the identities

$$(u)_{1/2}(u + \tfrac{1}{2})_{1/2} = u, \quad (-u)_{1/2}(-u - \tfrac{1}{2})_{1/2} = -u - \tfrac{1}{2}.$$

We can write solutions of (7.1) as

$$f_i^k(n_i) = \begin{cases} (n_i + a_k + \varepsilon_i)_{1/2} & \text{for} \quad i \geqslant k, \\ (-n_i - a_k - \varepsilon_i + \frac{1}{2})_{1/2} & \text{for} \quad i < k. \end{cases}$$

One can impose boundary conditions

$$\begin{aligned} x_k|_{n_k = -\alpha_k} &= 0 \quad \text{for} \quad k = 1, \dots, N, \\ x_k|_{n_{k-1} = -\alpha_k} &= 0 \quad \text{for} \quad k = 2, \dots, N, \end{aligned}$$

on the integer lattice $\mathbb{Z}^N$ for certain integers $\alpha_1 > \dots > \alpha_N$, which imitate the corresponding property of the continuous confocal coordinates. These boundary conditions are satisfied provided that

$$a_k - \alpha_k + \varepsilon_k = 0, \quad a_k - \alpha_k + \varepsilon_{k-1} = \frac{1}{2},$$

for which the shifts ε_k should satisfy $\varepsilon_{k-1} - \varepsilon_k = \frac{1}{2}$. Choosing $\varepsilon_k = -\frac{k}{2}$ and $a_k = \alpha_k + \frac{k}{2}$, we finally arrive at the solutions

$$f_i^k(n_i) = \begin{cases} (n_i + \alpha_k + \frac{k-i}{2})_{1/2} & \text{for} \quad i \geqslant k, \\ (-n_i - \alpha_k - \frac{k-i}{2} + \frac{1}{2})_{1/2} & \text{for} \quad i < k. \end{cases}$$

These are the functions introduced and studied in [BSST1], as solutions of the discrete Euler-Darboux-Poisson equations (cf. Appendix).

8 The case $N = 2$[1]

8.1 Classical confocal coordinate systems

We have seen that, given the family of confocal conics

$$\frac{x^2}{a+\lambda} + \frac{y^2}{b+\lambda} = 1, \tag{8.1}$$

the defining equations

$$\frac{x^2}{u+a} + \frac{y^2}{u+b} = 1, \quad \frac{x^2}{v+a} + \frac{y^2}{v+b} = 1 \tag{8.2}$$

of confocal coordinates $\{(u,v) : -a < u < -b < v\}$ on the plane give rise to the expressions

$$x^2 = \frac{(u+a)(v+a)}{a-b}, \quad y^2 = \frac{(u+b)(v+b)}{b-a}.$$

For an arbitrary re-parametrization of the coordinate lines, $u = u(s_1)$, $v = v(s_2)$, we obtain

$$x = \frac{f_1(s_1)f_2(s_2)}{\sqrt{a-b}}, \quad y = \frac{g_1(s_1)g_2(s_2)}{\sqrt{a-b}}, \tag{8.3}$$

where

$$\begin{cases} (f_1(s_1))^2 = u+a, \\ (g_1(s_1))^2 = -(u+b), \end{cases} \quad \begin{cases} (f_2(s_2))^2 = v+a, \\ (g_2(s_2))^2 = v+b. \end{cases} \tag{8.4}$$

Elimination of u and v leads to

$$(f_1(s_1))^2 + (g_1(s_1))^2 = a-b, \tag{8.5}$$
$$(f_2(s_2))^2 - (g_2(s_2))^2 = a-b. \tag{8.6}$$

The probably most obvious parametrization of solutions of these functional equations is by means of trigonometric/hyperbolic functions:

$$\begin{aligned} f_1(s_1) &= \sqrt{a-b}\,\cos s_1, & g_1(s_1) &= \sqrt{a-b}\ \sin s_1, \\ f_2(s_2) &= \sqrt{a-b}\,\cosh s_2\,, & g_2(s_2) &= \sqrt{a-b}\,\sinh s_2. \end{aligned}$$

Accordingly, we obtain the representation

$$\begin{pmatrix} x \\ y \end{pmatrix} = \sqrt{a-b} \begin{pmatrix} \cos s_1 \cosh s_2 \\ \sin s_1 \sinh s_2 \end{pmatrix} \tag{8.9}$$

of the confocal system of coordinates on the plane with the relation between (u,v) and (s_1,s_2) given by (8.4). This coordinate system is depicted in Figure 8.1.

[1] Two more examples can be found in Appendix B.

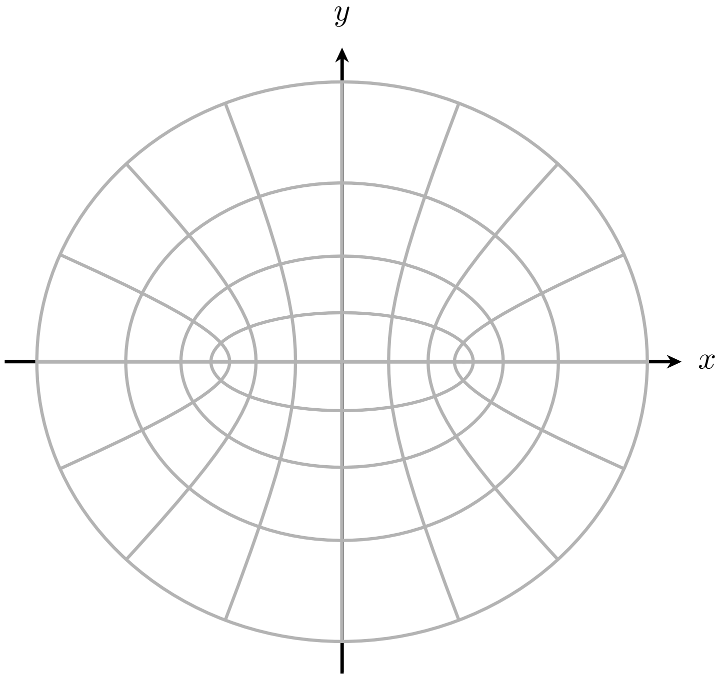

Figure 8.1. Two-dimensional classical confocal coordinate system (8.9) in terms of trigonometric functions with $a = 2$, $b = 1$.

8.2 Discrete confocal coordinate systems

For any discrete set of confocal quadrics (8.1), indexed by $u(n_1+\frac{1}{4}) \in \mathbb{R}$ and $v(n_2+\frac{1}{4}) \in \mathbb{R}$ with $n_1, n_2 \in \frac{1}{2}\mathbb{Z}$, we have introduced the discrete confocal quadrics defined by the equations of polarity relating nearest neighbors $\boldsymbol{x}(\boldsymbol{n})$ and $\boldsymbol{x}(\boldsymbol{n} + \frac{1}{2}\boldsymbol{\sigma})$:

$$\begin{aligned} \frac{x(\boldsymbol{n})x(\boldsymbol{n}+\frac{1}{2}\boldsymbol{\sigma})}{u(n_1+\frac{1}{4}\sigma_1)+a} + \frac{y(\boldsymbol{n})y(\boldsymbol{n}+\frac{1}{2}\boldsymbol{\sigma})}{u(n_1+\frac{1}{4}\sigma_1)+b} &= 1, \\ \frac{x(\boldsymbol{n})x(\boldsymbol{n}+\frac{1}{2}\boldsymbol{\sigma})}{v(n_2+\frac{1}{4}\sigma_2)+a} + \frac{y(\boldsymbol{n})y(\boldsymbol{n}+\frac{1}{2}\boldsymbol{\sigma})}{v(n_2+\frac{1}{4}\sigma_2)+b} &= 1. \end{aligned}$$

This is equivalent to

$$\begin{aligned} x(\boldsymbol{n})x(\boldsymbol{n}+\tfrac{1}{2}\boldsymbol{\sigma}) &= \frac{\big(u(n_1+\frac{1}{4}\sigma_1)+a\big)\big(v(n_2+\frac{1}{4}\sigma_2)+a\big)}{a-b}, \\ y(\boldsymbol{n})y(\boldsymbol{n}+\tfrac{1}{2}\boldsymbol{\sigma}) &= \frac{\big(u(n_1+\frac{1}{4}\sigma_1)+b\big)\big(v(n_2+\frac{1}{4}\sigma_2)+b\big)}{a-b}. \end{aligned}$$

According to Theorem 5.5, we can resolve this as follows:

$$x(\boldsymbol{n}) = \frac{f_1(n_1)f_2(n_2)}{\sqrt{a-b}}, \quad y(\boldsymbol{n}) = \frac{g_1(n_1)g_2(n_2)}{\sqrt{a-b}}, \tag{8.11}$$

where

$$\begin{cases} f_1(n_1)f_1(n_1+\frac{1}{2}) = u(n_1+\frac{1}{4}) + a, \\ g_1(n_1)g_1(n_1+\frac{1}{2}) = -\big(u(n_1+\frac{1}{4}) + b\big), \end{cases} \tag{8.12}$$

$$\begin{cases} f_2(n_2)f_2(n_2+\frac{1}{2}) = v(n_2+\frac{1}{4}) + a, \\ g_2(n_2)g_2(n_2+\frac{1}{2}) = v(n_2+\frac{1}{4}) + b. \end{cases} \tag{8.13}$$

Parametrization in terms of gamma functions. A solution of equations (8.12), (8.13) found in [BSST1] is given by $a = \alpha + \frac{1}{2}$, $b = \beta + 1$,

$$\begin{cases} f_1(n_1) = (n_1 + \alpha)_{1/2}, \\ g_1(n_1) = (-n_1 - \beta)_{1/2}, \end{cases} \qquad \begin{cases} f_2(n_2) = (n_2 + \alpha - \frac{1}{2})_{1/2}, \\ g_2(n_2) = (n_2 + \beta)_{1/2}, \end{cases}$$

so that

$$\begin{pmatrix} x(\boldsymbol{n}) \\ y(\boldsymbol{n}) \end{pmatrix} = \frac{1}{\sqrt{\alpha - \beta - \frac{1}{2}}} \begin{pmatrix} (n_1 + \alpha)_{1/2} \, (n_2 + \alpha - \frac{1}{2})_{1/2} \\ (-n_1 - \beta)_{1/2} \, (n_2 + \beta)_{1/2} \end{pmatrix}.$$

Parametrization in terms of trigonometric/hyperbolic functions. We obtain functional equations satisfied by the functions f_i, g_i by eliminating $u(n_1 + \frac{1}{4})$ and $v(n_2 + \frac{1}{4})$ from equations (8.12), (8.13):

$$f_1(n_1) f_1(n_1 + \tfrac{1}{2}) + g_1(n_1) g_1(n_1 + \tfrac{1}{2}) = a - b, \tag{8.14}$$

$$f_2(n_2) f_2(n_2 + \tfrac{1}{2}) - g_2(n_2) g_2(n_2 + \tfrac{1}{2}) = a - b. \tag{8.15}$$

By virtue of the addition theorems for trigonometric and hyperbolic functions, one easily finds solutions to these functional equations which approximate functions (8.7), (8.8):

$$f_1(n_1) = \sqrt{\frac{a-b}{\cos\frac{\delta_1}{2}}} \cos(\delta_1 n_1 + c_1), \quad g_1(n_1) = \sqrt{\frac{a-b}{\cos\frac{\delta_1}{2}}} \sin(\delta_1 n_1 + c_1), \tag{8.16}$$

and

$$f_2(n_2) = \sqrt{\frac{a-b}{\cosh\frac{\delta_2}{2}}} \cosh(\delta_2 n_2 + c_2), \quad g_2(n_2) = \sqrt{\frac{a-b}{\cosh\frac{\delta_2}{2}}} \sinh(\delta_2 n_2 + c_2). \tag{8.17}$$

Thus,

$$\begin{pmatrix} x(\boldsymbol{n}) \\ y(\boldsymbol{n}) \end{pmatrix} = \sqrt{\frac{a-b}{\cos\frac{\delta_1}{2} \, \cosh\frac{\delta_2}{2}}} \begin{pmatrix} \cos(\delta_1 n_1 + c_1) \, \cosh(\delta_2 n_2 + c_2) \\ \sin(\delta_1 n_1 + c_1) \, \sinh(\delta_2 n_2 + c_2) \end{pmatrix}. \tag{8.18}$$

The discrete coordinate curves $n_2 = \text{const}$ are to be interpreted as discrete ellipses. In order that they be closed curves, it is necessary to choose the lattice parameter δ_1 according to

$$\delta_1 = \frac{2\pi}{m}, \quad m \in \mathbb{N}.$$

One obtains a picture which is symmetric with respect to the coordinate axes if $c_1 = c_2 = 0$. The parameters $u(n_1 + \frac{1}{4})$ and $v(n_2 + \frac{1}{4})$ of the associated lattice of continuous confocal quadrics (8.2) are obtained from (8.12), (8.13) and (8.16), (8.17).

Figures 8.2–8.4 display a discrete confocal coordinate system for $a = 2$, $b = 1$, $m = 2$ and $\delta_2 = \delta_1$. In the continuous case encoded in the parametrisation (8.9), the foci on the x-axis correspond to $(s_1, s_2) = (0, 0)$ and $(s_1, s_2) = (\pi, 0)$. Their discrete analogs in the sublattice $\mathbb{Z}^2$ in Figure 8.3 (top) correspond to $(n_1, n_2) = (0, 0)$ resp. $(n_1, n_2) = (4, 0)$. The valence of these points is 2, as opposed to the regular points of valence 4. In the sublattice $(\mathbb{Z} + \frac{1}{2})^2$, the analogs of the foci are the "focal edges" connecting pairs of neighboring points of valence 3. For instance, the analog of the right focus is the edge $[\boldsymbol{x}(\frac{1}{2}, \frac{1}{2}), \boldsymbol{x}(\frac{1}{2}, -\frac{1}{2})]$. In the sublattices $\mathbb{Z} \times (\mathbb{Z} + \frac{1}{2})$ and $(\mathbb{Z} + \frac{1}{2}) \times \mathbb{Z}$, the analogs of the foci are the double points like $\boldsymbol{x}(0, \frac{1}{2}) = \boldsymbol{x}(0, -\frac{1}{2})$ and $\boldsymbol{x}(\frac{1}{2}, 0) = \boldsymbol{x}(-\frac{1}{2}, 0)$, both having valence 3 (see Figure 8.3, bottom). Figure 8.4 shows the confocal conics participating in the polarity relations of a discrete confocal coordinate system (8.18).

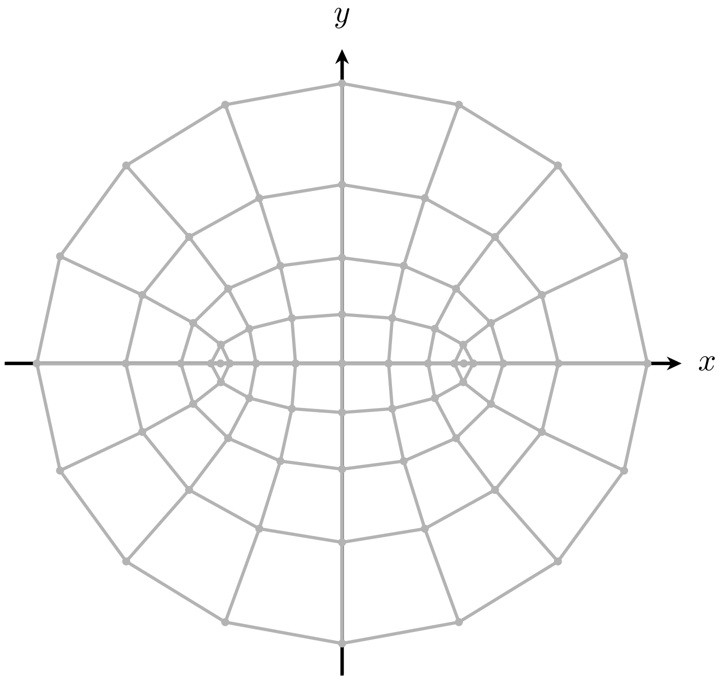

Figure 8.2. Two-dimensional discrete confocal coordinate system (8.18) on $\left(\frac{1}{2}\mathbb{Z}\right)^2$ in terms of trigonometric/hyperbolic functions with $a = 2$, $b = 1$, $m = 8$, $\delta_1 = \delta_2 = \frac{2\pi}{m}$, $c_1 = c_2 = 0$.

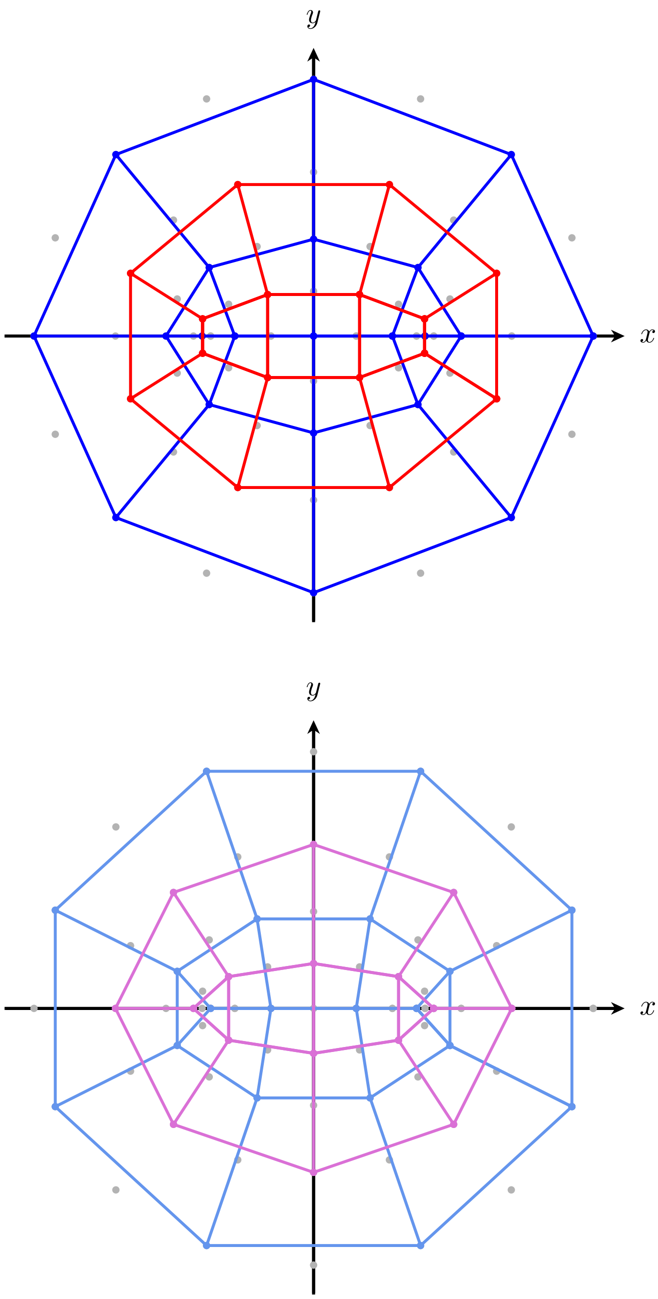

Figure 8.3. Pairs of dual orthogonal sublattices. Gray points show discrete confocal coordinates (8.18) on $\left(\frac{1}{2}\mathbb{Z}\right)^2$ with $a = 2$, $b = 1$, $m = 8$, $\delta_1 = \delta_2 = \frac{2\pi}{m}$, $c_1 = c_2 = 0$. (top) Sublattice on $\mathbb{Z}^2$ in blue and on $\left(\mathbb{Z} + \frac{1}{2}\right)^2$ in red. (bottom) Sublattice on $\mathbb{Z} \times (\mathbb{Z} + \frac{1}{2})$ in blue and on $(\mathbb{Z} + \frac{1}{2}) \times \mathbb{Z}$ in pink.

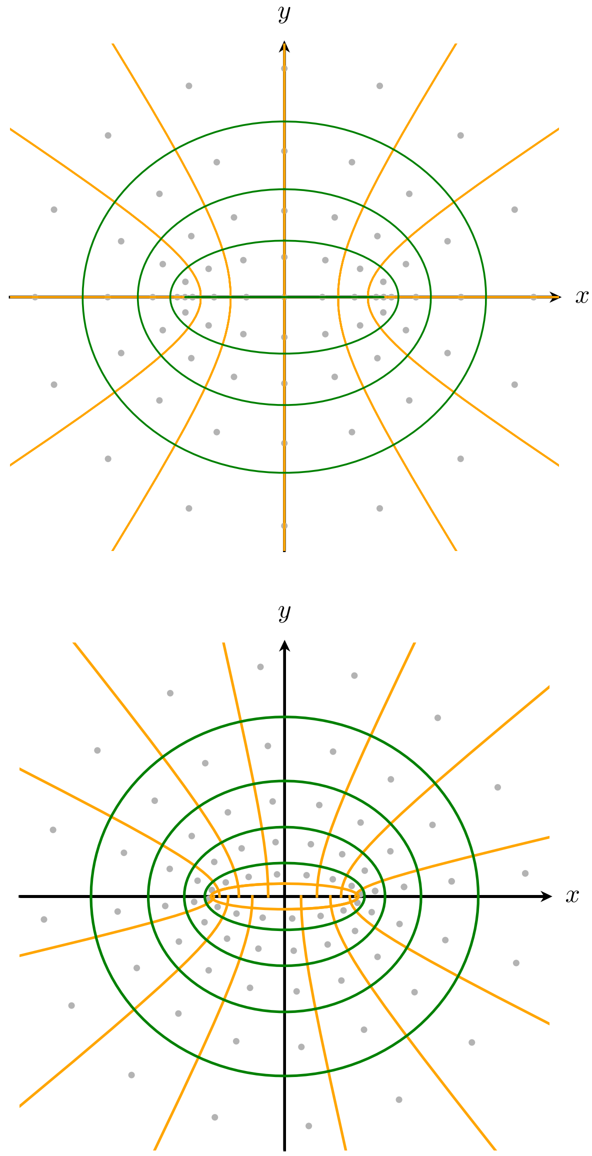

Figure 8.4. Polarity relation for discrete confocal conics. Gray points show discrete confocal coordinates (8.18) on $\left(\frac{1}{2}\mathbb{Z}\right)^2$ with $a = 2$, $b = 1$, $m = 8$, $\delta_1 = \delta_2 = \frac{2\pi}{m}$. The corresponding classical confocal conics which give rise to the polarity relation between gray points are shown in orange (for the values $u\left(n_1 + \frac{1}{4}\right)$) and green (for the values $v\left(n_2 + \frac{1}{4}\right)$). (left) Symmetric case with $c_1 = c_2 = 0$. All orange conics are hyperbolas and all green conics are ellipses. Note that near the coordinate axes those conics become degenerate and the polarity relation is not injective anymore. (right) Asymmetric case with $c_1 = 0.1$, $c_2 = 0.3$. Moving along the n_2-direction, the polarity across the y-axis is established by a conic with value $u\left(n_1 + \frac{1}{4}\right) < -a$, which is purely imaginary, while the polarity across the x-axis is established by a conic with value $u\left(n_1 + \frac{1}{4}\right) > -b$, which is an ellipse.

8.3 Parametrization by elliptic functions

The trigonometric/hyperbolic parametrization (8.7), (8.8) is not the only explicit solution to the functional equations (8.5), (8.6). One can find further ones in terms of elliptic functions. For instance, equation (8.5) admits the solution

$$f_1(s_1) = \sqrt{a-b}\ \mathrm{cn}(s_1, k_1), \quad g_1(s_1) = \sqrt{a-b}\ \mathrm{sn}(s_1, k_1) \tag{8.19}$$

with an arbitrary modulus k_1 (with (8.7) being the limiting case $k_1 \to 0$), or the solution

$$f_1(s_1) = \sqrt{a-b}\ \mathrm{dn}(s_1, k_1), \quad g_1(s_1) = \sqrt{a-b}\ k_1 \,\mathrm{sn}(s_1, k_1). \tag{8.20}$$

Similarly, equation (8.6) admits the solution

$$f_2(s_2) = \sqrt{a-b}\ \frac{1}{\mathrm{dn}(s_2, k_2)}, \quad g_2(s_2) = \sqrt{a-b}\ \frac{k_2 \,\mathrm{sn}(s_2, k_2)}{\mathrm{dn}(s_2, k_2)} \tag{8.21}$$

with an arbitrary modulus k_2 (with the limiting case (8.8) as $k_2 \to 1$). Further examples of solutions of (8.6) are:

$$f_2(s_2) = \sqrt{a-b}\ \frac{1}{\mathrm{sn}(s_2, k_2)}, \quad g_2(s_2) = \sqrt{a-b}\ \frac{\mathrm{cn}(s_2, k_2)}{\mathrm{sn}(s_2, k_2)}, \tag{8.22}$$

or

$$f_2(s_2) = \sqrt{a-b}\ \frac{1}{k_2'} \,\mathrm{dn}(s_2, k_2), \quad g_2(s_2) = \sqrt{a-b}\ \frac{k_2}{k_2'} \,\mathrm{cn}(s_2, k_2), \tag{8.23}$$

where $k_2' = \sqrt{1-k_2^2}$. All such solutions can be seen as based on relations between squares of theta functions, and are connected by simple transformations in the complex domain, but they have rather different properties in the real domain. For instance, in (8.21) one of the participating functions is odd and another is even, while in (8.22) both functions are odd and in (8.23) both functions are odd. On the other hand, in (8.21) and in (8.22) both participating functions have no singularities on the real axis, while in (8.23) both have simple poles at $s_2 = 2\mathsf{K}(k_2)$. Thus, the corresponding parametrizations of the confocal coordinates cover different regions of the plane $\mathbb{R}^2$ and have, in principle, different geometric features.

It turns out that any solution of the quadratic relations (8.5), (8.6) admits a corresponding solution of the bilinear relations (8.14), (8.15), the latter approximating the former in the continuum limit. These solutions can be derived with the help of the addition formulas for the theta functions (or for the Jacobi elliptic functions). As an example, we mention the addition formulas

$$\begin{aligned}
\mathrm{cn}(s,k)\,\mathrm{cn}(s+\eta,k) + \mathrm{sn}(s,k)\,\mathrm{sn}(s+\eta,k)\,\mathrm{dn}(\eta,k) &= \mathrm{cn}(\eta,k),\\
\mathrm{dn}(s,k)\,\mathrm{dn}(s+\eta,k) + k^2\,\mathrm{sn}(s,k)\,\mathrm{sn}(s+\eta,k)\,\mathrm{cn}(\eta,k) &= \mathrm{dn}(\eta,k),
\end{aligned}$$

which constitute bilinear analogs of the identities

$$\begin{aligned}
\mathrm{cn}^2(s,k) + \mathrm{sn}^2(s,k) &= 1,\\
\mathrm{dn}^2(s,k) + k^2\,\mathrm{sn}^2(s,k) &= 1.
\end{aligned}$$

As a consequence, we find the following two solutions of the functional equation (8.14):

$$f_1(n_1) = \alpha\,\mathrm{cn}(\delta n_1 + c_1, k_1), \quad g_1(n_1) = \beta\,\mathrm{sn}(\delta n_1 + c_1, k_1),$$

where

$$\alpha = \sqrt{\frac{a-b}{\mathrm{cn}(\frac{\delta}{2}, k_1)}}, \quad \beta = \sqrt{(a-b)\frac{\mathrm{dn}(\frac{\delta}{2}, k_1)}{\mathrm{cn}(\frac{\delta}{2}, k_1)}},$$

and

$$f_1(n_1) = \alpha\,\mathrm{dn}(\delta n_1 + c_1, k_1), \quad g_1(n_1) = \beta\,\mathrm{sn}(\delta n_1 + c_1, k_1),$$

where

$$\alpha = \sqrt{\frac{a-b}{\mathrm{dn}(\frac{\delta}{2}, k)}}, \quad \beta = k_1\sqrt{(a-b)\frac{\mathrm{cn}(\frac{\delta}{2}, k)}{\mathrm{dn}(\frac{\delta}{2}, k)}}.$$

They approximate solutions (8.19), resp. (8.20) in the continuum limit $\delta \to 0$.

In the following two sections, we will consider in detail two parametrizations of the continuous and discrete confocal coordinate systems of this kind with very remarkable geometric properties.

8.4 Confocal coordinates outside of an ellipse, diagonally related to a straight line coordinate system

Continuous case

Consider a coordinate system (8.3) with

$$\begin{aligned} f_1(s_1) &= \alpha_1 \operatorname{sn}(s_1,k), \quad g_1(s_1) = \beta_1 \operatorname{cn}(s_1,k),\\ f_2(s_2) &= \alpha_2 \frac{\operatorname{dn}(s_2,k)}{\operatorname{cn}(s_2,k)}, \quad g_2(s_2) = \beta_2 \frac{1}{\operatorname{cn}(s_2,k)}, \end{aligned} \tag{8.24}$$

where $s_1 \in [0, 2\mathsf{K}(k)]$ and $s_2 \in [0, \mathsf{K}(k))$, and the amplitudes α_1, β_1, α_2 and β_2 are chosen as follows:

$$\alpha_1 = \beta_1 = \sqrt{a-b}, \quad \alpha_2 = \frac{1}{k}\sqrt{a-b}, \quad \beta_2 = \frac{k'}{k}\sqrt{a-b},$$

where $k' = \sqrt{1-k^2}$. Observe that the modulus k in both pairs (f_1, g_1) and (f_2, g_2) is chosen to be the same. The remarkable geometric property mentioned above is this (cf. Figure 8.5):

Proposition 8.1. *In the coordinate system* (8.3), (8.24), *the points* (x, y) *with* $s_1 + s_2 = \xi = \text{const}$ *lie on straight lines. The same is true for points* (x, y) *with* $s_2 - s_1 = \eta = \text{const}$. *Moreover, all these lines are tangent to the ellipse*

$$\mathcal{E}_0 : \quad \frac{x^2}{a_0} + \frac{y^2}{b_0} = 1,$$

where

$$a_0 = \frac{1}{k^2}(a-b), \quad b_0 = \frac{(k')^2}{k^2}(a-b).$$

This ellipse belongs to the confocal family (8.1).

Proof. Due to the fact that the functions f_2, g_2 are even with respect to s_2, it is enough to demonstrate the second statement. We set $s_2 = s_1 + \eta$ and use addition theorems for elliptic functions to derive:

$$\begin{aligned} x(s_1, s_1+\eta) &= \frac{\sqrt{a-b}}{k} \frac{\operatorname{sn}(s_1)\operatorname{dn}(s_1)\operatorname{dn}(\eta) - k^2 \operatorname{sn}^2(s_1)\operatorname{cn}(s_1)\operatorname{sn}(\eta)\operatorname{cn}(\eta)}{\operatorname{cn}(s_1)\operatorname{cn}(\eta) - \operatorname{sn}(s_1)\operatorname{dn}(s_1)\operatorname{sn}(\eta)\operatorname{dn}(\eta)},\\ y(s_1, s_1+\eta) &= \frac{k'\sqrt{a-b}}{k} \frac{\operatorname{cn}(s_1) - k^2 \operatorname{sn}^2(s_1)\operatorname{cn}(s_1)\operatorname{sn}^2(\eta)}{\operatorname{cn}(s_1)\operatorname{cn}(\eta) - \operatorname{sn}(s_1)\operatorname{dn}(s_1)\operatorname{sn}(\eta)\operatorname{dn}(\eta)}. \end{aligned}$$

For these points, equation $Ax + By = C$ is satisfied with

$$\frac{\sqrt{a-b}}{k} A = -C \operatorname{sn}(\eta), \quad \frac{k'\sqrt{a-b}}{k} B = C \operatorname{cn}(\eta).$$

Obviously, for any η the coefficients A, B, C satisfy

$$a_0 \left(\frac{A}{C}\right)^2 + b_0 \left(\frac{B}{C}\right)^2 = 1$$

and the quantities a_0, b_0 obey $a_0 - b_0 = a - b$. □

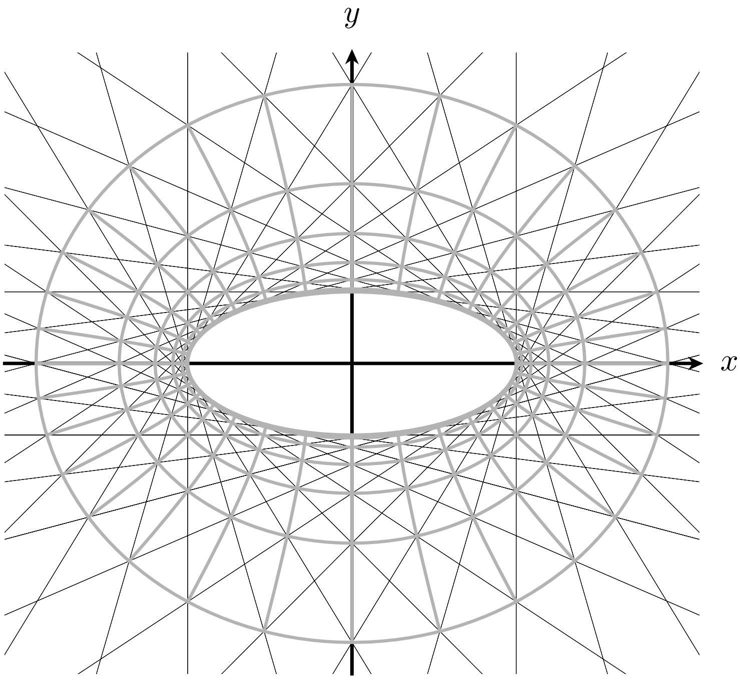

Figure 8.5. Two-dimensional continuous confocal coordinate system (8.3), (8.24) with $a = 2$, $b = 1$, $k = 0.9$. Points with $s_1 + s_2 =$ const as well as points with $s_1 - s_2 =$ const lie on straight lines which are tangent to an ellipse $\mathcal{E}_0$. The parametrization is only defined outside $\mathcal{E}_0$.

Discrete case and "elliptic" IC-nets

A solution of the functional equations (8.14) and (8.15) which approximates (8.24) in the continuum limit $\delta \to 0$, is given by

$$\begin{aligned} f_1(n_1) &= \hat{\alpha}_1 \operatorname{sn}(\delta n_1 + c_1, k), \quad & g_1(n_1) &= \hat{\beta}_1 \operatorname{cn}(\delta n_1 + c_1, k), \\ f_2(n_2) &= \hat{\alpha}_2 \frac{\operatorname{dn}(\delta n_2 + c_2, k)}{\operatorname{cn}(\delta n_2 + c_2, k)}, \quad & g_2(n_2) &= \hat{\beta}_2 \frac{1}{\operatorname{cn}(\delta n_2 + c_2, k)}. \end{aligned} \tag{8.25}$$

Using addition theorems for elliptic functions, we easily see that this is a solution if

$$\hat{\alpha}_1 = \sqrt{(a-b)\frac{\operatorname{dn}(\frac{\delta}{2}, k)}{\operatorname{cn}(\frac{\delta}{2}, k)}}, \quad \hat{\beta}_1 = \sqrt{\frac{a-b}{\operatorname{cn}(\frac{\delta}{2}, k)}},$$

and

$$\hat{\alpha}_2 = \frac{1}{k}\hat{\alpha}_1, \quad \hat{\beta}_2 = \frac{k'}{k}\hat{\beta}_1.$$

Here, the constants δ, k, c_1, c_2 are arbitrary except that $0 < k^2 < 1$ and $\operatorname{cn}(\frac{\delta}{2}, k) > 0$. However, for reasons of symmetry and closure, one should choose $c_1 = c_2 = 0$ and

$$\delta = \frac{\mathsf{K}(k)}{m}, \quad m \in \tfrac{1}{2}\mathbb{N},$$

so that the parameters n_i may be restricted to $n_1 \in [-2m, 2m]$ and $n_2 \in [0, m-\frac{1}{2}]$. The same computation as in the previous section allows us to show (cf. Figure 8.6):

Proposition 8.2. *The points (x, y) with $n_1 + n_2 = \xi =$ const lie on straight lines. The same is true for points (x, y) with $n_1 - n_2 = \eta =$ const. Moreover, all these lines are tangent to the ellipse*

$$\hat{\mathcal{E}}_0 : \quad \frac{x^2}{\hat{a}_0} + \frac{y^2}{\hat{b}_0} = 1,$$

where

$$\hat{a}_0 = (a-b)\frac{1}{k^2}\frac{\mathrm{dn}^2(\frac{\delta}{2},k)}{\mathrm{cn}^2(\frac{\delta}{2},k)}, \quad \hat{b}_0 = (a-b)\frac{(k')^2}{k^2}\frac{1}{\mathrm{cn}^2(\frac{\delta}{2},k)}.$$

This ellipse belongs to the confocal family (8.1)*, since* $\hat{a}_0 - \hat{b}_0 = a - b$.

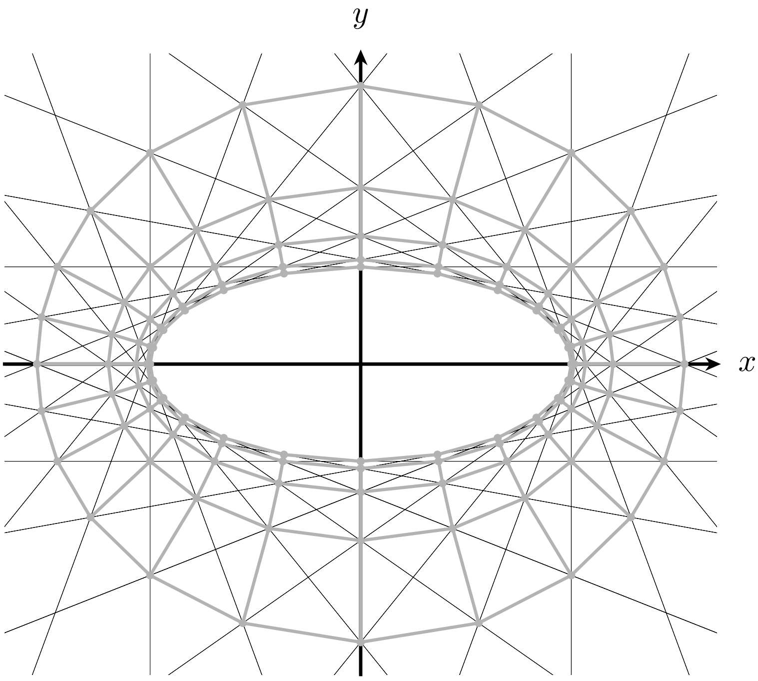

Figure 8.6. Two-dimensional discrete confocal coordinate system (8.11), (8.25) on $\left(\frac{1}{2}\mathbb{Z}\right)^2$ with $a = 2$, $b = 1$, $k = 0.9$, $m = 3$, $c_1 = c_2 = 0$. Points with $n_1 + n_2 = \mathrm{const}$ as well as points with $n_1 - n_2 = \mathrm{const}$ lie on straight lines which are tangent to an ellipse. The parametrization is only defined outside this ellipse.

Consider the case $c_2 = 0$. Then a short computation shows that the vertices of the innermost discrete ellipse $\boldsymbol{x}(n_1, 0)$ lie on the ellipse $\hat{\mathcal{E}}_0$. The tangent line to $\hat{\mathcal{E}}_0$ at the point $\boldsymbol{x}(n_1, 0)$ contains the vertices $\boldsymbol{x}(n_1 + m, m)$ and $\boldsymbol{x}(n_1 - m, m)$, $m \in \frac{1}{2}\mathbb{Z}_{\geqslant 0}$. In particular, this tangent line contains the edge $[\boldsymbol{x}(n_1 + \frac{1}{2}, \frac{1}{2}), \boldsymbol{x}(n_1 - \frac{1}{2}, \frac{1}{2})]$. In other words, the innermost discrete ellipse $n_2 = 0$ is inscribed in $\hat{\mathcal{E}}_0$, while the neighboring discrete ellipse $n_2 = \frac{1}{2}$ is circumscribed about $\hat{\mathcal{E}}_0$, with the points of contact being the vertices of the discrete ellipse $n_2 = 0$ (cf. Figure 8.7).

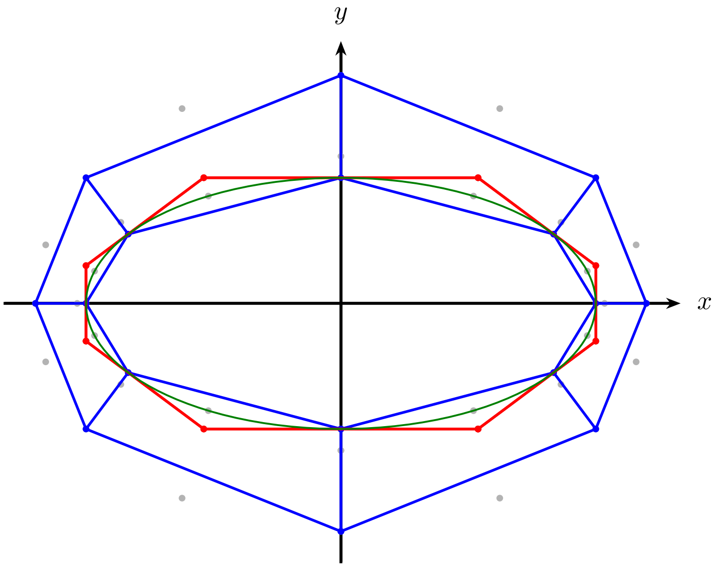

Figure 8.7. Gray points show discrete confocal coordinates (8.11), (8.25) on $\left(\frac{1}{2}\mathbb{Z}\right)^2$ with $a = 2$, $b = 1$, $k = 0.9$, $m = 2$, $c_1 = c_2 = 0$. The two dual sublattices on $\mathbb{Z}^2$ and on $\left(\mathbb{Z}+\frac{1}{2}\right)^2$ are shown in blue and in red, respectively. The innermost blue discrete ellipse, corresponding to $n_2 = 0$, is inscribed in $\hat{\mathcal{E}}_0$, while the neighboring red discrete ellipse, corresponding to $n_2 = \frac{1}{2}$, is circumscribed about $\hat{\mathcal{E}}_0$.

A further important observation is that the points (8.11) with f_1, f_2, g_1, g_2 given by (8.25) upon an affine transformation

$$(x, y) \mapsto (\alpha x, \beta y) \quad \text{with} \quad \alpha = \frac{\mathrm{cn}(\frac{\delta}{2}, k)}{\mathrm{dn}(\frac{\delta}{2}, k)}, \quad \beta = \mathrm{cn}(\tfrac{\delta}{2}, k) \tag{8.26}$$

lie on continuous conics given by the parametrization (8.24), i.e., on conics of the original confocal familiy (8.1). By the Theorem of Graves-Chasles (see [AB]), all elementary quadrilaterals of the diagonal net upon this affine transformation become circumscribed around circles. This means that the discrete confocal quadrics with the parametrization (8.11), (8.25) constitute affine images of "incircular nets" (IC-nets) studied in [AB]. An additional computation sketched in [BSST2] shows that, amazingly, the centers of all incircles coincide with the original points of the discrete confocal coordinate system.

Remark 8.1. As mentioned in [BSST1, Appendix A], the nets comprised by discrete quadrics, $\boldsymbol{x}(\mathbb{Z}\times\mathbb{Z})$, $\boldsymbol{x}((\mathbb{Z}+\frac{1}{2})\times(\mathbb{Z}+\frac{1}{2}))$, as well as $\boldsymbol{x}(\mathbb{Z}\times(\mathbb{Z}+\frac{1}{2}))$, $\boldsymbol{x}((\mathbb{Z}+\frac{1}{2})\times\mathbb{Z})$ (all of them being subnets of the incircle centers of an IC-net), are circular conical Koenigs nets. Note that the statement from [BSST1, Appendix A] that these nets are not separable, made on the basis of numerical experiments, was not correct.

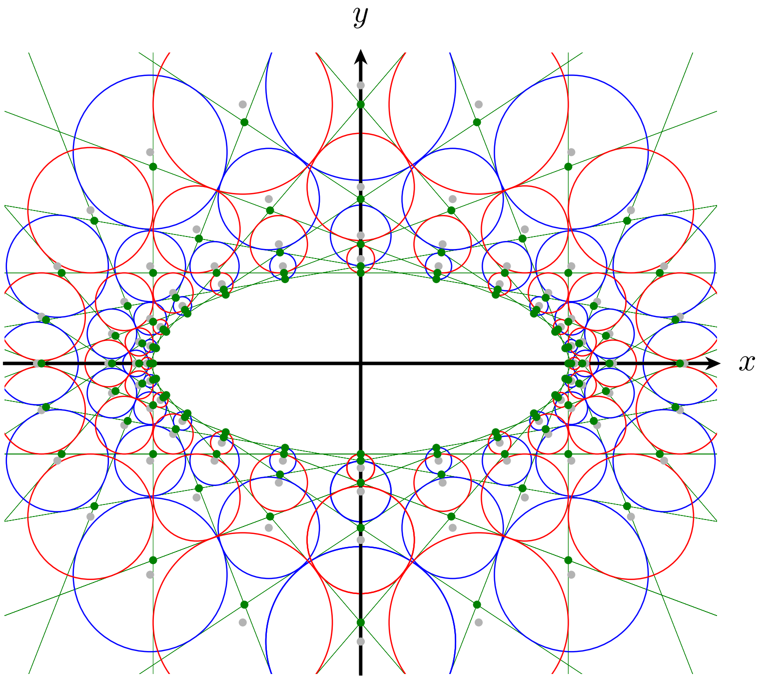

Figure 8.8. Grey points show discrete confocal coordinates (8.11), (8.25) on $\left(\frac{1}{2}\mathbb{Z}\right)^2$ with $a = 2$, $b = 1$, $k = 0.9$, $m = 3$, $c_1 = c_2 = 0$. Green points show the net after the affine transformation (8.26). The straight lines through the transformed net constitute two incircular nets. The grey points are the centers of the incircles.

8.5 Confocal coordinates outside of a hyperbola, diagonally related to a straight line coordinate system

Continuous case

Similar properties to those mentioned above has the following coordinate system:

$$
\begin{aligned}
f_1(s_1) &= \alpha_1 \operatorname{sn}(s_1, k), \quad & g_1(s_1) &= \beta_1 \operatorname{dn}(s_1, k), \\
f_2(s_2) &= \alpha_2 \frac{1}{\operatorname{sn}(s_2, k)}, \quad & g_2(s_2) &= \beta_2 \frac{\operatorname{cn}(s_2, k)}{\operatorname{sn}(s_2, k)},
\end{aligned}
\tag{8.27}
$$

where

$$\alpha_1 = k\sqrt{a-b}, \quad \alpha_2 = \beta_1 = \beta_2 = \sqrt{a-b}.$$

Proposition 8.3. *In the coordinate system* (8.3), (8.27), *the points* (x, y) *with* $s_1 + s_2 = \xi = \text{const}$ *lie on straight lines. The same is true for points* (x, y) *with* $s_2 - s_1 = \eta = \text{const}$. *Moreover, all these lines are tangent to the hyperbola (cf. Figure 8.9)*

$$\mathcal{H}_0 : \quad \frac{x^2}{a_0} - \frac{y^2}{c_0} = 1,$$

where

$$a_0 = k^2(a-b), \quad c_0 = (1-k^2)(a-b).$$

This hyperbola belongs to the confocal family (8.1).

Proof. Due to the fact that the functions f_2, g_2 are odd with respect to s_2, it is enough to demonstrate the second statement. We set $s_2 = s_1 + \eta$ and use addition theorems for elliptic functions to derive:

$$\begin{aligned} x(s_1, s_1+\eta) &= k\sqrt{a-b}\,\frac{\operatorname{sn}(s_1)\big(1-k^2\operatorname{sn}^2(s_1)\operatorname{sn}^2(\eta)\big)}{\operatorname{sn}(s_1)\operatorname{cn}(\eta)\operatorname{dn}(\eta)+\operatorname{cn}(s_1)\operatorname{dn}(s_1)\operatorname{sn}(\eta)},\\ y(s_1, s_1+\eta) &= \sqrt{a-b}\,\frac{\operatorname{dn}(s_1)\big(\operatorname{cn}(s_1)\operatorname{cn}(\eta)-\operatorname{sn}(s_1)\operatorname{dn}(s_1)\operatorname{sn}(\eta)\operatorname{dn}(\eta)\big)}{\operatorname{sn}(s_1)\operatorname{cn}(\eta)\operatorname{dn}(\eta)+\operatorname{cn}(s_1)\operatorname{dn}(s_1)\operatorname{sn}(\eta)}. \end{aligned}$$

For these points, equation $Ax + By = C$ is satisfied with

$$Ak\sqrt{a-b}\operatorname{cn}(\eta) = C\operatorname{dn}(\eta), \quad B\sqrt{a-b}\operatorname{cn}(\eta) = C\operatorname{sn}(\eta).$$

Obviously, for any η the coefficients A, B, C satisfy

$$a_0\left(\frac{A}{C}\right)^2 - c_0\left(\frac{B}{C}\right)^2 = \frac{\operatorname{dn}^2(\eta)}{\operatorname{cn}^2(\eta)} - \frac{(1-k^2)\operatorname{sn}^2(\eta)}{\operatorname{cn}^2(\eta)} = 1$$

and the quantities a_0, c_0 obey $a_0 + c_0 = a - b$. □

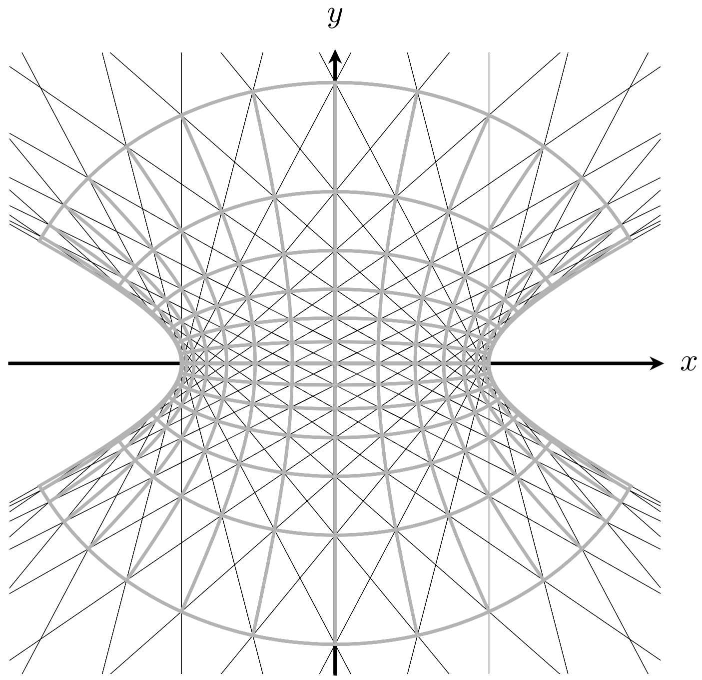

Figure 8.9. Two-dimensional continuous confocal coordinate system (8.3), (8.27) with $a = 2$, $b = 1$, $k = 0.9$. Points with $s_1 + s_2 =$ const as well as points with $s_1 - s_2 =$ const lie on straight lines which are tangent to a hyperbola $\mathcal{H}_0$. The parametrization is only defined outside $\mathcal{H}_0$.

Discrete case and "hyperbolic" IC-nets

A solution of (8.14), (8.15) which approximates (8.27) in the continuum limit $\delta \to 0$ reads:

$$\begin{aligned} f_1(n_1) &= \hat\alpha_1\operatorname{sn}(\delta n_1 + c_1, k), \quad g_1(n_1) = \hat\beta_1\operatorname{dn}(\delta n_1 + c_1, k),\\ f_2(n_2) &= \hat\alpha_2\frac{1}{\operatorname{sn}(\delta n_2 + c_2, k)}, \quad g_2(n_2) = \hat\beta_2\frac{\operatorname{cn}(\delta n_2 + c_2, k)}{\operatorname{sn}(\delta n_2 + c_2, k)}, \end{aligned} \tag{8.28}$$

where

$$\hat\alpha_2 = \frac{1}{k}\hat\alpha_1 = \sqrt{(a-b)\frac{\operatorname{cn}(\frac{\delta}{2},k)}{\operatorname{dn}(\frac{\delta}{2},k)}}, \quad \hat\beta_2 = \hat\beta_1 = \sqrt{\frac{a-b}{\operatorname{dn}(\frac{\delta}{2},k)}}.$$

Proposition 8.4. *The points (x, y) with $n_1 + n_2 = \xi = \text{const}$ lie on straight lines. The same is true for points (x, y) with $n_2 - n_1 = \eta = \text{const}$. Moreover, all these lines are tangent to the hyperbola (cf. Figure 8.10)*

$$\hat{\mathcal{H}}_0 : \quad \frac{x^2}{\hat{a}_0} - \frac{y^2}{\hat{c}_0} = 1,$$

where

$$\hat{a}_0 = (a-b)k^2 \frac{\operatorname{cn}^2(\frac{\delta}{2}, k)}{\operatorname{dn}^2(\frac{\delta}{2}, k)}, \quad \hat{c}_0 = (a-b)(1-k^2)\frac{1}{\operatorname{dn}^2(\frac{\delta}{2}, k)}.$$

This hyperbola belongs to the confocal family (8.1), since $\hat{a}_0 + \hat{c}_0 = a - b$.

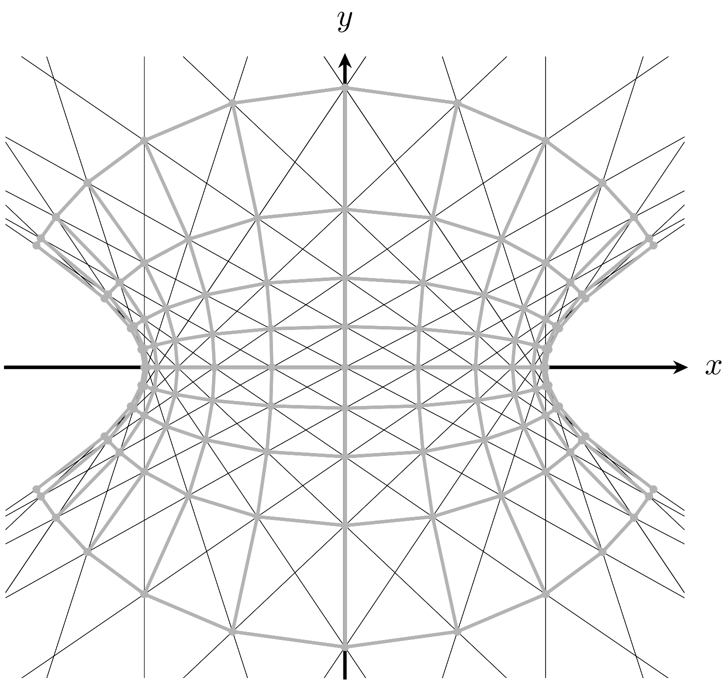

Figure 8.10. Two-dimensional discrete confocal coordinate system (8.11), (8.25) on $\left(\frac{1}{2}\mathbb{Z}\right)^2$ with $a = 2$, $b = 1$, $k = 0.9$, $m = 3$, $c_1 = c_2 = 0$. Points with $n_1 + n_2 = \text{const}$ as well as points with $n_1 - n_2 = \text{const}$ lie on straight lines which are tangent to a hyperbola. The parametrization is only defined outside this hyperbola.

An affine transformation converting the discrete confocal system (8.11) with (8.28) into "hyperbolic" IC-nets is characterized by

$$(x, y) \mapsto (\alpha x, \beta y) \quad \text{with} \quad \alpha = \frac{\operatorname{dn}(\frac{\delta}{2}, k)}{\operatorname{cn}(\frac{\delta}{2}, k)}, \quad \beta = \operatorname{dn}(\frac{\delta}{2}, k).$$

9 The case $N = 3$

9.1 Classical confocal coordinate systems

The defining equations

$$\begin{aligned}\frac{x^2}{u+a}+\frac{y^2}{u+b}+\frac{z^2}{u+c}&=1,\\ \frac{x^2}{v+a}+\frac{y^2}{v+b}+\frac{z^2}{v+c}&=1,\\ \frac{x^2}{w+a}+\frac{y^2}{w+b}+\frac{z^2}{w+c}&=1\end{aligned} \tag{9.1}$$

of confocal coordinates $\{(u, v, w) : -a < u < -b < v < -c < w\}$ in three dimensions give rise to the expressions

$$x^2 = \frac{(u+a)(v+a)(w+a)}{(a-b)(a-c)},$$

$$y^2 = \frac{(u+b)(v+b)(w+b)}{(b-a)(b-c)},$$

$$z^2 = \frac{(u+c)(v+c)(w+c)}{(c-a)(c-b)}.$$

For an arbitrary re-parametrization of the coordinate lines we obtain:

$$x = \frac{f_1(s_1)f_2(s_2)f_3(s_3)}{\sqrt{(a-b)(a-c)}}, \quad y = \frac{g_1(s_1)g_2(s_2)g_3(s_3)}{\sqrt{(a-b)(b-c)}}, \quad z = \frac{h_1(s_1)h_2(s_2)h_3(s_3)}{\sqrt{(a-c)(b-c)}},$$

where

$$\begin{cases} (f_1(s_1))^2 = u+a, \\ (g_1(s_1))^2 = -(u+b), \\ (h_1(s_1))^2 = -(u+c), \end{cases} \quad \begin{cases} (f_2(s_2))^2 = v+a, \\ (g_2(s_2))^2 = v+b, \\ (h_2(s_2))^2 = -(v+c), \end{cases} \quad \begin{cases} (f_3(s_3))^2 = w+a, \\ (g_3(s_3))^2 = w+b, \\ (h_3(s_3))^2 = w+c. \end{cases}$$

Elimination of u, v and w leads to functional equations

$$\begin{cases} (f_1(s_1))^2 + (g_1(s_1))^2 = a-b, \\ (f_1(s_1))^2 + (h_1(s_1))^2 = a-c, \end{cases} \quad \begin{cases} (f_2(s_2))^2 - (g_2(s_2))^2 = a-b, \\ (f_2(s_2))^2 + (h_2(s_2))^2 = a-c, \end{cases}$$

$$\begin{cases} (f_3(s_3))^2 - (g_3(s_3))^2 = a-b, \\ (f_3(s_3))^2 - (h_3(s_3))^2 = a-c. \end{cases}$$

There exists a solution parametrized in terms of Jacobi elliptic functions:

$$\begin{aligned} f_1(s_1) &= \sqrt{a-b}\,\mathrm{sn}(s_1,k_1), & g_1(s_1) &= \sqrt{a-b}\,\mathrm{cn}(s_1,k_1), & h_1(s_1) &= \sqrt{a-b}\,\frac{\mathrm{dn}(s_1,k_1)}{k_1}, \\ f_2(s_2) &= \sqrt{b-c}\,\frac{\mathrm{dn}(s_2,k_2)}{k_2}, & g_2(s_2) &= \sqrt{b-c}\,\mathrm{cn}(s_2,k_2), & h_2(s_2) &= \sqrt{b-c}\,\mathrm{sn}(s_2,k_2), \\ f_3(s_3) &= \sqrt{a-c}\,\frac{1}{\mathrm{sn}(s_3,k_3)}, & g_3(s_3) &= \sqrt{a-c}\,\frac{\mathrm{dn}(s_3,k_3)}{\mathrm{sn}(s_3,k_3)}, & h_3(s_3) &= \sqrt{a-c}\,\frac{\mathrm{cn}(s_3,k_3)}{\mathrm{sn}(s_3,k_3)}, \end{aligned}$$

where the moduli of the elliptic functions are defined by

$$k_1^2 = \frac{a-b}{a-c}, \quad k_2^2 = \frac{b-c}{a-c} = 1-k_1^2, \quad k_3 = k_1.$$

Hence, we obtain the representation

$$\begin{pmatrix} x \\ y \\ z \end{pmatrix} = \sqrt{a-c}\begin{pmatrix} \mathrm{sn}(s_1,k_1)\,\mathrm{dn}(s_2,k_2)\,\mathrm{ns}(s_3,k_3) \\ \mathrm{cn}(s_1,k_1)\,\mathrm{cn}(s_2,k_2)\,\mathrm{ds}(s_3,k_3) \\ \mathrm{dn}(s_1,k_1)\,\mathrm{sn}(s_2,k_2)\,\mathrm{cs}(s_3,k_3) \end{pmatrix} \tag{9.3}$$

of confocal coordinate systems in 3-space. If $\mathsf{K}(k)$ denotes the complete elliptic integral of the first kind, which constitutes the quarter-period of $\operatorname{sn}(s,k)$, then the parameters may be restricted to $s_1 \in [0, 4\mathsf{K}(k_1)]$, $s_2 \in [0, 4\mathsf{K}(k_2)]$ and $s_3 \in (0, 2\mathsf{K}(k_3))$. Three corresponding coordinate surfaces are depicted in Figure 9.1.

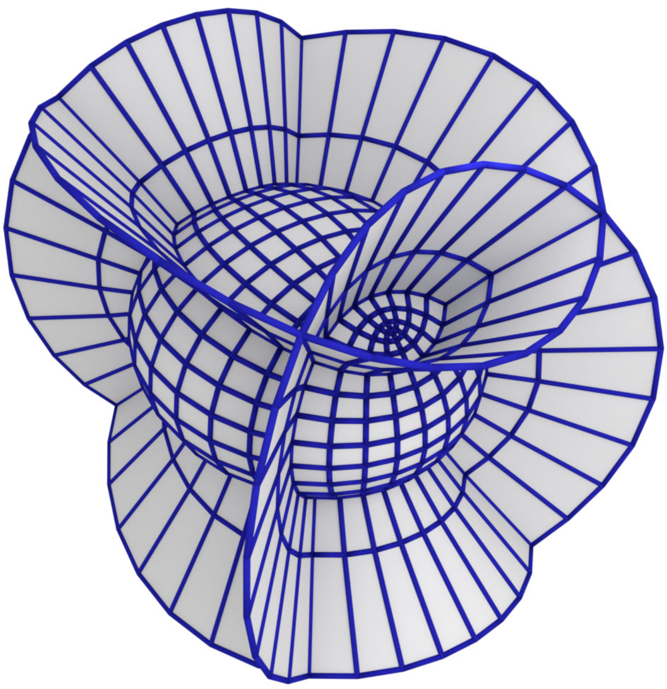

Figure 9.1. Three-dimensional classical confocal coordinate system (9.3) in terms of Jacobi elliptic functions with $a = 8$, $b = 4$, $c = 0$. One quadric of each signature is shown.

9.2 Discrete confocal coordinate systems

For any discrete set of confocal quadrics (9.1), indexed by $u(n_1 + \frac{1}{4})$, $v(n_2 + \frac{1}{4})$, and $w(n_3 + \frac{1}{4})$, we have introduced the discrete confocal quadrics defined by the equations of polarity relating nearest neighbors $\boldsymbol{x}(\boldsymbol{n})$ and $\boldsymbol{x}(\boldsymbol{n} + \frac{1}{2}\boldsymbol{\sigma})$:

$$\begin{aligned}
\frac{x(\boldsymbol{n})x(\boldsymbol{n}+\frac{1}{2}\boldsymbol{\sigma})}{u(n_1+\frac{1}{4}\sigma_1)+a} + \frac{y(\boldsymbol{n})y(\boldsymbol{n}+\frac{1}{2}\boldsymbol{\sigma})}{u(n_1+\frac{1}{4}\sigma_1)+b} + \frac{z(\boldsymbol{n})z(\boldsymbol{n}+\frac{1}{2}\boldsymbol{\sigma})}{u(n_1+\frac{1}{4}\sigma_1)+c} &= 1, \\
\frac{x(\boldsymbol{n})x(\boldsymbol{n}+\frac{1}{2}\boldsymbol{\sigma})}{v(n_2+\frac{1}{4}\sigma_2)+a} + \frac{y(\boldsymbol{n})y(\boldsymbol{n}+\frac{1}{2}\boldsymbol{\sigma})}{v(n_2+\frac{1}{4}\sigma_2)+b} + \frac{z(\boldsymbol{n})z(\boldsymbol{n}+\frac{1}{2}\boldsymbol{\sigma})}{v(n_2+\frac{1}{4}\sigma_2)+c} &= 1, \\
\frac{x(\boldsymbol{n})x(\boldsymbol{n}+\frac{1}{2}\boldsymbol{\sigma})}{w(n_3+\frac{1}{4}\sigma_3)+a} + \frac{y(\boldsymbol{n})y(\boldsymbol{n}+\frac{1}{2}\boldsymbol{\sigma})}{w(n_3+\frac{1}{4}\sigma_3)+b} + \frac{z(\boldsymbol{n})z(\boldsymbol{n}+\frac{1}{2}\boldsymbol{\sigma})}{w(n_3+\frac{1}{4}\sigma_3)+c} &= 1.
\end{aligned}$$

This is equivalent to

$$\begin{aligned}
x(\boldsymbol{n})x(\boldsymbol{n}+\tfrac{1}{2}\boldsymbol{\sigma}) &= \frac{\big(u(n_1+\frac{1}{4}\sigma_1)+a\big)\big(v(n_2+\frac{1}{4}\sigma_2)+a\big)\big(w(n_3+\frac{1}{4}\sigma_3)+a\big)}{(a-b)(a-c)}, \\
y(\boldsymbol{n})y(\boldsymbol{n}+\tfrac{1}{2}\boldsymbol{\sigma}) &= \frac{\big(u(n_1+\frac{1}{4}\sigma_1)+b\big)\big(v(n_2+\frac{1}{4}\sigma_2)+b\big)\big(w(n_3+\frac{1}{4}\sigma_3)+b\big)}{(b-a)(b-c)}, \\
z(\boldsymbol{n})z(\boldsymbol{n}+\tfrac{1}{2}\boldsymbol{\sigma}) &= \frac{\big(u(n_1+\frac{1}{4}\sigma_1)+c\big)\big(v(n_2+\frac{1}{4}\sigma_2)+c\big)\big(w(n_3+\frac{1}{4}\sigma_3)+c\big)}{(c-a)(c-b)}.
\end{aligned}$$

According to Theorem 5.5, these equations can be resolved as follows:

$$x(\boldsymbol{n}) = \frac{f_1(n_1)f_2(n_2)f_3(n_3)}{\sqrt{(a-b)(a-c)}}, \quad y(\boldsymbol{n}) = \frac{g_1(n_1)g_2(n_2)g_3(n_3)}{\sqrt{(a-b)(b-c)}}, \quad z(\boldsymbol{n}) = \frac{h_1(n_1)h_2(n_2)h_3(n_3)}{\sqrt{(a-c)(b-c)}}, \tag{9.4}$$

where

$$\left\{\begin{array}{l} f_1(n_1)f_1(n_1+\frac{1}{2}) = u(n_1+\frac{1}{4})+a, \\ g_1(n_1)g_1(n_1+\frac{1}{2}) = -(u(n_1+\frac{1}{4})+b), \\ h_1(n_1)h_1(n_1+\frac{1}{2}) = -(u(n_1+\frac{1}{4})+c), \end{array}\right. \qquad \left\{\begin{array}{l} f_2(n_2)f_2(n_2+\frac{1}{2}) = v(n_2+\frac{1}{4})+a, \\ g_2(n_2)g_2(n_2+\frac{1}{2}) = v(n_2+\frac{1}{4})+b, \\ h_2(n_2)h_2(n_2+\frac{1}{2}) = -(v(n_2+\frac{1}{4})+c), \end{array}\right.$$

$$\left\{\begin{array}{l} f_3(n_3)f_3(n_3+\frac{1}{2}) = w(n_3+\frac{1}{4})+a, \\ g_3(n_3)g_3(n_3+\frac{1}{2}) = w(n_3+\frac{1}{4})+b, \\ h_3(n_3)h_3(n_3+\frac{1}{2}) = w(n_3+\frac{1}{4})+c. \end{array}\right. \tag{9.5}$$

The solution of equations (9.5) in terms of gamma functions found in [BSST1] and reproduced for general N in Section 7, is given (in the first octant) by

$$\left\{\begin{array}{l} f_1(n_1) = (n_1+\alpha)_{1/2}, \\ g_1(n_1) = (-n_1-\beta)_{1/2}, \\ h_1(n_1) = (-n_1-\gamma-\frac{1}{2})_{1/2}, \end{array}\right. \qquad \left\{\begin{array}{l} f_2(n_2) = (n_2+\alpha-\frac{1}{2})_{1/2}, \\ g_2(n_2) = (n_2+\beta)_{1/2}, \\ h_2(n_2) = (-n_2-\gamma)_{1/2}, \end{array}\right.$$

$$\left\{\begin{array}{l} f_3(n_3 = (n_3+\alpha-1)_{1/2}, \\ g_3(n_3) = (n_3+\beta-\frac{1}{2})_{1/2}, \\ h_3(n_3) = (n_3+\gamma)_{1/2}, \end{array}\right.$$

with $\alpha > \beta > \gamma$ being three integers, and with the identification

$$a = \alpha + \tfrac{1}{2}, \quad b = \beta + 1, \quad c = \gamma + \tfrac{3}{2}.$$

On the other hand, the construction in Theorem 5.6 can be specialized in the case $N = 3$ as follows: the nine functions $f_i(n_i)$, $g_i(n_i)$, $h_i(n_i)$ satisfy the functional equations

$$\left\{\begin{array}{l} f_1(n_1)f_1(n_1+\frac{1}{2}) + g_1(n_1)g_1(n_1+\frac{1}{2}) = a-b, \\ f_1(n_1)f_1(n_1+\frac{1}{2}) + h_1(n_1)h_1(n_1+\frac{1}{2}) = a-c, \end{array}\right.$$

$$\left\{\begin{array}{l} f_2(n_2)f_2(n_2+\frac{1}{2}) - g_2(n_2)g_2(n_2+\frac{1}{2}) = a-b, \\ f_2(n_2)f_2(n_2+\frac{1}{2}) + h_2(n_2)h_2(n_2+\frac{1}{2}) = a-c, \end{array}\right.$$

$$\left\{\begin{array}{l} f_3(n_3)f_3(n_3+\frac{1}{2}) - g_3(n_3)g_3(n_3+\frac{1}{2}) = a-b, \\ f_3(n_3)f_3(n_3+\frac{1}{2}) - h_3(n_3)h_3(n_3+\frac{1}{2}) = a-c. \end{array}\right.$$

A solution of system (9.2) in terms of Jacobi elliptic functions reads:

$$\begin{array}{lll} f_1(n_1) = \alpha_1 \operatorname{sn}(\delta_1 n_1, k_1), & g_1(n_1) = \beta_1 \operatorname{cn}(\delta_1 n_1, k_1) & h_1(n_1) = \gamma_1 \operatorname{dn}(\delta_1 n_1, k_1), \\[2ex] f_2(n_2) = \alpha_2 \operatorname{dn}(\delta_2 n_2, k_2), & g_2(n_2) = \beta_2 \operatorname{cn}(\delta_2 n_2, k_2), & h_2(n_2) = \gamma_2 \operatorname{sn}(\delta_2 n_2, k_2), \\[2ex] f_3(n_3) = \alpha_3 \dfrac{1}{\operatorname{sn}(\delta_3 n_3, k_3)}, & g_3(n_3) = \beta_3 \dfrac{\operatorname{dn}(\delta_3 n_3, k_3)}{\operatorname{sn}(\delta_3 n_3, k_3)}, & h_3(n_3) = \gamma_3 \dfrac{\operatorname{cn}(\delta_3 n_3, k_3)}{\operatorname{sn}(\delta_3 n_3, k_3)}, \end{array} \tag{9.6}$$

where the moduli k_1, k_2, k_3 are defined as solutions of the following transcendental equations:

$$k_1^2 = \frac{a-b}{a-c} \cdot \frac{\operatorname{dn}^2(\frac{\delta_1}{2}, k_1)}{\operatorname{cn}^2(\frac{\delta_1}{2}, k_1)}, \quad k_2^2 = \frac{b-c}{a-c} \cdot \frac{\operatorname{dn}^2(\frac{\delta_2}{2}, k_2)}{\operatorname{cn}^2(\frac{\delta_2}{2}, k_2)}, \quad k_3^2 = \frac{a-b}{a-c} \cdot \frac{\operatorname{dn}^2(\frac{\delta_3}{2}, k_3)}{\operatorname{cn}^2(\frac{\delta_3}{2}, k_3)},$$

and the amplitudes $\alpha_1, \ldots, \gamma_3$ are given by

$$\alpha_1 = \sqrt{(a-b)\frac{\mathrm{dn}(\frac{\delta_1}{2}, k_1)}{\mathrm{cn}(\frac{\delta_1}{2}, k_1)}}, \quad \beta_1 = \frac{\alpha_1}{\sqrt{\mathrm{dn}(\frac{\delta_1}{2}, k_1)}}, \quad \gamma_1 = \frac{\alpha_1}{k_1\sqrt{\mathrm{cn}(\frac{\delta_1}{2}, k_1)}},$$

$$\gamma_2 = \sqrt{(b-c)\frac{\mathrm{dn}(\frac{\delta_2}{2}, k_2)}{\mathrm{cn}(\frac{\delta_2}{2}, k_2)}}, \quad \alpha_2 = \frac{\gamma_2}{k_2\sqrt{\mathrm{cn}(\frac{\delta_2}{2}, k_2)}}, \quad \beta_2 = \frac{\gamma_2}{\sqrt{\mathrm{dn}(\frac{\delta_2}{2}, k_2)}},$$

$$\alpha_3 = \sqrt{(a-c)\frac{\mathrm{cn}(\frac{\delta_3}{2}, k_3)}{\mathrm{dn}(\frac{\delta_3}{2}, k_3)}}, \quad \beta_3 = \frac{\alpha_3}{\sqrt{\mathrm{dn}(\frac{\delta_3}{2}, k_3)}}, \quad \gamma_3 = \frac{\alpha_3}{\sqrt{\mathrm{cn}(\frac{\delta_3}{2}, k_3)}}.$$

In order for the discrete confocal quadrics to respect the symmetries of their classical counterparts, we set

$$\delta_1 = \frac{\mathsf{K}(k_1)}{m_1}, \quad \delta_2 = \frac{\mathsf{K}(k_2)}{m_2}, \quad \delta_3 = \frac{\mathsf{K}(k_3)}{m_3}, \qquad m_i \in \mathbb{N}.$$

The parameters n_i may then be restricted to $n_1 \in [0, 4m_1]$, $n_2 \in [0, 4m_2]$ and $n_3 \in (0, 2m_3)$.

As in the 2-dimensional case, for arbitrary m_i, there exist special vertices of valence $\neq 4$ (cf. Figures 9.2 and 9.3) which are discrete analogs of the umbilic points on smooth confocal ellipsoids and two-sheeted hyperboloids. In the parametrization (9.3), these umbilic points are seen to be

$$\boldsymbol{x}(\varepsilon_1\mathsf{K}(k_1), \varepsilon_2\mathsf{K}(k_2), s_3), \quad \boldsymbol{x}(s_1, \varepsilon_2^*\mathsf{K}(k_2), \mathsf{K}(k_3))$$
$$\varepsilon_1, \varepsilon_2 \in \{1, 3\}, \quad \varepsilon_2^* \in \{0, 2\}$$

respectively. Their discrete analogues are given by the vertices

$$\boldsymbol{x}(\varepsilon_1 m_1, \varepsilon_2 m_2, n_3), \quad \boldsymbol{x}(n_1, \varepsilon_2^* m_2, m_3)$$
$$\varepsilon_1, \varepsilon_2 \in \{1, 3\}, \quad \varepsilon_2^* \in \{0, 2\}$$

which have valence 2 (cf. Figure 9.2) as may be inferred from the parametrization (9.6).

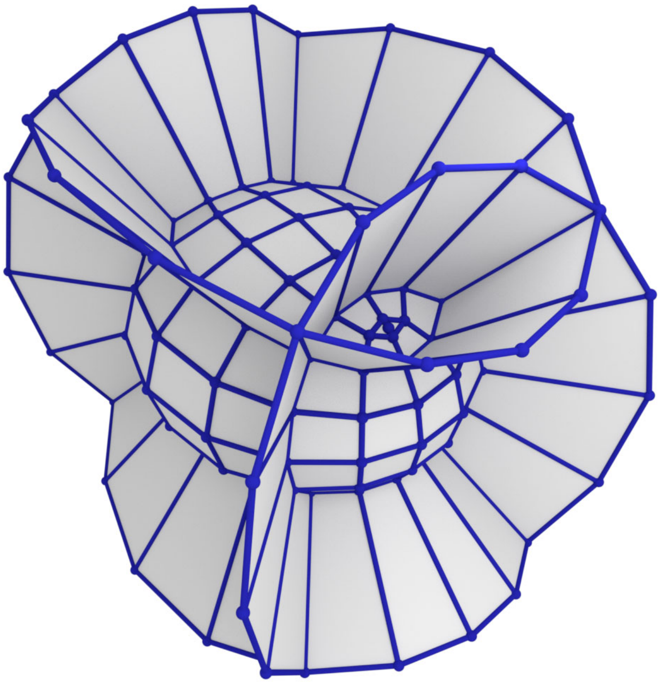

Figure 9.2. Three-dimensional discrete confocal coordinate system (9.4), (9.6) in terms of Jacobi elliptic functions on the sublattice $\mathbb{Z}^2$ with $a = 8$, $b = 4$, $c = 0$, $m = 4$. Three discrete quadrics are shown: a discrete two-sheeted hyperboloid for $n_1 = 2$, a discrete one-sheeted hyperboloid for $n_2 = 2$, and a discrete ellipsoid for $n_3 = 2$. A point of valence 2 on a discrete ellipsoid is a discrete analog of an umbilic point.

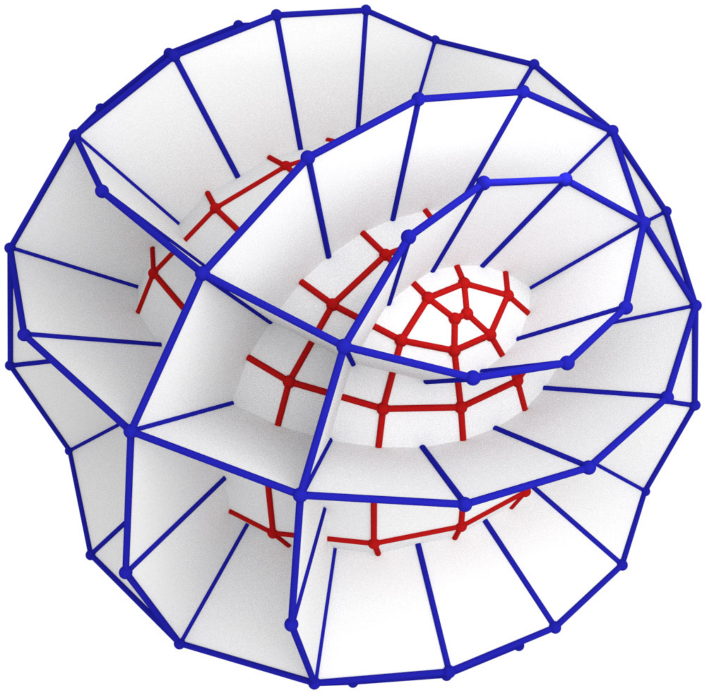

Figure 9.3. Discrete confocal coordinates with $a = 8$, $b = 4$, $c = 0$, $m = 4$. Discrete quadrics from the pair of dual orthogonal sublattices $\mathbb{Z}^3$ and $\left(\mathbb{Z} + \frac{1}{2}\right)^3$ are shown in blue and red respectively: two-sheeted hyperboloids $n_1 = 1, 2$, $n_2, n_3 \in \mathbb{Z}$, one-sheeted hyperboloids $n_2 = 1, 2$, $n_1, n_3 \in \mathbb{Z}$, ellipse $n_3 = 1.5$, $n_1, n_2 \in \mathbb{Z} + \frac{1}{2}$,

A Euler-Poisson-Darboux equation

A.1 Classical Euler-Poisson-Darboux equation

The discretization of confocal quadrics in [BSST1] was based on an integrable discretization of the Euler-Poisson-Darboux equation. We adapt the characterization of confocal coordinates in terms of the Euler-Poisson-Darboux equation to our present approach by arbitrary re-parametrization of the coordinate lines.

Consider the classical *Euler-Poisson-Darboux system*

$$\partial_{u_i}\partial_{u_j}\boldsymbol{x} = \frac{\gamma}{u_i - u_j}(\partial_{u_j}\boldsymbol{x} - \partial_{u_i}\boldsymbol{x}), \quad i, j \in \{1, \dots, N\}$$

with some constant $\gamma \in \mathbb{R}$. Under re-parametrization $u_i = u_i(s_i)$ this becomes

$$\partial_{s_i}\partial_{s_j}\boldsymbol{x} = \frac{\gamma}{u_i(s_i) - u_j(s_j)}\left(u_i'(s_i)\partial_{s_j}\boldsymbol{x} - u_j'(s_j)\partial_{s_i}\boldsymbol{x}\right). \tag{EPD$_\gamma$}$$

Confocal coordinates are given by certain factorizable solutions of this equation, and can be characterized as such.

Theorem A.1. *Let $\boldsymbol{x} = (x_1, \dots, x_N)$ be N independent factorizable solutions*

$$x_k(s_1, \dots, s_N) = \prod_{i=1}^{N} f_i^k(s_i)$$

of the Euler-Poisson-Darboux system (EPD$_\gamma$) *with $\gamma = \frac{1}{2}$ defined on a suitable domain*

$$\mathcal{U} = \{(s_1, \dots, s_N) \in \mathbb{R}^N \mid -a_1 < u_1(s_1) < -a_2 < u_2(s_2) < \cdots < -a_N < u_N(s_N)\}.$$

Then the net $\boldsymbol{x} : \mathcal{U} \to \mathbb{R}^N$ coincides with confocal coordinates (3.13)*, up to independent scaling along the coordinate axes $(x_1, \dots, x_N) \to (C_1x_1, \dots, C_Nx_N)$ with some $C_1, \dots, C_N > 0$.*

Proof. A factorizable function
$$x(s_1,\dots,s_N)=f_1(s_1)\cdots f_N(s_N)$$
is a solution of (EPD_γ), if and only if (compare [BSST1])
$$\frac{f_i'}{f_i}=\frac{u_i'}{2(u_i+a)},\quad i=1,\dots,N,$$
with some integration constant $a\in\mathbb{R}$. The general solution is, up to constant factors, given by
$$f_i(s_i)=\begin{cases}\sqrt{u_i(s_i)+a}, & \text{if}\quad u_i(s_i)>-a,\\ \sqrt{-(u_i(s_i)+a)}, & \text{if}\quad u_i(s_i)<-a.\end{cases}$$
Now N independent separable solutions $x_k(s_1,\dots,s_N)$, $1\leqslant k\leqslant N$ with constants of integration $a_1>\dots>a_N$ are, on the domain $\mathcal{U}$, given by
$$x_k(s_1,\dots,s_N)=D_k\prod_{i<k}\sqrt{-(u_i(s_i)+a_k)}\prod_{i\geqslant k}\sqrt{u_i(s_i)+a_k}$$
with some constants $D_k\neq 0$. The choice
$$D_k^{-1}=\prod_{i<k}\sqrt{a_i-a_k}\prod_{i>k}\sqrt{a_k-a_i}$$
is the unique scaling (up to a common factor) for which the parameter curves are pairwise orthogonal (see [BSST1]). ☐

A.2 Discrete Euler-Poisson-Darboux equation

It turns out that discrete confocal coordinate systems may also be characterized in terms of a discrete Euler-Poisson-Darbox equation.

Theorem A.2. *Discrete confocal coordinate systems given by* (5.9) *satisfy the discrete Euler-Poisson-Darboux system with* $\gamma=\frac{1}{2}$*:*
$$\Delta_i\Delta_j x_k=\frac{1}{u_i-u_j}\left(\Delta^{1/2}u_i\Delta_j x_k-\Delta^{1/2}u_j\Delta_i x_k\right),\qquad (\mathrm{dEPD}_{\gamma=\frac{1}{2}})$$
where $x_k=x_k(\boldsymbol{n})$ *and* $u_i=u_i(n_i+\frac{1}{4})$. *Here, the difference operator* Δ *acts according to* $\Delta_i f(\boldsymbol{n})=f(\boldsymbol{n}+\boldsymbol{e}_i)-f(\boldsymbol{n})$, *and*
$$\Delta^{1/2}u_i=u_i(n_i+\tfrac{3}{4})-u_i(n_i+\tfrac{1}{4}).$$

Conversely, let $\boldsymbol{x}=(x_1,\dots,x_N)$ *be* N *independent factorized solutions*
$$x_k(n_1,\dots,n_N)=\prod_{i=1}^N f_i^{(k)}(n_i)$$
of ($\mathrm{dEPD}_{\gamma=\frac{1}{2}}$) *with positive "discrete squares"*
$$f_i^{(k)}(n_i)f_i^{(k)}(n_i+\tfrac{1}{2})>0$$
defined on a suitable domain
$$\mathcal{U}=\Big\{(n_1,\dots,n_N)\in\left(\tfrac{1}{2}\mathbb{Z}\right)^N:\\ -a_1<u_1(n_1+\tfrac{1}{4})<-a_2<u_2(n_2+\tfrac{1}{4})<\dots<-a_N<u_N(n_N+\tfrac{1}{4})\Big\}.$$
Then the net $\boldsymbol{x}:\mathcal{U}\to\mathbb{R}^N$ *coincides with discrete confocal coordinates* (5.9), (5.10) *in the first hyperoctant, up to independent scaling along the coordinate axes* $(x_1,\dots,x_N)\to(C_1x_1,\dots,C_Nx_N)$ *with some constants* $C_1,\dots,C_N>0$.

Proof. First, we derive the discrete Euler-Poisson-Darboux equations satisfied by the discrete confocal coordinates given by (5.9). From equation (5.10) we obtain

$$\frac{f_i^{(k)}(n_i+1)}{f_i^{(k)}(n_i)} = \frac{u_i(n_i+\frac{3}{4})+a_k}{u_i(n_i+\frac{1}{4})+a_k},$$

which is equivalent to

$$\frac{\Delta f_i^{(k)}}{f_i^{(k)}} = \frac{\Delta^{1/2} u_i}{u_i+a_k}.$$

So, for $x_k(\boldsymbol{n}) = \prod_{i=1}^N f_i^{(k)}(n_i)$ we obtain:

$$\begin{aligned}
\Delta_i\Delta_j x_k &= \frac{\Delta^{1/2}u_i}{u_i+a_k}\frac{\Delta^{1/2}u_j}{u_j+a_k}x_k \\
&= \frac{1}{u_i-u_j}\left(\frac{\Delta^{1/2}u_i\Delta^{1/2}u_j}{u_j+a_k} - \frac{\Delta^{1/2}u_i\Delta^{1/2}u_j}{u_i+a_k}\right)x_k \\
&= \frac{1}{u_i-u_j}\left(\Delta^{1/2}u_i\Delta_j x_k - \Delta^{1/2}u_j\Delta_i x_k\right).
\end{aligned}$$

Conversely, a simple computation shows that a factorizable function

$$x(n_1,\ldots,n_N) = f_1(n_1)\cdots f_N(n_N)$$

is a solution of (dEPD$_{\gamma=\frac{1}{2}}$) if and only if

$$\Delta^{1/2}u_i\,\frac{f_i}{\Delta f_i} - u_i = \Delta^{1/2}u_j\,\frac{f_j}{\Delta f_j} - u_j = a,$$

with some constant of integration $a \in \mathbb{R}$. Equivalently,

$$\frac{\Delta f_i}{f_i} = \frac{\Delta^{1/2}u_i}{u_i+a} \quad\Leftrightarrow\quad \frac{f_i(n_i+1)}{f_i(n_i)} = \frac{u_i(n_i+\frac{3}{4})+a}{u_i(n_i+\frac{1}{4})+a}, \qquad i=1,\ldots,N.$$

Here the left-hand sides can be written as

$$\frac{f_i(n_i+1)}{f_i(n_i)} = \frac{F_i(n_i+\frac{3}{4})}{F_i(n_i+\frac{1}{4})},$$

where $F_i(n_i+\frac{1}{4}) = f_i(n_i)f_i(n_i+\frac{1}{2})$. Assuming that the discrete squares $F_i(n_i+\frac{1}{4})$ are positive, the general solution is, up to constant factors, given by

$$F_i(n_i+\tfrac{1}{4}) = \begin{cases} u_i(n_i+\frac{1}{4})+a, & \text{if } \ u_i(n_i+\frac{1}{4}) > -a, \\ -(u_i(n_i+\frac{1}{4})+a), & \text{if } \ u_i(n_i+\frac{1}{4}) < -a. \end{cases}$$

Now, take N independent factorizable solutions $x_k(n_1,\ldots,n_N)$, $1 \leqslant k \leqslant N$, with the constants of integration $a_1 > \cdots > a_N$. Define $\mathcal{U}$ as in (A.1) with these $a_1,\ldots,a_N$. Then, we find that

$$x_k(\boldsymbol{n})x_k(\boldsymbol{n}+\tfrac{1}{2}\boldsymbol{\sigma}) = D_k^2\prod_{i<k}-(u_i(n_i+\tfrac{1}{4}\sigma_i)+a_k)\prod_{i\geqslant k}(u_i(n_i+\tfrac{1}{4}\sigma_i)+a_k), \tag{A.2}$$

where $D_k \neq 0$ are constants. With the choice

$$D_k^{-2} = \prod_{i<k}(a_i-a_k)\prod_{i>k}(a_k-a_i),$$

expressions (A.2) coincide with (5.2). ☐

In the particular case $u_i(n_i+\frac{1}{4}) = n_i+\varepsilon_i$ we have $\Delta^{1/2}u_i = \frac{1}{2}$, and we recover the version of the discrete Euler-Poisson-Darboux equation from [BSST1]. An important integrability property of that equation holds true also for the more general version (dEPD$_{\gamma=\frac{1}{2}}$).

Proposition A.3. *Equation* (dEPD$_{\gamma=\frac{1}{2}}$) *is 3D-consistent.*

B More examples for the case $N = 2$

This appendix is not part of the original publication. It adds two more examples to Section 8.

B.1 Confocal coordinates, diagonally related to vertical lines and a hyperbolic pencil of circles

Continuous case

Consider a coordinate system (8.3) with

$$\begin{aligned} f_1(s_1) &= \sqrt{a-b}\; e^{s_1}, \quad g_1(s_1) = \sqrt{a-b}\; \sqrt{1-e^{2s_1}}, \\ f_2(s_2) &= \sqrt{a-b}\; e^{s_2}, \quad g_2(s_2) = \sqrt{a-b}\; \sqrt{e^{2s_2}-1}, \end{aligned} \tag{B.1}$$

where $s_1 < 0$ and $s_2 > 0$. The image is the first quadrant where the y-axis is approached in the limit $s_1 \to -\infty$. This parametrization is diagonally related to a hyperbolic pencil of circles which has the two foci of the confocal conics as limiting points. The following statement from [Ak] shows that the confocal ellipses, confocal hyperbolas, the pencil of circles, and the family of vertical lines constitute a *4-web* (see also [Ag]).

Proposition B.1. *The points (x, y) with $s_1 + s_2 = \text{const}$ lie on vertical lines. The points (x, y) with $s_2 - s_1 = \eta = \text{const}$ lie on circles with centers $(c(\eta), 0) = (\sqrt{a-b}\; \cosh(\eta), 0)$ and radii $r(\eta) = \sqrt{a-b}\; \sinh(\eta)$ (cf. Figure B.1).*

Proof. The first statement is equivalent to

$$f_1' f_2 - f_1 f_2' = 0.$$

For the second statement one computes that points (x, y) with $s_1 - s_2 = \eta = \text{const}$ satisfy

$$x^2 + y^2 - 2c(\eta)y + c(\eta)^2 - r(\eta)^2 = 0.$$

∎

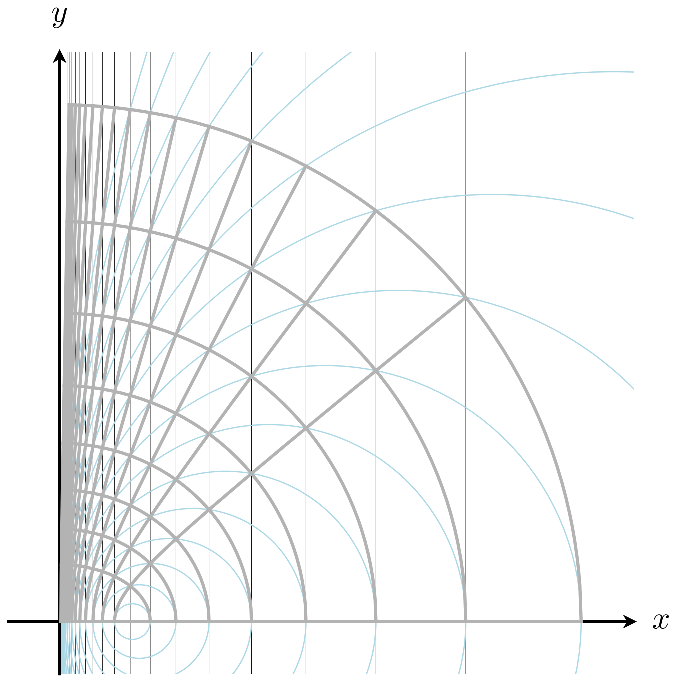

Figure B.1. Two-dimensional continuous confocal coordinate system (8.3), (B.1) with $a = 2$, $b = 1$. Points with $s_1 + s_2 =$ const lie on vertical lines, while points with $s_2 - s_1 =$ const lie on circles of a hyperbolic pencil which has as limiting points the two foci of the confocal conics.

Discrete case

A solution of the functional equations (8.14) and (8.15) which approximates (B.1) in the continuum limit $\delta \to 0$, is given by

$$\begin{aligned} f_1(n_1) &= \alpha_1 \, e^{\delta(n_1+c_1)}, \quad g_1(n_1) = \beta_1 \, \frac{\Gamma_{e^{-2\delta}}(-n_1 - c_1 + \frac{3}{4})}{\Gamma_{e^{-2\delta}}(-n_1 - c_1 + \frac{1}{4})}, \\ f_2(n_2) &= \alpha_2 \, e^{\delta(n_2+c_2)}, \quad g_2(n_2) = \beta_2 \, \frac{\Gamma_{e^{2\delta}}(n_2 + c_2 + \frac{3}{4})}{\Gamma_{e^{2\delta}}(n_2 + c_2 + \frac{1}{4})}, \end{aligned} \tag{B.2}$$

where

$$\begin{aligned} &\alpha_1 = \alpha_2 = \sqrt{a-b}, \\ &\beta_1 = \sqrt{a-b}\,\sqrt{1-e^{-2\delta}}, \quad \beta_2 = \sqrt{a-b}\,\sqrt{e^{2\delta}-1}, \end{aligned}$$

and Γ_q denotes the q-gamma function, which satisfies

$$\Gamma_q(z+1) = \frac{1-q^z}{1-q}\Gamma_q(z).$$

Boundary conditions $y|_{n_1=0} = 0$, $y|_{n_2=0} = 0$ may be achieved by setting $c_1 = \frac{1}{4}$, $c_2 = -\frac{1}{4}$.

Proposition B.2. *The points* (x, y) *with* $n_1 + n_2 =$ const *lie on vertical lines. Pairs of points*

$$(x, y) = \big(x(n_1 + \tfrac{1}{2}, n_2), y(n_1 + \tfrac{1}{2}, n_2)\big)$$

and

$$(\tilde{x}, \tilde{y}) = \big(x(n_1, n_2 + \tfrac{1}{2}), y(n_1, n_2 + \tfrac{1}{2})\big),$$

which are adjacent to the diagonal $n_2 - n_1 = \eta =$ const, *are related by the polarity*

$$x\tilde{x} + y\tilde{y} - c(\eta)\,(x + \tilde{x}) + c(\eta)^2 - r(\eta)^2 = 0$$

with respect to the circle with the center $(c(\eta), 0)$ *and the radius* $r(\eta)$*, where*

$$c(\eta) = \sqrt{a-b}\ \cosh(\delta(\eta + c_1 - c_2)), \quad r(\eta) = \sqrt{a-b}\ \sinh(\delta(\eta + c_1 - c_2))$$

(cf. Figure B.2).

The two classical confocal conics corresponding to the parameter values $u(n_1 + \frac{1}{4})$ *and* $v(n_2 + \frac{1}{4})$*, and the circle with center* $(c(\eta), 0)$ *and radius* $r(\eta)$*,* $\eta = n_2 - n_1$*, intersect at a point.*

This can be checked by a direct computation. There exists an analogous parametrization diagonally related to horizontal lines and an elliptic pencil of circles, both in the continuous case (see [Ak]) and in the discrete case.

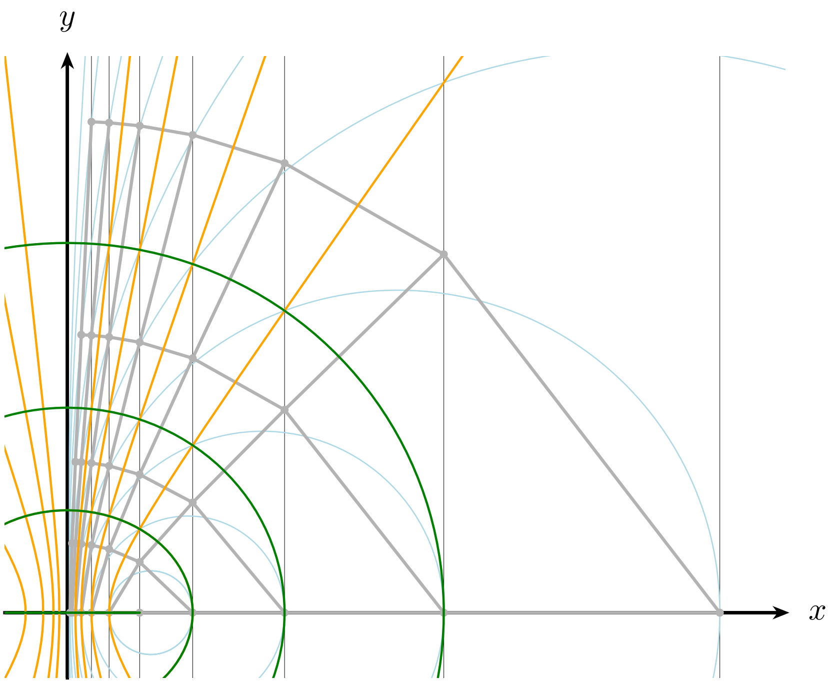

Figure B.2. Two-dimensional discrete confocal coordinate system (8.11), (B.2) with $a = 2$, $b = 1$, $c_1 = \frac{1}{4}$, $c_2 = -\frac{1}{4}$. Points with $n_1 + n_2 = \text{const}$ lie on vertical lines. In addition to the polarity relation given by the corresponding classical confocal ellipses (green) and hyperbolas (orange) two points adjacent to a diagonal $n_2 - n_1 = \text{const}$ also satisfy a polarity relation with respect to circles of a hyperbolic pencil.

B.2 Confocal coordinates, diagonally related to two families of concentric circles

Continuous case

Consider a coordinate system (8.3) with

$$\begin{aligned} f_1(s_1) &= \sqrt{a-b}\ s_1, \quad g_1(s_1) = \sqrt{a-b}\ \sqrt{1-s_1^2}, \\ f_2(s_2) &= \sqrt{a-b}\ s_2, \quad g_2(s_2) = \sqrt{a-b}\ \sqrt{s_2^2-1}, \end{aligned} \tag{B.3}$$

where $-1 < s_1 < 1$ and $s_2 > 1$. This parametrization is diagonally related to concentric circles with centers at the two foci of the confocal conics.

Proposition B.3. *The points* (x, y) *with* $s_1 + s_2 = \xi = \text{const}$ *lie on concentric circles with the center* $\left(-\sqrt{a-b}, 0\right)$ *and with the radii* $r(\xi) = \sqrt{a-b}\ \xi$*. The points* (x, y) *with* $s_2 - s_1 = \eta = \text{const}$ *lie on concentric circles with the center* $\left(\sqrt{a-b}, 0\right)$ *and with the radii* $r(\eta) = \sqrt{a-b}\ \eta$ *(cf. Figure B.3).*

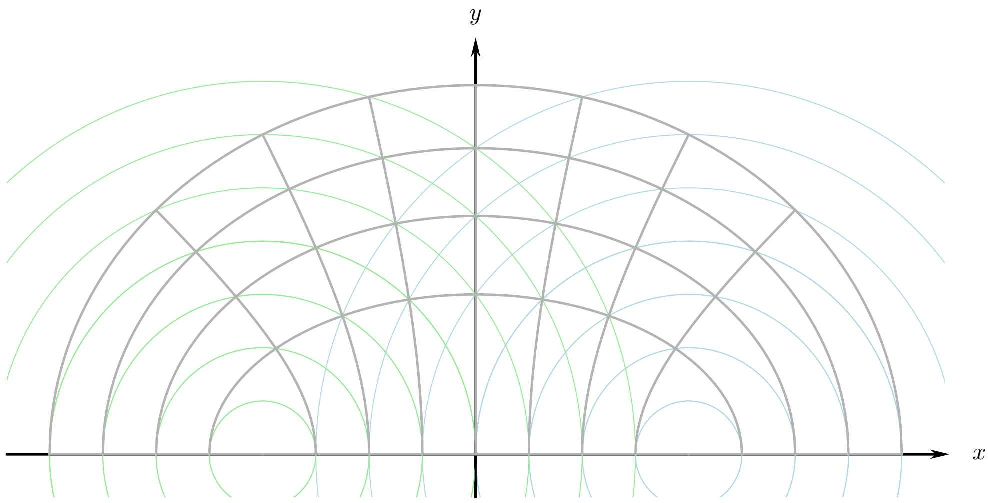

Figure B.3. Two-dimensional continuous confocal coordinate system (8.3), (B.3) with $a = 2$, $b = 1$. Points with $s_1 + s_2 = \text{const}$ and points with $s_2 - s_1 = \text{const}$ lie on concetric circles with centers at the two foci of the confocal family.

Discrete case

A solution of the functional equations (8.14) and (8.15) which approximates (B.3) in the continuum limit $\delta \to 0$, is given by

$$\begin{aligned} f_1(n_1) &= \alpha\delta(n_1 + c_1), \quad g_1(n_1) = \alpha(n_1 + c_1^+)_{1/2}(-(n_1 + c_1^-) + \tfrac{1}{2})_{1/2}, \\ f_2(n_2) &= \alpha\delta(n_1 + c_1), \quad g_2(n_2) = \alpha(n_2 + c_2^+)_{1/2}(n_2 + c_2^-)_{1/2}, \end{aligned} \tag{B.4}$$

where $\delta > 0$, $\alpha = \sqrt{a-b}$, $c_1, c_2 \in \mathbb{R}$, and

$$c_1^\pm = c_1 + \frac{1}{4} \pm \frac{\sqrt{16+\delta^2}}{4\delta}, \quad c_2^\pm = c_2 + \frac{1}{4} \pm \frac{\sqrt{16+\delta^2}}{4\delta}.$$

If we set $c_1 = c_2 = 0$, and

$$\delta = \frac{4}{\sqrt{(2l+1)^2 - 1}} \quad \Leftrightarrow \quad \frac{\sqrt{16+\delta^2}}{4\delta} = l + \frac{1}{2}$$

with some $l \in \mathbb{N}$, we may let $n_1 \in \left[-\frac{l+1}{2}, \frac{l+1}{2}\right]$, $n_2 \geqslant \frac{l}{2}$ and achieve boundary conditions

$$y\big|_{n_1 = -\frac{l+1}{2}} = y\big|_{n_1 = \frac{l+1}{2}} = 0, \quad y\big|_{n_2 = \frac{l}{2}} = 0.$$

Proposition B.4. *Pairs of points*

$$(x, y) = \big(x(n_1, n_2 - \tfrac{1}{2}), y(n_1, n_2 - \tfrac{1}{2})\big)$$

and

$$(\tilde{x}, \tilde{y}) = \big(x(n_1 + \tfrac{1}{2}, n_2), y(n_1 + \tfrac{1}{2}, n_2)\big),$$

which are adjacent to the diagonal $n_1 + n_2 = \xi = \text{const}$, *are related by polarity with respect to the circle with the center* $(c, 0) = (\sqrt{a-b}, 0)$ *and the radius* $r(\xi) = \sqrt{a-b}\,\delta(\xi + c_1 + c_2)$:

$$x\tilde{x} + y\tilde{y} - c\,(x + \tilde{x}) + c^2 - r(\xi)^2 = 0.$$

Similarly, pairs of points

$$(x, y) = \big(x(n_1 + \tfrac{1}{2}, n_2), y(n_1 + \tfrac{1}{2}, n_2)\big)$$

and

$$(\tilde{x},\tilde{y}) = \big(x(n_1,n_2+\tfrac{1}{2}), y(n_1,n_2+\tfrac{1}{2})\big),$$

which are adjacent to the diagonal $n_2 - n_1 = \eta = \text{const}$*, are related by polarity with respect to the circle with the center* $(-c,0)$ *and with the radius* $\hat{r}(\eta) = \sqrt{a-b}\,\delta(\eta + c_2 - c_1)$*:*

$$x\tilde{x} + y\tilde{y} + c\,(x+\tilde{x}) + c^2 - \hat{r}(\eta)^2 = 0$$

(cf. Figure B.4).

We remark that in this case the corresponding classical ellipses, hyperbolas, and circles participating in the polarity relations are not incident. The proof of all these statements is by direct computation.

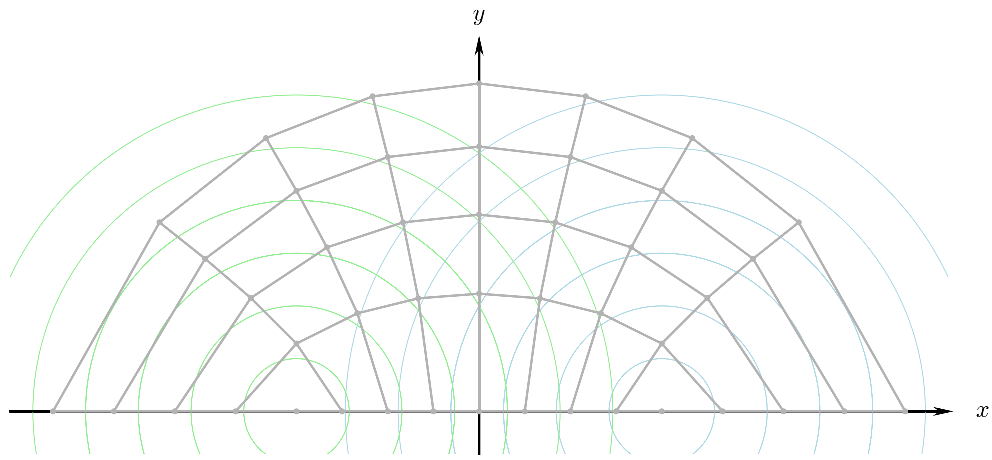

Figure B.4. Two-dimensional discrete confocal coordinate system (8.11), (B.4) with $a = 2$, $b = 1$, $c_1 = c_2 = 0$, $2l+1 = 7$. Points adjacent to a diagonal $n_2 - n_1 = \text{const}$ are related by polarity with respect to concentric circles with centers in the right focal point. Similarly, points adjacent to a diagonal $n_1 + n_2 = \text{const}$ are related by polarity with respect to concentric circles with centers in the left focal point.

References

[AVK] [AB] [Ar] [Bo] [BSST1] [BSST2] [BS] [CDS] [Da2] [DR] [EMOT] [FT] [IT] [Ja] [KS1] [KS2] [Kr] [LPWYW] [MT] [Mo] [PW] [Ve] [WW] [Za]

Chapter 3

Checkerboard incircular nets. Laguerre geometry and parametrisation

Alexander I. Bobenko[1], Wolfgang K. Schief[2], Jan Techter[1]

[1]Institut für Mathematik, TU Berlin,
Str. des 17. Juni 136, 10623 Berlin, Germany

[2]School of Mathematics and Statistics,
The University of New South Wales, Sydney, NSW 2052, Australia

Abstract. We present a procedure which allows one to integrate explicitly the class of checkerboard IC-nets which has recently been introduced as a generalisation of incircular (IC) nets. The latter class of privileged congruences of lines in the plane is known to admit a great variety of geometric properties which are also present in the case of checkerboard IC-nets. The parametrisation obtained in this manner is reminiscent of that associated with elliptic billiards. Connections with discrete confocal coordinate systems and the fundamental QRT maps of integrable systems theory are made. The formalism developed in this paper is based on the existence of underlying pencils of conics and quadrics which is exploited in a Laguerre geometric setting.

Acknowledgements. We are indebted to Yuri Suris for insightful comments and discussions. This research was supported by the DFG Collaborative Research Center TRR 109 "Discretization in Geometry and Dynamics". W.K.S. was also supported by the Australian Research Council (DP1401000851).

Geometriae Dedicata, Volume 204, Issue 1, February 2020, Pages 97-129,

This is a post-peer-review, pre-copyedit version of an article published in *Geometriae Dedicata*.
The final authenticated version is available online at: `https://doi.org/10.1007/s10711-019-00449-x`

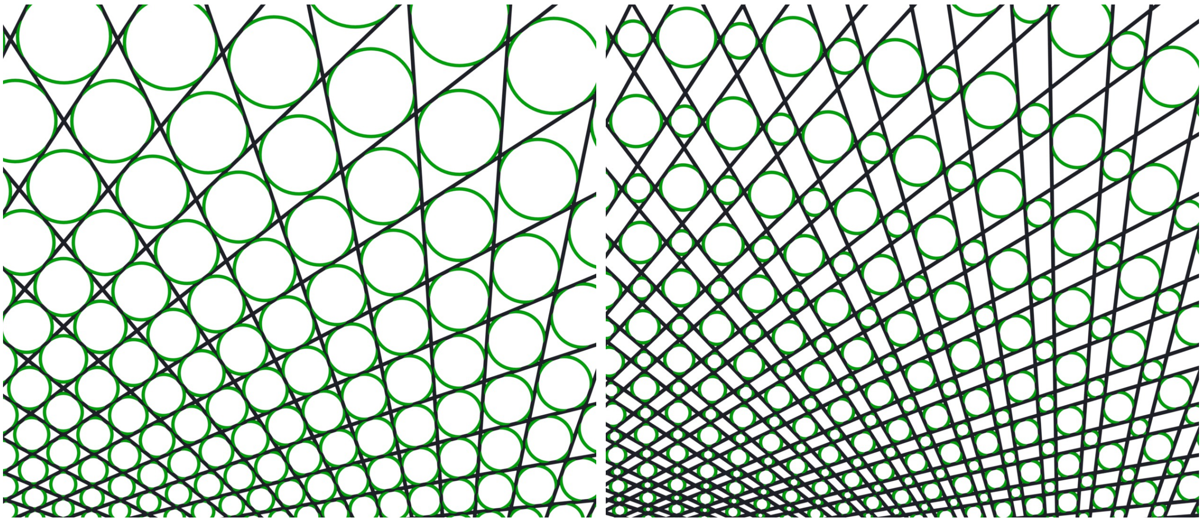

Figure 1.1. *Left:* An example of an IC-net. *Right:* An example of a checkerboard IC-net.

1 Introduction

The construction and geometry of *incircular nets* (IC-nets) and their generalisation to *checkerboard IC-nets* have recently been discussed in great detail in [AB]. IC-nets were introduced by Böhm [Bö] and are defined as congruences of straight lines in the plane with the combinatorics of the square grid such that each elementary quadrilateral admits an incircle as depicted in Figure 1.1 (left). IC-nets have a wealth of geometric properties, including the distinctive feature that any IC-net comes with a conic to which its lines are tangent. Another important aspect is that IC-nets discretise confocal quadrics. In fact, it has been observed in [BSST2] that IC-nets constitute particular instances of discrete confocal coordinate systems in the plane, which provides a first indication that IC-nets should be examined in the context of *integrable* discrete differential geometry [BS]. In this connection, it is noted that an integrable systems approach to the discretisation of confocal quadrics has been taken in [BSST1]. IC-nets are closely related to Poncelet(-Darboux) grids originally introduced by Darboux [Da1] and further studied in [LT] and [Sch].

Due to the combinatorial structure of IC-nets, their lines and circles may not be consistently oriented in such manner that these are in oriented contact. However, IC-nets are intimately related to checkerboard IC-nets which do exhibit this feature. Once again, the lines of checkerboard IC-nets have the combinatorics of the square grid but it is only required that every second quadrilateral admits an incircle, namely the "black" (or "white") quadrilaterals if the quadrilaterals of the net are combinatorially coloured like those of a checkerboard. An example of a checkerboard IC-net is displayed in Figure 1.1 (right).

Confocal checkerboard IC-nets constitute an important subclass of checkerboard IC nets and are characterised by their lines being tangent to a conic as in the case of IC-nets. This terminology is due to the remarkable fact that the points of intersection of the lines of a confocal checkerboard IC-net lie on conics which are confocal to the underlying conic.

In general, checkerboard IC-nets may be constructed in the following manner. One starts with a circle $\omega_{1,1}$ and four tangents ℓ_1, ℓ_2, m_1 and m_2. Subsequently, as indicated in Figure 1.2, one chooses four circles $\omega_{0,0}$, $\omega_{0,2}$, $\omega_{2,2}$ and $\omega_{2,0}$ which touch the pairs of lines forming the "corners" of the configuration of given lines. The four lines ℓ_0, ℓ_3, m_0, and m_3 being tangent to the respective pairs of circles are then fixed so that, in turn, the circles $\omega_{1,3}$ and $\omega_{3,1}$ are uniquely determined. An additional degree of freedom is obtained by choosing the circle $\omega_{3,3}$ Now, the entire checkerboard net is predetermined. Indeed, we first construct the lines ℓ_4 and m_4, then the circles $\omega_{4,0}$, $\omega_{4,2}$, $\omega_{0,4}$, $\omega_{2,4}$ and, finally, the lines ℓ_5 and m_5. The existence of the circle $\omega_{4,4}$ is non-trivial and follows from an incidence theorem [AB]. In Section 3, we present a simpler proof of this theorem, using the formalism developed in this paper. Iterative application of this theorem now generates a checkerboard IC-net of arbitrary size. In summary, a checkerboard IC-net

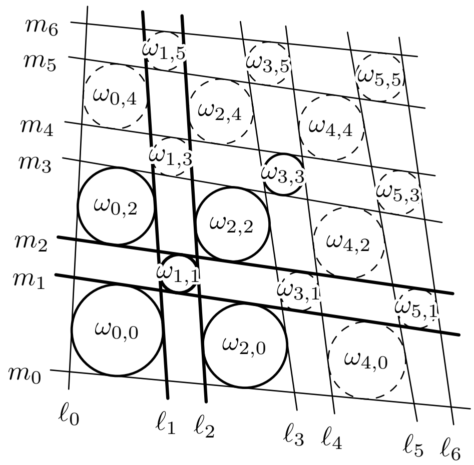

Figure 1.2. An elementary construction of a checkerboard IC-net

is uniquely determined by five neighbouring circles $\omega_{0,0}$, $\omega_{2,0}$, $\omega_{0,2}$, $\omega_{2,2}$, $\omega_{1,1}$ and the circle $\omega_{3,3}$. Thus, up to Euclidean motions and homotheties, checkerboard IC-nets form a real eight-dimensional family of nets.

The main objective of this paper is the explicit integration of (generic) checkerboard IC-nets in terms of Jacobi elliptic functions [NIST] similar to that of elliptic billiards [DR]. As a result, we establish explicit connections with, for instance, the discrete confocal coordinate systems mentioned above and the celebrated (symmetric) QRT mappings [QRT] which play a fundamental role in the theory of discrete integrable systems (see, e.g., [IR] and references therein). We also prove constructively the existence and provide examples of confocal checkerboard IC-nets which are closed (embedded) in the "azimuthal" direction. In order to achieve these results, we adopt a Laguerre geometric point of view which is natural due to the above-mentioned orientability of the lines and circles of checkerboard IC-nets. The necessary theoretical background of Laguerre geometry [BT, BS] is provided in the Appendix. Thus, we first determine the class of checkerboard IC-nets which may be mapped to confocal checkerboard IC-nets by means of real Laguerre transformations. Here, it is noted that, in the complex setting, all checkerboard IC-nets are Laguerre-equivalent to confocal checkerboard IC-nets. The classification of checkerboard IC-nets in the real setting is based on the standard classification of pencils of conics [Le] which emerges due to the important observation that any checkerboard IC-net admits an underlying pencil of quadrics. It should be noted that Laguerre geometry is indispensable in the investigation of IC-nets. Recently, this classical (but lesser-known) geometry has been applied to solve problems not only in geometry [SPG] but also in free-form architecture [PGB].

The second step in the procedure is to parametrise confocal checkerboard IC-nets. This is done via the base curve which is shared by the pencil of quadrics associated with any given checkerboard IC-net. These base curves are known to be just another avatar of so-called hypercycles [Bl] which constitute particular curves in the plane of degree 8. In fact, it is demonstrated that the lines of a checkerboard IC-net are tangent to a hypercycle. In the case of a confocal checkerboard IC-net, the hypercycle degenerates to the union of two identical conics with different orientations. The above-mentioned (hypercycle) base curves are of degree 4 and may be parametrised in terms of Jacobi elliptic functions. This will then lead to an explicit parametrisation of confocal checkerboard IC-nets and their Laguerre transforms. Furthermore, this parametrisation also applies to the generalised checkerboard IC-nets introduced at the end of the paper. Their geometric construction is very natural within the Laguerre-geometric framework established here and gives rise to a connection with "non-autonomous" QRT maps (see, e.g., [RJ] and references therein).

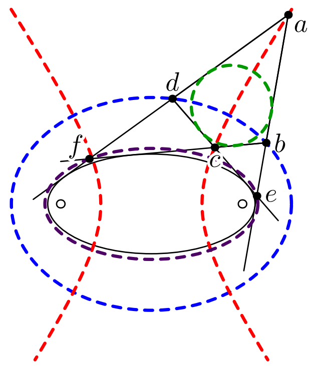

Figure 2.1. Graves–Chasles theorem

2 Checkerboard IC-nets. Definition and elementary properties

Checkerboard IC-nets have the combinatorics of a checkerboard, where all "black" quadrilaterals have inscribed circles (see Fig. 1.2). These were introduced in [AB].

Definition 2.1. *A checkerboard IC-net is comprised of oriented lines ℓ_i, m_j in the plane with $i, j \in \mathbb{Z}$ such that for any k and n the lines ℓ_{2k}, ℓ_{2k+1}, m_{2n}, m_{2n+1} as well as the lines ℓ_{2k-1}, ℓ_{2k}, m_{2n-1}, m_{2n} have a circle in oriented contact. The points of intersection $\ell_i \cap m_j$ are vertices of the corresponding quadrilateral lattice $\mathbb{Z}^2 \to \mathbb{R}^2$.*

Remark 2.1. We interpret the lines ℓ_i as combinatorially vertical and m_j as combinatorially horizontal. Checkerboard IC-nets become IC-nets when every second combinatorially horizontal strip and every second vertical strip degenerates in the sense that the two lines of such a strip coincide up to their orientation. Then, all remaining quadrilaterals admit inscribed circles, and all lines are non-oriented. An important property of IC-nets is that all their lines are tangent to a conic [AB]. The proof of this fact is based on the Graves-Chasles theorem [Da3, §174] (see also [IT]).

Theorem 2.2 (Graves–Chasles theorem)**.** *Suppose that all sides of a complete quadrilateral touch a conic α. Denote pairs of its opposite vertices by $\{\boldsymbol{a}, \boldsymbol{c}\}$, $\{\boldsymbol{b}, \boldsymbol{d}\}$, and $\{\boldsymbol{e}, \boldsymbol{f}\}$ (see Figure 2.1). Then, the following four properties are equivalent:*

(i) $(\boldsymbol{abcd})$ *circumscribes a circle,*

(ii) Points $\boldsymbol{a}$ *and* $\boldsymbol{c}$ *lie on a conic confocal with* α*,*

(iii) Points $\boldsymbol{b}$ *and* $\boldsymbol{d}$ *lie on a conic confocal with* α*,*

(iv) Points $\boldsymbol{e}$ *and* $\boldsymbol{f}$ *lie on a conic confocal with* α*.*

IC-nets are intimately related to a subclass of checkerboard IC-nets, namely confocal checkerboard IC-nets.

Definition 2.3. *[AB]. A checkerboard IC-net is called* confocal *if all lines of it are tangent to a conic.*

In fact, this class of checkerboard IC-nets constitutes a natural generalisation of IC-nets. However, in contrast to IC-nets, here, all circles and lines can be oriented so that the corresponding circles and lines are in oriented contact. Moreover, confocal checkerboard IC-nets can be regarded as subdivisions of IC-nets. This follows from the following lemma.

Lemma 2.4. *Let the six lines $\ell_0, \ell_1, \ell_2, m_0, m_1, m_2$ in Figure 2.2 (left) touch a conic. Then, any two of the incidences*

(i) ℓ_0, ℓ_1, m_0, m_1 *are tangent to a circle,*

(ii) ℓ_1, ℓ_2, m_1, m_2 *are tangent to a circle,*

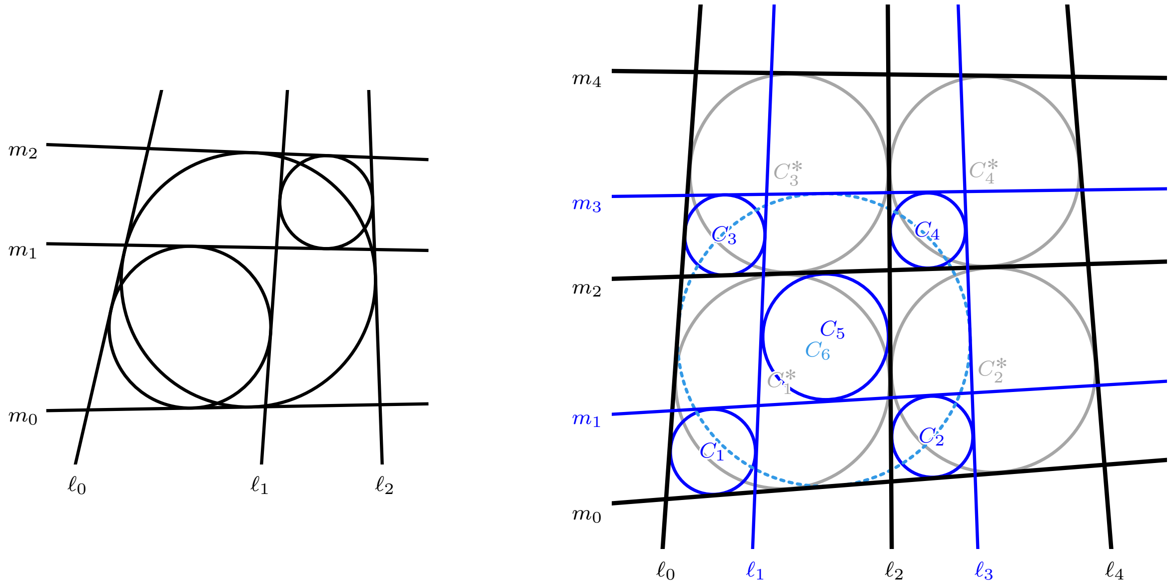

Figure 2.2. Confocal checkerboard IC-nets as subdivisions of IC-nets. *Left:* Illustration of the incidence Lemma 2.4. The initial configuration of six lines and two circles is such that the centres of the two circles and the point of intersection of the two common tangent lines are collinear. This is equivalent to demanding that the two initial circles and the two common tangent lines may be oriented in such manner that they are in oriented contact. *Right:* On the proof of Theorem 2.5.

(iii) ℓ_0, ℓ_2, m_0, m_2 *are tangent to a circle,*

imply the third one.

Proof. Let the lines $\ell_0, \ell_1, \ell_2, m_0, m_1, m_2$ be tangent to a conic α. Consider the three points of intersection $\ell_0 \cap m_0$, $\ell_1 \cap m_1$, $\ell_2 \cap m_2$. If, for instance, the two circles in (i) and (ii) exist then the Graves–Chasles theorem implies that the pairs of points $(\ell_0 \cap m_0, \ell_1 \cap m_1)$ and $(\ell_1 \cap m_1, \ell_2 \cap m_2)$ lie on conics confocal to α and, hence, on a common conic confocal to α. Application of the Graves–Chasles theorem to the third pair of points of intersection $(\ell_0 \cap m_0, \ell_2 \cap m_2)$ now implies that the circle in (iii) exists. $\square$

It is now evident that replacing pairs of diagonally neighbouring circles of a checkerboard IC-net by "large" circles inscribed in combinatorial 2×2 quadrilaterals as in Lemma 2.4 leads to four associated IC-nets. The converse is also true.

Theorem 2.5. *For every IC-net there exist one-parameter families of subdivisions into confocal checkerboard IC-nets with the same tangent conic* α.

Proof. In order to describe a subdivision of an IC-net into a checkerboard IC-net, one should consider a larger part of the net as shown in Figure 2.2 (right). Thus, let ℓ_{2n}, m_{2n} be the lines of an IC-net with tangent conic α as labelled in Figure 2.2 (right). Let us orient all lines ℓ_{2n} "down" and the lines m_{2n} "right". This choice of the orientation can be made precise, for example, as follows. Orient the circle C_1^* and choose the same orientation for the tangents ℓ_0, m_0, and the opposite orientation for ℓ_2, m_2. Orient C_2^* to have the same orientation as ℓ_2, m_0 and the opposite orientation to m_2. Let ℓ_4 have the opposite orientation to C_2^*. Proceed in this manner to specify the orientation of all circles and lines of the IC-net.

For a subdivision, choose an oriented line $_1$ which touches (the non-oriented conic) α and denote by C_1 the circle which is in oriented contact with ℓ_0, m_0 and ℓ_1. Let m_1 be the remaining line which is in oriented contact with C_1 and touches α. The circle C_2 is the unique circle which is in oriented contact with ℓ_2, m_0 and m_1, and C_3 is in oriented contact with ℓ_0, m_2 and ℓ_1. Define the lines ℓ_3 and m_3 by the requirement that they touch α and are in oriented contact with C_2 and C_3 respectively. By applying the Graves–Chasles theorem and the above lemma, one can now show that the lines ℓ_2, ℓ_3, m_2, m_3 have a common tangent circle C_4. Indeed, according to Lemma 2.4, the existence of the circles C_1 and the (original) circle C_1^* which touches the lines ℓ_0, ℓ_2, m_0, m_2 gives rise to a circle C_5 which is circumscribed by the lines ℓ_1, ℓ_2, m_1, m_2. The existence of the circles C_2, C_3, C_5 implies, in turn, that the points of intersection $\ell_0 \cap m_3, \ell_1 \cap m_2, \ell_2 \cap m_1, \ell_3 \cap m_0$ lie on a conic confocal to α. Accordingly, the lines ℓ_0, m_0, ℓ_3, m_3 circumscribe a circle C_6. A second application of Lemma 2.4 to the circles C_1^*, C_6 leads to the existence of the circle C_4.

Iterative application of the above procedure generates a checkerboard IC-net subdivision by adding oriented lines with odd indices ℓ_{2n+1}, m_{2n+1} and associated circles which are in oriented contact. The only free parameter of this subdivision is encoded in the line l_1. More precisely, due to the arbitrary choice of orientation of l_1, one obtains two one-parameter families of subdivisions. Another pair of one-parameter families of subdivisions is obtained by orienting all lines ℓ_{2n} "down" and the lines m_{2n} "left", prescribing the oriented line l_1, constructing the circle which is in oriented contact with ℓ_2, m_0 and l_1 and proceeding in a manner analogous to that described in the preceding. □

3 Laguerre geometric description of checkerboard IC-nets

It is natural to study checkerboard IC-nets in terms of Laguerre geometry. Such a description will allow us to prove fundamental properties of these nets and will finally lead to an explicit description of them. Here, we present a brief description of checkerboard IC-nets using the Blaschke cylinder model, consigning more details of Laguerre geometry to the Appendix.

Laguerre geometry in the plane deals with oriented circles and oriented straight lines. Lines

$$\{\boldsymbol{x} \in \mathbb{R}^2 : (\boldsymbol{v}, \boldsymbol{x})_{\mathbb{R}^2} = d\},$$

with unit normals $\boldsymbol{v} \in \mathbb{S}^1$ and $d \in \mathbb{R}$, can be put into correspondence with 3-tuples $(\boldsymbol{v}, d)$. Opposite 3-tuples $(\boldsymbol{v}, d)$ and $(-\boldsymbol{v}, -d)$ correspond to two different orientations of the same line. Thus, oriented lines are points of the *Blaschke cylinder*

$$\mathcal{Z} = \{\ell = (\boldsymbol{v}, d) \in \mathbb{R}^3 : |\boldsymbol{v}| = 1\} = \mathbb{S}^1 \times \mathbb{R} \subset \mathbb{R}^3.$$

Oriented circles

$$\{\boldsymbol{x} \in \mathbb{R}^2 : |\boldsymbol{x} - \boldsymbol{c}|^2 = r^2\}$$

with centres $\boldsymbol{c} \in \mathbb{R}^2$ and signed radii $r \in \mathbb{R}$ are in one-to-one correspondence with planes in $\mathbb{R}^3$ non-parallel to the axis of the Blaschke cylinder $\mathcal{Z}$:

$$S = \{(\boldsymbol{v}, d) \in \mathbb{R}^3 : (\boldsymbol{c}, \boldsymbol{v})_{\mathbb{R}^2} - d - r = 0\}.$$

Pairs of signed radii r and $-r$ correspond to two different orientations of the same circle. The intersection of such a plane S with $\mathcal{Z}$ consists of points of $\mathcal{Z}$ which represent lines in oriented contact with the corresponding circle, i.e., oriented lines which are tangent to the circle and exhibit corresponding orientation. Accordingly, the set of planes in $\mathbb{R}^3$ passing through a given point $\ell = (\boldsymbol{v}, d) \in \mathcal{Z}$ may be identified with the set of oriented circles in oriented contact with the oriented line ℓ. Finally, the set of planes in $\mathbb{R}^3$ passing through two points $\ell_1, \ell_2 \in \mathcal{Z}$, i.e., the set of planes containing the line $L = (\ell_1, \ell_2) \subset \mathbb{R}^3$, is identified with the set of oriented circles in oriented contact with the lines ℓ_1 and ℓ_2 (see Figure 3.1). The latter identification, together with the fact that four oriented lines are in contact with a common oriented circle if and only if the four corresponding points of the Blaschke cylinder are coplanar, will be crucial for the description of checkerboard IC-nets.

3.1 The Laguerre geometry of checkerboard IC-nets

As we have seen in Section 2, the following incidence theorem is of crucial importance for the elementary construction of checkerboard IC-nets.

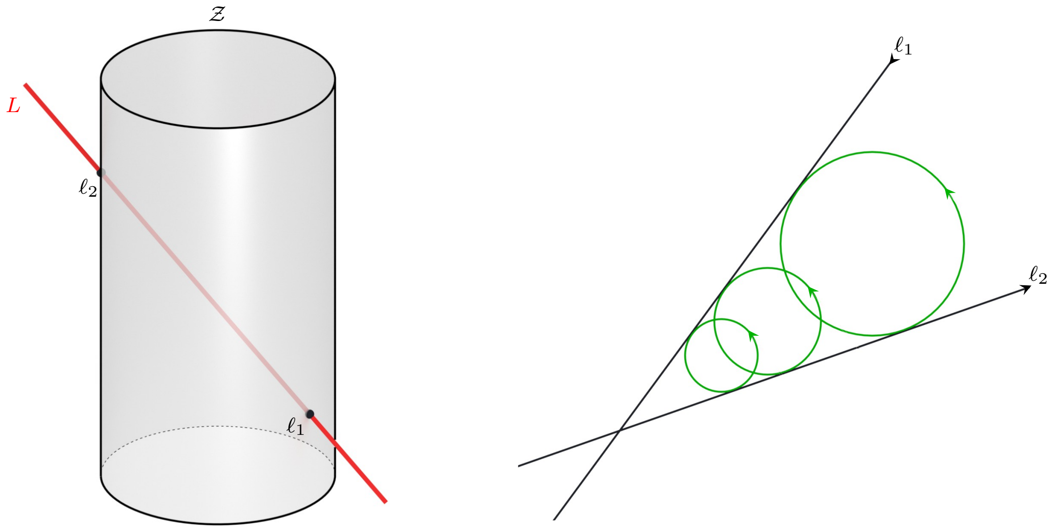

Figure 3.1. Blaschke cylinder model: Oriented lines are points $\ell \in \mathcal{Z}$ and oriented circles are planes S which do not intersect $\mathcal{Z}$ along its generators. Circles in oriented contact with two lines ℓ_1 and ℓ_2 are planes containing the line $L = (\ell_1, \ell_2)$.

Theorem 3.1. *(Checkerboard incircles incidence theorem) Let $\ell_1, \dots \ell_6$, $m_1, \dots, m_6$ be 12 oriented lines which are in oriented contact with 12 oriented circles $S_1, \dots, S_{12}$ as shown in Figure 3.2 (top), corresponding to "black" quadrilaterals of a 5×5 checkerboard IC-net. In particular, the lines ℓ_1, ℓ_2, m_1, m_2 are in oriented contact with the circle S_1, the lines ℓ_3, ℓ_4, m_1, m_2 are in oriented contact with the circle S_2 etc. Then, the 13th "black" checkerboard quadrilateral also has an inscribed circle, i.e., the lines ℓ_5, ℓ_6, m_5, m_6 have a common circle S_{13} in oriented contact.*

This theorem was originally proven in [AB]. Here, we give a slightly simpler proof which is also instrumental in the explicit integration of the nets. We assume that, modulo the existence of the 12 oriented circles, the 12 oriented lines are in general position. We begin with a simple lemma used in the proof.

Lemma 3.2. *Let p_1, p_2 be two points which belong to all members of a pencil of quadrics Q_t. Then, there exists a unique quadric $Q_{t_{12}}$ from the pencil which contains the whole line $L_{12} = (p_1, p_2)$. If the line $L_{34} = (p_3, p_4)$ associated with another pair of common points p_3, p_4 intersects the line L_{12} then the two quadrics $Q_{t_{12}}$ and $Q_{t_{34}}$ coincide.*

Proof. Even though we will apply this lemma to quadrics in $\mathbb{R}^3$, we will prove it in its natural projective setting. Thus, let q_1, q_2 be two quadratic forms generating the pencil with the quadratic form $q_t = q_1 + tq_2$. The points $p_1 = [v_1]$, $p_2 = [v_2]$ with v_1 and v_2 being homogeneous coordinates belong to all quadrics of the pencil iff $q_1(v_1) = q_1(v_2) = q_2(v_1) = q_2(v_2) = 0$. The line $L_{12} = (p_1, p_2)$ belongs to the quadric determined by $q_{t_{12}}$ iff $q_{t_{12}}(v_1, v_2) = 0$ so that $t_{12} = -\frac{q_1(v_1,v_2)}{q_2(v_1,v_2)}$. Vanishing of the denominator is the case when the line lies on the quadric determined by q_2. Moreover, if the line $L_{34} = (p_3, p_4)$ passing through another pair of common points p_3, p_4 intersects the line L_{12} then the point of intersection and p_3, p_4 belong to the quadric $Q_{t_{12}}$. Accordingly, the line L_{34} is contained in $Q_{t_{12}}$ so that $Q_{t_{12}} = Q_{t_{34}}$. □

Proof of Theorem 3.1. Here, it is convenient to interpret the statement of the theorem in terms of the Blaschke cylinder model. Thus, as explained above the lines L_i intersecting the Blaschke cylinder $\mathcal{Z}$ in the points ℓ_i and ℓ_{i+1} describe one-parameter sets of circles in oriented contact with the lines ℓ_i and ℓ_{i+1}. Some of the lines L_i and M_k intersect. For instance, the one-parameter families of circles corresponding to L_1 and M_1 contain the common circle S_1, corresponding to the plane determined by L_1 and M_1. We obtain the incidence picture shown in Figure 3.2 (bottom), wherein the points of intersection of the relevant pairs L_i, M_k are indicated by small circles. Moreover the lines L_i and L_{i+1} intersect since

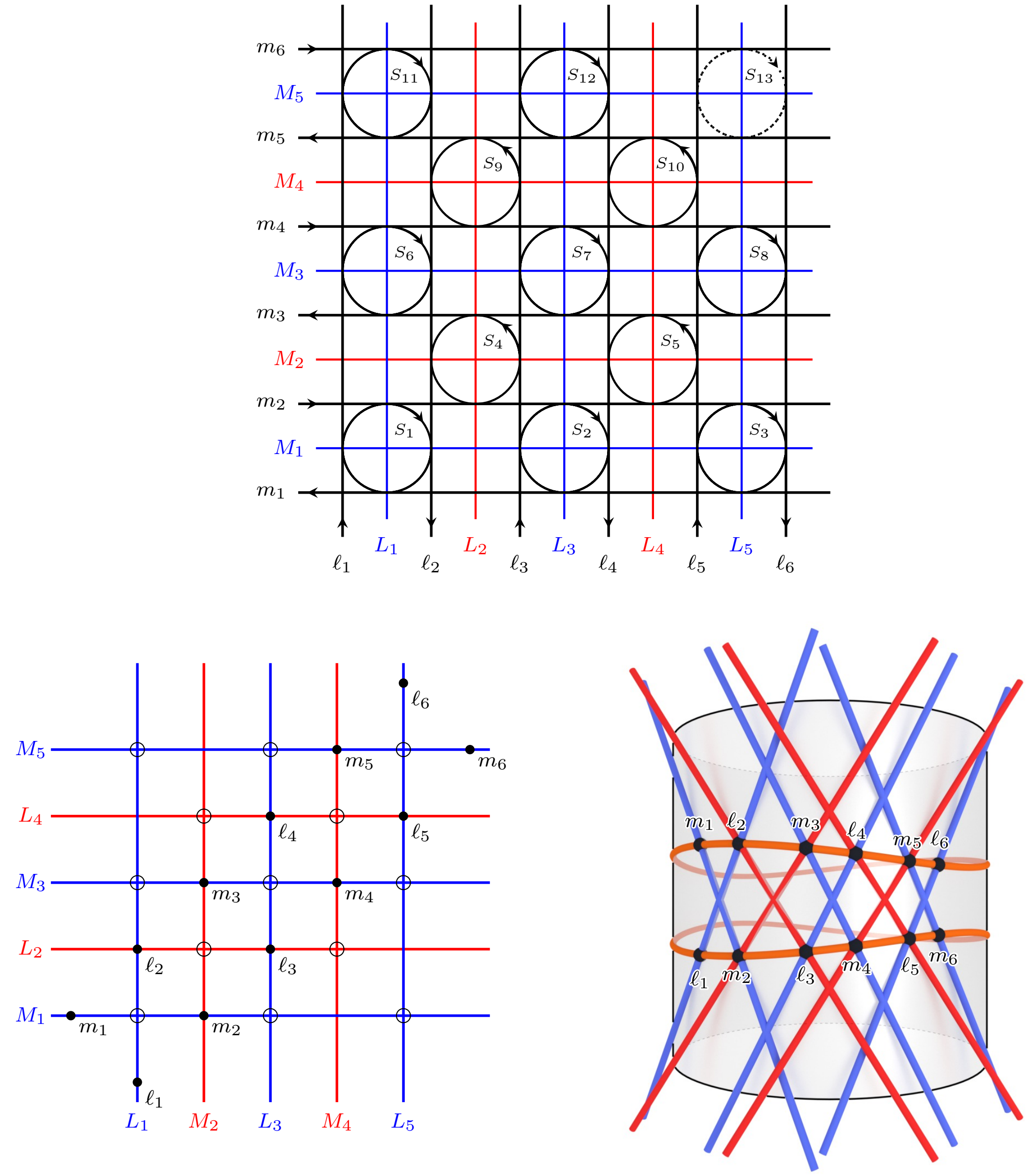

Figure 3.2. Checkerboard incircles incidence theorem. *Top:* Existence of the last circle S_{13}. *Bottom:* The Blaschke cylinder description. Pairs of intersecting lines L_i, M_k correspond to circles, whereas the points of intersection of the lines L_i, L_{i+1} and M_k, M_{k+1} encapsulate the common oriented lines ℓ_{i+1} and m_{k+1} respectively.

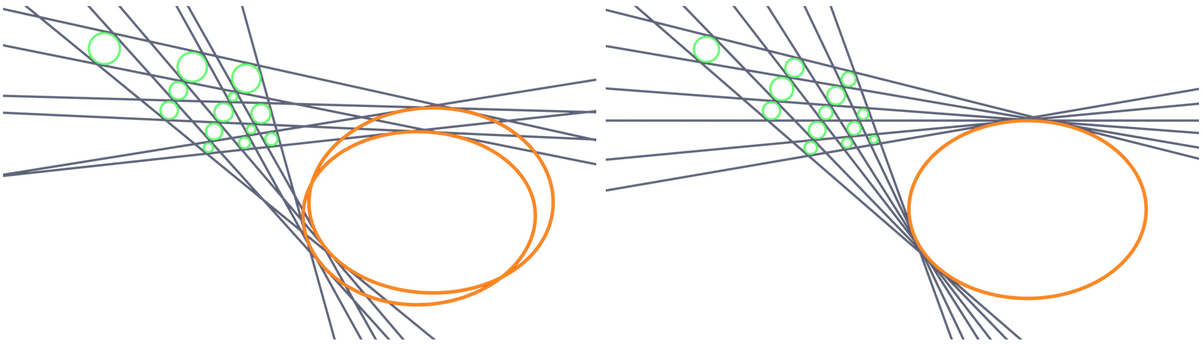

Figure 3.3. The lines of a checkerboard IC-net are tangent to a hypercycle. The hypercycle on the right consists of two coinciding ellipses of different orientations, encapsulating the tangent conic of a confocal checkerboard IC-net.

they pass through the same points in $\mathcal{Z}$ and so do the lines M_k and M_{k+1}. The points of intersection correspond to the lines ℓ_{i+1} and m_{k+1} respectively. For example $\ell_2 = L_1 \cap L_2$.

In order to prove the existence of the circle S_{13}, we have to show that the lines L_5 and M_5 intersect. We first note that the three lines L_1, L_3, L_5 determine a hyperboloid $\mathcal{H} \subset \mathbb{R}^3$ and recall that a line which intersects a quadric in three points is contained in the quadric. Accordingly, since M_1 and M_3 intersect the lines L_1, L_3, L_5, these are contained in $\mathcal{H}$. The intersection of the lines L_5 and M_5 is equivalent to the inclusion $M_5 \subset \mathcal{H}$. The latter property may be proven as follows.

Since ℓ_2, ℓ_3 belong to both quadrics $\mathcal{Z}, \mathcal{H}$, Lemma 3.2 implies that there exists a unique quadric $\tilde{\mathcal{H}}$ in the pencil of quadrics generated by $\mathcal{H}$ and $\mathcal{Z}$ which contains the whole line L_2. We now consider the three points $m_2, m_3, L_2 \cap M_2$ of M_2. Since m_2 and m_3 are common to $\mathcal{H}$ and $\mathcal{Z}$, these are contained in $\tilde{\mathcal{H}}$. Hence, $m_2, m_3, L_2 \cap M_2 \in \tilde{\mathcal{H}}$ so that $M_2 \subset \tilde{\mathcal{H}}$. This implies, in turn, that $\ell_4, \ell_5, L_4 \cap M_2 \in \tilde{\mathcal{H}}$ and, hence, $L_4 \subset \tilde{\mathcal{H}}$. Consequently, $m_4, L_2 \cap M_4, L_4 \cap M_4 \in \tilde{\mathcal{H}}$ so that $M_4 \subset \tilde{\mathcal{H}}$. In particular, m_5 lies in $\tilde{\mathcal{H}}$ (and $\mathcal{Z}$) and, therefore, in $\mathcal{H}$. Moreover, $L_1 \cap M_5$ and $L_3 \cap M_5$ lie in $\mathcal{H}$ which finally implies that $M_5 \subset \mathcal{H}$. □

It is observed that iterative application of Theorem 3.1 leads to the unique construction of an arbitrarily large checkerboard IC-net with lines L_n and M_n, $n \in \mathbb{Z}$. The hyperboloids $\mathcal{H}$ and $\tilde{\mathcal{H}}$ as constructed above then contain all lines L_{2k+1}, M_{2k+1} and L_{2k}, M_{2k} respectively. Thus, we have come to the important conclusion that a checkerboard IC-net encodes two quadrics which belong to a pencil containing the Blaschke cylinder $\mathcal{Z}$.

Corollary 3.3. *In the Blaschke cylinder model, the lines $L_{2k+1} = (\ell_{2k+1}, \ell_{2k+2})$, $M_{2k+1} = (m_{2k+1}, m_{2k+2})$ and $L_{2k} = (\ell_{2k}, \ell_{2k+1})$, $M_{2k} = (m_{2k}, m_{2k+1})$ associated with a checkerboard IC-net "in general position" are generators of hyperboloids $\mathcal{H}$ and $\tilde{\mathcal{H}}$ respectively which belong to a pencil of quadrics containing the Blaschke cylinder $\mathcal{Z}$.*

For future reference we denote the common curve of intersection of the above-mentioned quadrics by

$$\mathcal{C} = \mathcal{H} \cap \mathcal{Z} = \tilde{\mathcal{H}} \cap \mathcal{Z} = \mathcal{H} \cap \tilde{\mathcal{H}} \cap \mathcal{Z}.$$

Definition 3.4. *A (non-empty) curve of intersection of the Blaschke cylinder with a quadric is called a* hypercycle base curve.

The straight lines corresponding to the points of a hypercycle base curve are tangent to a curve in the plane which is generically of degree 8. This planar curve is called a *hypercycle* [Bl]. It is noted that a hypercycle base curve and the corresponding hypercycle are merely two different incarnations of the same object $\mathcal{C}$. In terms of this terminology, we have proven the following theorem (see Figure 3.3).

Theorem 3.5. *The lines of a checkerboard IC-net are tangent to a hypercycle.*

In the following, it is convenient to adopt a notion of genericity.

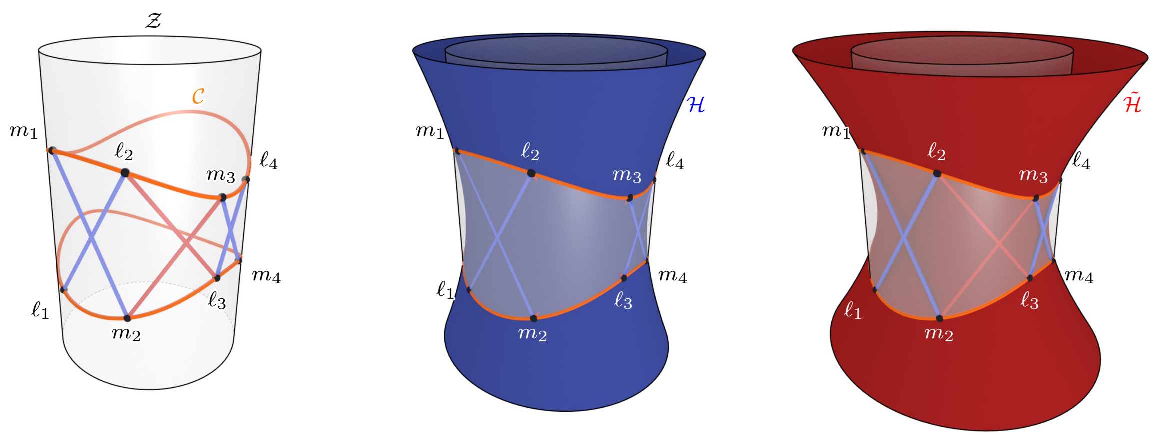

Figure 3.4. Construction of checkerboard IC-nets in the Blaschke cylinder model. The lines L_{2k+1}, M_{2k+1} (red) and L_{2k}, M_{2k} (blue) are generators of the quadrics $\mathcal{H}$ and $\tilde{\mathcal{H}}$ respectively.

Definition 3.6. *A quadric in $\mathbb{R}^3$ is termed* generic *if it does not contain the "point at infinity" on the axis of the Blaschke cylinder. A generic hypercycle base curve is the intersection of a generic quadric with the Blaschke cylinder. A pencil of quadrics containing the Blaschke cylinder is generic if one and, therefore, all quadrics of the pencil other than the Blaschke cylinder are generic. A checkerboard IC-net is generic if it is associated with a generic hypercycle base curve or, equivalently, a generic pencil of quadrics.*

We note that the standard square grid (appropriately oriented) does not constitute a generic checkerboard IC-net. Moreover, the above definition implies that the hypercycle base curve $\mathcal{C} \subset \mathcal{Z}$ associated with a generic quadric has bounded d-coordinate.

Corollary 3.7. *The lines of a generic checkerboard IC-net lie in bounded distance to the origin.*

3.2 Construction of checkerboard IC-nets

We are now in a position to formulate the construction of checkerboard IC-nets in the Blaschke cylinder model. One starts with two one-sheeted hyperboloids $\mathcal{H}, \tilde{\mathcal{H}}$ of a pencil of quadrics containing $\mathcal{Z}$ and two points ℓ_1, m_1 of the hypercycle base curve $\mathcal{C} = \mathcal{H} \cap \mathcal{Z}$. Let us make a choice and refer to one of the families of straight lines (generators) of the hyperboloid $\mathcal{H}$ as the L-family and the other one as the M-family. Make the choice of the L- and M-families on $\tilde{\mathcal{H}}$ as well. Now, the checkerboard IC-net is uniquely determined in the following sense. Label by L_1 the line from the L-family of $\mathcal{H}$ passing through ℓ_1 and denote by ℓ_2 its second point of intersection with $\mathcal{C}$. Similarly, the point $m_2 \in \mathcal{C}$ is the second point of intersection with $\mathcal{Z}$ of the M-line of $\mathcal{H}$ labelled by M_1 passing through m_1. Proceed further with the generators of the hyperboloid $\tilde{\mathcal{H}}$, where L_2 and M_2 are the L-line and M-line of $\tilde{\mathcal{H}}$ passing through ℓ_2 and m_2 respectively. The additional points of intersection with $\mathcal{C}$ are denoted by ℓ_3 and m_3 respectively. By alternating in this manner between the hyperboloids $\mathcal{H}$ and $\tilde{\mathcal{H}}$, the lines of a checkerboard IC-net ℓ_n and m_n represented as points of the hypercycle base curve which are connected by generators $L_n = (\ell_n, \ell_{n+1})$ and $M_n = (m_n, m_{n+1})$ may be constructed (see Figure 3.4). Thus, we conclude with the following theorem.

Theorem 3.8. **(Construction of checkerboard IC-nets in the Blaschke model)** *A checkerboard IC-net is uniquely determined by hyperboloids $\mathcal{H}, \tilde{\mathcal{H}}$ (with marked L- and M-families of generators on each hyperboloid) of a pencil of quadrics containing $\mathcal{Z}$ and two points ℓ_1, m_1 of the hypercycle base curve $\mathcal{C} = \mathcal{H} \cap \mathcal{Z}$.*

We now briefly discuss some illustrative classes of checkerboard IC-nets.

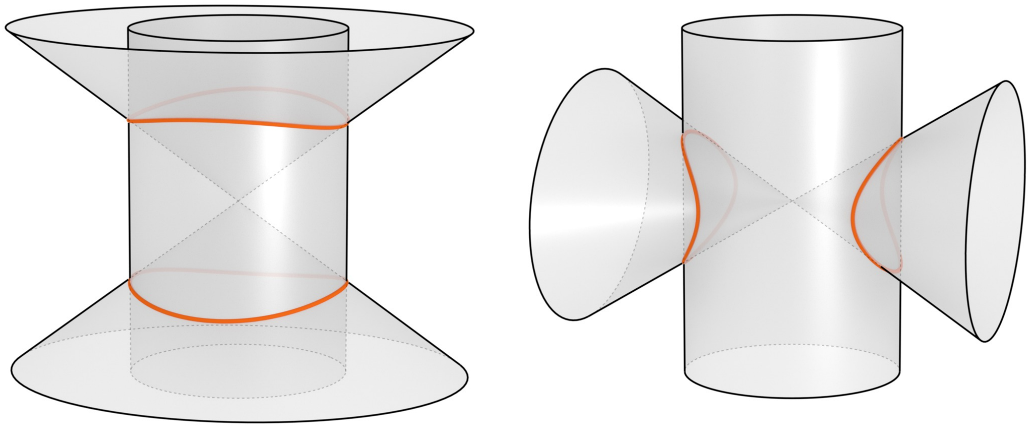

Figure 3.5. The elliptic and hyperbolic cones (3.3) and the hypercycle base curves of confocal checkerboard IC-nets in the Blaschke cylinder model.

(Confocal checkerboard) IC-nets

In [AB], confocal checkerboard IC-nets are characterised by the property that their lines are tangent to a conic. In this paper, we make the assumption that the conic is either an ellipse or a hyperbola so that, by means of a rotation and a translation (which constitute special Laguerre transformations, this conic may be brought into the form

$$\frac{x^2}{a} + \frac{y^2}{b} = 1. \tag{3.1}$$

Tangent lines to the conic are given by

$$\frac{xx_0}{a} + \frac{yy_0}{b} = 1$$

with

$$\frac{x_0^2}{a} + \frac{y_0^2}{b} = 1. \tag{3.2}$$

If we set $\boldsymbol{v} = (v, w)$ in the $(\boldsymbol{v}, d)$ description employed at the beginning of Section 3, this leads to $v = x_0 d/a$ and $w = y_0 d/b$ so that (3.2) may be expressed in terms of the cone

$$av^2 + bw^2 = d^2. \tag{3.3}$$

We refer to the latter as "elliptic" if $a > 0, b > 0$ and "hyperbolic" if $ab < 0$. The hypercycle base curve $\mathcal{C}$ is the intersection of the cone (3.3) with the Blaschke cylinder $v^2 + w^2 = 1$. It has two connected components and is symmetric with respect to the change of orientation $(v, w, d) \to (-v, -w, -d)$. In the plane, the two components of the hypercycle are the conic (3.1) equipped with two different orientations. Confocal checkerboard IC-nets are parametrised explicitly in Section 5.

As observed in Remark 2.1, any IC-net may be regarded as a (confocal) checkerboard IC-net by interpreting each line of the IC-net as a "double line", that is, two identical lines of opposite orientation represented by $\pm(v, w, d)$. Accordingly, one of the hyperboloids of the corresponding checkerboard IC-net constitutes a cone of the form (3.3). Indeed, the latter may be regarded as a characterisation of IC-nets in the context of checkerboard IC-nets.

Degeneration to rhombic checkerboard IC-nets

Hyperbolic confocal checkerboard IC-nets may be regarded as deformations of "rhombic" checkerboard IC-nets, that is, checkerboard IC-nets composed of identical rhombi. In order to show this, let $\mathcal{H}$ and $\tilde{\mathcal{H}}$ be the two hyperboloids underlying a hyperbolic checkerboard IC-net $\mathcal{N}$. Since the two hyperboloids belong to a pencil of quadrics, $\tilde{\mathcal{H}}$ may be regarded as a deformation of $\mathcal{H}$ with the parameter of the pencil playing the role of the deformation parameter. This implies, in turn, that we may interpret $\mathcal{N}$ as a deformation of a confocal checkerboard IC-net $\mathcal{N}_c$ for which $\tilde{\mathcal{H}} = \mathcal{H} = \mathcal{H}_c$ coincide. According to the construction of checkerboard IC-nets summarised in Theorem 3.8, $\mathcal{N}_c$ can only be non-trivial if the L-family on $\mathcal{H}$ coincides with the M-family on $\tilde{\mathcal{H}}$ (and vice versa), thereby representing the same family of generators on $\mathcal{H}_c$. Hence, we here assume that the choice of the L-and M-families on the hyperboloids associated with $\mathcal{N}$ has been made in such a manner that, in the limit $\tilde{\mathcal{H}} \to \mathcal{H}$, this non-triviality requirement is met.

The next step (see Figure 3.6) is to consider a one-parameter family of confocal checkerboard IC-nets $\mathcal{N}_c(\varepsilon)$ with underlying hyperboloids $\mathcal{H}_c(\varepsilon)$ given by

$$w_0^2 v^2 - v_0^2 w^2 = \varepsilon^2(\Delta^2 - d^2), \qquad \varepsilon \geqslant 0, \quad \Delta > 0$$

with $v_0^2 + w_0^2 = 1$, $v_0 w_0 \neq 0$ and

$$w_0^2 - \varepsilon^2 \Delta^2 > 0$$

for hyperbolicity of $\mathcal{N}(\varepsilon)$. In the limit $\varepsilon \to 0$, the hyperboloid $\mathcal{H}_c(0)$ degenerates to the union of the two planes

$$\mathcal{P}_\pm : \quad w_0 v \pm v_0 w = 0$$

passing through the axis of the Blaschke cylinder $\mathcal{Z}$, equipped with two special points on the axis given by

$$P_\pm = (0, 0, \pm\Delta).$$

In fact, it is easy to show that the generators of the hyperboloid $\mathcal{H}_c(\varepsilon)$ become straight lines passing through either P_+ or P_- as $\varepsilon \to 0$. Specifically, all lines L_n associated with the degenerate checkerboard IC-net $\mathcal{N}_c(0)$ in the Blaschke cylinder model lie in the plane $\mathcal{P}_-$, whereby all L_{2k} pass through P_-, while all L_{2k+1} pass through P_+. Similarly, all lines M_n lie in the plane $\mathcal{P}_+$ and all M_{2k} pass through P_-, while all M_{2k+1} pass through P_+. Moreover, without loss of generality, the lines of $\mathcal{N}_c(0)$ are given by $\ell_{2n} = (v_0, w_0, 4n\Delta)$, $\ell_{2n+1} = (-v_0, -w_0, -2(2n+1)\Delta)$, $m_{2n} = (v_0, -w_0, 4n\Delta)$, $m_{2n+1} = (-v_0, w_0, -2(2n+1)\Delta)$ so that $\mathcal{N}_c(0)$ is indeed of rhombic type.

It is observed that rhombic checkerboard IC-nets are non-generic since the corresponding hypercycle base curve $\mathcal{C}$ consists of four straight lines parallel to the axis of $\mathcal{Z}$. The simplest generic checkerboard IC-nets are obtained by "switching on" the parameter ε. The conics obtained by intersecting the quadric $\mathcal{H}_c(\varepsilon)$ with the $d = 0$ plane for some "small" ε are displayed in Figure 3.6 (left). It is important to note that the number of real base points of the pencil of conics in the $d = 0$ plane associated with the checkerboard IC-nets $\mathcal{N}_c(\varepsilon)$, that is, the number of points common to the conics of the pencil in the $d = 0$ plane is 4. This distinguishes hyperbolic confocal checkerboard IC-nets from elliptic confocal checkerboard IC-nets as discussed in detail in Section 5.

4 Checkerboard IC-nets as Laguerre transforms of confocal checkerboard IC-nets

We will now examine under what circumstances checkerboard IC-nets may be regarded as Laguerre transforms of confocal checkerboard IC-nets. The associated analysis may naturally be split into two parts.

4.1 Pre-normalisation

In homogeneous coordinates $\sim (v, w, 1, d)$, the quadratic forms of the pencil of quadrics associated with a confocal checkerboard IC-net with normalised conics (3.1) are diagonal. Indeed, the cone (3.3) and the Blaschke cylinder $v^2 + w^2 = 1$ generate the whole pencil. It is easy to see that the converse statement is also true if we include in our definition of confocal checkerboard IC-nets the case of the lines being "tangent" to a degenerate ellipse or hyperbola corresponding to $a > 0$, $b \to 0$ or $b > 0$, $a \to 0$. In this case, all lines pass through the two focal points. The cases $a < 0$, $b \to 0$ or $b < 0$, $a \to 0$ may be excluded

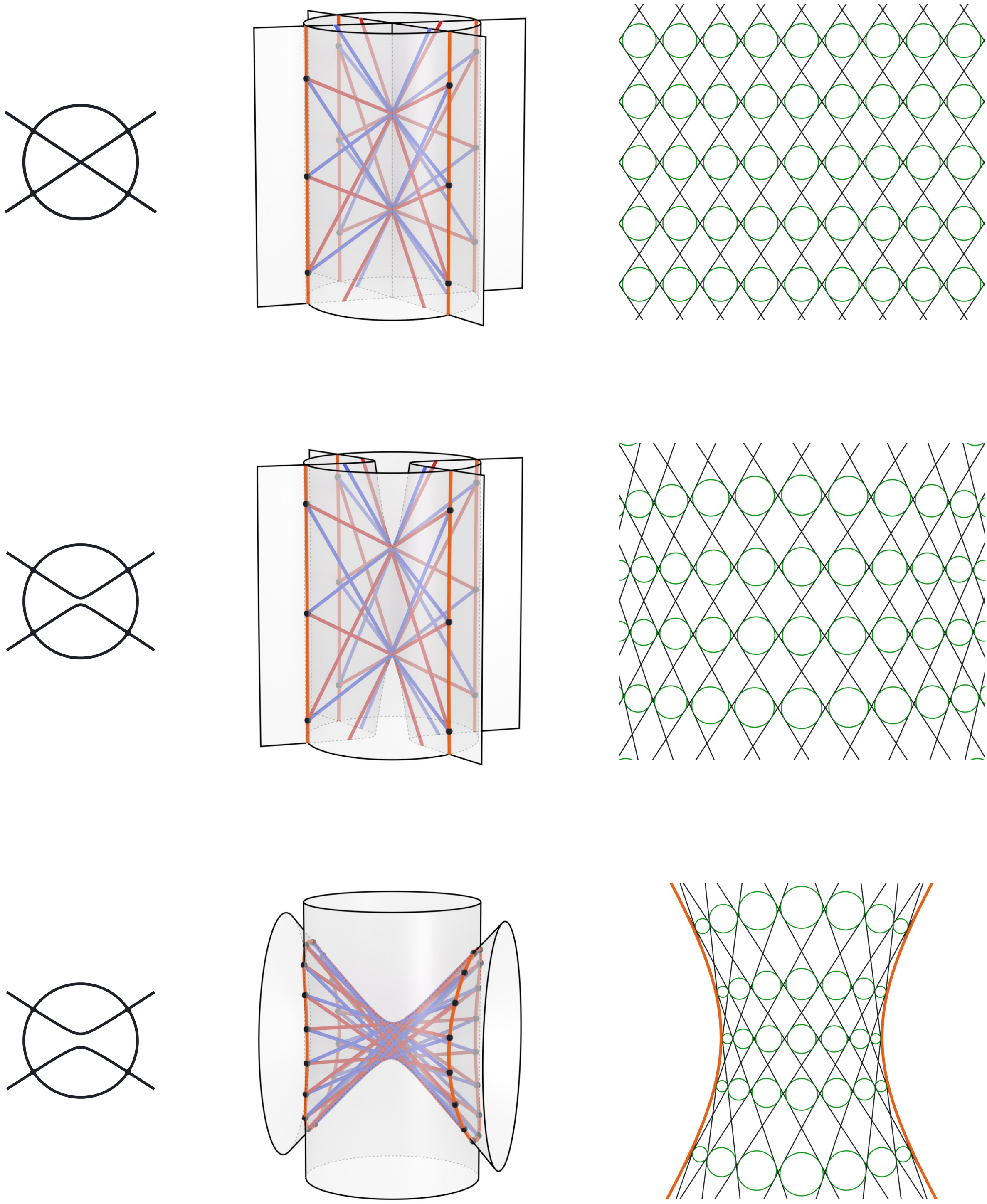

Figure 3.6. Deformation of a rhombic checkerboard IC-net. *Top to bottom:* A rhombic checkerboard IC-net. A slightly deformed "almost rhombic" checkerboard IC-net with equal hyperboloids $\mathcal{H} = \tilde{\mathcal{H}}$. A hyperbolic checkerboard IC-net from a larger deformation with equal hyperboloids $\mathcal{H} = \tilde{\mathcal{H}}$. *Left to right:* Conics in the $d = 0$ plane (The corresponding pencil has 4 base points). The checkerboard IC-net in the Blaschke cylinder model. The checkerboard IC-net in the plane.

since the hypercycle base curve consists of only two points corresponding to two lines which only differ in their orientation and which may not be used to construct a proper checkerboard IC-net.

Theorem 4.1. *A generic checkerboard IC-net is confocal with its lines being tangent to a normalised conic of the form* (3.1) *if and only if the quadratic forms of the associated pencil of quadrics are diagonal in homogeneous coordinates* $\sim (v, w, 1, d)$.

The above theorem implies that a pencil of quadrics associated with a general (that is, non-normalised) confocal checkerboard IC-net is diagonalisable by Laguerre transformations of the form (A.6) (Appendix) since Euclidean motions constitute particular Laguerre transformations. On the other hand, since the lines of confocal checkerboard IC-nets are tangent to two copies of the same conic which have two different orientations, a Laguerre transformation separates those two copies and one obtains a hypercycle which consists of two possibly intersecting pieces (see Figure 3.3). It is therefore natural to investigate the question of the diagonalisability of generic pencils of quadrics which are not necessarily associated with confocal checkerboard IC-nets. Thus, we now consider a generic checkerboard IC-net with $\mathcal{H}$ being one of its corresponding generic hyperboloids so that the diagonalisability of the associated pencil of quadrics is equivalent to the diagonalisability of $\mathcal{H}$. Let $(\tilde{Q}_{i,j})_{i,j=1,\ldots,4}$ be the symmetric matrix of its quadratic form in coordinates $(v, w, 1, d)$. Our genericity assumption is equivalent to $\tilde{Q}_{4,4} \neq 0$. The normalisation $\tilde{Q}_{4,4} = -1$ therefore leads to

$$\tilde{Q} = \begin{pmatrix} \tilde{S} & a \\ a^T & -1 \end{pmatrix},$$

where $\tilde{S}$ is a symmetric matrix, and $a \in \mathbb{R}^3$. By means of a Laguerre transformation (A.5) (Appendix) with the matrix

$$A = \begin{pmatrix} 1 & 0 \\ a^T & 1 \end{pmatrix},$$

$\tilde{Q}$ is brought into the block diagonal form

$$Q = A^T \tilde{Q} A = \begin{pmatrix} S & 0 \\ 0 & -1 \end{pmatrix}, \tag{4.1}$$

where S is symmetric. Furthermore, the matrix Q may be diagonalised by a Laguerre transformation A' only if it is of the form

$$A' = \begin{pmatrix} B & 0 \\ 0 & 1 \end{pmatrix}$$

with $B \in O(2, 1)$. Hence, we conclude that the pencil of quadrics associated with a generic checkerboard IC-net is diagonalisable by a Laguerre transformation if and only if there exists a $B \in O(2, 1)$ such that

$$B^T S B$$

is diagonal, where S is defined by (4.1).

4.2 Diagonalisation

In the preceding, it has been demonstrated that the question of whether or not a checkerboard IC-net may be Laguerre-transformed into a confocal checkerboard IC-net may be answered by determining the class of symmetric 3×3 matrices S which may be diagonalised according to

$$S \to B^T S B, \quad B \in O(2, 1).$$

It is important to note that S represents the conic intersection of the quadric

$$(v\ w\ 1) S \begin{pmatrix} v \\ w \\ 1 \end{pmatrix} = d^2 \tag{4.2}$$

Type	Type and multiplicity of base points	# of real base points	Type and multiplicity of degenerate conics	Type and multiplicity of roots
Ia	$1,1,1,1$	4	$\times,\times,\times$	$1,1,1$
Ib	$1,1,(1,\bar{1})$	2	$\times,\circ,\bar{\circ}$	$1,(1,\bar{1})$
Ic	$(1,\bar{1}),(1,\bar{1})$	0	$\times,\bullet,\bullet$	$1,1,1$
IIa	$2,1,1$	3	$2\times,\times$	$2,1$
IIb	$2,(1,\bar{1})$	1	$2\bullet,\times$	$2,1$
IIIa	$2,2$	2	$2\Vert,\times$	$2,1$
IIIb	$(2,\bar{2})$	0	$2\Vert,\bullet$	$2,1$
IV	$3,1$	2	$3\times$	3
V	4	1	$3\Vert$	3

Figure 4.1. The classification of real pencils of conics. There exist four different types of degenerate conics. ($\times$) Two real intersecting lines. ($\circ$) Two non-intersecting complex lines. ($\bullet$) Two complex conjugate lines which intersect in a real point. ($\Vert$) A real double line.

and the plane $d = 0$. Since the matrix $Z = \mathrm{diag}(1,1,-1)$ representing the "Blaschke circle" $v^2 + w^2 = 1$ is invariant under the action of the group $O(2,1)$, the matrix S is diagonalisable if and only if the one-parameter family of matrices

$$S^\lambda = S + \lambda Z$$

encoding the pencil of conics $\mathcal{P}$ spanned by the conic associated with S and the Blaschke circle is diagonalisable. It is noted that the roots of the characteristic cubic polynomial

$$P(\lambda) = \det S^\lambda$$

correspond to the degenerate conics of $\mathcal{P}$. Furthermore, it is evident that S is diagonal if and only if one conic in $\mathcal{P}$ different from the Blaschke circle (and therefore any conic) is symmetric with respect to the v- and w-axes.

We will now demonstrate that diagonalisability may be characterised in terms of the real base points of the pencil $\mathcal{P}$, that is, the points (on the Blaschke circle) common to all conics of $\mathcal{P}$ (or, equivalently, any particular pair of conics of $\mathcal{P}$). The proof of the following theorem is based on the standard classification of pencils of conics [Le] in terms of the number and nature of the base points which are determined by the roots of the quartic equation, representing the common solutions of $v^2 + w^2 = 1$ and $(4.2)_{d=0}$. This classification is in one-to-one correspondence with the number and nature of roots of the characteristic polynomial $P(\lambda)$ associated with any pencil. The present theorem is a variant of a theorem [Le] which states that a symmetric matrix S is diagonalisable by means of a *projective* transformation if and only if the corresponding pencil is of type Ia, Ic, IIIa or IIIb in the classification tabled in Figure 4.1. Normal forms of degenerate conics associated with this classification are depicted in Figure 4.2.

Theorem 4.2. *The matrix S may be diagonalised if and only if the associated pencil of conics $\mathcal{P}$ has four, two double or no real base points, that is, if $\mathcal{P}$ is of type Ia, Ic, IIIa or IIIb.*

Proof. If S is diagonal then the associated pencil $\mathcal{P}$ is symmetric with respect to the v- and w-axes. This symmetry cannot be present in types other than Ia, Ic, IIIa or IIIb. Conversely, it is necessary to show that if the pencil is of any of those four types then $\mathcal{P}$ can be made symmetric or, equivalently, S^λ is diagonalisable for one $\lambda \neq \infty$.

Ia) Four real base points. In this case, we may apply a projective transformation which transforms the Blaschke circle into an ellipse and maps the four base points to the four vertices of a rectangle which is symmetric with respect to the v- and w-axes. An appropriate subsequent affine transformation then

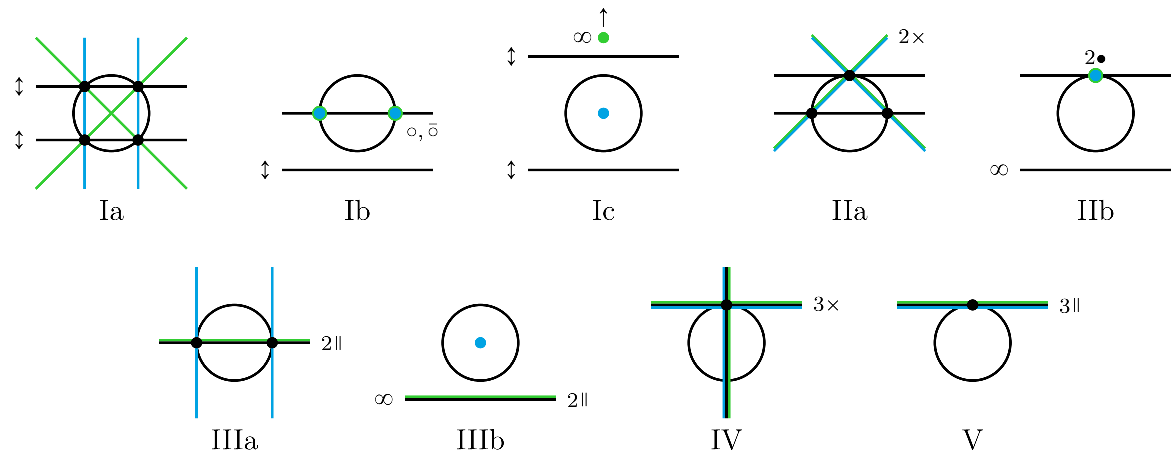

Figure 4.2. Degenerate conics of real pencils of conics containing the Blaschke circle. For each type, a normal form is shown with respect to projective transformations which preserve the Blaschke circle. For types I, the normal form still depends on one parameter, which is indicated by $\updownarrow$. The ∞ symbol indicates that the line (point) is chosen to be the line at infinity (the point at infinity in the designated direction).

maps the ellipse to the Blaschke circle without affecting the symmetry of the rectangle. The composition of these two transformations constitutes an $O(2,1)$ transformations since it leaves the Blaschke circle invariant. This compound transformation results in a symmetric distribution of the base points and, hence, the transformed pencil is symmetric.

IIIa) Two real double base points. In this case, there exists a degenerate conic consisting of two real lines which touch the Blaschke circle. A suitable combination of a projective and an affine transformation sends the vertex of this degenerate conic to infinity and maps the intermediate ellipse back to the Blaschke circle. The degenerate conic may therefore be transformed into $w^2 = 1$ which is symmetric.

Ic) Four complex base points. In this case, there exists a degenerate conic consisting of two intersecting real lines which do not intersect the Blaschke circle. A suitable combination of a projective and an affine transformation sends the vertex of this degenerate conic to infinity and maps the intermediate ellipse back to the Blaschke circle. The degenerate conic may therefore be transformed into $(w-a)(w+b) = 0$, where $a, b > 1$. It is not difficult to show that a suitable hyperbolic rotation in the $(\tilde{w}, \tilde{z})$-plane (with $(\tilde{w}, \tilde{z}) \sim (w, 1)$) leads to $a = b$ so that the degenerate conic simplifies to $w^2 = a^2$ which is symmetric.

IIIb) Two complex double base points. In this case, there exists a degenerate conic consisting of two coinciding real lines which do not intersect the Blaschke circle. A suitable combination of a projective and an affine transformation sends this double line to infinity and maps the intermediate ellipse back to the Blaschke circle. The transformed double line is therefore given by $\tilde{z}^2 = 0$ which is symmetric. □

In summary, it has been established that the matrix S may be diagonalised if and only if the associated pencil of conics $\mathcal{P}$ has four, two double or no real base points. This leads to the following characterisation.

Theorem 4.3. *A generic checkerboard IC-net is Laguerre-equivalent to a confocal checkerboard IC-net if and only if the hypercycle base curve of the associated pencil of quadrics consists of two non-degenerate loops on the Blaschke cylinder which are either disjoint or transversal.*

Proof. Since the statement to be proven is invariant under Laguerre transformations, it suffices to examine the nature of the base curves of "normal forms" of generic pencils of quadrics. These are determined by the normal forms of the associated pencils of conics. The normal forms of degenerate conics which together with the Blaschke circle span pencils of conics of types Ia, Ic and IIIa, IIIb have been derived in the proof of the preceding theorem. In a similar manner, the remaining types of pencils may be treated. Accordingly, one obtains the classification of pencils of quadrics displayed in Figure 4.3. The associated base curves are also depicted in Figure 4.3. It is noted that the base curves of types Ic_+ and IIIb_- are empty and, therefore, do not correspond to a hypercycle. The types Ia and Ic_- are associated with a double hyperbola and a double ellipse respectively, while the types IIIa_+, IIIa_- and IIIb_+ correspond to the special cases of the hypercycle consisting of two points, a double line and a double circle respectively. As pointed out in connection with Theorem 4.1, the case of a double line does not give rise to a proper checkerboard IC-net. Accordingly, we find that confocal checkerboard IC-nets are captured by the types Ia, Ic_-, IIIa_+ and IIIb_+ which confirms the assertion of the theorem. □

Remark 4.1. A stronger notion of genericity is obtained by considering only those checkerboard IC-nets which are generically generated by means of the iterative geometric construction of checkerboard IC-nets described in Section 4. In this case, generic checkerboard IC-nets are of types Ia, $\mathrm{Ib}_\pm$ and Ic_- so that the case of two transversal components of the hypercycle base curve cannot occur and must be removed from the above theorem.

Type	Normal form of a degenerate quadric	Type and multiplicity of degenerate quadrics
Ia	$w^2 - a^2 = \underset{(-)}{+} d^2, \quad 0 < a < 1$	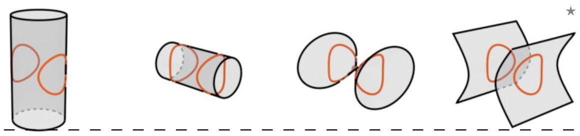
$\mathrm{Ib}_\pm$	$w(bw-1) = \pm d^2, \quad \lvert b \rvert < 1$	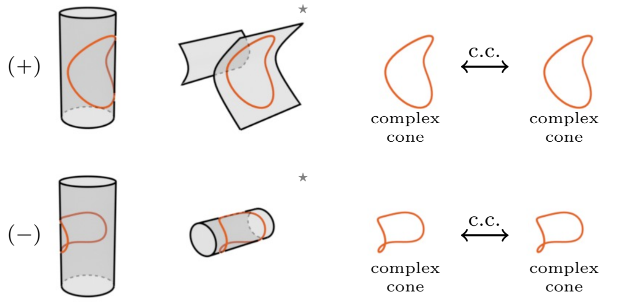
$\mathrm{Ic}_\pm$	$w^2 - a^2 = \pm d^2, \quad a > 1$	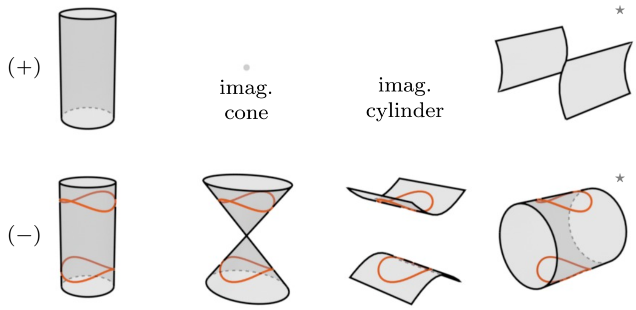
$\mathrm{IIa}_\pm$	$w(w-1) = \pm d^2$	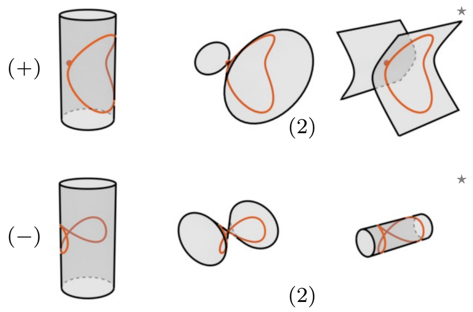
$\mathrm{IIb}_\pm$	$(w-1) = \pm d^2$	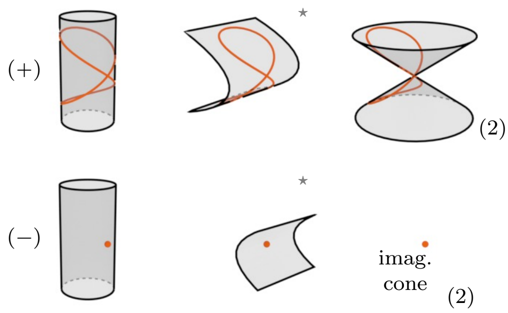

$\mathrm{IIIa}_\pm$	$w^2 = \pm d^2$	
$\mathrm{IIIb}_\pm$	$1 = \pm d^2$	
IV	$(w-1)v = \substack{+\\(-)}d^2$	
$\mathrm{V}_\pm$	$(w-1)^2 = \pm d^2$	
O	$0 = \substack{+\\(-)}d^2$	

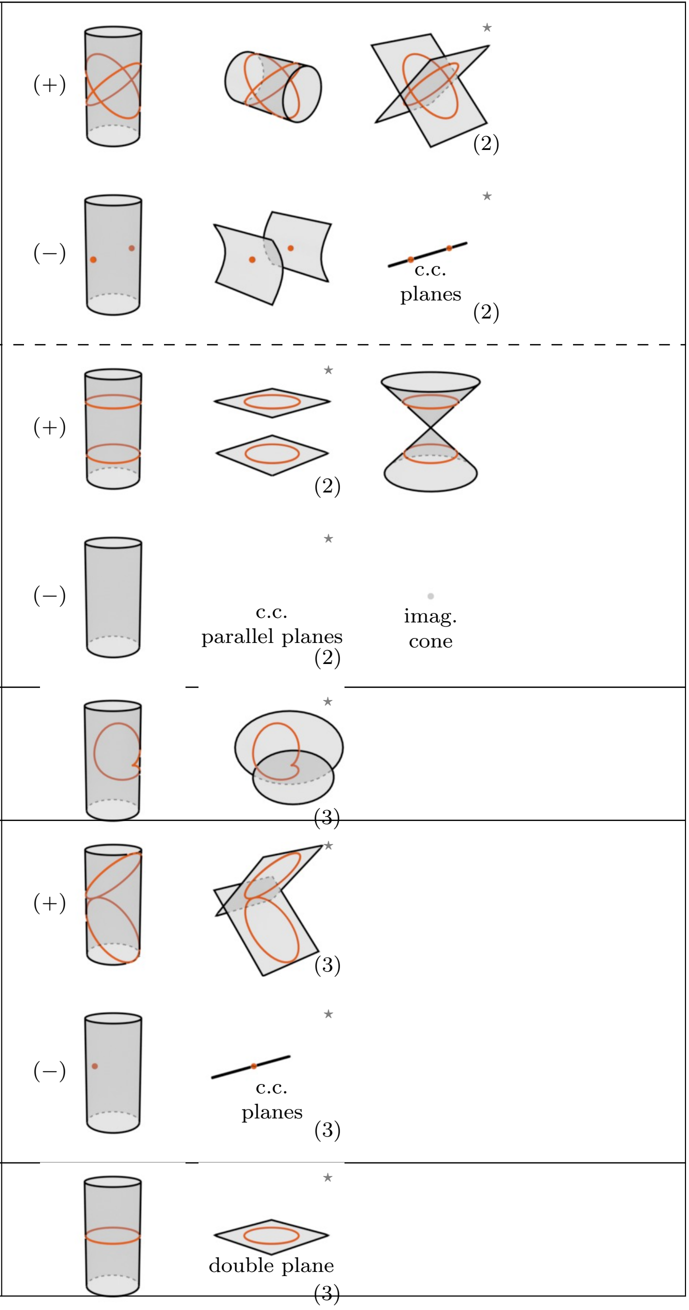

Figure 4.3. Normal forms of degenerate quadrics of generic pencils, corresponding to the classification of different types of planar pencils of conics listed and illustrated in Figures 4.1 and 4.2. These are obtained by "adding" a $\pm d^2$ term to the algebraic representation of the degenerate conics depicted in Figure 4.2. However, type O corresponds to the case $S = 0$ which does not encode a pencil of conics in the (v, w)-plane. Note that types Ia, IV, and O each generate only one class, that is, different signs in $\pm d^2$ lead to equivalent pencils. Types Ic_+ and IIIb_- correspond to empty hypercycles. For each type, a normal form of one degenerate quadric is given which spans the generic pencil together with the Blaschke cylinder. Furthermore, for each type, all degenerate quadrics are shown together with the hypercycle base curve. The multiplicity is given if greater than 1, and a $\star$ indicates that the degenerate quadric corresponds to the normal form recorded in the second column of the table.

5 An elliptic function representation of confocal checkerboard IC-nets

Explicit parametrisations of confocal checkerboard IC-nets and their Laguerre transforms may now be obtained by parametrising the hypercycle base curves associated with a pencil of quadrics in terms of elliptic functions.

5.1 Elliptic confocal checkerboard IC-nets

It is recalled that "elliptic" confocal checkerboard IC-nets, that is checkerboard IC-nets the lines of which are tangent to an ellipse

$$\frac{x^2}{\alpha^2} + \frac{y^2}{\beta^2} = 1, \tag{5.1}$$

correspond to a pencil of quadrics

$$(\alpha^2 + \lambda)v^2 + (\beta^2 + \lambda)w^2 = d^2 + \lambda \tag{5.2}$$

generated by an elliptic cone and the Blaschke cylinder, namely

$$\alpha^2 v^2 + \beta^2 w^2 = d^2, \quad v^2 + w^2 = 1. \tag{5.3}$$

In the following, we assume that $\alpha^2 \geqslant \beta^2$ without loss of generality. The associated base curve is the set of all points (v, w, d) obeying the pair (5.3). This corresponds to types Ic_- or IIIb_+ of the classification of pencils of quadrics with the two components of the base curve being mapped into each other by $d \to -d$. The nature of any quadric $\mathcal{H}$ in the pencil (5.2) depends on the value of the associated parameter λ. Accordingly, there exist two cases.

The case $\boldsymbol{\lambda \geqslant 0}$

In this case, the quadric $\mathcal{H}$ constitutes a one-sheeted hyperboloid (or a cone for $\lambda = 0$) which is aligned with the Blaschke cylinder. If we now parametrise v and w in terms of Jacobi elliptic functions [NIST] cn and sn respectively then the general solution of (5.3) is given by

$$\boldsymbol{v}_\pm(\psi) = \begin{pmatrix} v(\psi) \\ w(\psi) \\ d_\pm(\psi) \end{pmatrix} = \begin{pmatrix} \mathrm{cn}(\psi, k) \\ \mathrm{sn}(\psi, k) \\ \pm\alpha\,\mathrm{dn}(\psi, k) \end{pmatrix}, \quad k = \sqrt{1 - \frac{\beta^2}{\alpha^2}}, \tag{5.4}$$

where ψ constitutes the parameter along the (two components of the) base curve. Any pair of points on the two components of the base curve may be represented by

$$\boldsymbol{v}_\pm(\psi_0), \quad \boldsymbol{v}_\mp(\psi_1), \quad \psi_1 = s + \psi_0 \tag{5.5}$$

for any fixed choice of the above signs. If we demand that, for fixed s, the one-parameter family of lines

$$\boldsymbol{l}(\psi_0, t) = \boldsymbol{v}_\pm(\psi_0) + t[\boldsymbol{v}_\mp(\psi_1) - \boldsymbol{v}_\pm(\psi_0)], \quad t \in \mathbb{R} \tag{5.6}$$

consist of generators of the quadric $\mathcal{H}$ then we obtain a relationship between the parameters s and λ which is to be independent of ψ_0. Indeed, insertion of $\boldsymbol{l}$ into (5.2) produces

$$v(\psi_0)v(\psi_1)(\alpha^2 + \lambda) + w(\psi_0)w(\psi_1)(\beta^2 + \lambda) = d_\pm(\psi_0)d_\mp(\psi_1) + \lambda.$$

It is observed that, geometrically, the latter merely represents the fact that the points $\boldsymbol{v}_\pm(\psi_0)$ and $\boldsymbol{v}_\mp(\psi_1)$ are required to lie in the tangent planes to the hyperboloid (5.2) at those two points. Now, comparison with the general identity [NIST]

$$\begin{gathered} c_s\,\mathrm{sn}(\psi_0, k)\,\mathrm{sn}(\psi_1, k) + c_c\,\mathrm{cn}(\psi_0, k)\,\mathrm{cn}(\psi_1, k) = c_d\,\mathrm{dn}(\psi_0, k)\,\mathrm{dn}(\psi_1, k) + 1 \\ c_s = \mathrm{dc}(s, k) + c_d(1 - k^2)\,\mathrm{nc}(s, k), \quad c_c = \mathrm{nc}(s, k) + c_d\,\mathrm{dc}(s, k) \end{gathered} \tag{5.7}$$

for elliptic functions with $\psi_1 = \psi_0 + s$ shows that it is required that

$$\begin{aligned}\alpha^2 + \lambda &= \lambda\,\mathrm{nc}(s,k) - \alpha^2\,\mathrm{dc}(s,k)\\ \beta^2 + \lambda &= \lambda\,\mathrm{dc}(s,k) - \alpha^2(1-k^2)\,\mathrm{nc}(s,k).\end{aligned}$$

Since the latter two conditions coincide, we conclude that

$$\lambda = \alpha^2\frac{\mathrm{dc}(s,k)+1}{\mathrm{nc}(s,k)-1} = \alpha^2\,\mathrm{cs}^2\left(\frac{s}{2},k\right) \geqslant 0 \tag{5.8}$$

so that any family of generators of the quadric (5.2) for $\lambda \geqslant 0$ is encoded via the parametrisation (5.4)-(5.6) in an appropriately chosen parameter s. In other words, a translation of the argument ψ in the parametrisation (5.4) by some fixed quantity s together with a change of the component of the base curve gives rise to a family of generators of a unique quadric $\mathcal{H}$ of the pencil. The second family of generators is obtained by letting $s \to -s$.

The case $-\alpha^2 \leqslant \lambda \leqslant -\beta^2$

This case corresponds to the remaining one-sheeted hyperboloids (and an elliptic and hyperbolic cylinder for $\lambda = -\alpha^2$ and $\lambda = -\beta^2$ respectively) of the pencil (5.2) which are aligned with the v-axis. It is now convenient to introduce an additional parameter ε in the parametrisation (5.4) according to

$$\boldsymbol{v}_\pm^\varepsilon(\psi) = \begin{pmatrix}\mathrm{cn}(\psi,k)\\ \varepsilon\,\mathrm{sn}(\psi,k)\\ \pm\alpha\,\mathrm{dn}(\psi,k)\end{pmatrix}, \quad \varepsilon^2 = 1$$

and consider two points

$$\boldsymbol{v}_\pm^\varepsilon(\psi_0), \quad \boldsymbol{v}_\mp^{-\varepsilon}(\psi_1), \quad \psi_1 = s + \psi_0 \tag{5.9}$$

on any fixed component of the base curve. Then, the lines

$$\boldsymbol{l}(\psi_0,t) = \boldsymbol{v}_\pm^\varepsilon(\psi_0) + t[\boldsymbol{v}_\mp^{-\varepsilon}(\psi_1) - \boldsymbol{v}_\pm^\varepsilon(\psi_0)], \quad t \in \mathbb{R} \tag{5.10}$$

turn out to be generators on any hyperboloid $\mathcal{H}$ given by (5.2) for

$$\lambda = -\beta^2\,\mathrm{nd}^2\left(\frac{s}{2},k\right).$$

Once again, for any fixed λ in the current range, there exists an $|s|$ such that the generators of the associated quadric $\mathcal{H}$ which pass through the base curve are parametrised by (5.10). The two signs of s correspond to the two families of generators of $\mathcal{H}$.

Construction of elliptic confocal checkerboard IC-nets

In order to illustrate the construction of checkerboard IC-nets from pencils of quadrics presented in Section 3, we consider two quadrics $\mathcal{H}$ and $\tilde{\mathcal{H}}$ of the pencil (5.2) corresponding to a pair of parameters s and $\tilde{s}$ which are related to $\lambda, \tilde{\lambda} > 0$ by (5.8). It is recalled that any point (v,w,d) of the base curve is in one-to-one correspondence with a line

$$vx + wy = d.$$

In this sense, we refer to (v,w,d) as a point on the Blaschke cylinder or a line in the (x,y)-plane. The first ("vertical") family of lines of the elliptic confocal checkerboard is then given by

$$\begin{aligned}\boldsymbol{v}_{2n}^v &= \boldsymbol{v}_+(\psi_0^v + n(s+\tilde{s})),\\ \boldsymbol{v}_{2n+1}^v &= \boldsymbol{v}_-(\psi_0^v + n(s+\tilde{s}) + s),\end{aligned} \qquad n \in \mathbb{Z},$$

where ψ_0^v is arbitrary and corresponds to one of the "initial conditions" of the construction. The second ("horizontal") family of lines is associated with the two other families of generators of $\mathcal{H}$ and $\tilde{\mathcal{H}}$ encoded in the parameters $-s$ and $-\tilde{s}$ respectively. Accordingly, the construction of confocal checkerboard IC-nets in this case may be summarised as follows.

Theorem 5.1. *For any pairs of parameters $\alpha \geqslant \beta > 0$ and ψ_0^v, ψ_0^h and $s, \tilde{s}$, the lines*

$$\begin{aligned} \boldsymbol{v}_{2n}^v &= \boldsymbol{v}_+(\psi_0^v + n(s+\tilde{s})), \\ \boldsymbol{v}_{2n+1}^v &= \boldsymbol{v}_-(\psi_0^v + n(s+\tilde{s}) + s), \\ \boldsymbol{v}_{2n}^h &= \boldsymbol{v}_+(\psi_0^h - n(s+\tilde{s})), \\ \boldsymbol{v}_{2n+1}^h &= \boldsymbol{v}_-(\psi_0^h - n(s+\tilde{s}) - s), \end{aligned} \qquad \begin{aligned} \boldsymbol{v}_\pm(\psi) &= \begin{pmatrix} \mathrm{cn}(\psi,k) \\ \mathrm{sn}(\psi,k) \\ \pm\alpha\,\mathrm{dn}(\psi,k) \end{pmatrix} \\ k &= \sqrt{1-\frac{\beta^2}{\alpha^2}}. \end{aligned} \tag{5.11}$$

form a (confocal) checkerboard IC-net and are tangent to the ellipse

$$\frac{x^2}{\alpha^2} + \frac{y^2}{\beta^2} = 1.$$

The parameters $s, \tilde{s}$ determine the associated hyperboloids $\mathcal{H}, \tilde{\mathcal{H}}$ of the pencil

$$(\alpha^2+\lambda)v^2 + (\beta^2+\lambda)w^2 = d^2 + \lambda$$

according to

$$\lambda = \alpha^2\,\mathrm{cs}^2\left(\frac{s}{2}, k\right).$$

"Embedded" elliptic confocal checkerboard IC-nets are obtained by requiring periodicity, that is,

$$s + \tilde{s} = 4\mathsf{K} + \frac{4\mathsf{K}}{N}, \quad N \in \mathbb{N}, \tag{5.12}$$

where the quarter-period $\mathsf{K}(k)$ of the Jacobi elliptic functions is given by the complete elliptic integral of the first kind, and demanding that the two families of lines $\boldsymbol{v}^v$ and $\boldsymbol{v}^h$ coincide up to their orientation. The latter may be achieved by relating the parameters ψ_0^v and ψ_0^h according to

$$\psi_0^v = 2\mathsf{K} + \psi_0^h - s$$

so that

$$\boldsymbol{v}_{2n}^v = -\boldsymbol{v}_{-2n+1}^h, \quad \boldsymbol{v}_{2n+1}^v = -\boldsymbol{v}_{-2n}^h.$$

If we now parametrise the constraint (5.12) by

$$s = 2\mathsf{K} + \frac{4\mathsf{K}}{N} - \kappa, \quad \tilde{s} = 2\mathsf{K} + \kappa,$$

where κ is the arbitrary parameter, then

$$\psi_0^h = \psi_0^v + \frac{4\mathsf{K}}{N} - \kappa. \tag{5.13}$$

For $\kappa = 0$, the lines $\boldsymbol{v}_{2n}^v$ and $\boldsymbol{v}_{2n-1}^v$ coincide up to their orientation and the quadric $\tilde{\mathcal{H}}$ becomes the cone $(5.3)_1$ since $\tilde{s} = 2\mathsf{K}$ so that $\tilde{\lambda} = 0$. Hence, as discussed in Section 3, an elliptic IC-net is obtained as depicted in Figure 5.1 (left) for $N = 32$ and $\psi_0^v = 0.2$. Here, $\alpha = 2$ and $\beta = 1$. As κ increases, the coinciding lines separate and the circles of zero radius between the coinciding lines enlarge so that a non-degenerate confocal checkerboard emerges with $\tilde{\mathcal{H}}$ being a proper hyperboloid. An elliptic confocal checkerboard IC-net for $\kappa = 0.1$ is displayed in Figure 5.1 (right).

5.2 Hyperbolic confocal checkerboard IC-nets

The lines of "hyperbolic" confocal checkerboard IC-nets are tangent to a hyperbola given by, without loss of generality,

$$\frac{x^2}{\alpha^2} - \frac{y^2}{\beta^2} = 1.$$

In terms of the Blaschke model, the associated pencil of quadrics

$$(\alpha^2+\lambda)v^2 - (\beta^2-\lambda)w^2 = d^2 + \lambda \tag{5.14}$$

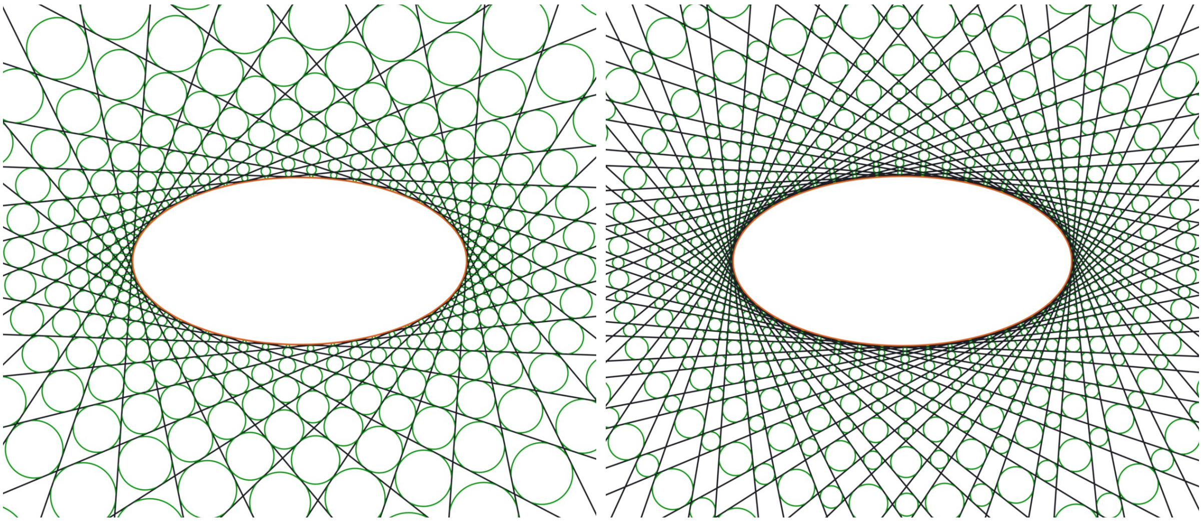

Figure 5.1. Periodic elliptic confocal checkerboard IC-nets for $\alpha = 2$, $\beta = 1$, $N = 32$. *Left:* $\kappa = 0$, corresponding to the degenerate case of an IC-net. *Right:* $\kappa = 0.1$.

is generated by the pair of quadrics

$$\alpha^2 v^2 - \beta^2 w^2 = d^2, \quad v^2 + w^2 = 1.$$

The base curve is the intersection of these two quadrics (and all members of the pencil), corresponding to type Ia_- of the classification of pencils of quadrics. The two components of the base curve are mapped into each other via $v \to -v$. As in the elliptic case, the base curve may be parametrised in terms of elliptic functions and one has to distinguish between two cases.

The case $-\alpha^2 \leqslant \lambda \leqslant 0$

In this case, any quadric $\mathcal{H}$ constitutes a one-sheeted hyperboloid (or a cone for $\lambda = 0$ and an elliptic cylinder for $\lambda = -\alpha^2$) which is aligned with the v-axis. It is then readily verified that

$$\boldsymbol{v}_\pm(\psi) = \begin{pmatrix} v_\pm(\psi) \\ w(\psi) \\ d(\psi) \end{pmatrix} = \begin{pmatrix} \pm \operatorname{dn}(\psi, k) \\ k \operatorname{sn}(\psi, k) \\ \alpha \operatorname{cn}(\psi, k) \end{pmatrix}, \quad k = \sqrt{\frac{\alpha^2}{\alpha^2 + \beta^2}} \tag{5.15}$$

covers all points of these two components. Given any two points of the form (5.5) on the two components of the base curve, one may now determine the corresponding quadric $\mathcal{H}$ of the pencil which contains the lines (5.6) as generators for fixed s and all ψ_0. A calculation along the lines of the previous subsection reveals that the pencil parameter λ linked to the parameter s is given by

$$\lambda = -\alpha^2 \operatorname{cn}^2\left(\frac{s}{2}, k\right). \tag{5.16}$$

The case $\lambda \geqslant \beta^2$

This case corresponds to the remaining two-sheeted hyperboloids $\mathcal{H}$ (or a hyperbolic cylinder for $\lambda = \beta^2$) of the pencil (5.14) which are aligned with the Blaschke cylinder. In analogy with the elliptic case, it is convenient to introduce a parameter ε in the parametrisation

$$\boldsymbol{v}_\pm^\varepsilon(\psi) = \begin{pmatrix} \pm \operatorname{dn}(\psi, k) \\ k \operatorname{sn}(\psi, k) \\ \varepsilon\alpha \operatorname{cn}(\psi, k) \end{pmatrix}, \quad \varepsilon^2 = 1$$

of the base curve. Then, any pair of points of the type (5.9) on any fixed component of the base curve may be connected by a line (5.10) which constitutes a generator of the quadric (5.14) for

$$\lambda = (\alpha^2 + \beta^2) \operatorname{ds}^2\left(\frac{s}{2}, k\right)$$

independently of the value of ψ.

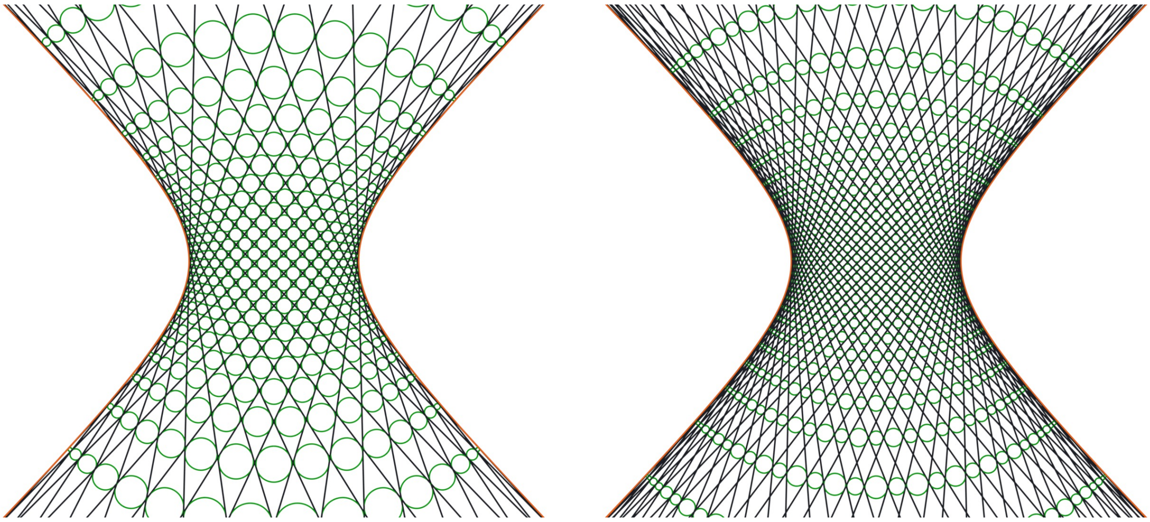

Figure 5.2. Periodic hyperbolic confocal checkerboard IC-nets for $\alpha = \beta = 1$, $N = 32$. *Left:* $\kappa = 0$, corresponding to the degenerate case of an IC-net. *Right:* $\kappa = 0.1$.

Construction of hyperbolic confocal checkerboard IC-nets

Once again, as an illustration, we now consider two quadrics $\mathcal{H}$ and $\tilde{\mathcal{H}}$ of the pencil (5.14) defined via the relation (5.16) by given parameters s and $\tilde{s}$. The formulae (5.11) for the two families of lines of the corresponding confocal checkerboard IC-nets remain valid in the current hyperbolic case but $\boldsymbol{v}_\pm$ and k are now defined by (5.15). In fact, the conditions (5.12)-(5.13) for embeddedness are likewise applicable. Thus, for $\kappa = 0$, one obtains hyperbolic IC-nets as illustrated in Figure 5.2 (left) for $N = 32$, $\psi_0^v = 0.2$ and $\alpha = \beta = 1$. Furthermore, a hyperbolic confocal checkerboard IC-net for $\kappa = 0.1$ is depicted in Figure 5.2 (right).

5.3 IC-nets and discrete confocal conics

We conclude this section by relating IC-nets to the discrete confocal conics proposed in [BSST1, BSST2]. For brevity, we focus on the class of IC-nets which is subsumed by the class of elliptic checkerboard IC-nets captured by Theorem 5.1. These IC-nets are associated with the choice $\tilde{s} = 2\mathsf{K}$, corresponding to a cone as the corresponding quadric $\tilde{\mathcal{H}}$. Thus, if we set $s = 2\mathsf{K} + \delta$ and $\psi_0^{v/h} = \delta n_0^{v/h}$ then the explicit parametrisation (5.11) leads to the following corollary.

Corollary 5.2. *The (coinciding pairs of non-oriented) lines of an elliptic IC-net of the type captured by Theorem 5.1 may be represented by the lines*

$$\boldsymbol{v}_{n_1}^v = \boldsymbol{v}(\delta(n_0^v + n_1)), \quad \boldsymbol{v}_{n_2}^h = \boldsymbol{v}(\delta(n_0^h - n_2)), \quad n_i \in \mathbb{Z}, \tag{5.17}$$

where

$$\boldsymbol{v}(\psi) = \begin{pmatrix} v(\psi) \\ w(\psi) \\ d(\psi) \end{pmatrix} = \begin{pmatrix} \mathrm{cn}(\psi, k) \\ \mathrm{sn}(\psi, k) \\ \alpha\,\mathrm{dn}(\psi, k) \end{pmatrix}, \quad k = \sqrt{1 - \frac{\beta^2}{\alpha^2}}. \tag{5.18}$$

In the sense of Laguerre geometry, the quadruples of oriented lines

$$\boldsymbol{v}_{n_1}^v, \quad \boldsymbol{v}_{n_2}^h, \quad -\boldsymbol{v}_{n_1+1}^v, \quad -\boldsymbol{v}_{n_2+1}^h$$

are tangent to circles so that, by construction,

$$\begin{vmatrix} 1 & v_{n_1}^v & w_{n_1}^v & d_{n_1}^v \\ 1 & v_{n_2}^h & w_{n_2}^h & d_{n_2}^h \\ 1 & -v_{n_1+1}^v & -w_{n_1+1}^v & -d_{n_1+1}^v \\ 1 & -v_{n_2+1}^h & -w_{n_2+1}^h & -d_{n_2+1}^h \end{vmatrix} = 0 \tag{5.19}$$

which coincides with the known identity [NIST]

$$\begin{vmatrix} 1 & \operatorname{sn}(z_1,k) & \operatorname{cn}(z_1,k) & \operatorname{dn}(z_1,k) \\ 1 & \operatorname{sn}(z_2,k) & \operatorname{cn}(z_2,k) & \operatorname{dn}(z_2,k) \\ 1 & \operatorname{sn}(z_3,k) & \operatorname{cn}(z_3,k) & \operatorname{dn}(z_3,k) \\ 1 & \operatorname{sn}(z_4,k) & \operatorname{cn}(z_4,k) & \operatorname{dn}(z_4,k) \end{vmatrix} = 0, \quad z_1 + z_2 + z_3 + z_4 = 0 \tag{5.20}$$

for Jacobi elliptic functions if one identifies the arguments in (5.19) and (5.20) appropriately. The point of intersection $(x_\times, y_\times)$ of two lines $\boldsymbol{v}^v_{n_1}$ and $\boldsymbol{v}^h_{n_2}$ is given by the solution of the two linear equations

$$v^v_{n_1} x_\times + w^v_{n_1} y_\times = d^v_{n_1}, \quad v^h_{n_2} x_\times + w^h_{n_2} y_\times = d^h_{n_2}. \tag{5.21}$$

If we now make the change of variables

$$\begin{aligned} n_1 &= m_2 + m_1, \quad \xi_1 = \delta\left[m_1 + \frac{1}{2}(n^v_0 + n^h_0)\right] \\ n_2 &= m_2 - m_1, \quad \xi_2 = \delta\left[m_2 + \frac{1}{2}(n^v_0 - n^h_0)\right], \end{aligned}$$

leading to

$$\boldsymbol{v}^v = \boldsymbol{v}(\xi_1 + \xi_2), \quad \boldsymbol{v}^h = \boldsymbol{v}(\xi_1 - \xi_2),$$

where we have suppressed the dependence on $m_i \in \frac{1}{2}\mathbb{Z}$, then consideration of the sum and the difference of the linear equations (5.21) and application of the addition theorems for Jacobi elliptic functions produces the following result.

Theorem 5.3. *The points of intersection of the pairs of lines* $(\boldsymbol{v}^v_{m_2+m_1}, \boldsymbol{v}^h_{m_2-m_1})$ *of the elliptic IC-nets* (5.17), (5.18) *are given by the compact formulae*

$$x_\times = \alpha \operatorname{cd}(\xi_1,k)\operatorname{dc}(\xi_2,k), \quad y_\times = \alpha(1-k^2)\operatorname{sd}(\xi_1,k)\operatorname{nc}(\xi_2,k) \tag{5.22}$$

with

$$\xi_1 = \delta\left[m_1 + \frac{1}{2}(n^v_0 + n^h_0)\right], \quad \xi_2 = \delta\left[m_2 + \frac{1}{2}(n^v_0 - n^h_0)\right]. \tag{5.23}$$

These lie on the conics

$$\frac{x^2_\times}{\lambda^e(\xi_2)} + \frac{y^2_\times}{\mu^e(\xi_2)} = 1, \quad \frac{x^2_\times}{\lambda^h(\xi_1)} + \frac{y^2_\times}{\mu^h(\xi_1)} = 1, \tag{5.24}$$

where

$$\begin{aligned} \lambda^e &= \alpha^2 \operatorname{dc}^2(\xi_2,k), \qquad \mu^e = \alpha^2(1-k^2)\operatorname{nc}^2(\xi_2,k) \\ \lambda^h &= \alpha^2 k^2 \operatorname{cd}^2(\xi_1,k), \quad \mu^h = -\alpha^2 k^2(1-k^2)\operatorname{sd}^2(\xi_1,k), \end{aligned}$$

which are confocal to the ellipse of contact (5.1).

Proof. It is straightforward to verify that ξ_1 and ξ_2 as given by (5.23) obey the quadratic relations (5.24). Moreover, since

$$\lambda^e - \mu^e = \lambda^h - \mu^h = \alpha^2 k^2 = \alpha^2 - \beta^2,$$

the conics (5.24) are indeed in the set of confocal conics defined by the ellipse (5.1). □

As proven in [AB], the centres of the circles of IC-nets lie on affine transforms of confocal conics. Hence, the algebraic structure of their coordinates should coincide with that of the points of intersection of pairs of lines as given by (5.22). In order to confirm this assertion, it is observed that the centre $(x_\odot, y_\odot)$ and the radius $r_\odot$ of any particular circle are determined by solving any three equations of the linear system

$$v x_\odot + w y_\odot - r_\odot = d, \quad \boldsymbol{v} \in \{\boldsymbol{v}^v_{n_1}, \boldsymbol{v}^h_{n_2}, -\boldsymbol{v}^v_{n_1+1}, -\boldsymbol{v}^h_{n_2+1}\}.$$

Elimination of $r_\odot$ leads to the pair of equations

$$\begin{aligned} (v^v_{n_1} - v^h_{n_2})x_\odot + (w^v_{n_1} - w^h_{n_2})y_\odot &= (d^v_{n_1} - d^h_{n_2}) \\ (v^v_{n_1+1} - v^h_{n_2+1})x_\odot + (w^v_{n_1+1} - w^h_{n_2+1})y_\odot &= (d^v_{n_1+1} - d^h_{n_2+1}). \end{aligned} \tag{5.25}$$

Once again, the addition theorems for Jacobi elliptic functions and the double- and half-“angle” formulae [NIST]

$$\begin{aligned}\operatorname{sn}(2z,k) &= \frac{2\operatorname{sn}(z,k)\operatorname{cn}(z,k)\operatorname{dn}(z,k)}{1-k^2\operatorname{sn}^4(z,k)}\\ \operatorname{sn}^2(\tfrac{1}{2}z,k) &= \frac{1-\operatorname{cn}(z,k)}{1+\operatorname{dn}(z,k)}\end{aligned}$$

give rise to a compact form of its solution.

Theorem 5.4. *The centres of the circles of the elliptic IC-nets* (5.17), (5.18) *are given by*

$$\begin{aligned}x_\odot &= \alpha\operatorname{dc}(\tfrac{\delta}{2},k)\operatorname{cd}(\xi_1,k)\operatorname{dc}(\xi_2+\tfrac{\delta}{2},k)\\ y_\odot &= \alpha(1-k^2)\operatorname{nc}(\tfrac{\delta}{2},k)\operatorname{sd}(\xi_1,k)\operatorname{nc}(\xi_2+\tfrac{\delta}{2},k).\end{aligned} \tag{5.26}$$

These constitute the vertices of a discrete confocal coordinate system on the plane, that is, there exist functions $f(m_1), g(m_1)$ and $\tilde{f}(m_2), \tilde{g}(m_2)$ such that

$$\begin{pmatrix}x_\odot\\ y_\odot\end{pmatrix} = \frac{1}{\sqrt{a-b}}\begin{pmatrix}f(m_1)\tilde{f}(m_2)\\ g(m_1)\tilde{g}(m_2)\end{pmatrix} \tag{5.27}$$

and

$$\begin{aligned}f(m_1)f(m_1+\tfrac{1}{2}) + g(m_1)g(m_1+\tfrac{1}{2}) &= a-b\\ \tilde{f}(m_2)\tilde{f}(m_2+\tfrac{1}{2}) - \tilde{g}(m_2)\tilde{g}(m_2+\tfrac{1}{2}) &= a-b,\end{aligned} \tag{5.28}$$

where $a-b=\alpha^2k^2$.

Proof. The structure of the solution (5.26) of the linear system (5.25) shows that it factorises according (5.27). If we choose the scaling of the functions f, g and $\tilde{f}, \tilde{g}$ in such a manner that

$$\begin{aligned}f &= |\alpha k|\sqrt{\operatorname{dc}(\tfrac{\delta}{2},k)\operatorname{cd}(\xi_1,k)}\\ \tilde{f} &= \alpha\sqrt{\operatorname{dc}(\tfrac{\delta}{2},k)\operatorname{dc}(\xi_2+\tfrac{\delta}{2})}\\ g &= |\alpha k|\sqrt{1-k^2}\sqrt{\operatorname{nc}(\tfrac{\delta}{2},k)\operatorname{sd}(\xi_1,k)}\\ \tilde{g} &= \alpha\sqrt{1-k^2}\sqrt{\operatorname{nc}(\tfrac{\delta}{2},k)\operatorname{nc}(\xi_2+\tfrac{\delta}{2})}\end{aligned} \tag{5.29}$$

then it may be verified that the difference equations (5.28) are indeed satisfied. Here, we have assumed that $\operatorname{cn}(\tfrac{\delta}{2},k)>0$, which is compatible with the continuum limit $\delta\to 0$. The other case may be dealt with in a similar manner but requires the introduction of factors of the type $(-1)^{m_1}$ and $(-1)^{m_2}$ in the definitions of f, g and $\tilde{f}, \tilde{g}$ respectively. This corresponds to “superdiscrete” IC-nets which do not admit a continuum limit. Finally, since the pair (5.27), (5.28) characterises discrete confocal coordinate systems on the plane [BSST2], the proof is complete. □

Remark 5.1. Up to the shift of the argument $\xi_2\to\xi_2+\frac{\delta}{2}$ and the affine transformation

$$(x_\odot, y_\odot)\to(Ax_\odot, By_\odot),\qquad A=\operatorname{cd}(\tfrac{\delta}{2},k),\quad B=\operatorname{cn}(\tfrac{\delta}{2},k).$$

the formulae (5.22) and (5.26) coincide. This confirms that the centres $(x_\odot, y_\odot)$ lie on affine transforms of the confocal conics associated with the ellipse (5.1). Equivalently, this implies that the affine transforms $(A^{-1}x_\times, B^{-1}y_\times)$ are likewise vertices of a discrete confocal coordinate system. In fact, the points $(x_\odot, y_\odot)$ and $(A^{-1}x_\times, B^{-1}y_\times)$ are part of the same (extended) discrete confocal coordinate system of $(\frac{1}{2}\mathbb{Z})^2$ combinatorics. Another implication of this connection is that the functions f, g and $\tilde{f}, \tilde{g}$ as given by (5.29) satisfy the algebraic identities

$$Af^2+Bg^2=a-b,\quad A\tilde{f}^2-B\tilde{g}^2=a-b. \tag{5.30}$$

The latter constitute the algebraic constraints on discrete confocal coordinate systems as defined by (5.27), (5.28) which give rise to the privileged IC-net-related discrete confocal coordinate systems touched upon in the preceding. These have been discussed in detail in [BSST2].

Remark 5.2. If we eliminate, for instance, g between $(5.28)_1$ and $(5.30)_1$ then we obtain a first-order difference equation for f, namely

$$(A^2 - B^2)f_{\frac{1}{2}}^2 f^2 + 2(a-b)B^2 f_{\frac{1}{2}} f - (a-b)A(f_{\frac{1}{2}}^2 + f^2) + (a-b)^2(1-B^2) = 0,$$

where $f = f(m_1)$, $f_{\frac{1}{2}} = f(m_1 + \frac{1}{2})$. The latter may be regarded as a first integral of a difference equation of second order. Indeed, if we regard B^2 as the associated constant of integration then elimination of B leads to

$$f_1 = \frac{F^1(f_{\frac{1}{2}}) - fF^2(f_{\frac{1}{2}})}{F^2(f_{\frac{1}{2}}) - fF^3(f_{\frac{1}{2}})} \tag{5.31}$$

with

$$F^1(f_{\frac{1}{2}}) = 2(a-b)f_{\frac{1}{2}}, \quad F^2(f_{\frac{1}{2}}) = f_{\frac{1}{2}}^2 + (a-b)A, \quad F^3(f_{\frac{1}{2}}) = 2Af_{\frac{1}{2}} \tag{5.32}$$

and $f_1 = f(m_1 + 1)$. Remarkably, (5.31), (5.32) constitutes a particular symmetric case of an 18-parameter family of integrable reversible mappings of the plane known as QRT maps [QRT]. These play a fundamental role in the theory of discrete integrable systems and are known to be parametrisable in terms of elliptic functions, which is in agreement with the parametrisation of IC-nets presented in the preceding.

6 Generalised checkerboard IC-nets

The construction of checkerboard IC-nets in terms of the Blaschke cylinder model as described in Section 3 may immediately be generalised in a natural manner. Thus, for any given pencil of quadrics which contains the Blaschke cylinder $\mathcal{Z}$, we first select two ("horizontal" and "vertical") sequences of hyperboloids $\mathcal{H}_n^h$ and $\mathcal{H}_n^v$ belonging to this pencil. We then choose two points ℓ_1 and m_1 of the associated hypercycle base curve and iteratively construct two sequences of points ℓ_n and m_n on the hypercycle base curve by "moving along" generators L_n and M_n of the corresponding hyperboloids $\mathcal{H}_n^h$ and $\mathcal{H}_n^v$ respectively, that is,

$$L_n = (\ell_n, \ell_{n+1}) \subset \mathcal{H}_n^h, \quad M_n = (m_n, m_{n+1}) \subset \mathcal{H}_n^v.$$

If, for any i, k, the two hyperboloids $\mathcal{H}_i^h$ and $\mathcal{H}_k^v$ coincide and the corresponding generators L_i and M_k have been chosen in such a manner that they are not in the same family of generators of the common hyperboloid then the lines ℓ_i, ℓ_{i+1} and m_k, m_{k+1} circumscribe an oriented circle. In particular, if $\mathcal{H}_n :=$ $\mathcal{H}_n^h = \mathcal{H}_n^v$ and $\mathcal{H}_{n+2} = \mathcal{H}_n$ then standard checkerboard IC-nets are retrieved. An example of a generalised checkerboard IC-net in the case of period 4, that is, $\mathcal{H}_{n+4} = \mathcal{H}_n$ is displayed in Figure 6.1 (left). Another example of period 4 which involves only three hyperboloids with $\mathcal{H}_{4n+1} = \mathcal{H}_1$, $\mathcal{H}_{2n+2} = \mathcal{H}_2$, $\mathcal{H}_{4n+3} = \mathcal{H}_3$ is also depicted in Figure 6.1 (right).

In algebraic terms, the construction of generalised checkerboard IC-nets may be implemented as follows. Here, we focus on a pencil of quadrics which has already been normalised so that

$$(a+\lambda)v^2 + (b+\lambda)w^2 = d^2 + \lambda$$

with underlying normalised cone and Blaschke cylinder

$$av^2 + bw^2 = d^2, \quad v^2 + w^2 = 1.$$

Any prescribed sequence of (suitably constrained) pencil parameters λ_n then corresponds to a sequence of hyperboloids $\mathcal{H}_n$ which, in the following, represents one of $\mathcal{H}_n^h$ or $\mathcal{H}_n^v$. The procedure described below may then also be applied to the other sequence of hyperboloids. Now, given a point $\boldsymbol{v}_n = (v_n, w_n, d_n)$ (that is, either ℓ_n or m_n) on the hypercycle base curve, the two choices for the point $\boldsymbol{v}_{n+1}$ corresponding to the pair of generators of the hyperboloid $\mathcal{H}_n$ passing through $\boldsymbol{v}_n$ are obtained by intersecting the hypercycle base curve with the tangent plane of $\mathcal{H}_n$ at $\boldsymbol{v}_n$. Algebraically, this is expressed by

$$(a+\lambda)v_n v_{n+1} + (b+\lambda)w_n w_{n+1} = d_n d_{n+1} + \lambda. \tag{6.1}$$

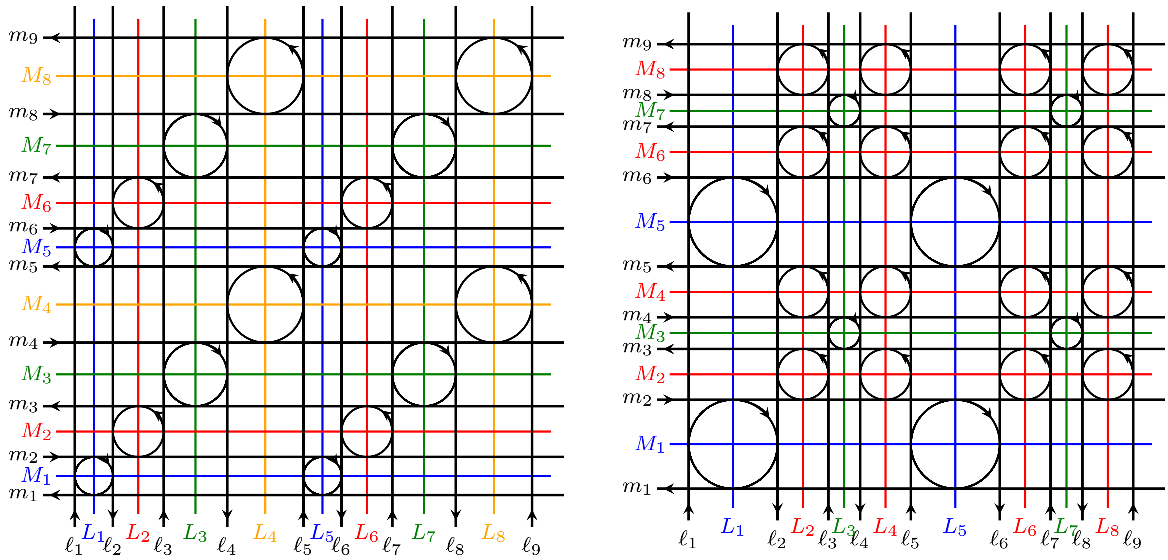

Figure 6.1. Examples of generalised checkerboard IC nets involving three (right) and four (left) different hyperboloids.

If we eliminate v_{n+1} and w_{n+1} between this tangency condition and the hypercycle base curve constraints

$$av_{n+1}^2 + bw_{n+1}^2 = d_{n+1}^2, \quad v_{n+1}^2 + w_{n+1}^2 = 1 \tag{6.2}$$

then we obtain a quartic in d_{n+1} which, by construction, contains the factor $(d_{n+1} - d_n)^2$. Accordingly, we are left with a symmetric and biquadratic relation between d_{n+1} and d_n which reads

$$\kappa_d(d_n^2 d_{n+1}^2 + ab) + d_n^2 + d_{n+1}^2 + 2\kappa_v\kappa_w d_n d_{n+1} = 0, \tag{6.3}$$

where

$$\kappa_v = \frac{\lambda^2 + 2a\lambda + ab}{\lambda^2 - ab}, \quad \kappa_w = \frac{\lambda^2 + 2b\lambda + ab}{\lambda^2 - ab}, \quad \kappa_d = 4\frac{\lambda(\lambda + a)(\lambda + b)}{(\lambda^2 - ab)^2}.$$

For a given point $\boldsymbol{v}_n$, the two choices for the point $\boldsymbol{v}_{n+1}$ therefore correspond to the two roots of the quadratic (6.3). In order to verify algebraically the uniqueness of the components v_{n+1} and w_{n+1} once d_{n+1} has been fixed, it is convenient to be aware of the pair of linear equations (in v_{n+1} and w_{n+1})

$$\kappa_w a v_n v_{n+1} + \kappa_v b w_n w_{n+1} + d_n d_{n+1} = 0, \quad \kappa_v v_n v_{n+1} + \kappa_w w_n w_{n+1} = 1 \tag{6.4}$$

which may be extracted from the compatible system (6.1), (6.2). One may directly verify that the pair (6.4) may be combined to reproduce the tangency condition (6.1).

We observe in passing that for any given sequence λ_n, the biquadratic equation (6.3) may be regarded as a non-autonomous extension of the first integral of a particular member of the symmetric class of QRT maps alluded to at the end of the previous section. In the case of standard confocal checkerboard IC-nets, the coefficients of the biquadratic are of period 2. Non-autonomous QRT maps with periodic coefficients and their relation to discrete Painlevé equations have been discussed in detail in [RGW].

As an illustration of the above formalism, we consider the "elliptic" case analogous to that discussed in Section 5.1, that is,

$$a = \alpha^2, \quad b = \beta^2, \quad \lambda \geqslant 0.$$

Then, any given sequence s_n determines both the hyperboloids $\mathcal{H}_n$ according to

$$\lambda_n = \alpha^2 \operatorname{cs}^2\left(\frac{s_n}{2}, k\right), \quad k = \sqrt{1 - \frac{\beta^2}{\alpha^2}}$$

and, via $\operatorname{sgn}(s_n)$, to which families the generators (L_n or M_n) belong. The solution of the system (6.3), (6.4) is given by

$$\boldsymbol{v}_n = \begin{pmatrix} \operatorname{cn}(\psi_n, k) \\ \operatorname{sn}(\psi_n, k) \\ (-1)^n \alpha \operatorname{dn}(\psi_n, k) \end{pmatrix}, \quad \psi_{n+1} = \psi_n + s_n$$

and the coefficients κ_v, κ_w and κ_d read

$$\kappa_v = \operatorname{nc}(s_n, k), \quad \kappa_w = \operatorname{dc}(s_n, k), \quad \kappa_d = \alpha^{-2} \operatorname{sc}^2(s_n, k)$$

so that the relations (6.4) are seen to encode the classical "pencil" of addition theorems (5.7) for Jacobi elliptic functions.

We conclude by translating the construction of "periodic" generalised checkerboard IC-nets in terms of the Blaschke model into a direct geometric construction in the plane with suitably prescribed Cauchy data. Here, we consider the case $\mathcal{H}_n^h = \mathcal{H}_n^v = \mathcal{H}_n$. We first observe that if we prescribe the line m_1 and the lines ℓ_n which are in oriented contact with a given hypercycle then a corresponding generalised checkerboard IC-net for which each quadruplet of lines $\ell_n, \ell_{n+1}, m_n, m_{n+1}$ is in oriented contact with a circle is uniquely determined. Indeed, there exists a unique line m_2 which is in oriented contact with the hypercycle and the unique circle in oriented contact with the lines ℓ_1, ℓ_2 and m_1. In this manner, all lines m_n may be constructed iteratively. In the periodic case $\mathcal{H}_{n+N} = \mathcal{H}_n$, $N \geqslant 2$ for which the circles inscribed in the quadruples of lines $\ell_n, \ell_{n+1}, m_{n+kN}, m_{n+kN+1}$ are required to exist (cf. Figure 6.1 (left) for $N = 4$), it is sufficient to prescribe the lines m_1 and $\ell_1, \ldots, \ell_{N+1}$. In order to make good this assertion, we first construct the lines $m_2, \ldots, m_{N+1}$ in the manner described above. The triples of lines m_1, m_2, ℓ_{N+1} and ℓ_1, ℓ_2, m_{N+1} then give rise to associated circles in oriented contact which, in turn, determine the lines ℓ_{N+2} and m_{N+2} via oriented contact with the respective circle and the hypercycle. By virtue of Lemma 3.2, the existence of these two circles and the circle circumscribed by the lines ℓ_1, ℓ_2, m_1, m_2 now implies that the lines $L_1 = (\ell_1, \ell_2), M_1 = (m_1, m_2)$ and $L_{N+1} = (\ell_{N+1}, \ell_{N+2}), M_{N+1} = (m_{N+1}, m_{N+2})$ are generators of the same hyperboloid which one may denote by $\mathcal{H}_1 = \mathcal{H}_{N+1}$ and, moreover, that L_{N+1} and M_{N+1} are not in the same family of generators of $\mathcal{H}_1$. This guarantees the existence of a circle which is in oriented contact with the quadruple of lines $\ell_{N+1}, \ell_{N+2}, m_{N+1}, m_{N+2}$. Iterative application of this procedure now generates the entire generalised checkerboard IC-net of period N. Finally, we merely mention that generalised checkerboard IC-nets of the type displayed in Figure 6.1 (right) are determined by lines m_1 and $\ell_1, \ell_2, \ell_3, \ell_4$ which are in oriented contact with a hypercycle.

A Laguerre geometry

Here, we present the basic facts about Laguerre geometry, focussing on the Blaschke cylinder model employed in this paper for studying checkerboard IC-nets. We begin with the more fundamental Lie sphere geometry. Lie sphere geometry in the plane is the geometry of oriented circles and lines. These are described as elements of the Lie quadric

$$\mathcal{L} = P(\mathbb{L}^{3,2}), \quad \mathbb{L}^{3,2} = \{x \in \mathbb{R}^{3,2} | < x, x >_{\mathbb{R}^{3,2}} = 0\}.$$

Let e_1, e_2, e_3, e_4, e_5 be an orthonormal basis with signature $(+++--)$. For our purposes, another basis $e_1, e_2, e_5, e_\infty, e_0$ defined by

$$e_0 = \frac{1}{2}(e_4 - e_3), \quad e_\infty = \frac{1}{2}(e_4 + e_3), \quad < e_0, e_\infty > = -\frac{1}{2}$$

turns out to be more convenient. Elements of $\mathcal{L}$ with non-vanishing e_0-component are identified with oriented circles $|\boldsymbol{x} - \boldsymbol{c}|^2 = r^2$, centred at $\boldsymbol{c} \in \mathbb{R}^2$ and of radius $r \in \mathbb{R}$:

$$s = \boldsymbol{c} + r e_5 + (|\boldsymbol{c}|^2 - r^2) e_\infty + e_0. \tag{A.1}$$

Points are circles of radius $r = 0$, and oriented lines $(\boldsymbol{v}, \boldsymbol{x})_{\mathbb{R}^2} = d$ are elements of $\mathcal{L}$ with vanishing e_0-component:

$$p = \boldsymbol{v} + e_5 + 2d e_\infty. \tag{A.2}$$

The incidence $< p, s >= 0$ is the condition

$$(\boldsymbol{c}, \boldsymbol{v}) - r = d \tag{A.3}$$

of oriented contact of a circle and a line.

The Lie sphere transformation group $PO(3,2)$ acting on $P(\mathbb{R}^{3,2})$ preserves the Lie quadric $\mathcal{L}$ and maps oriented circles and lines to oriented circles and lines, preserving oriented contact. Its subgroup of Laguerre transformations preserves the set of straight lines or, equivalently, the hyperplane

$$\mathsf{P} = \text{span}\{e_1, e_2, e_5, e_\infty\} = \{w \in \mathbb{R}^{3,2} | < w, e_\infty >= 0\}.$$

Direct computation shows that the elements of $PO(3,2)$ preserving the hyperplane P are of the form

$$\begin{pmatrix} \lambda B & 0 & \alpha \\ b^T & 1 & \nu \\ 0 & 0 & \lambda^{-2} \end{pmatrix}$$

in the basis $e_1, e_2, e_5, e_\infty, e_0$, where

$$B \in O(2,1), \quad b \in \mathbb{R}^{2,1}, \quad \alpha = \frac{\lambda}{2} Bb, \quad \nu = \frac{\lambda}{4}(b,b)_{\mathbb{R}^{2,1}}, \quad \lambda \in \mathbb{R}.$$

In order to pass to the *Blaschke cylinder model* of Laguerre geometry, we confine ourselves to the subspace $\mathcal{P} = \text{span}\{e_1, e_2, e_5, e_\infty\}$. Elements of this space can be identified with straight lines, described (projectively) by

$$\tilde{p} = \tilde{\boldsymbol{v}} + \tilde{s} e_5 + 2\tilde{d} e_\infty$$

as points of the Blaschke cylinder

$$\mathcal{Z} = \{[\tilde{p}] \in P(\mathbb{R}^{2,1,1}) | |\tilde{\boldsymbol{v}}|^2 = \tilde{s}^2\}. \tag{A.4}$$

Identification with (A.2) is made via the normalisation of the e_0-component: $\boldsymbol{v} = \tilde{\boldsymbol{v}}/\tilde{s}$, $d = \tilde{d}/\tilde{s}$. It is noted that the symmetry with the description of circles (A.1) in Lie sphere geometry is no longer present in the Blaschke cylinder model, and oriented circles are described as the sets of all straight lines in oriented contact, i.e., the sets of lines satisfying the condition (A.3), that is

$$S = \{(\boldsymbol{v}, d) \in \mathbb{R}^3 | (\boldsymbol{c}, \boldsymbol{v})_{\mathbb{R}^2} - r = d\}.$$

Furthermore, Laguerre transformations restricted to the subspace of lines $\mathsf{P} = \text{span}\{e_1, e_2, e_5, e_\infty\}$ are of the form

$$A = \begin{pmatrix} \lambda B & 0 \\ b^T & 1 \end{pmatrix}. \tag{A.5}$$

Theorem A.1. *The group of Laguerre transformations in the Blaschke (projective) cylinder model (in the basis e_1, e_2, e_5, e_∞) is represented by matrices of the form* (A.5)*, where $B \in O(2,1)$, $b \in \mathbb{R}^{2,1}$, $\lambda \in \mathbb{R}$. These transformations preserve the Blaschke cylinder* (A.4)*.*

We conclude by observing that Euclidean motions

$$\boldsymbol{x} \to \tilde{\boldsymbol{x}} = R\boldsymbol{x} + \Delta, \quad R \in O(2), \quad \Delta \in \mathbb{R}^2$$

are particular Laguerre transformations, the corresponding matrix of which is given by (A.5) with

$$B = \begin{pmatrix} R^T & 0 \\ 0 & 1 \end{pmatrix}, \quad b = \begin{pmatrix} 2R\Delta \\ 0 \end{pmatrix} \tag{A.6}$$

and $\lambda = 1$.

References

[AB] [Bl] [BT] [BSST1] [BSST2] [BS] [Bö] [Da1] [Da3] [DR] [IR] [IT] [LT] [Le] [NIST] [PGB] [QRT] [RGW] [RJ] [Sch] [SPG]

Bibliography

[Ag] S.I. Agafonov. Confocal conics and 4-webs of maximal rank, arxiv:1912.01817v1 (2019).

[AVK] A.A. Akhmetshin, Yu.S. Vol'vovskij, I.M. Krichever. *Discrete analogs of the Darboux-Egorov metrics*, Proc. Steklov Inst. Math., (1999), **225**, 16–39.

[Ak] A.V. Akopyan. 3-Webs generated by confocal conics and circles. *Geometriae Dedicata*, (2017).

[AB] A.V. Akopyan, A.I. Bobenko. Incircular nets and confocal conics, *Trans. AMS* **370:4** (2018) 2825–2854.

[ABST] A.V. Akopyan, A.I. Bobenko, W.K. Schief, J. Techter. On mutually diagonal nets on (confocal) quadrics and 3-dimensional webs, arXiv:1908.00856, (2019).

[Ar] V.I. Arnold. *Mathematical methods of classical mechanics*, Graduate Texts in Mathematics, Vol. 60, 2nd ed. Springer-Verlag, New York, (1989), xvi+508 pp.

[Bl] W. Blaschke. Untersuchungen über die Geometrie der Speere in der Euklidischen Ebene, Separatdruck aus "Monatshefte f. Mathematik u. Physik", XXI, Hamburg (1910).

[BT] W. Blaschke, G. Thomsen. *Vorlesungen über Differentialgeometrie und Geometrische Grundlagen von Einsteins Relativitätstheorie. III. Differentialgeometrie der Kreise und Kugeln*, Springer, Berlin-Heidelberg (1929).

[Bo] A.I. Bobenko. Discrete conformal maps and surfaces, *Symmetries and Integrability of Difference Equations (Canterbury, 1996)* (P. A. Clarkson, F. W. Nijhoff, eds.), London Math. Soc. Lecture Notes, (1999), vol. 255, Cambridge University Press, pp. 97–108.

[BPR] A.I. Bobenko, H. Pottmann, T. Rörig. Multi-Nets. Classification of Discrete and Smooth Surfaces with Characteristic Properties on Arbitrary Parameter Rectangles, *Discrete & Computational Geometry* (2019).

[BSST1] A.I. Bobenko, W.K. Schief, Y.B. Suris, J. Techter. On a discretization of confocal quadrics. I. An integrable systems approach, *Journal of Integrable Systems*, Volume 1, Issue 1, January 2016, xyw005, `https://doi.org/10.1093/integr/xyw005`

[BSST2] A.I. Bobenko, W.K. Schief, Y.B. Suris, J. Techter. On a discretization of confocal quadrics. II. A geometric approach to general parametrizations, *International Mathematics Research Notices*, Volume 2020, Issue 24, December 2020, Pages 10180–10230, `https://doi.org/10.1093/imrn/rny279`

[BST] A.I. Bobenko, W.K. Schief, J. Techter. Checkerboard incircular nets. Laguerre geometry and parametrisation, *Geometriae Dedicata*, Volume 204, Issue 1, February 2020, Pages 97-129, `https://doi.org/10.1007/s10711-019-00449-x`

[BS] A.I. Bobenko, Y.B. Suris. *Discrete differential geometry. Integrable structure.* Graduate Studies in Mathematics, Vol. 98. AMS, Providence, (2008).

[Bö] W. Böhm. Verwandte Sätze über Kreisvierseitnetze, *Arch. Math. (Basel)* **21** (1970) 326–330.

[Ca] E. Casas-Alvero. *Analytic Projective Geometry*, EMS Textbooks in Mathematics (2014).

[CDS] J. Cieśliński, A. Doliwa, P.M. Santini. The integrable discrete analogues of orthogonal coordinate systems are multi-dimensional circular lattices, *Phys. Lett. A*, (1997), **235**, 480–488.

[Da1] G. Darboux. *Leçons sur la Théorie Générale des Surfaces et les Applications Géométriques du Calcul Infinitésimal* **2, 3**, Gauthier-Villars, Paris (1887, 1889).

[Da2] G. Darboux. *Leçons sur les systèmes orthogonaux et les coordonnées curvilignes. Principes de géométrie analytique*, Gauthier-Villars, Paris, (1910), 567 pp.

[Da3] G. Darboux. *Principes de Géométrie Analytique*, Gauthier-Villars (1917).

[dC] M.P. do Carmo. *Differential geometry of curves and surfaces*, Prentice Hall (1976).

[DR] V. Dragović, M. Radnović. Poncelet Porisms and Beyond. Integrable Billiards, Hyperelliptic Jacobians and Pencils of Quadrics, *Frontiers in Mathematics*, Birkhäuser, Basel (2011).

[Ei1] L.P. Eisenhart. Triply conjugate systems with equal point invariants, *Ann. of Math.* (2), (1919), Vol. 20, No. 4, pp. 262–273.

[Ei2] L.P. Eisenhart. *A treatise on the differential geometry of curves and surfaces*, Dover, New York, (1960).

[EMOT] A. Erdélyi, W. Magnus, F. Oberhettinger, F.G. Tricomi. *Higher transcendental functions. Vol. III. Elliptic and automorphic functions, Lamé and Mathieu functions.* Based, in part, on notes left by Harry Bateman. McGraw-Hill, New York-Toronto-London, 1955, xvii+292 pp.

[FT] D. Fuchs, S. Tabachnikov. *Mathematical omnibus. Thirty lectures on classic mathematics*, AMS, Providence, (2007), xvi+463 pp.

[GGR] I.M. Gelfand, M.I. Graev, V.S. Retakh. General hypergeometric systems of equations and series of hypergeometric type, *Russ. Math. Surv.*, (1992), Vol. 47, pp. 1–88.

[IR] A. Iatrou, J.A.G. Roberts. Integrable mappings of the plane preserving biquadratic invariant curves, *J. Phys. A: Math. Gen.* **34** (2001) 6617–6636.

[Iz] I. Izmestiev. Spherical and hyperbolic conics, *Eighteen Essays in non-Euclidean Geometry, EMS*, (2019).

[IT] I. Izmestiev, S. Tabachnikov. Ivory's theorem revisited, *J. Integrable Systems* **2** (2017) xyx006.

[Ja] C.G.J. Jacobi. *Vorlesungen über analytische Mechanik. Berlin 1847/48*, Lecture notes prepared by Wilhelm Scheibner. Dokumente zur Geschichte der Mathematik, 8. Vieweg, Braunschweig, (1996). lxx+353 pp.

[Ki] W. Killing. *Der Flächenbüschel zweiter Ordnung*, Dissertation (1872).

[Kl] F. Klein. *Vorlesungen über nicht-euklidische Geometrie.*, Die Grundlehren der math.Wiss. 26, Springer, (1928).

[KS1] B.G. Konopelchenko, W.K. Schief. Three-dimensional integrable lattices in Euclidean spaces: Conjugacy and orthogonality, *Proc. R. Soc. London A*, (1998), Vol. 454, pp. 3075–3104.

[KS2] B.G. Konopelchenko, W.K. Schief. Integrable discretization of hodograph-type systems, hyperelliptic integrals and Whitham equations, *Proc. Royal Soc. A*, (2014), Vol. 470, No. 2172, 20140514, 21 pp.

[Kr] I.M. Krichever. Algebraic-geometric n-orthogonal curvilinear coordinate systems and the solution of associativity equations, *Funct. Anal. Appl.* **31** (1997), 25–39.

[LT] M. Levi, S. Tabachnikov. The Poncelet grid and billiards in ellipses, *The American Mathematical Monthly* **114** (2007) 895–908.

[Le] H. Levy. *Projective and Related Geometries*, Macmillan, New York (1964).

[LPWYW] Y. Liu, H. Pottmann, J. Wallner, Y.-L. Yang, W. Wang. Geometric modelling with conical meshes and developable surfaces, *ACM Trans. Graphics* **25**, no. 3 (2006), 681–689.

[MT] A.E. Mironov, I.A. Taimanov. Orthogonal curvilinear coordinate systems that correspond to singular spectral curves, *Proc. Steklov Inst. Math.* (2006), no. 4(255), 169—184.

[Mo] J. Moser. Geometry of quadrics and spectral theory, In: *The Chern Symposium 1979*, Springer, New York-Berlin, (1980), pp. 147–188.

[NIST] *NIST Digital Library of Mathematical Functions* (online at dlmf.nist.gov), National Institute of Standards and Technology, U.S. Department of Commerce (2010–2018).

[PGB] H. Pottmann, P. Grohs, B. Baschitz. Edge offset meshes in Laguerre geometry, *Adv. Comp. Math.* **33:1** (2010) 45–73.

[PW] H. Pottmann, J. Wallner. The focal geometry of circular and conical meshes, *Adv. Comp. Math.*, (2008), **29**, no. 3, 249–268.

[QRT] G.R.W. Quispel, J.A.G. Roberts, C.J. Thompson. Integrable mappings and soliton equations II, *Physica D* **34** (1989) 183–192.

[RGW] A. Ramani, B. Grammaticos, R. Willox. Generalized QRT mappings with periodic coefficients, *Nonlinearity* **24** (2011) 113–126.

[RJ] J.A.G. Roberts, D. Jogia. Birational maps that send biquadratic curves to biquadratic curves, *J. Phys. A: Math. Theor.* **48** (2015) 08FT02.

[Sch] R.E. Schwartz. The Poncelet grid, *Advances in Geometry* **7** (2007) 157–175.

[SPG] M. Skopenkov, H. Pottmann, P. Grohs. Ruled Laguerre minimal surfaces, *Math. Z.* **272** (2012) 245–274.

[So] D.M.Y. Sommerville. *Analytical geometry of three dimensions*, Cambridge University Press, Cambridge, (1934).

[SS] A. Sym, A. Szereszewski. On Darboux's Approach to R-Separability of Variables, *SIGMA* **7** (2011).

[Ts] E. Tsukerman. Discrete conics as distinguished projective images of regular polygons, *Discrete Comput. Geom.*, (2015), Vol. 53, No. 4, pp. 691–702.

[Ve] A.P. Veselov. Confocal surfaces and integrable billiards on the sphere and in the Lobachevsky space, *J. Geom. Phys.*, (1990), vol. 7, no. 1, 81—107.

[WW] E.T. Wittaker, G.N. Watson. *A Course of Modern Analysis.* Cambridge University Press, Cambridge, (1927).

[Za] V.E. Zakharov. Description of the n-orthogonal curvilinear coordinate systems and Hamiltonian integrable systems of hydrodynamic type. I. Integration of the Lamé equations, *Duke Math. J.* **94**, no. 1, (1998), 103–139.